

SEQUENCE STRATIGRAPHY OF THE MID-ATLANTIC COASTAL PLAIN: AN
EVALUATION OF EUSTASY, SEDIMENT SUPPLY VARIATIONS, AND PASSIVE-
AGGRESSIVE TECTONISM

by

ANDREW A. KULPECZ

A dissertation submitted to the
Graduate School-New Brunswick
Rutgers, The State University of New Jersey

In partial fulfillment of the requirements

For the degree of

Doctor of Philosophy

Graduate Program in Geological Sciences

Written under the direction of

Dr. Kenneth G. Miller, Sr.

And approved by

New Brunswick, NJ

October, 2008

ABSTRACT OF THE DISSERTATION

Sequence Stratigraphy of the mid-Atlantic Coastal Plain: An Evaluation of Eustasy,
Sediment Supply Variations, and Passive-Aggressive Tectonism

By ANDREW A. KULPECZ

Dissertation Director:

Dr. Kenneth G. Miller, Sr.

This study uses high resolution geochronology (from biostratigraphy and Sr-isotope age estimates), lithofacies analysis (from continuous coreholes), and geophysical log correlations to develop a detailed framework of sequence and facies distribution across the U.S. mid-Atlantic margin. This allows the evaluation, and quantification (through one-dimensional backstripping), of the influence of eustatic, tectonic, and sediment supply changes on the Late Cretaceous-Pleistocene U.S. mid-Atlantic margin and the post-impact section of the late Eocene Chesapeake Bay Impact Structure (CBIS). Studies of late Cretaceous sequences from the New Jersey Coastal Plain provide a long-term (35 myr), high resolution (> 1 myr) record of paleodeltaic evolution on the New Jersey Coastal Plain and document five primary phases of margin evolution in response to eustatic change, two long-lived fluvial axes, variations in sediment budget, and thermoflexural basement subsidence. This study demonstrates the facies variability of mixed-influence (wave- and tide- influenced) deltaic systems, but also documents the

long-term stability of deltaic facies systems on the 10^6 - 10^7 yr scale, with cyclically repeating systems tracts controlled by eustatic change.

Studies of the Cenozoic southern mid-Atlantic Coastal Plain and CBIS post-impact section reveal significant unconformities and the discontinuous preservation of sequences during the Oligocene, lower Miocene, and late-middle Miocene, when coeval deltaic sections in New Jersey are thick and widespread, implicating regional “passive-aggressive” non-thermal tectonic changes. We explain these observations by the differential movement (uplift and excess subsidence) of basement structures in response to variations in intraplate stress. Stratigraphic observations provide low-end estimates of uplift as 10-50 m/ 1-5 myr, while backstripping quantifies periods of excess subsidence of 10-75 m/5-10 myr. Comparison of CBIS and regional backstripped records shows the post-impact evolution was not only dominated by eustasy and regional tectonics, but also the time-dependent compaction of impact-generated materials responsible for excess subsidence on the scale of 285 ± 50 m in the late Eocene that progressively decreased to 20 ± 15 m by the late Miocene. These studies demonstrate that while eustasy provides the template for sequence deposition globally, regional tectonics (uplift and subsidence), local effects (impact processes) and sediment supply dictate the regional preservation of sequences.

ACKNOWLEDGMENTS

On the seemingly endless voyage towards the completion of one's dissertation, there are countless people who help along the way. These range from faculty advisors and committee members, who lend guidance, assistance, and the constructive criticism invaluable to such an undertaking, to fellow graduate students and friends, who provide valuable discussion, debate, and emotional outlets during long hours of data collection and writing. Family members also share in much of the credit, for without their positive attitude, prayer, and encouragement, much of these efforts would go for naught.

I would especially like to thank my advisor, Ken Miller, for the countless hours of mentoring and discussion. Furthermore, he is the only person to actually read all 250 plus pages of this dissertation in its seemingly infinite permutations- a very notable achievement! His sense of humor helped temper many situations, and his mentorship stands as the most influential factor on my advancement as a geoscientist. I would also like to thank Peter Sugarman and Jim Browning, whose comments and eager assistance over the last six years has not gone unappreciated. They are always good for a sarcastic remark to get you back on the right track. Finally, I would like to thank committee members Greg Mountain and Michelle Kominz, who helped considerably through the reading of this dissertation and the initial research proposal. Michelle deserves much credit for the development of the backstripping model used in Chapter 3, and I am deeply appreciative of all her efforts and guidance.

I would especially like to thank the many generations of Rutgers graduate students, faculty, and staff who have helped out during my tenure on the “Banks of the Old Raritan.” The many hours with my officemates (Ashley, Svetlana, and Aimee) have yielded many great memories, and their sense of humor made the process much easier. I would like to thank Ryan Earley for his assistance with graphics design programs, as his vast knowledge saved many hours of troubleshooting. I thank the many people who took the time to caffeinate at the student center (Jim Wright, Don Monteverde, Mark Baum, Ian Saginor, and Sam Henderson), and for the valuable conversations that took place on these treks. I thank the residents of the Green Building for their positive attitude, and laughs along the way. I deeply appreciate the opportunity to instruct laboratories and learn from great names like Gail Ashley and Ken Miller, and for the opportunity to teach Planet Earth for the last two years. The lessons learned along the way will stay with me through the rest of my career. Without the assistance of the support staff of the Department of Geological Sciences, this journey would have been significantly more difficult. I thank Jovani Reaves, Johanny Zabala, Keith Sproul, and Bob Baldi for their help along the way: it was very much appreciated.

I am grateful for those who helped with the collection of data sets used in this study: Lloyd Mullikin and Don Monteverde of the New Jersey Geological Survey; Gene Cobbs III and his USGS drill team; David Powars, Greg Gohn, Wright Horton, and Lucy Edwards from the USGS for their contributions on the Eyreville and Exmore cores; Travis Hayden from Western Michigan University for his discussions and help regarding backstripping; Mark Feigenson for the use of his Mass Spectrometer and clean lab; and

Dr.'s Jeff Greenberg, Stephen Moshier, and James Clark of Wheaton College who started me down this long, long road.

Finally, I thank my wonderful wife who put up with countless hours of whining and writing during this arduous process. Her positive attitude and love allowed the completion of this chapter of our life, as did her financial support! I thank my family and family-in-law, who were always good for a pat on the back (and a kick in the rear) when they deemed it necessary. I would have finished sooner if it weren't for the illustration of my father's Ph.D.! I would like to thank my many friends who feigned interest and kindly tolerated many hours of geology talk: Maz, Jack, Chip, Scott, Adam, Chris, Bob, Pat, Jesús, Theo, and Josiah.

Table of Contents

Abstract of the Dissertation.....	ii
Acknowledgements.....	iii
Table of Contents.....	vi
List of Tables.....	xi
List of Illustrations.....	xii
Introduction to the Dissertation.....	1
Geologic Background of the mid-Atlantic margin.....	3
The Chesapeake Bay Impact Structure.....	9
The Sequence Stratigraphic Method.....	11
Objectives and Overview of Chapters.....	14
References.....	18
Figure Captions.....	24
Figures and Tables.....	26
 Chapter 1: Response of Late Cretaceous Migrating Deltaic Facies Systems to Sea Level, Tectonics, and Sediment Supply Changes, New Jersey Coastal Plain, U.S.A.	29
Abstract.....	29
Introduction.....	30
Geologic Background.....	32
Methodology.....	35
Cores and Correlation of Geophysical Logs.....	35
Mapping.....	38

Data and Results.....	40
Early Cenomanian-Early Turonian Sequences.....	40
Mid-Turonian-Coniacian Sequences.....	42
Santonian Sequence.....	45
Uppermost Santonian-Campanian Sequences.....	46
Maastrichtian Sequence.....	48
Discussion.....	50
Deltaic Facies Models.....	50
Paleogeographic Evolution of Late Cretaceous Deltas, New Jersey	
Margin.....	55
Controls on the Distribution of Sequences and Facies.....	60
Sea-Level Changes.....	60
Sediment Supply and Source Location.....	61
Basement Structure and Subsidence.....	65
Conclusions.....	67
Acknowledgements.....	69
References.....	70
Figures Captions.....	76
Figures and Tables.....	80

Chapter 2: Post-Impact Evolution of the Chesapeake Bay Impact Structure: Eustasy,	
Passive-Aggressive Tectonism, and Impactite Compaction.....	90
Abstract.....	90

Introduction.....	91
Methods.....	96
Data and Results- Exmore Corehole.....	103
Late Eocene Sequence(s).....	104
Oligocene Sequences.....	105
Sequence C5 (Lower Miocene).....	107
Sequence C6 (Middle Miocene).....	108
Sequence C7 (Middle Miocene).....	109
Sequence C8 (Middle Miocene).....	110
Sequence M1 or LST Sequence SM (Upper Miocene).....	112
Sequence SM (Upper Miocene).....	114
Sequences Ea1 and Ea2 (Upper Miocene).....	116
Pleistocene Sequences.....	118
Discussion.....	119
Post-Impact Evolution of the CBIS.....	119
Eustatic Variations.....	122
Impactite Compaction.....	124
Passive-Aggressive Tectonism: Regional Insights and Controlling Mechanisms.....	126
Regional Sediment Supply Variations.....	133
Conclusions.....	135
Acknowledgements.....	136
References.....	137

Figure Captions.....	146
Figures and Tables.....	153
Chapter 3: Quantifying Regional Tectonics and Impact-Related Effects: Backstripping the Inner Crater, Chesapeake Bay Impact Structure, Virginia, U.S.A.....	166
Abstract.....	166
Introduction.....	167
Methods.....	174
Data.....	179
Results.....	183
Time-Dependent Compaction Model	183
R1 Results	185
Discussion.....	188
Integration with R2 Results and Controls on Post-Impact Evolution.....	188
Late Eocene- Excess Accommodation and “Shoaling-Upwards”	
Trends.....	189
Late Eocene-early Oligocene Uplift within the CBIS.....	191
Miocene through Pliocene Trends and Sea-Level Estimates.....	193
Quantifying Oligocene and Miocene Uplift and Unconformity	
Genesis.....	196
Discussion of tectonic mechanisms.....	198
Conclusions.....	204
References.....	206
Figure Captions.....	214

Figures and Tables.....	219
Appendices.....	233
Conclusions of the Dissertation.....	237
Late Cretaceous New Jersey.....	237
Regional Studies of the Chesapeake Bay Impact Structure.....	239
Quantifying Impact-Effects and Regional Tectonism.....	240
Future Work.....	242
References.....	245
Figure Captions.....	247
Figures.....	248
Curriculum Vitae.....	250

LIST OF TABLES

Table 2.1. Table shows the Sr- isotopic age ranges for sequences recovered at the three coreholes used in this study; Bethany Beach (Browning et al., 2006); Eyreville (Browning et al., this volume); and Exmore (this study). All ages are in Ma. Undated (no carb) indicates that intervals provided insufficient carbonate material to extract Sr-ratios. The letters “xxx” indicate the absence of a sequence at a corehole.....	162
Table 2.2. Table summarizes the primary lithologic, paleoenvironmental, and regional thickness trends of strata from Delaware/ New Jersey to the CBIS and southern Virginia.....	163
Table 2.3. Criteria used for sequence boundary analysis for the Eyreville corehole. A confidence level of ‘2’ indicates that there is a substantial hiatus, and the presence of several key defining characteristics. A confidence level of ‘1’ indicates a shorter hiatus, or a poorly defined sequence boundary.....	164
Table 2.4. Criteria used for sequence boundary analysis for the Exmore corehole. A confidence level of ‘2’ indicates that there is a substantial hiatus, and the presence of several key defining characteristics. A confidence level of ‘1’ indicates a shorter hiatus, or a poorly defined sequence boundary. Age estimates with superscript “*” represent ages derived from correlation with nearby coreholes.....	165
Table 3.1. Chart shows sample depth, sequence, paleoenvironmental interpretation, abundant benthic fauna, biofacies interpretations, and paleodepth estimates for the Eyreville corehole.....	230
Table 3.2. Backstripping inputs for the Eyreville corehole. Thickness is in meters, density is in g/cm ³ , % clay-sand-silt is out of 100, sorting (1 = dirty, 4= clean), Age (Ma), paleoenvironmental interpretation from core, and water depth estimates.....	231
Table 3.3. Backstripping inputs for the Exmore corehole. Thickness is in meters, density is in g/cm ³ , % clay-sand-silt is out of 100, sorting (1 = dirty, 4= clean), Age (Ma), paleoenvironmental interpretation from core, and water depth estimates.....	232

LIST OF ILLUSTRATIONS

Figure I.1. Location map showing the mid-Atlantic margin extending from northern New Jersey to North Carolina. The landward edge of the Baltimore Canyon trough is modified from Olsson (1980) and is marked by the dashed red line. The outline of the Chesapeake Bay Impact Structure is modified from Powars and Bruce (1999). The basement structure contour is modified from Owens and Gohn (1985). Coreholes used in this study are marked by red dot: A- Ancora, NJ; AC- Atlantic City, NJ; B- Bayside, VA; BB- Bethany Beach, DE; BR- Bass River, NJ; CM- Cape May, NJ; CZ- Cape May Zoo, NJ; D- Dismal Swamp, VA; E- Eyreville, VA; F- Fentress, VA; IB- Island Beach, NJ; JB- Jenkins Bridge, VA; K- Kiptopeke, VA; L- Langley, VA; M- MW4-1, VA; MV- Millville, NJ; OC- Ocean City, NJ; SG- Sea Girt, NJ; and X- Exmore, VA. Black dots indicate some of the geophysical logs used in this study.....26

Figure I.2. Regional correlation section showing the distribution of stratigraphic units modified from Olsson et al. (1988). Data based on biostratigraphy and lithology from a series of deep coreholes spanning the mid-Atlantic Coastal Plain (noted at top of chart). Note the presence of the South Jersey high, Salisbury embayment, and Norfolk arch and their respective roles on regional sedimentation.....27

Figure I.3. Anatomy of a typical “coarsening-upwards” sequence found on the U.S. mid-Atlantic Coastal Plain (modified from Miller et al., 2004; Browning et al., 2006; Kulpecz et al., 2008). Upper Cretaceous units from the New Jersey Coastal Plain tend to exhibit a stronger deltaic influence, while Cenozoic sequences typically exhibit shelf-to-shoreface shallowing upwards successions. The typical gamma ray and resistivity log signatures are included.....28

Figure 1.1. Location map shows the location of ODP 174AX coreholes and additional geophysical logs used in this study. The location of basement structures is represented by the form line (in light gray) from Owens (1970). Coreholes (large gray circles, capital letters, boxed labels): AN- Ancora; BR- Bass River; MV- Millville; SG- Sea Girt. Geophysical logs (small circles, lowercase letters): Ap- Asbury Park; Bm- Browns Mills; Bu- Buena; Cw- Chatsworth; Do- Dorothy; Fr- Freehold; Hw- Howell; Ib- Island Beach; Ja- Jackson; La- Lavallette; Lb- Long Branch; Lh- Lakehurst; Lk- Lakehurst; Lw- Lakewood; Pp- Point Pleasant; Pw- Pittman West; Sh- Seaside Heights; Sm- South Mantoloking; Sp- Seaside Park; T1, T2, T3, T4, T5- Toms River area; Wg- Warren Grove; Wi- Williamstown; Wm- Woodmansie; Wt- Williamstown. OB represents an outcrop of the Magothy II sequence in Old Bridge, NJ. The inset map (after Poag and Sevon, 1989) presents a regional view with modern river courses and source terrains (filled with gray): H- Hudson River; D- Delaware River; S- Susquehanna River; C- Connecticut River; CA- Central Appalachian Highlands; A- Adirondack Highlands; NE- New England Highlands; and NJ- New Jersey.....80

Figure 1.2. Generalized lithostratigraphy (after Owens and Gohn, 1985), sequence stratigraphy (after Miller et al., 2004), and hydrostratigraphy (after Zapeczka, 1989) of the Upper Cretaceous New Jersey Coastal Plain.....81

Figure 1.3. Anatomy and well-log signature of typical New Jersey Upper Cretaceous sequences showing the primary lithologic components, their relationship to sequence stratigraphic units, and their characteristic gamma-ray and resistivity log characteristics (after Miller et al., 2004).....82

Figure 1.4. Paleogeographic maps showing the depositional evolution of Late Cretaceous deltaic facies. The thickness of highstand sands is represented by 10 m contour intervals. Facies are represented by both color and symbol where appropriate: AP- alluvial plain; CS- crevasse splay; DF- delta front; DP- delta plain and paleosols; ES- estuary; F- fluvial; L/S- lagoon and swamp; PD- prodelta; S- marine shelf; SF- shoreface; and TC- Tidal channel to Tidal delta. “Funnel, bell and box, and serrated” refer to the characteristic gamma log signatures of deltaic facies (listed to the left of each log) that are used to correlate facies away from continuous coreholes (after Rider, 2002). Approximate vertical scales are displayed to the right of each log signature.....83

Figure 1.5. Strike cross section of Upper Cretaceous sequences of the northern New Jersey Coastal Plain showing typical well-log characteristics. Correlation between ODP 174AX corehole Sea Girt (SG) and geophysical logs Lakewood (Lw) and Toms River (T3) shows the advantage of using both resistivity and gamma-log data (e.g., T3), particularly in identifying thin HST sand units.....84

Figure 1.6. Isopach maps of the Cenomanian Bass River sequences (I, II, III) from core and geophysical log data. Arrows represent the inferred location of sediment sources, with solid arrows representing a primary source and dashed arrows indicating a weaker secondary source. Contour interval is 3 meters. Large gray circles represent coreholes; small black circles represent well locations.....85

Figure 1.7. Subdivisions of the Magothy Formation showing sequences, facies, and log characteristics from the four ODP 174AX coreholes. Magothy sequences thicken to the north and contain diverse shallow marine to delta-plain facies. Outcrop photograph of the Old Bridge Member of the Magothy Formation (Magothy II sequence), Old Bridge, New Jersey. Note the change in orientation of the outcrop face represented by the thin black line. The letters indicate: A) an irregular-based interval of gray to white clean clays with fine-grained quartz sand; B) an irregular-based (30-40 cm) channel incised into clayey and sandy substrates; C) flaser and wavy beds of black to dark gray micaceous, organic clay draped over small (1-2 cm) ripples and planar cross-beds of fine- to medium-grained quartz sand; D) planar cross stratification; and E) interlaminated (3-5 mm) black micaceous clay with yellow to gray fine quartz sands.....86

Figure 1.8. Isopach maps of the Turonian-Coniacian Magothy sequences (I, II, III, IVA, IVB) from core and geophysical log data. Solid arrows represent a primary sediment source and dashed arrows indicate a weaker secondary source. Contour interval is 3 meters. Large gray circles represent coreholes; small black circles represent well locations.....87

Figure 1.9. Isopach maps of the Santonian, Campanian, and Maastrichtian sequences (Cheesequake, Merchantville, upper Englishtown, Marshalltown, and Navesink) from core and geophysical log data. Solid arrows represent a primary sediment source and dashed arrows indicate a weaker secondary source. Contour interval is 3 meters. Large gray circles represent coreholes; small black circles represent well locations.....88

Figure 1.10. Chart shows: (1) Composite sequence recovery; (2) backstripped sea-level estimates (from Miller et al., 2005); (3) onshore depocenter isopach maps (contour interval 20 meters); (4) offshore depocenter isopach maps from Poag and Sevon (1989) (contour interval 100 meters); (5) inferred sediment source (black circle indicates primary role, open circle indicates secondary); and (6) appropriate facies system. The two isopach sets do not represent the same ages, as is indicated by each map title.....89

Figure 2.1. Location map of the mid-Atlantic margin showing the distribution of coreholes and geophysical logs used in this study. Yellow dots represent USGS coreholes, red dots represent ODP 150X and 174AX coreholes, while black dots are geophysical logs. Coreholes used in this study are further identified by letter; E- Eyreville (Browning et al., this volume; Edwards et al., this volume; Gohn et al., in press); X- Exmore; K- Kiptopeke; F- Fentress; D- Dismal Swamp (Powars and Bruce, 1999); C- Cape Charles (Gohn et al., 2007); B- Bayside (Horton et al., 2008); L- Langley (Horton et al., 2005a); CM- Cape May (Sugarman et al., 2007); and BB- Bethany Beach (Browning et al, 2006). Well logs shown in Figure 3 are identified by letters; Ea- Eastville; Ta- Tasley; Ha- Hallwood; Wa- Wallops Island; Sh- Snow Hill; Wo- Wor-Dd80; Oa- Ocean City C30A; and Ob- Ocean City C43B. The regional transect (Fig. 3) is represented by the blue line that runs from A-A1. Figure 2 occurs along this same line, and depicts the wells within the CBIS. The outline of the CBIS is modified from Powars and Bruce (1999). An approximate basement contour (adapted from Olsson, 1988) marks the primary basement features of the mid-Atlantic Margin: 1) the Norfolk arch; 2) Salisbury embayment; and 3) South Jersey high. The base map is adapted from USGS Digital Line Graph 1:2,000,000, 1990.....152

Figure 2.2. Corehole-well log cross section from Langley, VA–Bethany Beach, DE (A-A1) modified from Gohn et al. (in press). Bethany Beach (Browning et al., 2006), Langley, Kiptopeke, Cape Charles, Exmore are coreholes; Eastville and Tasley are gamma ray logs. Sequence ages based on age-depth plots primarily using Sr-isotopes. Sequences C1-10 and M1 defined at Bethany Beach (Browning et al., 2006) while YK, Ea1, Ea2, and SM were first identified at Eyreville (Browning et al., this volume; this study). Blue lines represent sequence boundaries. Wavy red lines indicate coalesced sequence boundaries where one or more sequences are absent. Blue age ranges at Langley and Kiptopeke are established from biostratigraphy (Edwards et al., 2005; Powars and Bruce, 1999). Green ages are single Sr-age estimates from Powars and Bruce (1999). Lithologic columns are coded by the following colors: bright yellow- coarse quartz sand; pale yellow- fine quartz sand; blue- carbonate sand; brown- silt and clay; green- glauconite sand; and pink/white- mica or other. The underlying diagram of the CBIS is not to scale, and is intended to show the position of post-impact sequences

relative to crater morphology. Note the change in transect orientation at Kiptopeke from N-S to NE-SW.....153

Figure 2.3. Regional corehole-well log transect from Fentress, VA to Bethany Beach, DE (A-A1) showing Oligocene-Pleistocene sequence distribution as defined at the Bethany Beach (Browning et al., 2006), Eyreville (Browning et al., this volume), and Exmore coreholes (this study). Published reports were used to supplement correlations outside the crater (e.g., Powars and Bruce, 1999; Olsson et al., 1987). Thin blue lines represent sequence boundaries. Thick wavy red lines indicate coalesced sequence boundaries where one or more sequences are absent. Thin green lines indicate significant contacts or hiatuses identified from lithologic or biostratigraphic breaks from previous studies. Dotted lines indicate lower confidence in correlations, while hachured areas indicate insufficient data to render interpretations. Sequences are packaged and color coded by time. Blue age ranges at Langley and Kiptopeke are established from biostratigraphy (Edwards et al., 2005; Powars and Bruce, 1999). Green ages are single Sr-age estimates from Powars and Bruce (1999). The underlying diagram of the CBIS is not to scale, and is intended to show the position of post-impact sequences relative to crater morphology. Note the change in transect orientation at Kiptopeke from N-S to NE-SW.....154

Figure 2.4. Generalized transgressive-regressive, “shallowing-upwards” sequence of the Cenozoic mid-Atlantic Margin (modified from Miller et al., 1996; Miller et al., 2004; and Kulpecz et al., 2008). Diagram depicts the relationships between paleoenvironment, lithology, sequence components, and geophysical log character.....155

Figure 2.5. Diagram shows age-depth relationships for the early through late Miocene sequences identified within the Exmore corehole. Sequence boundaries identified in core are represented by the thick horizontal red lines. Blue lines extend from the lower to upper unconformities and indicate the time represented by a sequence, assuming a consistent sedimentation rate. Horizontal blue bars represent dinocyst zones from De Verteuil and Norris (1996). Zone DN6 at 513 ft represents a reinterpretation of De Verteuil and Norris (1996) sample 1712-22 by L. Edwards. The inferred ages for the top and base of each sequence are annotated. Black circles represent valid Sr- isotope datum points, while red circles represent Sr- isotope ranges compromised by diagenetic alteration. Error bars are included for all dates. Red shading represents the error range for each sequence. Lithologic units are from Powars et al. (1992), Powars and Bruce (1999), and Powars et al. (2005).). Lithologic columns are coded by the following colors: bright yellow- coarse quartz sand; pale yellow- fine quartz sand; blue- carbonate sand; brown- silt and clay; green- glauconite sand; and pink/white- mica or other....156

Figure 2.6. Figure shows lithologic, geochronologic, and sequence stratigraphic interpretations of the Exmore corehole. From left to right: 1) Gamma log response; 2) percent lithology (color key described in Figure 2); 3) depth column; 4) Sr- isotope dates; 5) paleoenvironmental interpretations; 6) sequence stratigraphic interpretations (e.g., systems tracts, MFS, etc.); 7) the identified sequence; and 8) respective

lithostratigraphic Formation. Solid horizontal red lines indicate sequence boundaries identified from core, while dashed red lines represent potential sequence boundaries. Dashed blue lines represent the position of Maximum Flooding Surfaces identified from core and geophysical logs. Lithologic units are from Powars et al. (1992), Powars and Bruce (1999), and Powars et al. (2005). IHST- lower Highstand Systems Tract; uHST- upper Highstand Systems Tract; TST- Transgressive Systems Tract; LST- Lowstand; FS- Flooding surface; MFS- Maximum Flooding Surface; Chop- Choptank Fm.; and NN-Newport News Beds.). Lithologic columns are coded by the following colors: bright yellow- coarse quartz sand; pale yellow- fine quartz sand; blue- carbonate sand; brown- silt and clay; green- glauconite sand; and pink/white- mica or other.....157

Figure 2.7. See Figure 2.6 caption.....158

Figure 2.8. Diagram shows the temporal distribution of sequences for three coreholes (Exmore, Eyreville, and Bethany Beach) plotted against oxygen isotope data (Miller et al., 2005). Geochronology of each sequence was derived from Sr- isotope age analysis, with biostratigraphy at Bethany Beach and Eyreville (Browning et al., 2006; this volume). Hachured sequences are poorly dated. Oxygen 18 inflections represent ice volume increases, are marked by the arrowed blue lines, and identified next to the right axis.....159

Figure 2.9. Map showing the distribution of subsurface terranes, boundaries, and key structural elements across the mid-Atlantic Magrin (modified from Maguire et al., 2004 and Glover et al., 1997). Terranes are colored according to the underlying key. Blue dashed lines represent major synforms (b- Shellburne Falls and Chester domes; d- Connecticut Valley-Gaspé Synclinorium) while orange dashed lines represent major antiforms (a- Manhattan prong-Berkshire Massif; c- Prehlan dome-Bronson Hill anticlinorium). The mid-Atlantic coastline and CBIS are overlain to add geographic perspective. Terranes and other features are identified by letters: rr- Roanoke Rapids; ch- Charleston; ha- Hatteras; bc- Brompton-Cameron; and cm- central Maine. JRSZ marks the James River Structural Zone (northern edge of the Norfolk arch) from Powars (2000). Horton et al. (2005a, b) note the presence of Avalon basement at the Bayside corehole, different from the shown map.....160

Figure 2.10. Diagram shows the preservation of sequences (in time) plotted against geographic distance (south to north transect from Fentress, VA to Island Beach, NJ). The basement contour is modified from Olsson et al., 1989). Faint red background is used to represent regional hiatuses.....161

Figure 3.1. Location map showing the mid-Atlantic Coastal Plain and the location of the CBIS, key basement features, and the location of backstripped records used in this study. Coreholes are coded by color and letter: BB- Bethany Beach, DE; X- Exmore, VA; E- Eyreville, VA; K- Kiptopeke, VA; L- Langley, VA; M- MW4-1, VA; F- Fentress, VA; and D- Dismal Swamp, VA. New backstripped records from Eyreville and Exmore are unique to this study, while the other coreholes are modified from Hayden et al. (2008).

Red circles indicate coreholes used in the construction of the New Jersey sea-level estimates (Miller et al., 2005; Kominz et al., 2008).....219

Figure 3.2. Diagram shows the data inputs for backstripping from the Eyreville (Browning et al., submitted) and Exmore (Kulpecz et al., submitted) coreholes. Plots include the percentage lithology (brown- clay/silt; pale yellow- fine sand; bright yellow- medium/coarse sand; green- glauconite; blue- carbonate; white- other), age interpretations for each sequence (based on bio- and Sr-isotope stratigraphy, sequence name, benthic zone interpretations, and lithofacies/paleoenvironmental interpretation. Biofacies U- *Uvigerina*; Bul- *Bulimina*; Hanz- *Hanzawaia*; Non; *Nonionella*; and Elph- *Elphidium* are defined by the studies of Miller et al. (1997). Biofacies A-G are defined by Pekar et al. (1997) while ‘n’ indicates no foraminifera. Lithofacies: USF- upper shoreface; LSF- lower shoreface; Est.- Estuarine; while p- proximal and d- distal.....220

Figure 3.3. Eyreville fraction porosity data is from Sanford et al. (submitted) and provides the data set for our time-dependent compaction model. The compaction models for Eyreville and Exmore are shown next to the physical data. Each multi-colored line represents a time-step (see key below for both age after impact and true geologic age) in the time-dependent compaction of these impact materials.....221

Figure 3.4. Figure presents the litho- and biofacies models used for paleodepth assignment. Lithofacies are modified from the wave-dominated shoreface model of Browning et al. (2006), while benthic foraminiferal biofacies for Miocene sequences are from Miller et al. (1997; shown on lithofacies diagram) and Oligocene sequences from Pekar et al. (1997; noted in blue beneath lithofacies diagram).....222

Figure 3.5. The lower three graphs depict different scenarios of time-dependent compaction and the sensitivity of the models to changes in c and t_0 . Model C represents the maximum compaction scenario; Model A represents the best-case scenario (used in this study); and Model D represents the end-case of no time-dependent compaction (impactite compacts as a function of depth). The sensitivity of R1 and R2 results to changes in model inputs are portrayed at the top of the page. R1 results are plotted against the theoretical subsidence curve of McKenzie (1978). Each scenario is color coded to match the appropriate model.....223

Figure 3.6. Backstripped R1 results from Eyreville (red) and Exmore (green). ‘Tsubs’ is defined as tectonic subsidence (minimum, best, maximum, and sed) while ‘WD’ stands for water depth.....224

Figure 3.7. New backstripped R1 estimates from Eyreville (red) and Exmore (green) plotted against the previous records of Hayden et al. (2008) and Browning et al. (2006). The regional hiatuses of Gohn et al. (2008) and Kulpecz et al. (submitted) are represented by the semi-transparent boxes. The base of the graph classifies the events that shaped the post-impact evolution of the CBIS, as defined by Hayden et al. (2008) and this study. The black bar represents the impact event.....225

Figure 3.8. Backstripped R2 estimates from Eyreville (red) and Exmore (green) plotted against the eustatic estimates of Kominz et al. (2008). Purple indicates the best eustatic estimate, while the black line represents the approximated lowstand sea level estimates. Light and dark purple depict minimum and maximum values, respectively. The light blue line represents long-term sea level, while the orange line represents long-term sea level from New Jersey with a slab correction (to account for dynamic topographic changes). Error ranges of CBIS estimates are represented by the broad color fills.....226

Figure 3.9. Thermal anomaly model of Hayden et al. (2008) that shows the normal geothermal gradient, the post-impact cooling from the deposition of cold impact materials after impact, the maximum subsidence event, and subsequent uplift phase and restoration of a new geothermal gradient (higher than original values due to the low thermal conductivity of impactites and post-impact sediments).....227

Figure 3.10. Figure depicts the geographic distribution of unconformities during the Oligocene, lower Miocene, and upper middle Miocene established from regional studies by Kulpecz et al. (submitted) and Powars and Bruce (1999). Thickness of these intervals in New Jersey, Delaware, and Maryland is established from geophysical log correlation (Kulpecz et al., submitted) and reports and publications from coreholes drilled by the Ocean Drilling Program (e.g., Browning et al., 2006; Sugarman et al., 2007; etc.). Note the different contour intervals between maps. Blank areas on the coastal plain indicate the presence of known unconformities.....228

Figure 3.11. Graph depicts the amplitude and timing of important mechanisms responsible for tectonic uplift and subsidence on typical passive margins. Lithospheric flexure and intraplate stress values are derived from Cloetingh (1988) and Karner et al. (1993). Dynamic topographic ranges are from Mueller et al. (2008). Thermoflexural subsidence estimates are from Steckler and Watts (1978) and Kominz et al. (1998), while lower crustal flow is derived from Westaway (2007). The dashed line for the upper intraplate stress box represents high amplitudes of uplift tied to major stress field reorganizations (e.g., Cloetingh, 1988; Cloetingh et al., 1990).....229

Figure C.1. Location map of the mid-Atlantic margin showing the location of ODP Leg 150X and 174AX coreholes (red dots) that could be used for extensive mapping of Cenozoic sequences. JB represents the location of the Jenkins Bridge (USGS) corehole, a vital component for improving regional correlations across the Delmarva Peninsula...248

Figure C.2. Isopach map showing the thickness and distribution of Paleocene sequences on the New Jersey Coastal Plain. Red dots indicate the location of ODP Leg 174 AX coreholes used in Kulpecz et al. (2008), while black dots indicate geophysical logs used for correlation. Thickness trends mirror those of the Late Cretaceous identified by Kulpecz et al. (2008), but further mapping is required to establish the distribution of Eocene- late Miocene sequences on the Coastal Plain.....249

INTRODUCTION

The U.S. mid-Atlantic margin is one of the most intensely studied sedimentary basins in the world, due in part to its proximity to the greater New York, Philadelphia, and Washington D.C. metropolitan area, and the many academic institutions therein. Studies of this region date back to the 19th century, when Charles Lyell (1845), seeking comparison to equivalent sections in the United Kingdom, described the sedimentary units of the New Jersey Coastal Plain. In subsequent decades, numerous studies described the physical and hydrologic characteristics of mid-Atlantic sediments (e.g., Weller and Knapp, 1907; Sanford, 1913; Cedarstrom, 1945), predominantly relying on outcrop lithostratigraphy to classify the stratigraphic record. The maturation of the plate tectonic theory in the 1960's and 1970's led to a major reevaluation of "passive margin" evolution, and led to numerous studies that evaluated mechanisms behind the stratigraphic development of the mid-Atlantic margin: eustasy (global sea-level change), tectonic uplift and subsidence, and sediment supply.

Driven by an era of rapid natural resource exploration in the 1970's (accompanied by the collection of seismic profiles from numerous sedimentary basins), the birth of seismic stratigraphy (the recognition of seismic reflections as geochronologic markers and facies indicators useful for the stratigraphic interpretation; Vail and Mitchum, 1977) provided a powerful tool for basin analysis. Increases in seismic resolution enabled the "outcrop scale" facies interpretations previously unavailable to previous studies, greatly increasing the accuracy of subsurface interpretations. The integration of seismic data with cores,

geophysical logs, paleontology, and outcrop studies led to the advent of sequence stratigraphy, the use of genetically-related, unconformably bounded units and stratal surfaces to interpret the stratigraphic record (e.g. Vail et al., 1977; Posamentier et al., 1988). Although this advance revolutionized the classification of sedimentary sections, many questions still remain concerning the origin of sequences and the mechanisms that control their evolution; namely the relationship between changes in accommodation (capacity for sediment to accumulate) and the nature of base-level lowering in response to variations in eustasy and tectonism. Furthermore, changes in sediment supply can complicate interpretations, as variable rates of sediment delivery can enhance or diminish unconformity genesis on regional scales and significantly influence the character of lithofacies (e.g., Christie-Blick, 1991; Reynolds et al., 1991; Kulpecz et al., 2008).

Identifying and differentiating the roles of eustasy, tectonics, and sediment supply on sedimentation remains necessary to fully understand the evolution of sequences on the U.S. mid-Atlantic and other margins. By developing a regional sequence stratigraphic framework and quantifying eustatic change and tectonic subsidence (through one-dimensional backstripping), one can distinguish global signals (glacioeustasy) from regional processes (margin tectonics) and localized effects (deltaic lobe position, impact-related effects), allowing for a comprehensive evaluation of the mechanisms at play. The mid-Atlantic Coastal Plain, the area stretching from Long Island, New York to Cape Fear, North Carolina (Fig. 1), provides an excellent natural laboratory for evaluating these processes. This study utilizes numerous continuous coreholes and geophysical logs from New Jersey, Delaware, Maryland, and Virginia to develop a sequence stratigraphic

framework and evaluate the regional distribution of sequences and facies. Furthermore, the late Eocene Chesapeake Bay Impact Structure (CBIS), located beneath the modern Chesapeake Bay and Delmarva Peninsula (Fig. 1; Poag et al., 1994), provides a unique opportunity to evaluate impact-related processes, framed within the context of passive margin evolution. The overarching goal of this study is to present a high-resolution geochronologic analysis of the mechanisms that influence margin sedimentation, focusing on sections from the Late Cretaceous (New Jersey Coastal Plain) and Cenozoic (late Eocene-Pleistocene from Delaware, Maryland, and Virginia). In each chapter, we comment on the role of eustasy, thermoflexural subsidence, non-thermal tectonics, and changes in sediment supply, and discuss how these factors affected the deposition, preservation, and characteristics of sequences.

Geologic Background of the mid-Atlantic Margin

The U.S. mid-Atlantic Coastal Plain consists of a series of eastward thickening wedges of unconsolidated fluvio-deltaic and marine sediments that prograde seaward across the continental shelf (Owens and Sohl, 1969). These strata lie unconformably over an irregular, deformed, and faulted Paleozoic crystalline basement. Thermoflexural basement subsidence (e.g., Kominz et al., 1998), periodic non-thermal tectonic uplift of basement structure (e.g., Brown et al., 1972; Kulpecz et al., submitted), sea level change (e.g., Miller et al., 2005), and sediment supply variations have played significant roles in the stratigraphic development of the Atlantic margin since the Triassic- early Jurassic separation of North America from northwestern Africa (Klitgord et al., 1988).

The underlying basement structure of mid-Atlantic Coastal Plain is controlled by a succession of alternating embayments and arches (from north to south: Long Island platform, Raritan embayment, South Jersey high, Salisbury embayment, Norfolk arch, Albemarle embayment, Cape Fear arch; Fig. 1; Owens and Gohn, 1985) that extend inland from the offshore Baltimore Canyon Trough, a large (60-100 km wide) sedimentary basin that parallels the middle Atlantic margin (Grow and Sheridan, 1988; Grow et al., 1988). The Baltimore Canyon Trough yields the thickest sedimentary section of the Atlantic margin, an 14 km-thick post-rift section (Lower Mesozoic clastics and carbonates overlain by Upper Mesozoic and Cenozoic marine sediments) off the coast of New Jersey and seaward of the hinge zone, the transition between relatively “unstretched” continental crust and extensively heated and thinned crust (Poag, 1979; Watts, 1981; Grow et al., 1988). These Cretaceous and Cenozoic sediments thin landward of the hinge zone and reach a maximum thickness of less than 1-1.5 km in the southern New Jersey Coastal Plain (Poag, 1979; Olsson, 1980), but exceed 2-3 km in the Salisbury embayment underlying Maryland and Virginia (Fig. 2; Olsson et al., 1988). Other studies (Horton et al., 1989; Maguire et al., 2004) note the presence of numerous fault-bounded terranes that comprise the Paleozoic basement underlying the coastal plain (some of which are reactivated during the extensional rift-phase of the margin; e.g., the border fault of the Newark Basin; Schlische, 1992; Withjack et al., 1998), adding another layer of complexity to the margin.

Although subsidence of the Atlantic margin began roughly 195 Ma following the cessation of rifting and onset of oceanic crust production in the north Atlantic, it was not until the Late Jurassic and Early Cretaceous that areas now landward of the hinge zone were covered by marine sediments (Grow and Sheridan, 1988; Watts and Steckler, 1979). This is attributed to the coupling of thermal and flexural tectonic subsidence of the Atlantic margin, controlled by the initial amount of heating, degree of lithospheric thinning during the rifting process, and subsequent cooling and thermal contraction. The crust experienced ~ 250-300% of extension seaward of the hinge zone that resulted in as much as 20 km of thinning towards the outer shelf (Watts, 1981; Watts, 1982). As a result, early thermal cooling and subsidence was greatest seaward of the hinge line.

Progressive cooling of the crust resulted in increased flexural strength and rigidity (Watts, 1981). Subsequent loading of thick sedimentary packages across the shelf induced flexural subsidence of the margin and updip coastal plain. This flexural response accounts for the “coastal onlap” of younger sedimentary packages “overstepping” older units landward of the hinge zone (Watts, 1981). Thermoflexural subsidence and the first significant sedimentation of the mid-Atlantic Coastal Plain began about 120 Ma (although thin Jurassic sediments were recovered deep within the Salisbury embayment; Fig. 2; Olsson et al., 1988), significantly lagging offshore post-rift subsidence (Watts, 1981; 1982).

Although post-rift lithospheric cooling and the flexural response to offshore sediment loading are the dominant contributors to “classic” Atlantic-type passive margin

subsidence (Watts and Steckler, 1979; Kominz et al., 1998), periods of non-thermal subsidence and uplift have occurred on this margin (e.g., Brown et al., 1972; Owens and Gohn, 1985; Owens et al., 1997). While numerous studies attempted to link regional sedimentation patterns to the underlying basement structure, the small number of coreholes that penetrate basement, lack of deep regional seismic data, and low seismicity along active faults north of the Cape Fear arch (Seeber and Armbruster, 1988; Weems and Lewis, 2002) cloud their influence on sequence deposition. Early investigations of the Atlantic Margin (Owens and Sohl, 1969; Owens and Gohn, 1985) recognized sequences as the fundamental building blocks of the coastal plain and cited regional (although ambiguous) tectonics as the dominant mechanism controlling their development. Brown et al. (1972) described these structures as a series of wrench fault-bounded grabens, while Owens et al. (1997) attributed regional stratigraphic differences to “rolling basins” or broad warping (~100-200 km wavelength) of the crust.

While studies from New Jersey and Delaware (Kominz et al., 1998, 2008) show that tectonics have been largely “passive” and thermoflexural in origin across much of the northern mid-Atlantic coastal plain, significant regional unconformities across the Cape Fear and Norfolk arches implicate periods of uplift, erosion, and non-preservation (Olsson et al., 1988; Weems and Lewis, 2002; Kulpecz et al., submitted). The recent development of a high-resolution (> 1 myr) sequence stratigraphic framework across the mid-Atlantic Margin (New Jersey, Delaware) and within the CBIS (Virginia) provides the proper geochronologic resolution to identify such non-thermal events (Miller et al., 2005; Browning et al., 2006; Browning et al., submitted; Kulpecz et al., submitted).

This distribution of regional sequences reveals significant periods of non-thermal tectonic uplift and excess subsidence at a scale of tens of meters in 1-5 myr, overprinting subsidence from simple lithospheric cooling and flexure. This style of “passive-aggressive” tectonism characterizes passive margins otherwise dominated by thermoflexural subsidence. Although these observations confirm the presence of significant unconformities, the mechanism behind their genesis is uncertain.

Recent studies have suggested several mechanisms as the cause of regional uplift, down-flexure, and movement of existing basement structures. These include variations in intraplate stress (e.g., Cloetingh, 1988; Karner et al., 1993) and density-driven mantle processes related to the interaction of eastern North America with the subducted Farallon plate (e.g., Mueller et al., 2008; Spasojević et al., 2008). Furthermore, the interaction of the margin to large sediment loads (excess subsidence of Browning et al., 2006 and flexural bulge of Galloway, 1989) and variations in lower crustal flow from the erosion of hinterland material must also be considered (e.g., Westaway, 2007). This study will explore the possible influences of these mechanisms on margin sedimentation.

While tectonic subsidence was critical in the early development of the margin, eustasy has played an important role on margin sedimentation as the onshore coastal plain records numerous sea-level events from the Late Cretaceous (e.g. Olsson, 1991; Miller et al., 2004) throughout the Cenozoic (e.g. Miller et al., 1997). Sea-level change, and more appropriately global changes in ice volume (glacioeustasy), appears to determine the template of available sequences on the Atlantic Margin by altering the availability of

accommodation through variations in base-level (e.g., Pittman and Golovchenko, 1983). Olsson (1991) linked the timing of New Jersey Coastal Plain sequences to those of Haq et al. (1987), necessitating a “global” mechanism for their genesis. Extensive drilling of the New Jersey shelf-slope (ODP Legs 150 and 174A) and coastal plain (ODP Leg 150X and 174AX) identified 33 Cenozoic sequences and linked Oligocene-Miocene sequence boundaries with $\delta^{18}\text{O}$ increases, implicating a glacioeustatic control on sequence genesis (Miller et al., 1998). Recently, Kulpecz et al. (submitted) noted the strong correspondence of late Eocene-Pliocene sequence boundaries and $\delta^{18}\text{O}$ isotope increases within and around the CBIS, implicating eustasy as the driver behind sequence boundary genesis. The timing and number of Cenozoic sequences from the studies of Miller et al. (2005) are consistent with the results of Haq et al. (1987), implicating a glacioeustatic control for sequence boundary formation. However, differences in sequence expression (both temporal and physical) indicate that regional and local forces exist and that the mechanisms are not entirely global in origin.

Variations in sediment supply also influence the distribution and expression of sequences across the mid-Atlantic Coastal Plain. Variations in sediment budget can affect sequence thickness, the position of key stratal surfaces, and the expression of litho- and biofacies (e.g., Reynolds et al., 1991). The mid-Atlantic region was influenced by several major fluvial systems during the Cenozoic (Poag and Sevon, 1989). The ancestral Susquehanna, Potomac, Delaware, and Hudson Rivers, as well as several smaller rivers (e.g. Raritan, James, Yorktown, etc.), each influenced regional sedimentation. Changes in sediment input, tied to variation in the rates of Appalachian uplift and denudation, are reflected by

different styles of regional sedimentation. Kulpecz et al. (2008) demonstrated that two deltaic systems that controlled the distribution of sequences, facies and hydrogeologic units during the Late Cretaceous in New Jersey. Similarly, Sugarman et al. (1995) documented deltaically influenced Miocene sections in New Jersey with a likely paleo-Delaware and possible paleo-Hudson source. Coeval Miocene sections in Delaware reveal little deltaic influence and resemble wave-dominated shoreline facies (Browning et al., 2006), while equivalent sections in Maryland and Virginia appear fully marine and are dominated by shelf facies (e.g., Powars and Bruce, 1999). Although variations in sediment supply cannot alone cause the formation of sequence boundaries (Christie-Blick et al., 1991), they can dramatically alter the expression of sequences on a regional scale and obscure the influence of eustasy and tectonics (e.g., the sediment starved setting of the Oligocene as we later discuss). Substantial changes in thickness of Cenozoic sections across the mid-Atlantic Coastal Plain indicate that tectonics and/or sediment supply variations significantly alter the geometry of sequences on regional and local scales.

The Chesapeake Bay Impact Structure

A unique feature of the mid-Atlantic margin is the late Eocene (35.45 Ma; Pusz et al., in press) Chesapeake Bay Impact Structure (CBIS), a remarkably intact 85-km diameter crater that underlies the Chesapeake Bay area and lower Delmarva Peninsula (Fig. 1) (Poag et al., 1994). The CBIS is unique because of its position on a passive continental shelf and its status as one of only a handful of well-preserved marine-impacts (Sanford et al., 2004). The impact location on a deep continental shelf disrupted the normally

“passive” sedimentation of the margin and facilitated the deposition of marine sediments immediately following the catastrophic resurge and crater-fill of impactites, mega-block breccia, and tsunamites (Poag et al., 1994). This rapid return to normal marine processes inhibited subsequent erosion and degradation of the crater that plagues the later interpretation of other terrestrial structures. Post-impact sedimentation deposited 150-450 m of late Eocene to recent marine sediments atop the impact structure (Powars and Bruce, 1999).

Scientific investigations of CBIS date back to its discovery from marine seismic profiles (Poag et al., 1994) and impact-breccia penetrated by coreholes (Powars and Bruce, 1999). Extensive drilling by the United States Geological Survey completed a series of 5 coreholes that penetrated post-impact and impact sections. Cooperative drilling of the Eyreville-1 corehole (USGS, DOSECC, ICDP, state geological surveys, and academic institutions, including Rutgers) was completed in May 2006, providing a thick (444 m) expanded upper Eocene through Pliocene post-impact section with near perfect recovery (Fig. 1). These sediments provide a high resolution view of Cenozoic sea-level change and tectonics when compared to coeval sections to the north. Although previous studies have examined the litho-and biostratigraphy of post-impact strata, a majority of the interpretation has been largely lithostratigraphic (e.g., Powars and Bruce, 1999). These sediments provide a unique opportunity evaluate the genetic evolution of CBIS strata in regards to: 1) the unique mechanisms that dictate sequence preservation within the crater (impactite compaction, crustal rebound, thermal effects, and fault-related subsidence) and; 2) the processes of global sea-level change, regional tectonic subsidence and uplift,

and sediment input. To understand the sedimentary response to these mechanisms, the CBIS must be studied from a sequence stratigraphic perspective.

The Sequence Stratigraphic Method

Sequence stratigraphy, the use of genetically-related unconformity-bounded units and their constituent systems tracts to correlate sedimentary sequences on regional scales, revolutionized the geologic understanding of many sedimentary basins, including the mid-Atlantic margin (e.g., Olsson, 1991). The discipline was born from numerous outcrop studies, and the subsequent recognition that facies association and key surfaces visible in outcrops were detectable in seismic data (e.g., Mitchum et al., 1977). Although the definitions and terminology of sequence stratigraphic elements have been debated for several decades, the widely accepted definition of a ‘sequence’ is that of Exxon Production Research (EPR), which defines a sequence as “a stratigraphic unit composed of a relatively conformable succession of genetically related strata and bounded at its top and base by unconformities or their correlative conformities (Mitchum et al, 1977).”

These sedimentary sequences and bracketing unconformities provide a method for evaluating the processes that control the development of sedimentary architecture on both passive and active margins. These range from glacioeustasy to changes in the prevailing tectonic regime (subsidence versus uplift) to variations in sediment supply (Pitman and Golovchenko, 1983). They are also essential in predicting the distribution of important economic resources, namely hydrocarbons (Vail et al., 1977), freshwater aquifers

(Sugarman and Miller., 1997), and potential sites for carbon capture and sequestration (CCS).

Posamentier and Vail (1988) determined that each unconformity bounded depositional sequence was composed of a succession of systems tracts, or distinct depositional systems of unique geometry (and seismic characteristics) that form in response to different phases of eustatic (or tectonic) change. The lowstand systems tract (LST) is generally deposited during periods of relative sea-level fall and the earliest stages of sea-level rise. The LST is generally comprised of a basal unconformity overlain by a lowstand fan (submarine fans fed by incised valleys that bypass the shelf) and lowstand wedge of fine-grained slope deposits (Posamentier and Vail, 1988). Lowstand systems tracts are generally not represented in the New Jersey Coastal Plain due to its updip position on the margin (Fig 3; e.g., Miller et al., 1998). The transgressive-systems tract (TST) is deposited after the first major flooding event (representing relative sea-level rise), and is composed of a succession of retrogradational or “backstepping” sedimentary packages (Fig 3; Posamentier and Vail, 1988). The Maximum Flooding Surface (MFS), often represented by a condensed sedimentary section, forms in response to the highest rate of relative sea-level rise and caps the TST. The Highstand systems tract (HST) forms during the eustatic highstand and is characterized by the seaward progradation (and at times aggradation) of parasequences. These prograding sediments are often composed of fluvial, deltaic, nearshore, and offshore marine facies, conformably overlies the TST, and is generally capped by an unconformity formed during subsequent eustatic lowering (Posamentier and Vail, 1988).

Numerous studies (e.g., Van Wagoner et al., 1990; Van Wagoner, 1995) describe a typical “sequence” as consisting of a basal unconformity with an abrupt basin-ward shift (or shallowing) in facies across the boundary, subsequently overlain by transgressive deposits of the TST and coarse-grained units of the HST. Typical Upper Cretaceous and Cenozoic sequences of the mid-Atlantic Coastal Plain are substantially different, consisting of a coarsening upwards succession from marine shelf to shallow marine and nonmarine facies (Fig. 3). These differences are attributed to the updip position of mid-Atlantic Coastal Plain strata, far away from the focus of lowstand deposition and major fluvial incision farther offshore. In the deltaically influenced New Jersey Coastal Plain, these sequences consist of a basal unconformity and overlying middle-neritic glauconite shelf sands (TST) (Fig. 3). These are overlain by medial-prodelta silty clay (lower HST) capped by upper delta-front quartz sand and occasional delta plain sediments (upper HST). Cenozoic sequences from Maryland, Delaware, and Virginia are often represented by middle to inner shelf silt and clay (TST) overlain by lower shoreface fine sand (Fig. 3; lower HST), upper shoreface and foreshore coarse quartz sand, and occasional estuarine facies (upper HST; Browning et al., 2006). Lowstand (LST) facies are rarely recovered in core (occasional LST deposits are preserved within incised valleys; Kulpecz et al., submitted).

On the mid-Atlantic margin, sequence boundaries in core and outcrop are represented by distinct characteristics such as lag gravels, phosphorite concentrations, rip-up clasts, extensive burrowing and bioturbation, gamma ray inflections, and a sharp unconformable contact (Miller et al, 2004; Sugarman et al., 1995). Sequence boundaries are also

distinguished on the basis of geochronologic hiatuses from planktonic foraminifera, calcareous nannofossils and Sr-isotope age estimates. Although each sequence boundary is unique, each of these methods can be used to indicate significant periods of nondeposition and erosion (Sugarman et al., 1995; Olsson et al., 1988).

Objectives and Overview of Chapters

The overarching objective of this study is to evaluate the relative influence of eustatic, tectonic, and sediment supply changes on the U.S. mid-Atlantic margin using high resolution geochronology (from biostratigraphy and Sr-isotope age estimates), lithofacies analysis (from continuous coreholes), and geophysical log correlation to develop a detailed framework of sequence distribution and character across the margin.

Furthermore, the post-impact section of the late Eocene Chesapeake Bay Impact Structure offers numerous continuous coreholes and a unique opportunity to differentiate and quantify (through one-dimensional backstripping) regional trends from impact-related processes (impactite compaction, fault-related subsidence, etc.).

This dissertation is divided into three chapters, each of which has been published in a peer-reviewed journal, or has been written in manuscript format for submission. The first chapter, “Response of Late Cretaceous migrating deltaic facies systems to sea level, tectonics, and sediment supply changes, New Jersey Coastal Plain, U.S.A.” was published in the *Journal of Sedimentary Research* (Kulpecz et al., 2008). This paper presents a long-term (35 myr), high resolution (> 1 myr) record of paleodeltaic evolution

on the New Jersey Coastal Plain, and documents five primary phases of margin evolution in response to eustatic change, two long-lived fluvial systems, variations in sediment budget, and classic thermoflexural basement subsidence. This study demonstrates the widely known variability of mixed-influence (wave- and tide- influenced) deltaic systems, but also documents the long-term stability of deltaic facies systems on the 10^6 - 10^7 yr scale, with cyclically repeating systems tracts controlled by eustatic change. This study further demonstrates that although eustasy provides the template for sequence deposition, regional tectonics and sediment supply dictate the regional preservation of sequences. Observations from this research were also published in Sugarman et al. (2005) and Browning et al. (2008).

The second chapter, “Post-impact evolution of the Chesapeake Bay Impact Structure: eustasy, passive-aggressive tectonism, and impactite compaction,” was submitted to the Geological Society of America Special Publication on the CBIS, and is currently under consideration for publication (Kulpecz et al., submitted). In this paper, we use the Eyreville and Exmore, VA cores to provide the first continuous, high-resolution ($> \sim 1$ myr) chronostratigraphic records linking the inner crater and annular trough of the CBIS, and place them within a regional sequence stratigraphic framework extending from northern North Carolina through Delaware. Sequence boundaries preserved within the CBIS and across the mid-Atlantic region correlate with $\delta^{18}\text{O}$ increases, indicating a primary glacioeustatic control. However, regional comparisons show that sequences are preserved and cut out in different time intervals across the margin, including significant regional unconformities (or thin, patchy sequences) during the Oligocene (~ 35 -27 Ma),

lower Miocene (27-18 Ma), and late-middle Miocene (13-8.4 Ma) that correspond to the CBIS and nearby Norfolk arch. Many of these unconformities are equivalent to thick, deltaic sections preserved in New Jersey, implicating a mechanism other than eustasy for these regional differences. We explain these observations by: 1) the long-term compaction of impact-generated materials; 2) the differential tectonic movement of crustal blocks in response to variations in intraplate stress, and; 2) regional changes in sediment supply. Portions of this research were published in Gohn et al. (2008), as well as two companion papers submitted to the same Geological Society of America Special Publication (Edwards et al., submitted; Browning et al., submitted).

The final chapter, “Quantifying regional tectonics and impact-related effects: backstripping the inner crater, Chesapeake Bay Impact Structure, Virginia, U.S.A.,” is written in manuscript format and will be submitted to a peer-reviewed publication pending additional revision (Kulpecz et al., in prep). This manuscript utilizes previous studies of the CBIS (Gohn et al., 2008; Hayden et al., 2008; Kulpecz et al., submitted; Browning et al., submitted) to generate inputs for one-dimensional backstripping (an inverse modeling technique that removes the effects of sediment compaction and loading to estimate tectonic subsidence) of the Eyreville corehole within the inner crater of the CBIS. Backstripping enables the quantification of rates and amplitudes of impact-related effects, regional tectonic uplift and subsidence, and eustasy for the post-impact section. We also generate a new time-dependent compaction model for the compaction of impact-materials, one of the first applications of such a model to backstripping.

Comparison of backstripped records in and around the CBIS reveals several interesting trends: 1) the time-dependent compaction of impact-generated materials strongly influenced deposition within the inner crater, shown by the growth of most post-impact sequences into the CBIS and excess subsidence of 285 ± 50 m in the late Eocene that progressively decreased to 20 ± 15 m by the late Miocene; 2) excess accommodation within the annular trough was 115 ± 50 m in the late Eocene, but decreased significantly by the Oligocene due to a thinner (~ 200 m) impactite column; 3) late Eocene-early Oligocene shallowing of 95-225 m likely resulted from a major eustatic fall and the removal of a large negative thermal anomaly; 4) regional unconformities during the Oligocene, lower Miocene, and upper middle Miocene contrast with thick sections in New Jersey and Delaware, and appear to correspond with known basement structural boundaries; 5) the comparison of backstripped R2 results with eustatic curves establishes minimum levels of uplift required for unconformity genesis (15-100 m/ 1-5 myr); and 6) unlike much of the mid-Atlantic margin, this segment of the margin exhibits distinct periods of “passive-aggressive” non-thermal tectonic uplift (15-100 m /1-5 myr) and excess subsidence (10-55/10 myr, with peaks of 75-100 m/5 myr).

We conclude that while eustasy is largely responsible for changes in accommodation and the margin-wide genesis of sequence boundaries, the vertical movement of basement structures in response to intraplate stress, depocenter loading, and other tectonic mechanisms, results in significant differential preservation of sequences across the margin. The post-impact section of the CBIS, although strongly influenced by the initial impact and subsequent long-term compaction of impact materials, is dominated by

regional tectonic patterns after the latest Eocene and may provide valid eustatic estimates for the late Miocene and Pliocene.

References

- Brown, P.M., Miller, J.A., and Swain, F.M., 1972, Structural and stratigraphic, and spatial distribution of permeability of the Atlantic Coastal Plain, North Carolina to New York: U.S. Geological Survey Professional Paper 796, p. 1-79.
- Browning, J.V., Miller, K.G., McLaughlin, P.P., Kominz, M.A., Sugarman, P.J., Monteverde, D., Feigenson, M.D., and Hernández, J.C., 2006, Quantification of the effects of eustasy, subsidence, and sediment supply on Miocene sequences, Mid-Atlantic margin of the United States: Geological Society of America Bulletin, v. 118, p. 567-588.
- Browning, J.V., Miller, K.G., Sugarman, P.J., Kominz, M.A., McLaughlin, P.P., and Kulpecz, A.A., 2008, A 100 million year record of sequences, sedimentary facies and sea-level change from Ocean Drilling Program onshore coreholes, U.S. Mid-Atlantic coastal plain: Basin Research, v. 20, p. 227-248.
- Browning, J.V., Miller, K.G., McLaughlin, P.P., Jr., Edwards, L.E., Powars, D.S., Kulpecz, A.A., Wade, B.S., and Feigenson, M.D., *submitted*, Post-impact integrated litho-, sequence, Sr-isotopic, and bio-stratigraphy of the Eyreville corehole, Chesapeake Bay impact structure inner basin: Geological Society of America Special Publication.
- Cedarstrom, D.J., Geology and ground-water resources of the coastal plain in southeastern Virginia: Virginia Geological Survey Bulletin 63, 384 p.
- Christie-Blick, N., 1991, Onlap, offlap, and the origin of unconformity-bounded depositional sequences: Marine Geology, v. 97, p. 35-56.
- Cloetingh, S., 1988, Intraplate stresses: a tectonic cause for third-order cycles in apparent sea level?: Society of Economic Paleontologists and Mineralogists Special Publication, v. 42, p. 19-29.
- Edwards, L.E., Powars, D.S., Wade, B.S., Self-Trail, J.M., Kulpecz, A.A., Browning, J.V., Miller, K.G., McLaughlin, P.P., Jr., and Elbra, T., *submitted*, Geologic columns for the ICDP-USGS Eyreville A and C coreholes, Chesapeake Bay Impact Structure: Post-Impact Sediments, 0 to 444 m depth: Geological Society of America Special Publication.

- Galloway, W.E., 1989, Genetic stratigraphic sequences in basin analysis II: Application to northwest Gulf of Mexico Cenozoic basin: *American Association of Petroleum Geologists Bulletin*, v. 73, p. 143-154.
- Gohn, G.S., Koeberl, C., Miller, K.G., Reimold, W.U., Browning, J.V., Cockell, C.S., Horton, J.W., Jr., Kenkmann, T., Kulpecz, A.A., Powards, D.S., Sanford, W.E., and Voytek, M.A., 2008, Deep Drilling Yields New Insights into the Chesapeake Bay Impact Event: *Science*, v. 320, p. 1740-1745
- Grow, J.A., and Sheridan, R.E., 1988, U.S. Atlantic continental margin: a typical Atlantic-type or passive continental margin, *in* Sheridan, R.E., Grow, J.A., eds., *The Atlantic Continental Margin, U.S.: Boulder, Colorado, The Geological Society of America, Geology of North America*, v. 1-2, p. 1-7.
- Grow, J.A., Klitgord, K.D., and Schlee, J.S., 1988, Structure and evolution of the Baltimore Canyon Trough, *in* Sheridan, R.E., Grow, J.A., eds., *The Atlantic Continental Margin, U.S.: Boulder, Colorado, The Geological Society of America, Geology of North America*, v. 1-2, p. 269-290.
- Haq, B.U., Hardenbol, J., and Vail, P.R., 1987, Chronology of fluctuating sea levels since the Triassic (250 million years ago to present): *Science*, v. 235, p. 1156-1167.
- Hayden, T., Kominz, M., Powars, D.S., Edwards, L.E., Miller, K.G., Browning, J.V., and Kulpecz, A.A., 2008, Impact effects and regional tectonic insights: Backstripping the Chesapeake Bay impact structure: *Geology*, v. 36, p. 327-330.
- Horton, J.W., Jr., Drake, A.A., Jr., and Rankin, D.W., 1989, Tectonostratigraphic terranes and their Paleozoic boundaries in the central and southern Appalachians: *Geological Society of America Special Paper 230*, p. 213-245.
- Karner, G.D., Driscoll, N.W., Weissel, J.K., 1993, Response of the lithosphere to in-plane force variations: *Earth and Planet Science Letters*, v. 114, p. 397-416.
- Klitgord, K.D., Hutchinson, D.R., and Schouten, H., 1988, U.S. Atlantic continental margin; structural and tectonic framework, *in* Sheridan, R.E., Grow, J.A., eds., *The Atlantic Continental Margin, U.S.: Boulder, Colorado, The Geological Society of America, Geology of North America*, v. 1-2, p. 19-56.
- Kominz, M.A., Miller, K.G., and Browning, J.V., 1998, Long-term and short-term global Cenozoic sea-level estimates: *Geology*, v. 26, p. 311-314.
- Kominz, M.A., Browning, J.V., Miller, K.G., Sugarman, P.J., Mizintseva, S., and Scotese, C.R., 2008, Late Cretaceous to Miocene sea-level estimates from the New Jersey and Delaware coastal plain coreholes: and error analysis: *Basin Research*, v. 20, p. 211-226.

- Kulpecz, A.A., Miller, K.G., Sugarman, P.J., and Browning, J.V., 2008, Response of Late Cretaceous migrating deltaic facies systems to sea level, tectonics, and sediment supply changes, New Jersey Coastal Plain U.S.A.: *Journal of Sedimentary Research*, v. 78, p. 112-129.
- Kulpecz, A.A., Miller, K.G., Browning, J.V., Edwards, L.E., Powars, D.S., McLaughlin, P.P., Jr., Harris, A.D., Feigenson, M.D., *submitted*, Post-impact of the Chesapeake Bay impact structure: eustasy, passive-aggressive tectonism, and impactite compaction: *Geological Society of America Special Publication XX*, XX
- Lyell, C., 1845, Notes on the Cretaceous strata of New Jersey, and other parts of the United States bordering the Atlantic: *Quarterly Journal of the Geological Society of London*, v. 1, p. 55-60.
- Maguire, T.J., Sheridan, R.E., and Volkert, R.A., 2004, Geophysical modeling of the northern Appalachian Brompton-Cameron, Central Maine, and Avalon terranes under the New Jersey Coastal Plain: *Journal of Geodynamics*, v. 37, p. 457-485.
- Miller, K.G., Wright, J.D., and Fairbanks, R.G., 1991, Unlocking the ice house: Oligocene-Miocene oxygen isotopes, eustasy, and margin erosion: *Journal of Geophysical Research*, v. 96, p. 6829-6848.
- Miller, K.G., Browning, J.V., Pekar, S.F., and Sugarman, P.J., 1997, Cenozoic evolution of the New Jersey Coastal Plain: Changes in sea level, tectonics, and sediment supply, *in* Miller, K.G., and Snyder, S.W. eds., *Proceedings of the Ocean Drilling Program, Scientific results, Volume 150X: College Station, Texas, Ocean Drilling Program*, p. 361-373.
- Miller, K.G., Mountain, G.S., Browning, J.V., Kominz, M.A., Sugarman, P.J., Christie-Blick, N., Katz, M.E., and Wright, J.D., 1998, Cenozoic global sea-level, sequences, and the New Jersey transect: Results from coastal plain and slope drilling: *Reviews of Geophysics*, v. 36, p. 569-601.
- Miller, K.G., Sugarman, P.J., Browning, J.V., Kominz, M.A., Olsson, R.K., Feigenson, M.D., and Hernandez, J.C., 2004, Upper Cretaceous sequences and sea-level history, New Jersey Coastal Plain, *Geological Society of America Bulletin*, v. 116, p. 368-393.
- Miller, K.G., Kominz, M.A., Browning, J.V., Wright, J.D., Mountain, G.S., Katz, M.E., Sugarman, P.J., Cramer, B.S., Christie-Blick, N., and Pekar, S.F., 2005, The Phanerozoic record of global sea-level change: *Science*, v. 310, p. 1293-1298.
- Mitchum, R.M., Vail, P.R., and Thompson, S., 1977, The depositional sequence as a basic unit for stratigraphic analysis: *American Association of Petroleum Geologists Memoir*, v. 26, p. 53-62.

- Mueller, R.D., Sdrolias, M., Gaina, C., Steinberger, B., and Heine, C., 2008, Long-term sea-level fluctuations driven by ocean basin dynamics: *Science*, v. 319, p. 1357-1362.
- Olsson, R.K., 1980, The New Jersey Coastal Plain and its relationship with the Baltimore Canyon Trough, *in* Manspeizer, W., ed., *Field studies of New Jersey geology and guide to field trips: 52nd annual meeting of the New York State Geological Association*, Newark, N.J., p. 116-129.
- Olsson, R.K., Gibson, T.G., Hansen, H.J., and Owens, J.P., 1988, Geology of the northern Atlantic Coastal Plain: Long Island to Virginia, *in* Sheridan, R.E., and Grow, J.A., eds., *The Atlantic Coastal Margin, U.S.: Boulder, Colorado, Geological Society of America, Geology of North America*, v. 1-2, p. 87-105.
- Olsson, R.K., 1991, Cretaceous to Eocene sea-level fluctuations on the New Jersey margin: *Sedimentary Geology*, v. 70, p. 195-208.
- Owens, J.P., and Sohl, N.F., 1969, Shelf and deltaic paleoenvironments in the Cretaceous-Tertiary formations of the New Jersey Coastal Plain, *in* Subitsky, S., ed., *Geology of selected areas in New Jersey and eastern Pennsylvania and guidebook of excursions: Rutgers University Press, New Brunswick, N.J.*, p. 235-278.
- Owens, J.P., and Gohn, G.S., 1985, Depositional history of the Cretaceous series in the U.S. Atlantic Coastal Plain: Stratigraphy, paleoenvironments, and tectonic controls of sedimentation, *in* Poag, C.W., ed., *Geologic evolution of the United States Atlantic Margin: New York, Van Nostrand Reinhold*, p.25-86.
- Owens, J.P., Miller, K.G., and Sugarman, P.J., 1997, Lithostratigraphy and paleoenvironments of the Island Beach borehole, New Jersey Coastal Plain Drilling Project, *In* Miller K.G., and Snyder, S.W., eds. *Proceedings of the Ocean Drilling Program, Scientific Results*, v. 150X, p. 15-24.
- Pittman, W.C., III, and Golovchenko, X., 1983, The effect of sea-level change on the shelf edge and slope of passive margins: *Society of Economic Paleontologists and Mineralogists Special Publication*, v. 33, p. 41-58.
- Poag, C.W., 1979, Stratigraphy and depositional environments of the Baltimore Canyon Trough, *American Association of Petroleum Geologists Bulletin*, v. 63, p. 1452-1466.
- Poag, C.W., and Sevon, W.D., 1989, A record of Appalachian denudation in postrift Mesozoic and Cenozoic sedimentary deposits of the U.S. middle Atlantic continental margin: *Geomorphology*, v. 2, p. 119-157.

- Poag, C.W., Koeberl, C., and Reimhold, W.U., 2004, *The Chesapeake Bay Crater*, Springer, New York, 522p.
- Posamentier, H.W., and Vail, P.R., 1988, Eustatic controls on clastic deposition II--sequence and systems tract models: Society of Economic Paleontologists and Mineralogists Special Publication, v. 42, p. 125-154.
- Posamentier, H.W., Jervey, M.T., and Vail, P.R., 1988, Eustatic controls on clastic deposition I -- Conceptual framework: Society of Economic Paleontologists and Mineralogists Special Publication, v. 42, p. 109-124.
- Powars, D.S., and Bruce, T.S., 1999, The effects of the Chesapeake Bay impact crater on the geologic frame-work and the correlation of hydrogeologic units of southeastern Virginia, south of the James River: U.S. Geological Survey Professional Paper 1612, 82 p.
- Pusz, A., Miller, K.G., Wright, J.D., and Kent, D.V., submitted March 2008, Global carbon cycle perturbation associated with late Eocene impacts: Geological Society of America Special Publication.
- Reynolds, D.J., Steckler, M.S., and Coakley, B.J., 1991, The role of sediment load in sequence stratigraphy; the influence of flexural isostasy and compaction, *in* Cloetingh, S., ed., Special Section on Long-Term Sea-Level Change: Journal of Geophysical Research, v. 96, p. 6931-6949.
- Sanford, S., 1913, The underground water resources of the Coastal Plain Province of Virginia: Virginia Geological Survey Bulletin 5, 361 p., 1 pl.
- Sanford, W.E., Gohn, G.S., Powars, D.S., Horton, J.W., Jr., Edwards, L.E., Self-Trail, J.M., and Morin, R.H., 2004, Drilling the central crater of the Chesapeake Bay impact structure: A first look: Eos Transactions, v. 85, p. 369, 377.
- Schlische, R.W., 1992, Structural and stratigraphic development of the Newark extensional basin, eastern North America: Evidence for the growth of basin and its bounding structures: Geological Society of America Bulletin, v. 104, p. 1246-1263.
- Seeber, L., and Armbruster, J.G., 1988, Seismicity along the Atlantic seaboard of the U.S.: Intraplate neotectonics and earthquakes, *in* Sheridan, R., and Grow, J., eds., The Atlantic continental margin, U.S.: Geological Society of America, Decade of North American Geology, v. I-2, p.437-444.
- Spasojević, S., Liu, L., Gurnis, M., and Muller, R.D., 2008, The case for dynamic subsidence of the U.S. east coast since the Eocene: Geophysical Research Letters, v. 35, L0835, doi: 10.1029/2008GL033511.

- Sugarman, P.J., Miller, K.G., Bukry, D., and Feigenson, M.D., 1995, Uppermost Campanian-Maestrichtian strontium isotopic, biostratigraphic, and sequence stratigraphic framework of the New Jersey Coastal Plain: *Geological Society of America Bulletin*, v. 107, p.19-37.
- Sugarman, P.J., and Miller, K.G., 1997, Correlation of Miocene sequences and hydrogeologic units, New Jersey Coastal Plain, *Sedimentary Geology*, v. 108, p. 3-18.
- Sugarman, P.J., Miller, K.G., Browning, J.V., Kulpecz., A.A., McLaughlin, P.P., Jr., Monteverde, D.H., 2005, Hydrostratigraphy of the New Jersey Coastal Plain: Sequences and facies predict the continuity of aquifers and confining units: *Stratigraphy*, v. 2, p. 259-275.
- Vail, P.R., and Mitchum, R.M., Jr., 1977, Seismic stratigraphy and global changes of sea level, Part 1: Overview, in Payton, C.E., editor, *Seismic stratigraphy- applications to hydrocarbon exploration*, American Association of Petroleum Geologists, Memoir 26 p.51-52
- Vail, P.R., Mitchum, R.M., Jr., Todd, R.G., Widimier, J.M., Thompson, S., III, Sangree, J.B., Bubbs, J.N., and Hatlelid, W.G., 1977, Seismic stratigraphy and global changes of sea level: *American Association of Petroleum Geologists Memoir*, v. 26, p. 49-212.
- Van Wagoner, J.C., Mitchum, R.M., Campion, K.M., and Rahmanian, V.D., 1990, Siliciclastic sequence stratigraphy in well logs, cores, and outcrops: concepts for high-resolution correlation of time and facies: *AAPG Methods in Exploration Series* 7, 55 p.
- Van Wagoner, J.C., 1995, Sequence stratigraphy and marine to nonmarine facies architecture of foreland basin strata, Book Cliffs, Utah, U.S.A., *in* Van Wagoner, J.C., and Bertram, G.T., eds., *Sequence Stratigraphy of Foreland Basin Deposits: AAPG Memoir* 64, p. 137-224.
- Watts, A.B., and Steckler, M.S., 1979, Subsidence and eustasy at the continental margin of eastern North America, American Geophysical Union, Maurice Ewing Symposium Series 3, p. 218-234.
- Watts, A.B., 1981, The U.S. Atlantic continental margin: Subsidence history, crustal structure, and thermal evolution: *in* Bally, A.B., ed., *Geology of passive continental margins: History, structure, and sedimentologic record (with special emphasis on the Atlantic margin)*, American Association of Petroleum Geologists Education Course Notes Series, No. 19, p. 2-i-2-75.
- Watts, A.B., 1982, Tectonic subsidence, flexure, and global changes of sea level: *Nature*, v. 297, p. 469-474.

- Weems, R.E., and Lewis, W.C., 2002, Structural and tectonic setting of the Charleston, South Carolina region: Evidence from the Tertiary stratigraphic record: Geological Society of America Bulletin, v. 114, p. 24-42.
- Weller, S., and Knapp, G.N., 1907, A report on the Upper Cretaceous paleontology of New Jersey, based upon the stratigraphic studies of George N. Knapp: New Jersey Geological Survey, Paleontology series 4, 1106p.
- Westaway, R., 2007, Late Cenozoic uplift of the eastern United States revealed by fluvial sequences of the Susquehanna and Ohio river systems: coupling between surface processes and lower crustal flow: Quaternary Science Reviews, v. 26, p. 2823-2843.
- Withjack, M.O., Schlische, R.W., and Olsen, P.E., 1998, Diachronous rifting, drifting, and inversion on the passive margin of central eastern North America: an analog for other passive margins: American Association of Petroleum Geologists Bulletin, v. 82, p. 817-835.

Figure Captions

Figure 1. Location map showing the mid-Atlantic margin extending from northern New Jersey to North Carolina. The landward edge of the Baltimore Canyon trough is modified from Olsson (1980) and is marked by the dashed red line. The outline of the Chesapeake Bay Impact Structure is modified from Powars and Bruce (1999). The basement structure contour is modified from Owens and Gohn (1985). Coreholes used in this study are marked by red dot: A- Ancora, NJ; AC- Atlantic City, NJ; B- Bayside, VA; BB- Bethany Beach, DE; BR- Bass River, NJ; CM- Cape May, NJ; CZ- Cape May Zoo, NJ; D- Dismal Swamp, VA; E- Eyreville, VA; F- Fentress, VA; IB- Island Beach, NJ; JB- Jenkins Bridge, VA; K- Kiptopeke, VA; L- Langley, VA; M- MW4-1, VA; MV- Millville, NJ; OC- Ocean City, NJ; SG- Sea Girt, NJ; and X- Exmore, VA. Black dots indicate some of the geophysical logs used in this study.

Figure 2. Regional correlation section showing the distribution of stratigraphic units modified from Olsson et al. (1988). Data based on biostratigraphy and lithology from a series of deep coreholes spanning the mid-Atlantic Coastal Plain (noted at top of chart). Note the presence of the South Jersey high, Salisbury embayment, and Norfolk arch and their respective roles on regional sedimentation.

Figure 3. Anatomy of a typical “coarsening-upwards” sequence found on the U.S. mid-Atlantic Coastal Plain (modified from Miller et al., 2004; Browning et al., 2006; Kulpecz et al., 2008). Upper Cretaceous units from the New Jersey Coastal Plain tend to exhibit a stronger deltaic influence, while Cenozoic sequences typically exhibit shelf-to-shoreface shallowing upwards successions. The typical gamma ray and resistivity log signatures are included.

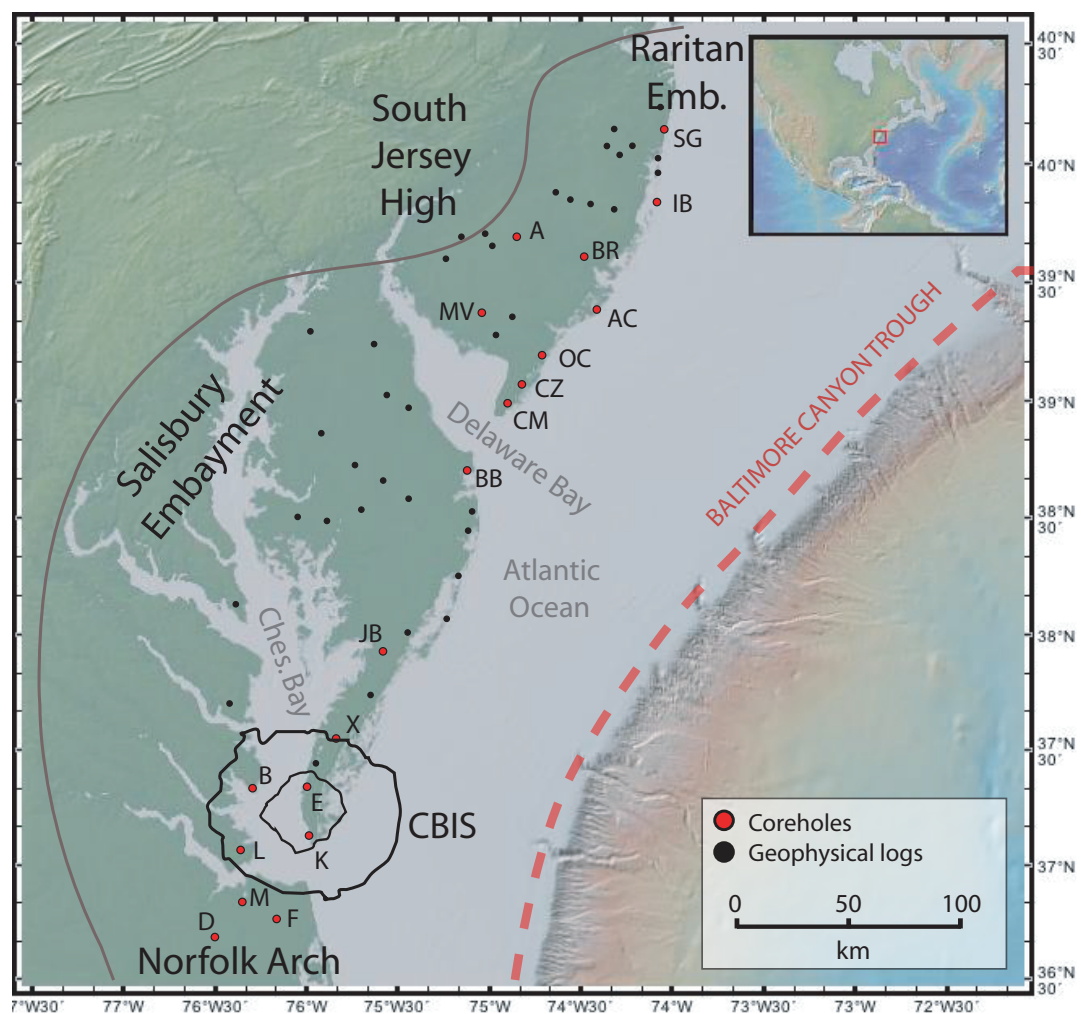


Figure 1

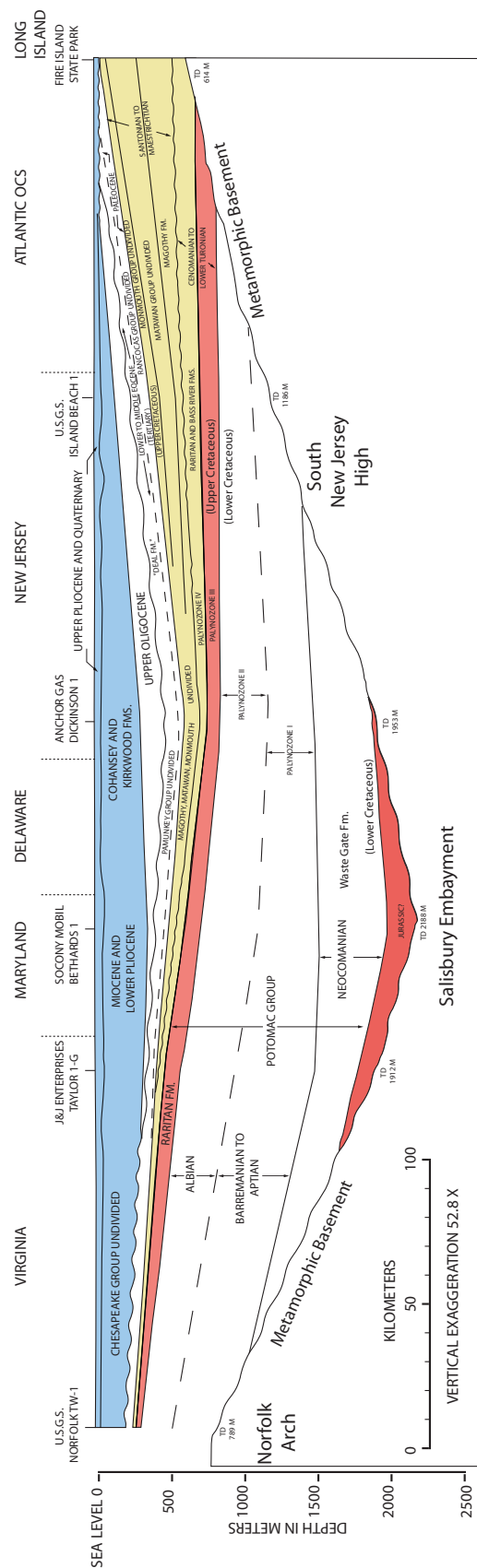


Figure 2

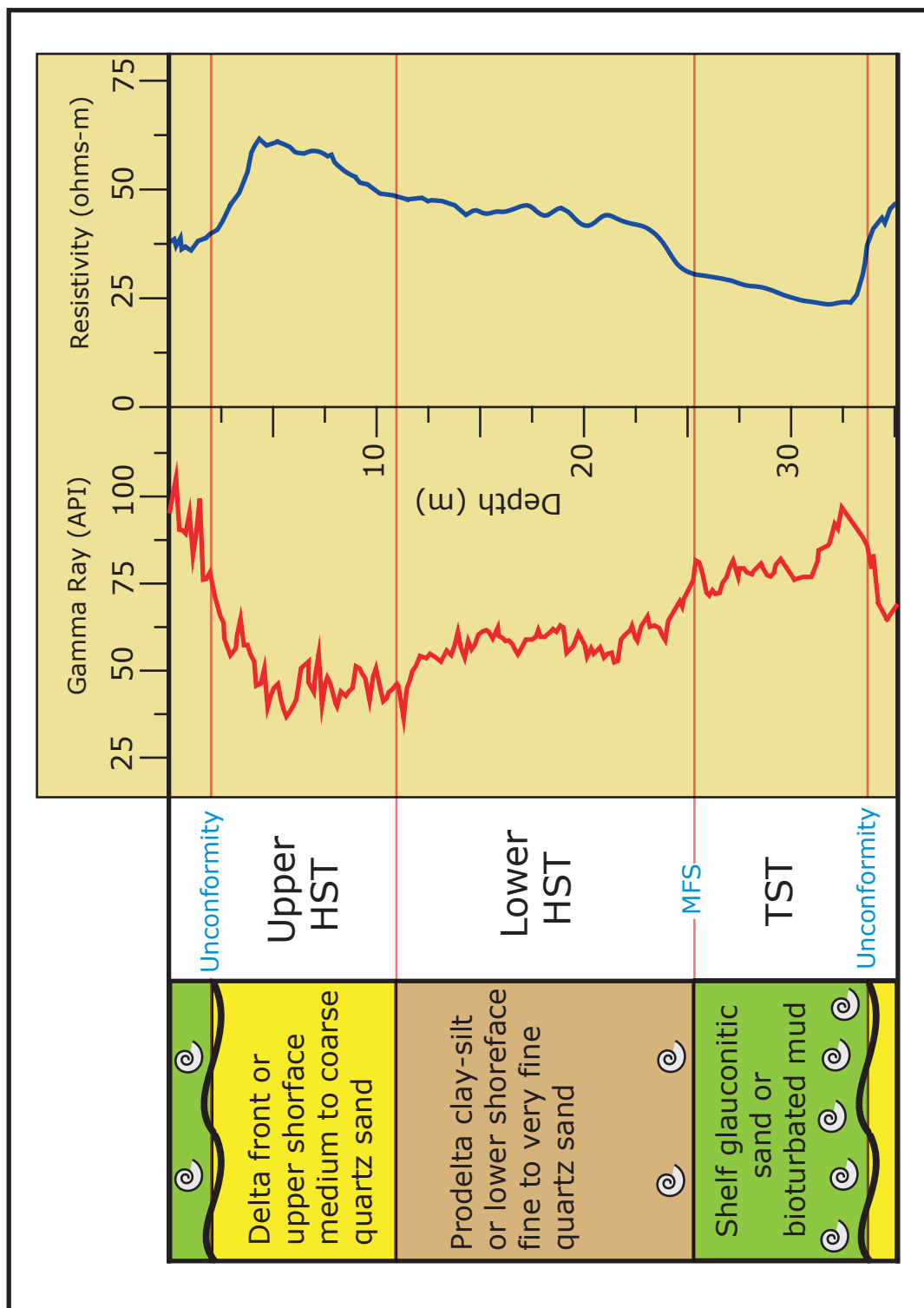


Figure 3

Chapter 1: Response of Late Cretaceous Migrating Deltaic Facies Systems to Sea Level, Tectonics, and Sediment Supply Changes, New Jersey Coastal Plain, U.S.A.

This chapter was published as Kulpecz, A.A., Miller, K.G., Sugarman, P.J., and Browning, J.V., 2008, Response of Late Cretaceous Migrating Deltaic Facies Systems to Sea Level, Tectonics, and Sediment Supply Changes, New Jersey Coastal Plain, U.S.A.: *Journal of Sedimentary Research*, v.78, p.112-129.

Abstract: Paleogeographic, isopach, and deltaic lithofacies mapping of thirteen depositional sequences established a 35 myr high resolution (> 1 Myr) record of Late Cretaceous wave- and tide- influenced deltaic sedimentation. We integrate sequences defined on the basis of lithologic, biostratigraphic, and Sr-isotope stratigraphy from core with geophysical log data from 28 wells to further develop and extend methods and calibrations of well-log recognition of sequences and facies variations. This study reveals the northeastward migration of depocenters from the Cenomanian (ca. 98 Ma) through the earliest Danian (ca. 64 Ma) and documents five primary phases of paleodeltaic evolution in response to long-term eustatic changes, variations in sediment supply, the location of two long-lived fluvial axes, and thermoflexural basement subsidence: (1) Cenomanian-early Turonian deltaic facies exhibit marine and nonmarine facies and are concentrated in the central coastal plain; (2) high sediment rates, low sea level, and high accommodation rates in the northern coastal plain resulted in thick, marginal to nonmarine mixed-influenced deltaic facies during the Turonian-Coniacian; (3) comparatively low sediment rates and high long-term sea level in the Santonian resulted

in a sediment-starved margin with low deltaic influence; (4) well-developed Campanian deltaic sequences expand to the north and exhibit wave reworking and longshore transport of sands; and (5) low sedimentation rates and high long-term sea level during the Maastrichtian resulted in the deposition a sediment-starved glauconitic shelf. Our study illustrates the widely known variability of mixed-influence deltaic systems, but also documents the relative stability of deltaic facies systems on the 10^6 - 10^7 yr scale, with long periods of cyclically repeating systems tracts controlled by eustasy. Results from the Late Cretaceous further show that although eustasy provides the template for sequences globally, regional tectonics (rates of subsidence and accommodation), changes in sediment supply, proximity to sediment input, and flexural subsidence from depocenter loading determines the regional to local preservation and facies expression of sequences.

Introduction

Sequence stratigraphy, the use of unconformity-bounded units and their constituent facies to correlate sedimentary sequences on regional scales (Mitchum et al., 1977), has been a powerful tool in predicting the distribution of important economic resources such as hydrocarbon reservoirs (Vail et al., 1977) and groundwater aquifers (Sugarman and Miller 1997; Sugarman et al., 2006). The application of sequence stratigraphic principles revolutionized our understanding of the New Jersey Coastal Plain (e.g., Olsson, 1991) and established the Mid-Atlantic Margin as a natural laboratory for examining the fundamental mechanisms that control deposition on passive margins (Miller et al., 1998a; Miller et al., 2005). Processes that control deposition on this, and other margins, include

eustasy (Miller et al., 2005), changes in the prevailing tectonic regime (subsidence versus uplift) (e.g., Browning et al., 2006), and variations in sediment supply (Pitman and Golovchenko, 1983; Poag and Sevon, 1989; Reynolds et al., 1991).

The sequence stratigraphic method has also proven useful in examining the evolution of deltaic systems. Sequence boundaries and flooding surfaces (e.g., Galloway, 1989) represent temporally significant surfaces that can be used to establish the paleogeographic history of a deltaic margin or chart the distribution of facies through time and space. These studies of deltaic systems range in scope from the robust data sets of the Gulf of Mexico (Galloway, 1989; Galloway et al., 2000; Combellas-Bigott, and Galloway, 2006) and Western Canada (Plint, 2003), to high-resolution outcrop studies of the Cretaceous Western Interior Seaway that evaluate the higher-order response of deltaic sequences, parasequences, and facies to forcing mechanisms (e.g., Bhattacharya and Walker, 1991; Lee et al., 2007; Gani and Bhattacharya, 2007; Davies et al., 2006). Although these studies have contributed greatly to our understanding of ancient deltaic systems, many face complications such as complex tectonic histories and difficulty establishing geochronologic control due to shallow and nonmarine facies. Because each margin offers a unique blend of eustatic, tectonic, and sediment supply controls, differentiating the sedimentary response to each can be very difficult.

While the New Jersey Coastal Plain does not afford the broad regional picture of the Gulf of Mexico, or the detail of outcrop-scale facies analyses, it offers a long-term (~ 35 Myr) record of eustatically forced Late Cretaceous deltaic sequences with high temporal

resolution (> 1 Myr) from the work of the Ocean Drilling Program Leg 174AX (Miller et al., 1998b; Miller et al., 1999; Miller et al., 2003; Sugarman et al., 2006: summarized in Miller et al., 2004 and this study). Because deposition occurred on a passive margin dominated by consistent thermoflexural subsidence (Kominz et al., 1998; Miller et al., 2004), this study avoids many of the difficulties associated with tectonically active settings.

The main objectives of this study are to: (1) reconstruct the Late Cretaceous paleogeographic evolution of this deltaic margin; (2) examine the response of deltaic facies, highstand sands, and eustatically forced depositional sequences to post-rift thermoflexural subsidence and higher-frequency autogenic fluvial axis switching and sediment supply variations; and (3) evaluate the relative influences of wave, tidal, and fluvial processes on deltaic sedimentation during the Late Cretaceous.

Geologic Background

Upper Cretaceous sequences of the New Jersey Coastal Plain (Fig. 1) typically represent transgressive-regressive coarsening-upward successions from marine shelf to shallow marine, fluvio-deltaic, and nonmarine environments (Owens and Gohn, 1985; Sugarman et al., 1995). Late Cretaceous (e.g., Olsson, 1991; Miller et al., 2004) and Cenozoic (e.g., Miller et al., 1991; Miller et al., 1998a) strata record numerous unconformities (interpreted as sequence boundaries) caused by eustatic falls since the initial deposition of marine units during the Cenomanian (ca. 100 Ma) (Fig. 2) (Olsson et al., 1988; Miller et

al., 2004). Coastal-plain sediments were deposited atop a series of basement structures: (1) the Salisbury Embayment, a large basin centered near Salisbury, MD; (2) the Raritan Embayment, located at the modern confluence of the Raritan and Hudson Rivers in Raritan Bay; and (3) the South Jersey High, a minor arch that divides the two embayments (Fig. 1) (Owens and Gohn, 1985). The coastal plain was eroded during the global sea-level lowstands of the Plio-Pleistocene (Stanford et al., 2001), resulting in the exposure of Upper Cretaceous and Cenozoic strata.

The recognition of sequences as fundamental building blocks of the stratigraphic record greatly improved the understanding of New Jersey Coastal Plain stratigraphy and its controlling mechanisms. Owens and Sohl (1969) and Owens and Gohn (1985) identified transgressive-regressive coarsening-upwards cycles on the basis of recurrent glauconitic beds, physical unconformities, and biostratigraphic hiatuses and tied their cyclicity to regional tectonic processes. Olsson et al. (1988; Olsson, 1991) identified and dated eight Upper Cretaceous New Jersey sequences and linked their origin to multiple Late Cretaceous marine transgressions (Albian through Maastrichtian), consistent with the eustatic control of Haq et al. (1987). Sugarman et al. (1995) integrated Sr-isotope stratigraphy with a biostratigraphic and lithostratigraphic framework to improve stratigraphic control ($< \sim 1$ my) of coastal plain sequences.

The New Jersey Coastal Plain Drilling Project drilled eleven onshore coreholes as part of the Ocean Drilling Program (ODP) New Jersey Sea Level/Mid-Atlantic Transect (NJ-MAT). ODP Legs 150 and 150X targeted Cenozoic sequences onshore at three sites and

on the continental slope and established a link between Oligocene-middle Miocene sequence boundaries and glacioeustatic fall (Miller et al., 1996; Miller et al., 1991; Miller et al., 1998a). ODP Leg 174AX continued onshore drilling at eight sites, four of which targeted Upper Cretaceous strata (Bass River, Ancora, Millville, and Sea Girt) (Fig. 1). Results from these four coreholes identified and dated at least 11 (and as many as 18) sequences (Fig. 2) (Miller et al., 2003; Miller et al., 2004). Sequence boundaries in core are identified by: (1) a sharp unconformable contact; (2) lag gravels; (3) rip-up clasts; (4) extensive burrowing and bioturbation; (5) overstepping of facies successions; and (6) biostratigraphic and geochronologic hiatuses determined from benthic foraminiferal assemblages and Sr-isotope data (Miller et al., 2004; Sugarman et al., 1995). Although each sequence boundary is unique, together these methods can be used to indicate significant periods of nondeposition and erosion (Olsson et al., 1988; Sugarman et al., 1995). Water-depth variations within the sequences were established from lithofacies and biofacies analyses.

The studies by Miller et al. (2005) established the New Jersey margin as an excellent location for extracting estimates of global sea level for the Late Cretaceous and Cenozoic due to the well-preserved record of marine sediments and simple thermoflexural subsidence. One-dimensional backstripping (an inverse modeling technique that accounts for compaction, loading, subsidence, and paleodepth to determine accommodation rates and eustasy) indicates that large (> 20 m), rapid (< 1 Myr), and possibly glacioeustatic sea-level changes occurred during the Late Cretaceous (Miller et

al., 2003; Miller et al., 2004; Miller et al., 2005; Van Sickle et al., 2004; Sugarman et al., 2005).

Although Miller et al. (2004) identified 11-16 late Cretaceous New Jersey sequences and genetically linked them to eustasy, the understanding of subsurface sequence distribution is inherently limited due to the small number (four) of onshore coreholes that penetrate Upper Cretaceous strata and the large distances (~ 65 km) that separate coreholes.

Without a detailed understanding of sequence expression across the coastal plain, the respective influences of global sea-level change, tectonic subsidence, and sediment supply remain clouded. In this study, geophysical logs bridge the gaps between coreholes, lending a sub-regional perspective to the distribution of coastal plain sequences, the paleogeography of deltaic facies systems, and a chronology of depocenter migration.

Methodology

Cores and Correlation of Geophysical Logs

This study uses gamma and electric logs from ODP Leg 174AX (Miller et al., 1998a; Miller et al., 1999; Miller et al., 2006; Sugarman et al., 2005) to establish a characteristic geophysical log signature for the sequences and lithofacies identified by Miller et al. (2004) and Lanci et al. (2002). This signature was used to identify sequences from logs lacking core control, allowing high-resolution (better than meter scale) mapping across

the coastal plain, identification of sedimentary facies, and generation of a paleogeographic framework.

Sequence depocenters are identified by the thickest preserved intervals of a given sequence on the coastal plain. Although erosion occurs during base-level lowerings (forming the unconformities critical to this study), geographic variations in erosion do not appear to control the observed differences in thickness. This is established from: (1) similar age estimates of the sediments immediately above and below unconformities observed in core; (2) comparable thickness ratios of systems tracts within sequences; and (3) the preservation of well-developed upper highstand systems tracts (uHST) in most sequences, indicating that erosion was not severe enough to remove entire systems tracts.

Geophysical logs have been used to interpret paleoenvironments and correlate depositional facies since Serra and Sulpice (1975) used spontaneous potential (SP) and resistivity logs to unravel the depositional history of strata in the Gulf of Mexico. Gamma logs, a measure of naturally occurring radiation in sediment, have become a useful tool for log-based facies interpretation, particularly in siliciclastic fluvio-deltaic environments with good lithologic control from core, cuttings, or chip samples. Because fine-grained sediments, clays, glauconite sands, and phosphorites retain high levels of radiogenic elements, gamma logs are considered a good indicator of lithology (Rider, 2002).

Within a transgressive-regressive sequence, gamma logs typically exhibit: (1) a sharp positive deflection moving upward across a basal unconformity; (2) high values (e.g., ~

100-150 API units) in middle-neritic glauconite shelf sands and clays representing the transgressive systems tract (TST) of Posamentier and Vail (1988); (3) intermediate values (e.g., ~ 50-100 API units) in prodelta silty clays representing the lower highstand systems tract (LHST); (4) relatively low values (e.g., ~ 10-40 API units) in medium to coarse sands of the upper highstand systems tract (uHST); and (5) a rapid deflection to high values representing a sequence boundary and return to fine-grained glauconitic units (Fig. 3) (e.g., Lanci et al., 2002). Because the coarse upper-delta-plain or nearshore sands are also the primary groundwater aquifers of the coastal plain, resistivity logs (the measure of pore fluid resistance to an electrical current) generally exhibit high values (e.g., ~ 50-150 ohms-m) in coarser-grained intervals and significantly lower values (e.g., ~ 10-50 ohms-m) in finer-grained “confining” intervals (e.g., transgressive clays) (Fig. 3) (Keys and MacCary, 1971). This is attributed to the high resistance of fresh water to the application of an electrical current, and the status of clays as a strong conductor coupled with lower porosity (and thus pore-water content) than sands. Although most sequences reflect the above patterns, varying sedimentation rates and levels of lowstand erosion can alter the expression of a sequence across the coastal plain (e.g., thin or absent highstand sands). Care must be taken to avoid oversimplified and incorrect interpretations (Rider, 1990).

Gamma and electric logs have characteristic geometries that are useful for facies interpretation (Rider, 2002). Gradual negative deflections capped by a sharp return to high gamma values, also referred to as “funnel” geometry, characterize a variety of sedimentary facies. These can consist of regressive shelf to delta front, prograding estuary, crevasse splay, and shoreface facies (Fig.4) (Finley and Tyler, 1986; Rider,

2002). Conversely, a sharp negative shift overlain by a gradual positive deflection (a “bell” shape) can represent transgressive shelf, fining-upward fluvial channel (e.g., point bar), distributary channel, and wave-dominated delta front facies (Fig. 4) (Finley and Tyler, 1986; Rider, 2002). Trough-shaped low gamma values sharply bracketed by high gamma values can represent deltaic distributary and channel facies (Fig. 4) (Rider, 2002). A “serrated” gamma signature can characterize swamp, marsh, lake, and levee facies (Finley and Tyler, 1986; Rider, 2002). Upper-delta-plain environments exhibit a variety of the log patterns discussed above, including floodplain paleosols that show high-amplitude, sharp, positive spikes in the middle of coarser-grained intervals (e.g., channel facies) (Fig. 4). By themselves, gamma and electric logs interpretations are thus non-unique. In this study, we calibrate downhole logs and continuous cores (including lithologic and paleontologic control) to provide accurate paleoenvironmental interpretations that can be extended beyond core control to wells across the coastal plain.

Mapping

Detailed subsurface maps and cross sections of 13 Late Cretaceous sequences were generated using the sequence stratigraphic model of Miller et al. (1998a, 2004). In addition, 11 paleogeographic maps and accompanying sand thickness maps were created for sequences that exhibit shallow to non-marine facies. Twenty-eight geophysical logs obtained from the New Jersey Geological Survey and industry sources were used to compliment the existing four ODP Leg 174AX coreholes at Bass River, Ancora, Millville, and Sea Girt (Fig. 1). Wells were selected for inclusion into the database on the

basis of geographic location (e.g., satisfying areas of poor coverage), depth (substantial penetration through Upper Cretaceous section), and adequate quality.

Selected wells were required to include a gamma log, although it was preferred that they also include additional electric (primarily resistivity) logs. The combination of gamma and resistivity logs can offset the difficulty of correlating subtle lithologic changes in very fine-grained or glauconitic intervals (Fig. 5). If a sandy unit is not recorded on the gamma ray log, high resistivity readings might indicate its presence and prevent incorrect interpretation and correlation. Spontaneous potential and sonic logs provided an additional data source when gamma log correlation was unclear. Although this study relied heavily on geophysical log data as a method for correlation, physical and biostratigraphic data from ODP cores were used to constrain log signatures and account for sub-regional facies changes.

Downhole logs allow mapping of sandbodies within sequences. Sand isopach maps (depicted by 10 m contours on the paleogeographic maps) measured the total HST sand thickness per sequence. “Sands” were defined as intervals with gamma measurements lower than 75 API, although inconsistencies in older logs (acquired prior to the standardization of gamma tools) necessitated calibration to known measurements from the nearest corehole. In heterogeneous lithologies (e.g., lagoon, crevasse splay, delta plain), fine-grained intervals were subtracted from the total unit thickness to yield net sand thickness.

Low sedimentation rates, deep-water marine facies (less sensitive to base-level variations), unfossiliferous zones, and poor core recovery can complicate the identification and correlation of sequences. For this reason, coupled with the inherent limitations of resolution in detailed well log correlation, this analysis of Upper Cretaceous sequence distribution focused on mapping the most significant and pronounced sequences of the New Jersey Coastal Plain. As a result, the subdivisions of the Merchantville (I, II, III) and Navesink (I, II) sequences proposed by Miller et al. (2004) have been omitted because of their thin (< 10 ft, 3 m) expression in outer-shelf facies (e.g., contained entirely within intervals rich in glauconite and clay).

Data and Results

Early Cenomanian-Early Turonian Sequences

The identification of characteristic geophysical log signatures for sequences and facies in New Jersey is unique to this study and enabled the mapping of sequences first identified by Miller et al. (2004) across the coastal plain. To emphasize the critical link between sequence components, lithofacies, and log character, previously published sequence descriptions are referenced for each sequence. Three sequences (Bass River I, II, III) were identified in the Bass River Formation (Sugarman et al., 2005). The Bass River I sequence is dated as early to mid-Cenomanian (Pollen Zone IV) and unconformably overlies the fluvial and terrestrial mottled clays and paleosols of the Barremian-lowermost Cenomanian Potomac Formation. The Bass River II sequence is mid-

Cenomanian whereas Bass River III, the uppermost and thickest of the sequences, is upper Cenomanian-lower Turonian (Fig. 2) (Miller et al., 2004). Bass River sequences generally “shallow” upwards from: (1) neritic glauconite sand and clay (TST); (2) prodelta clay and silt (IHST); and (3) delta front to shoreface quartz sands (uHST) (Miller et al., 1998b; Miller et al., 1999; Miller et al., 2006; Sugarman et al., 2005).

Each sequence is characterized by a coarsening upwards “funnel” gamma log signature, although local variations can result in a “serrated” or “box” character (Fig. 5). The lack of thick upper HST clean coarse quartz sands often results in relatively high gamma values, highlighting the importance of resistivity logs and their peak values in these thin, sandy water-bearing intervals to identify highstand deposits.

Isopach maps of the Bass River sequences reveal pervasive, downdip (seaward) thickening toward the central and southern coastal plain (Fig. 6). Bass River I is 10-15 m thick across most of the coastal plain, although: (1) several coastal sections exceed 15 m; (2) a comparatively thick “finger” (>15 m) extends updip from the coast towards central New Jersey; and (3) the thickest interval (~ 21 m) is located in the southern coastal plain (Fig. 6). Highstand delta front sands are thickest in the central coastal plain (10.9 m), but grade to shoreface sands ~ 1-2 m thick to the south (Fig. 4). The Bass River II sequence is thick across the coastal plain (~ 24 m) but thins to the west at Ancora (~ 8-10 m) and to the south at Millville (9.7 m). Thick values (24-27 m) in the central coastal plain could represent a localized depocenter during the mid-Cenomanian (Fig. 6). Highstand sands range from 10 to 11.5 m across the central and northern coastal plain and vary from delta-

front to fluvial in origin. Thin (1-3.5 m) delta-plain sands dominate the southern coastal plain. The Bass River III is the thickest (and most variable) Cenomanian sequence inasmuch as it: (1) thickens to 77.7 m at Island Beach; (2) thins to the west (6-8 m); and (3) thins to the south at Millville (14.1 m). Highstand sands thicken to 10 m at Bass River, but are otherwise thin (1-5 m) and fine-grained across much of the coastal plain.

Mid-Turonian-Coniacian Sequences

Five Turonian-Coniacian sequences (Magothy I, II, III, IVA, and IVB) were identified in the coarse-grained Magothy Formation, one of New Jersey's primary aquifers and the upper unit of the PRM aquifer system (Fig. 2) (Zapeczka, 1989). Correlation using pollen zonation after Christopher (1982) reveals a discontinuous and patchy distribution for Magothy sequences. The lowermost Magothy I is dated as pollen Zone IV (mid-Turonian) at Bass River, Millville, and Sea Girt (Miller et al. 1999; Miller et al. 2006; Sugarman et al., 2005). The Magothy II, the oldest sequence recovered at Ancora, is assigned to pollen Zone V (late Turonian), indicating that the Magothy I was cut out (Miller et al., 1999). The Magothy III sequence is assigned to pollen zone V and was recovered at all four coreholes (Miller et al., 1998; Miller et al., 1999; Miller et al., 2006; Sugarman et al., 2005). Two Coniacian (Pollen Zone VII) Magothy sequences (IVA and IVB) were penetrated only at the Sea Girt corehole and are restricted to the northern coastal plain (Miller et al., 2006).

The Sea Girt corehole provided an expanded Turonian-Coniacian section that allows the first core and log samples of the IVA and B sequences near local outcrops of the Magothy Formation (Miller et al., 2006). Sugarman et al. (2006) informally linked the recovered sequences (pending further analyses) to outcrop-defined members of the Magothy Formation (Fig. 7) on the basis of lithology: the (1) Sayreville Sand Member (Magothy I); (2) South Amboy Fire Clay and Old Bridge Sand Members (Magothy II); (3) Amboy Stoneware Clay Member (Magothy III); (4) the Morgan Beds Member (Magothy IV A); and (5) the Cliffwood Beds Member (Magothy IVB).

Although Magothy sequences consist of a diverse system of deltaic facies (Fig. 7), they maintain fairly consistent well-log signatures across the coastal plain (Fig. 5). The delta-front and fluvial sands of the Magothy I and III (Miller et al., 1998b; Miller et al., 1999) are easily distinguishable by significant gamma-ray troughs (and high resistivity values) separated by the high gamma peaks of the Magothy II clays and paleosols (Fig. 5). In the northern coastal plain, the delta-front sands of Magothy IVA form four distinct gamma spikes that resemble a “serrated” log pattern (Fig. 7). The overlying delta-front and bay to lagoon sands of the Magothy IVB sequence exhibit a similar low amplitude “choppy” gamma interval capped by a sharp deflection to high values of the overlying Cheesequake Formation. The Magothy IV sequences maintain these signatures until they gradually pinch out in the central coastal plain (Fig. 4).

Thickness trends of Magothy sequences fall into two distinct groups: (1) the lower (Magothy I, II, III) sequences that are present throughout the coastal plain (Fig. 8); and

(2) the upper (IVA, IVB) sequences that are limited to the north (Fig. 8). The Magothy I sequence is widespread but discontinuous, grading from thick intervals in the central coastal plain (18.6 m) to the point of no recovery at Ancora. Northern sections show a patchy distribution from 7.6 to 15.2 m and the sequence thins to 3.4 m in the south (Fig. 8). Thick highstand sands are concentrated in the central (12-18 m) and northern (14.6 m) coastal plain and range from delta front to crevasse splay (Fig. 4). Sands become significantly thinner (> 1 m) towards Millville. The Magothy II sequence reveals two primary depocenters: (1) a thick section in the northeast reaches 18.3-21.3 m; and (2) a thick western interval measures +26 m at Ancora (Fig. 8). Thick highstand fluvial sands (16-25 m) at Ancora are consistent with these observations. The Magothy III sequence thickens eastward from thin (Ancora: 7.9 m) or absent to thick intervals at Sea Girt (19.7 m) and Dorothy (17.2 m). Intermediate sections (9.1-13.7 m) characterize much of the central coastal plain. The thickest highstand sands (9-14.6 m) are found around Ancora and throughout the central coastal plain.

The upper Magothy (IVA, B) sequences are restricted to the northern coastal plain and were only recovered at the Sea Girt corehole, though logs allow correlation in the north (Fig. 8). The Magothy IVA thickens to 17.5 m in the northeast and thins consistently to the south before pinching out in the central coastal plain (Fig. 8). The Magothy IVB thickens to twin northern “bulls-eye” depocenters at Sea Girt (17.8 m) and Freehold (16.2 m) and is similarly absent from the southern coastal plain (Fig. 8). Patterns of highstand sand thickness are consistent with overall sequence thickness trends for the Magothy IVA

and IVB and represent an array of fluvial channel, delta-front, and lagoonal sands (Fig. 4).

Santonian Sequence

A comparatively thin (8-26 ft, 2.4-7.9 m) lower to middle Santonian Cheesequake sequence is identified in cores (Miller et al., 1998b; Miller et al., 1999) and correlated to the glauconitic clayey silt of the Cheesequake Formation of outcrop (Fig. 2) (Owens et al., 1998). The Cheesequake Formation and sequence is dominated by inner-shelf to middle-shelf facies and bracketed by distinct unconformities with the Magothy and Merchantville Formations (Miller et al., 2004).

The Cheesequake sequence is correlated across the coastal plain on the basis of its geophysical log signature and position between the glauconitic clays of the Merchantville Formation (high gamma values) and the coarse quartz sands of the Magothy Formation (low gamma, high resistivity). Dual gamma spikes often mark the gradation from basal glauconitic clays and sands (TST) to fine quartz sands (HST), although a series of smaller peaks within the sequence represent the interplay of clayey glauconite beds and coarser lithology (Fig. 5).

The Cheesequake sequence exhibits gentle, downdip thickening from 3-4.2 m to its maximum thickness of 7.9 m at Bass River. The sequence thins to the south (2.4-3.4 m), possibly representing the influence of the South Jersey High. No significant onshore

depocenters or significant quantities of shallow marine highstand sands are apparent during the Santonian, a reflection of deposition on a sediment-starved shelf with weak northern and southern sources. For this reason, paleogeographic and deltaic facies maps were not created for the Cheesequake sequence.

Uppermost Santonian-Campanian Sequences

Three predominantly Campanian sequences were identified from core: (1) the uppermost Santonian to mid-Campanian Merchantville sequence; (2) the mid-Campanian upper Englishtown sequence; and (3) the upper Campanian Marshalltown sequence (Fig. 2) (Miller et al., 2004). Unlike Bass River and Magothy sequences, some Campanian sequences encompass multiple Upper Cretaceous lithostratigraphic units. The Merchantville sequence consists of the Merchantville, Woodbury, and lower Englishtown Formations (Miller et al., 2004). The upper Englishtown sequence corresponds to its lithologic namesake (Owens et al., 1998), and the Marshalltown sequence consists of the Marshalltown, Wenonah, and Mount Laurel Formations (Fig. 2) (Miller et al., 2004).

The Merchantville sequence exhibits classic funnel geometry on the gamma log (Fig. 5) and a “coarsening upwards” gradational succession of glauconite clay and sand, micaceous clay, and fine quartz sand (Miller et al., 1998b; Miller et al., 1999). The HST of the sequence (lower Englishtown Formation) is a moderate coastal-plain aquifer (Zapeczka, 1989) and exhibits high resistivity values (Fig. 2). The Merchantville sequence thickens downdip and northeast from thin western sections (46.5 m) to 89.3 m at Island

Beach, the thickest upper Cretaceous sequence observed on the coastal plain. Thick intervals (60.9-73.1 m) are visible across the central and northern coastal plain, but the sequence thins towards the South Jersey High (Fig. 9). Highstand sands are thickest along the central coast and inland (10-14 m) and consist of interbedded delta-front and prodelta deposits. Shoreface sands in the north range from 6.7 to 8 m, whereas the southern coastal plain exhibits thin (3-5 m) shelf sands (Fig. 4).

The geophysical log signature of the upper Englishtown sequence, an important northern aquifer composed largely of quartz sand, varies significantly along dip. In the northern coastal plain, thick delta-front sections are easily distinguished by their “box-like” appearance in gamma logs and high resistivity values (Fig. 5). The sequence thins consistently to the south around Millville and becomes increasingly fine-grained, glauconitic, and assumes a gradational “funnel” gamma signature. Although resistivity values are “muted” in these fine-grained intervals, the upper sand of the sequence prevails across the coastal plain. The upper Englishtown sequence is thickest in the northeastern coastal plain around Sea Girt (45.7-51.8 m) and thins west of Toms River (33.5 m). Highstand sands are generally 20-29 m thick around Sea Girt and grade to ~ 10 m around the central coastal plain (Fig. 4). Thinning of the sequence (8.3 m) and highstand sands (6 m) around Millville could indicate increasing distance from a strong deltaic northern source (Fig. 9).

The Marshalltown sequence shallows upward from glauconite clay and sand, to micaceous clay and clean quartz sands (Miller et al., 1998b; Miller et al., 1999). This

results in “funnel” geometry for gamma and resistivity values. The largest gamma spike (+150 API units) of the New Jersey Coastal Plain marks the sequence boundary between the Mount Laurel HST sand (upper Marshalltown sequence) and the glauconitic Navesink sequence (Fig. 5). This reworked interval is glauconite-rich and includes concentrations of phosphate pebbles, rip-up clasts, and represents a lowstand systems tract (LST) lag deposit of the overlying Navesink sequence (Miller et al., 2004). The Marshalltown sequence thickens seaward and exhibits two primary depocenters (central and northern) divided by a thin interval (21.3-27.4 m) (Fig. 9). The northern depocenter thickens to 43.6-47.4 m along the northeastern coast, whereas the southern depocenter is thickest at Bass River (44.5 m) and gradually thins to 32.3 m at Ancora. Very thin intervals characterize the southern coastal plain (8.1 m at Millville), just 30 km south of Bass River (Fig. 9). Thick highstand delta-front sands (21-25.6 m) occur across the central coastal plain but become finer-grained and thin to < 1 m shelf sands at Millville. Deposition during the Campanian indicates a north-northeast shift in the sedimentation of the New Jersey Coastal Plain similar to Turonian-Coniacian trends (Magothy sequences) (Fig. 8). Cenomanian-lower Turonian sequences exhibit depocenters in the central and southern coastal plain, whereas Turonian-Campanian sequences thicken towards the north.

Maastrichtian Sequence

The Maastrichtian to lowermost Danian Navesink sequence consists of fossiliferous glauconite clays and sands (Fig. 2) (Miller et al., 1998b; Miller et al., 1999). This interval

is characterized by high gamma values and low resistivity values, although sandier intervals (e.g., Redbank, Tinton Formations) may exhibit slight resistivity peaks (Fig. 5). The Cretaceous-Paleogene (K-P) impact event is preserved in most Navesink sections and is marked by spherule layers, Cretaceous chalk fragments, and a major gamma peak that is only exceeded by the uppermost layer of the Mount Laurel sand (Olsson et al., 1997; Miller et al., 1998a). These two peaks dominate the gamma log signature and allow easy identification of the Navesink Formation, although reworking and bioturbation of the K-P boundary can obscure the identification of the upper sequence boundary (Fig. 5).

Thickness variations of the Navesink sequence appear largely unrelated to dip. The northernmost wells of the study area represent the thickest intervals (26.2 m). An east-west-trending band of thin Navesink (9.1-10.1 m) in the south central coastal plain divides similarly thick (13.7-18.2 m) southern and central deposits (Fig. 9). This relatively thick southern section is not consistent with the majority of Cenomanian-Campanian sequences that thin south of the Bass River corehole. The lack of a clear depocenter paired with relative thickening to the south could indicate: (1) deep-water environments with low sediment input; and/or (2) decreased influence of basement structure on margin deposition. Paleogeographic and facies distribution maps were not created for the Navesink sequence due to the abundance of shelfal facies and absence of shallow marine highstand sands.

Discussion

Deltaic Facies Models

The analysis of deltaic systems has long been defined by the tripartite system of Galloway (1975), who used the relative influence of tidal, wave, and fluvial processes to classify delta morphology. Subsequent studies have shown that deltas and facies arrangements evolve through a broad spectrum of stages as a function of changes in sedimentation rates, eustasy, and rates of accommodation. Bhattacharya and Giosan (2003) show that deltas can exhibit wave-, tide-, and river-dominated facies across different lobes (e.g., Danube delta), suggesting that different classifications of delta can exist under the similar conditions (e.g., microtidal) within a delta system. Furthermore, deltas can evolve from tide- to wave-dominated over relatively short time periods. The Mekong delta shifted from tide-dominated to tide- and wave-dominated over the last 4 kyr (Ta et al., 2002), while seasonal variations in wind and wave energy can also influence facies characteristics (Yang et al., 2005). It is therefore simplistic to assume that 35 Myr of Late Cretaceous sedimentation can be exclusively pinned to a three-end-member modern analog system defined by deposition during global sea-level highstands.

Despite these limitations of delta classification, wave, fluvial, and tidal processes distinctly influence facies deposition, sedimentary characteristics (on a variety of scales), and the distribution and geometry of subsurface units. Lithofacies analysis from continuous core, coupled with our use of geophysical logs to establish paleogeographic maps and the lateral relationships of deltaic facies, reveals the widely known variability

of deltaic systems. However, we also document the relative stability of deltaic facies systems on the 10^6 - 10^7 yr scale (Fig. 10), with long periods of cyclically repeating systems tracts controlled by eustasy punctuated by facies shifts controlled by long-term sea level and shifting fluvial-deltaic sources (Fig. 4).

Early studies (Owens and Sohl, 1969; Owens and Gohn, 1985) recognized the deltaic origin of Upper Cretaceous New Jersey Coastal Plain strata, and subsequent lithofacies analyses by Miller et al. (2004) tied the observed shelf, prodelta, and shallow marine facies to a “mixed” tide- and wave-influenced modern Niger delta facies model (Allen, 1970). Characteristics of these deltaic facies that we observe in core are: (1) thin middle-neritic to outer-neritic glauconite sands and clays (60-200 m paleodepths determined from benthic foraminiferal analysis); (2) common, thick prodelta micaceous clays and silts (20-60 m paleodepths); (3) generally thick delta-front, nearshore, and shoreface fine to coarse quartz sands (0-20 m paleodepths); (4) delta-plain sands, silts, and clays; and (5) fine- to medium-grained fluvial, estuarine, and tidal-channel quartz sands; (6) back-barrier lagoon and swamp organic-rich clays and sands; (7) levee and crevasse-splay sands; (8) upper-delta-plain and lower-delta-plain interfluvial mudplain clays and paleosols (Miller et al., 1998b; Miller et al., 1999; Miller et al., 2003; Miller et al., 2004; Miller et al., 2006; Sugarman et al., 2005). The middle-neritic to outer-neritic facies compose the basal TST packages observed in the Bass River, Cheesequake, Merchantville, Marshalltown, and Navesink Formations (Miller et al. 2004). Prodelta facies compose the lower HST found in the Bass River, Woodbury, upper Englishtown, and Marshalltown Formations. Coarse-grained delta-front to shoreface facies represent

the upper HST observed in the Bass River, lower Englishtown, upper Englishtown, and Mount Laurel Formations (Miller et al., 2004). A majority of the marginal-marine to nonmarine facies are restricted to the Magothy Formation (Fig. 7), although they are occasionally observed in other sections (Miller et al., 2004).

Discerning the influence of wave, fluvial, and tidal processes on deltaic sediments in fully marine units can be difficult. Instead, careful examination of marginal to shallow marine facies proximal to the littoral zone can offer a snapshot of the processes that shape deltaic facies patterns. The paleogeographic distribution of facies can also be very useful in determining the relative influence, inasmuch as tidally influenced sandbodies tend to be shore perpendicular, while wave-dominated sandbodies are often arcuate, shore parallel, and show evidence of wave reworking and lateral transport by longshore currents (e.g., Allen, 1970; Van Andel, 1967; Fisher and McGowan, 1969).

Paleogeographic maps reveal several examples of wave influence on sandbody geometry and deltaic facies patterns: (1) Thick (+20 m) delta-front sands of the Marshalltown sequence (Mount Laurel Formation) grade rapidly (> 10-20 km) across the central coastal plain into similarly thick (21 m) shoreface sands to the northeast. These sands become progressively thinner farther north along the paleoshoreline, indicating increasing distance from the primary sediment input (Fig. 4). (2) A similar transition is visible in the upper Englishtown sequence, although shoreface sands are visible to the southwest of the main depocenter. Thick 10-29 m delta-front deposits of the central and northern coastal plain transition to thinner (~ 10 m) shoreface sands to the south at Ancora, although this lateral facies change occurs over ~ 40 km (Fig. 4). (3) Thin (< 10 m) delta-front and

shoreface deposits of the Merchantville sequence (lower Englishtown Formation) are juxtaposed in the northern coastal plan around Sea Girt and Toms River. This transition occurs over a very short distance ($< 5\text{-}10\text{ km}$), with shoreface sands becoming more abundant to the northeast (Fig. 4). (4) Both the Bass River I and II sequences exhibit delta-front sands in the central coastal plain that pass into thin shoreface sands in the southern coastal plain (Ancora and Millville area). Because this facies change occurs over the course of $40\text{-}50\text{ km}$, it casts doubt on a wave-reworked genesis (Fig. 4). While these shore-parallel transitions from thick delta-front deposits to shoreface sands could simply represent the contrast between deltaic and interdeltic segments of a margin (particularly facies shifts that occur over long segments of a coastline), we believe that the rapid scale of these changes ($> 10\text{-}40\text{ km}$) and comparable thicknesses of the delta-front and shoreface facies attest to wave reworking and consequent redistribution of sand by longshore drift.

While paleogeographic maps are useful in determining longshore variations in facies character and potential wave influence, discerning the orientation of tidally influenced sandbodies exceeds the spatial resolution of this study due to the geographic distribution of wells and coreholes. Determining the tidal influence of a sedimentary unit can be very difficult from core, necessitating further integration with outcrops. However, because most of the Late Cretaceous deltaic facies are either fully marine or nonmarine, few candidate sequences with nearshore to marginal marine facies are available for extracting tidal influence.

Observations from an outcrop of the Magothy II sequence in Old Bridge, NJ (~ 30 km to the northwest of the Sea Girt corehole) reveal sedimentary characteristics consistent with strong tidal influence on deposition. These include: (1) abundant flaser and wavy beds of black to dark gray micaceous, organic clay draped over small (1-2 cm) ripples and planar cross beds of fine- to medium-grained quartz sand; (2) interlaminated (3-5 mm) black micaceous clay with yellow to gray fine quartz sands; (3) numerous sets of large (50-100 cm thick) trough and planar cross beds interbedded with intervals of clean gray to white clays; (4) 1-2 cm diameter scours and irregular reactivation surfaces; (5) irregular-based (30-40 cm to 2 m) channels incised into clayey and sandy substrates; (6) rare bidirectional cross bedding with clay drapes; and (7) presence of rare 4-8 cm long *Skolithos* burrows, hinting at a marginal-marine environment of deposition (Fig. 7). These criteria support our interpretation of either a tidal channel or tidal delta for the Magothy II sequence at this locality.

Although the Old Bridge outcrop of the Magothy II offers only a brief snapshot of 35 Myr of Late Cretaceous deltaic sedimentation, facies identified throughout the Magothy sequences in core and from logs (e.g., tidal channel) support the identification of tidal influence. The presence of tidal channels, estuarine deposits, and extensive lagoons and swamps, coupled with broad sandbody trends derived from paleogeographic maps of the Turonian-Coniacian, is consistent with a mixed wave- and tide-dominated delta. The absence of marginal-marine facies throughout the Campanian, Santonian, and Cenomanian makes the identification of tidal influence difficult, but does not preclude it.

Paleogeographic Evolution of Late Cretaceous Deltas, New Jersey Margin

The paleogeographic reconstruction of Late Cretaceous deposition in the New Jersey Coastal Plain was generated using sequence boundaries as geochronologic markers. Facies analysis of the deposits directly underlying these sequence boundaries provided the geographic distribution of deltaic facies during the regressive highstand systems tract. A series of paleogeographic maps and highstand sandbody isopach maps (Fig. 4) were integrated with total sequence isopach maps (Figs. 6-9) and observations from the offshore New Jersey margin (Poag and Sevon, 1989) to construct a comprehensive record of New Jersey margin deposition, depocenter migration, and Late Cretaceous deltaic evolution.

This depositional history records the long-term signal of coastal onlap characteristic of post-rift passive margins (Grow, 1980), apparent in the transition from the fully terrestrial and fluvial Albian Potomac Formation (deposited in prior to the Bass River sequences) to the strong marine influence on deltaic facies during the Late Cretaceous (Miller et al. 2004). Thermoflexural subsidence is modulated by higher-frequency variations in sediment supply, flexural subsidence from sediment loading of the shelf, and third-order eustatic changes. Analysis of paleogeography and depocenter migration reveals five primary phases of Late Cretaceous margin deposition:

(1) Cenomanian-early Turonian Bass River I-III sequences exhibit the first evidence of marine strata on the coastal plain and the onset of 35 Myr of Late Cretaceous deltaic

margin sedimentation. The paleoshoreline was oriented slightly more NE-SW than modern trends, representing the disparity of rapidly prograding delta fronts versus slower progradation of southern shoreface deposits (Fig. 4).

Deposition of the Bass River I and II sequences saw northern and central fluvial systems supply a broad delta front in the central coastal plain. These sands: (1) transition into prodelta and thin glauconitic shelf sands farther offshore; and (2) grade alongshore into thinner shoreface sands to the southwest, likely representing a transition to the bordering interdeltic margin (Fig. 4). While Bass River I and II also record extensive delta-plain and fluvial sediments (supported by outcrop studies of the time-equivalent and updip Raritan Formation; Owens and Gohn, 1985), Bass River III deposition is characterized by significant shoreline retreat (the result of higher sea level; Miller et al. 2005) and consists of thick, well-defined marine delta-front, prodelta, and shelf facies.

Sequence and sand depocenters are concentrated along the south-central coastal plain and are relatively stable through the Cenomanian-early Turonian, likely the result of a stable northern to central source and sediment supply. These results are consistent with offshore interpretations that identify a major depocenter off the coast of central New Jersey. A northern source appears to feed an offshore depocenter and bypass the northern coastal plain, resulting slightly thinner intervals (Poag and Sevon, 1989) (Fig. 10).

(2) A major northeast shift in depocenter location occurs during the late Turonian-Coniacian (Magothy sequences) associated with a long-term phase of low sea level

(Miller et al., 2005), the establishment of two sediment delivery systems (northern and southern sources), a significant influx of sediment to the mid-Atlantic Margin (Poag and Sevon, 1989), and increased subsidence in the Raritan Embayment (Fig. 10). These sequences thicken substantially offshore toward the Long Island Platform, where sections exceed 350 m (Fig. 10) (Poag and Sevon, 1989).

Late Turonian-Coniacian deltaic sequences exhibit a wide array of marginal to nonmarine facies that are unique to Late Cretaceous deltaic sedimentation. These include delta and alluvial plain, paleosols, fluvial channel, levee, crevasse splay, lagoon, swamp, estuarine, and tidal channel to delta facies observed in core and outcrop (Miller et al., 1998b; Miller et al., 1999; Miller et al., 2006; Sugarman et al., 2005).

Paleogeographic analysis reveals several interesting trends of Turonian-Coniacian deltaic sedimentation: (1) The Magothy I sequence consists of thick delta-front deposits, but also exhibits delta-plain and fluvial and estuarine deposits across the southern and northern coastal plain. (2) No marine facies are recorded in the Magothy II sequence due to substantial progradation of the shoreline. Two extensive fluvial systems are visible in the northern and southern coastal plain, while thin alluvial and delta plain paleosols are abundant throughout (Fig. 4). (3) The Magothy III sequence records the highest diversity of facies observed in core, and consists of a substantial delta front with abundant fluvial, crevasse-splay, lagoon, and swamp deposits across much of the coastal plain. (4) The Magothy IVA and IVB sequences are preserved only in the northern coastal plain, and record extensive nonmarine delta-plain, fluvial-channel, and coastal lagoon to swamp

facies that border thin delta-front sands to the east (Fig. 4). The restricted distribution of these northern sequences represents the dominance of a strong northern source and ample accommodation in the Raritan Embayment.

(3) Santonian deposition is characterized by a sediment-starved glauconitic shelf (Miller et al. 2004). No significant depocenters or deltaically influenced facies are visible on the coastal plain, representing a major transgression caused relatively high sea level and a significant reduction of local siliciclastic input (Fig. 10).

(4) The Campanian is characterized by thick northern depocenters, although several secondary central depocenters are also evident. This is consistent with offshore intervals that record thick sections east of northern New Jersey (Fig. 10) (Poag and Sevon, 1989). Campanian trends indicate the influence of both sediment sources: (1) the southern source was the primary control of a large tide- and wave-dominated delta (Merchantville sequence) as evidenced by a major depocenter on the south-central coastal plain; (2) the northern source deposited thick delta-front sands across the northern coastal plain (upper Englishtown sequence); and (3) significant northern and central depocenters of the Marshalltown sequence indicate both sediment sources were significant contributors to deposition (Fig. 10).

Delta-plain deposits are absent during the Campanian, and sequences exhibit a strong marine influence with significant accumulations of delta-front sands, prodelta sandy, silty clays, and glauconitic shelf sands (Fig. 4). Campanian sequences also document the rapid

lateral transition from thick delta-front to shoreface facies, implicating significant wave reworking and longshore transport of this mixed-influence Cretaceous delta (Fig. 4).

(5) Maastrichtian deposition exhibits gradual thickening to the north and south while offshore maps exhibit broad contours that extend gently across the shelf towards a depocenter located ~ 300 km to the east. The relatively thin and sediment-starved Maastrichtian Navesink sequence exhibits little influence from either source due to low sedimentation rates and deep paleodepths (middle to outer neritic; Miller et al., 2003) tied to high sea level (Miller et al., 2005). This period of deposition is unique because it: (1) Lacks primary onshore depocenters; (2) is the only upper Cretaceous sequence to thicken toward the southern coastal plain; and (3) exhibits shelf facies with little to no deltaic influence from either sediment source.

The paleogeographic distribution of sequences reveals that shifting northern and southern sediment sources fed large deltaic systems and onshore and offshore depocenters. A northward shift in deposition from the Cenomanian to the Campanian resulted from a dominant northern source, a weakened southern source, and persistent thickening into the Raritan Embayment. The progressive shift from marginal and nonmarine deltaic facies in the Turonian-Coniacian to fully marine deltaic facies in the Campanian represents continued thermoflexural subsidence and a long-term rise in sea level.

Controls on the Distribution of Sequences and Facies

Late Cretaceous sequences and deltaic facies systems of the New Jersey Coastal Plain reflect the interplay of several variables: (1) eustatic variations dominate the timing of sequences, systems tracts, and generation of bounding disconformities; (2) differential flexural subsidence of the continental crust across the margin provides excess accommodation in the Raritan Embayment relative to the South Jersey High; (3) changes in tectonic uplift and weathering of Appalachian source terrains affects the rate and location (e.g., dominant fluvial axes) of sediment supply, influences the expression and characteristics of deltaic facies, and may have a positive feedback on the basement response to sediment loading.

Sea-Level Changes

Third-order sea-level changes are well documented for the Late Cretaceous (Miller et al., 2005). One-dimensional backstripping estimates from New Jersey Coastal Plain coreholes identified 11 (and as many as 18) sea-level cycles from 100 to 65 Ma with amplitudes as great as ~ 50 m (Miller et al., 2005). These sea-level changes are the principal driver behind base-level changes, unconformity genesis, and the timing of transgressions, regressions, and systems tracts on the New Jersey Coastal Plain.

Because thermoflexural subsidence is the dominant tectonic component of evolution of passive margins, New Jersey offers an excellent location to examine the evolution of

eustatically forced sequences and deltaic facies. Periods of elevated or low sea level have a distinct effect on shoreline position and the types of deltaic facies that are recorded on the coastal plain. High sea level in the Campanian resulted in marine deltaic facies, while low Turonian-Coniacian sea level resulted in the deposition of marginal to nonmarine deltaic facies. However, eustasy alone does not account for the variability of deltaic facies across the coastal plain.

Our results from the Late Cretaceous show that although eustasy provides the template for sequences globally, regional tectonics (rates of subsidence and accommodation), autogenic changes in sediment supply, proximity to sediment input, and local subsidence from depocenter loading determines the preservation of sequences in a particular region.

Sediment Supply and Source Location

The integration of Cenomanian-Maastrichtian paleogeographic and isopach maps of New Jersey sequences establishes a chronology of depocenter migration and documents the importance of two dominant sediment sources (northern and southern) on the distribution of deltaic sequences and facies. Changes in deltaic facies patterns and sandbody character appear to result from: (1) variations in sediment supply; (2) changes in source location and/or the dominance of a particular source; (3) proximity of sandbodies to a sediment source; and (4) the modifying effects of wave and tidal energy on deltaic facies distributions. These changes in sediment source location and sediment

yield are superimposed on longer trends of basement subsidence and third-order eustatic variations.

For this study, the terms “northern” and “southern” source replace the “ancient-Hudson” and “ancient-Delaware” of Poag and Sevon (1989), who used the names to represent inferred locations of Appalachian drainage. Although fault patterns in Paleozoic basement may constrain the location of the modern Hudson River into the Cretaceous (lending a degree of permanence to its impact on New Jersey margin deposition), little work has addressed the issue and its precise location remains uncertain before the Plio-Pleistocene (Stanford et al., 2001). Similarly, the geological context and Cretaceous path of the modern Delaware River is unknown, although southern source was likely located around the central coastal plain, much farther north than the modern Delaware River. Poag and Sevon (1989) infer the Adirondack Highlands as the primary source of ancient-Hudson sediment, with some influence from the western New England Highlands, while the ancient-Delaware is fed by the Central Appalachian Highlands (Fig. 1).

Long-term trends reveal the gradual shift of depocenters from the central to northern New Jersey Coastal Plain from the Cenomanian (ca. 98 Ma) to the Campanian (ca. 72 Ma). This reflects the nature of a two-sediment-source system and variations in sediment supply tied to extrabasinal uplift and increased weathering of source terrains (Poag and Sevon, 1989). Peak rates ($21 \text{ km}^3/\text{Myr}$) of Late Cretaceous sediment accumulation on the mid-Atlantic Margin occurred during the Coniacian, representing a phase of tectonic uplift and intense weathering of the Appalachian hinterland (Poag and Sevon, 1989). This

large influx of sediments is reflected by the rapid seaward progradation of the shoreline and preservation of extensive delta-plain deposits on the New Jersey Coastal Plain (Magothy sequences). The concentration of Magothy depocenters in the northern coastal plain implies a higher sediment load in the northern source than the southern source. Observations from the coastal plain are consistent with offshore data that shows large amounts of coarse, deltaic material deposited across New Jersey shelf, a function of high sediment rates “flooding” the system (Poag and Sevon, 1989).

Conversely, periods of low to dormant uplift and weathering are characterized by a reduction in the amount of sediment delivered to the coast by the fluvial systems. Deposition during these intervals can be characterized by a retreat of the shoreline and the onset of largely sediment-starved, glauconitic shelves across the New Jersey Coastal Plain (although sea level also plays an important role). While the Maastrichtian exhibits substantial sediment accumulation rates ($11 \text{ km}^3/\text{Myr}$) across the mid-Atlantic Margin, most of this sediment is derived from sources to the north and south of New Jersey (Poag and Sevon, 1989). As a result, there is little evidence of any deltaic influence in New Jersey during these time periods, with the only shallow sands identified as distal lower shoreface in the Sea Girt corehole (Sugarman et al., 2005). Although the Cenomanian experiences extremely low regional sediment accumulation rates ($2 \text{ km}^3/\text{Myr}$), the thickest intervals are located 100 km east of New Jersey. As a result, relatively thin but well-defined deltaic sequences are preserved across the New Jersey Coastal Plain while coeval sections are thin to absent across much of the mid-Atlantic Coastal Plain (Poag and Sevon, 1989).

Proximity to fluvial axes and active deltaic lobes plays an important role in sequence thickness and the character (e.g., lithology, grain size, porosity, permeability) of deltaic sandbodies. Several sequences (Cenomanian and Campanian) exhibit thick delta-front sands that grade laterally into thinner shoreface sands over relatively short distances (5-50 km). While several of these could simply represent interdeltic zones of the margin (“shore-zones” of Galloway, 2001), it appears that large amounts of deltaically derived sand are reworked by wave action and redistributed by longshore currents. Such lateral variations in facies and sandbody character are important to understand, particularly in the application of ancient deltaic systems to hydrocarbon and hydrogeologic studies. The gradation from thick, porous delta-front sand to thinner, finer-grained lower-shoreface sands observed throughout upper Cretaceous sequences can significantly alter the viability of reserves. In non-hydrocarbon-bearing regions, these sandy intervals are also important aquifers, particularly in densely populated areas such as the greater New York-New Jersey-Philadelphia metropolitan area. Understanding the process and scale of such changes can be critical in effectively managing groundwater resources.

While the marine delta front is generally the locus of sand deposition of the Late Cretaceous New Jersey delta, the associated progradation of the delta often preserves an extensive delta plain where many nonmarine facies have significant quantities of sand. Most of the thick, coarse sands are found in fluvial to tidal channels that dissect the ancient delta plain. However, additional sandbodies can be uncovered in crevasse-splay, levee, lagoon, swamp, and bay deposits, although the lateral continuity of these

sandbodies is limited and difficult to constrain with sporadic core and well coverage.

Many of these sandy intervals are heterolithic accumulations of sand with paleosols and floodplain muds and clays, limiting their utility for hydrologic purposes on the coastal plain.

Basement Structure and Subsidence

While thermal subsidence and subsequent flexural loading is the dominant form of subsidence on passive margins (Watts and Steckler, 1979; Watts, 1982; Kominz et al., 1998), a series of basement embayments and arches influence the structural fabric of the Atlantic Coastal Plain. This trend is manifest in New Jersey with the southern Salisbury Embayment, the smaller northern Raritan Embayment, and the intervening South Jersey High (Fig. 1) (Olsson et al., 1988).

Isopach maps of upper Cretaceous sequences reveal the ubiquitous influence of the Raritan Embayment and South Jersey High on sequence distribution. Three Cenomanian-lower Turonian Bass River sequences exhibit thinning onto the South Jersey High (Fig. 10). Five Turonian-Coniacian Magothy sequences and three Campanian sequences thicken into the northern Raritan Embayment and similarly thin onto the South Jersey High (Fig. 10). Although they have influenced deposition since the Early Cretaceous, the genesis and behavior of these structural features is unclear (Olsson et al., 1988).

Brown et al. (1972) defined the tectonic framework of the coastal plain as a regional system of crustal segments that formed fault-bounded grabens as a result of far-field compression on wrench-fault zones. Differential subsidence along these fault-bounded “segments” was thought to deposit thick sedimentary sections in these embayments versus bordering basement highs. However, the existence of these large faults is unclear. Although active faulting has been observed across the Atlantic Coastal Plain south of the Salisbury Embayment (at Charleston, South Carolina; Weems and Lewis, 2002), the New Jersey Coastal Plain shows no evidence of syndepositional faulting (Kominz et al., 1998), though antecedent faults such as the Cornwall-Kelvin fault under the Raritan Embayment (Drake and Woodward, 1963) and a southern fault trending under Cape May (Taylor et al., 1968) could have provided inherited basement structure that influenced sequences (Browning et al., 2006). However, isopach mapping reveals no direct evidence of significant faulting during the Late Cretaceous such as large (+ 15 m) thickness variations over short distances (~ 2 km), growth packages, or erratic contours.

Variations in sequence thickness in the New Jersey Coastal Plain appear to result from “normal” passive-margin thermoflexural subsidence (Watts and Steckler, 1979; Kominz et al., 1998) and the consequent flexural response of progressive point loading of thick sedimentary packages into the Raritan Embayment and farther offshore by a northern sediment source. This loading caused positive feedback and increased flexural subsidence that accentuated the existing basement fabric and increased accommodation rates for subsequent units. The thinning of units onto the South Jersey High may represent a

peripheral bulge (e.g., Galloway, 1989) caused by the progressive flexural response to Early Cretaceous and subsequent loading in the Salisbury and Raritan embayments.

Isopach mapping reveals trends that validate thermoflexural subsidence as the primary control of regional accommodation and sedimentation, namely the persistent thickening into the Raritan Embayment, thinning onto the South Jersey High, and broad continuous contours that extend across the coastal plain (Fig. 10). Similar to the work of Galloway (1989; Galloway et al., 2000) and Browning et al. (2006), we find that the position of embayments and structural highs can be largely attributed to syndepositional flexural subsidence due to large prograding sedimentary wedges across the shelf.

Conclusions

We use core and geophysical log correlation to map upper Cretaceous sequences and deltaic facies across the New Jersey Coastal Plain and evaluate and refine well-log predictions in the absence of core control. Core-log correlations from four continuously cored ODP sites (Ancora, Bass River, Millville and Sea Girt) establish a clear link between the identified sequences (based on lithology, biostratigraphy, and Sr-isotope dating) and their respective gamma-ray and resistivity geophysical log signatures.

Paleogeographic, isopach, and deltaic lithofacies mapping of thirteen depositional established a 35 million year, high-resolution (> 1 Myr) record of Late Cretaceous deltaic sedimentation of the New Jersey Coastal Plain. Our study illustrates the widely known

variability of deltaic systems, but also documents the relative stability of deltaic facies systems on the 10^6 - 10^7 yr scale, with long periods of cyclically repeating systems tracts controlled by eustasy.

This study reveals five primary phases of margin evolution during the Late Cretaceous: (1) Cenomanian-early Turonian deltaic facies shift from delta plain to fully marine and are thickest in the central coastal plain; (2) high sediment rates, low sea level, and high accommodation rates in the northern coastal plain resulted in thick, marginal to nonmarine mixed-influenced deltaic facies during the Turonian-Coniacian; (3) comparatively low sediment rates and high sea level during the Santonian resulted in a sediment-starved margin without clear deltaic influence; (4) Campanian deltaic sequences thicken to the north and exhibit wave reworking and longshore transport of sands; and (5) low sedimentation rates and high long-term sea level during the Maastrichtian resulted in a sediment-starved glauconitic shelf.

Deltaic facies characteristics are strongly influenced by long-term eustatic changes, allogenic variations in sediment supply, and proximity to two long-lived fluvial axes. Sequence depocenters migrate gradually northeastward from the Cenomanian (ca. 98 Ma) through the earliest Danian (ca. 64 Ma) and reflect the position of active sediment sources and flexural subsidence due to large prograding sediment loads on the coastal plain and offshore shelf.

Results from the Late Cretaceous show that although eustasy provides the template for sequences globally, regional tectonics (rates of subsidence and accommodation), autogenic changes in sediment supply, proximity to sediment input, and flexural subsidence from depocenter loading determines the regional to local preservation and facies expression of sequences.

Acknowledgments

We thank members of the New Jersey Coastal Plain Drilling Project for their assistance in the collection of datasets from the ODP Leg 174AX coreholes. We also thank Lloyd Mullikin and Donald Monteverde of the New Jersey Geological Survey for providing access to the many geophysical logs used in this study. Thanks go to Greg Mountain and Gail Ashley for evaluations of the material. Additional thanks go to A. Guy Plint and Bill Harris for reviews of an earlier version of this manuscript. We would especially like to thank Editor Colin P. North and Associate Editor Mike Blum for their constructive criticism and helpful comments regarding this paper. We thank Ryan Earley for technical assistance with several of the figures presented in this paper. The Ocean Drilling Program provided core samples used in this study. Supported by National Science Foundation grants OCE 0084032, EAR97-08664, EAR99-09179, EAR03-07112, a scholarship from the Society of Petrophysicists and Well Log Analysts, and the New Jersey Geological Survey.

References

- Allen, J.R.L., 1970, Sediments of the modern Niger delta, a summary and review, *in* Morgan, J.P., ed., Deltaic Sedimentation; Modern and Ancient: Society of Economic Paleontologists and Mineralogists, Special Publication 15, p. 138-151.
- Bhattacharya, J., and Giosan, L., 2003, Wave-influenced deltas: geomorphological implications for facies reconstruction: *Sedimentology*, v. 50, p. 187-210.
- Bhattacharya, J., and Walker, R.G., 1991, River- and wave-dominated depositional systems of the Upper Cretaceous Dunvegan Formation, northwestern Alberta: *Bulletin of Canadian Petroleum Geology*, v. 39, p. 165-191.
- Brown, P.M., Miller, J.A., and Swain, F.M., 1972, Structural and stratigraphic, and spatial distribution of permeability of the Atlantic Coastal Plain, North Carolina to New York: United States Geological Survey, Professional Paper 796, p. 1-79.
- Browning, J.V., Miller, K.G., McLaughlin, P.P., Kominz, M.A., Sugarman, P.J., Monteverde, D., Feigenson, M.D., and Hernandez, J.C., 2006, Quantification of the effects of eustasy, subsidence, and sediment supply on Miocene sequences, U.S. mid-Atlantic Margin: *Geological Society of America, Bulletin*, v. 118, p. 657-588.
- Christopher, R.A., 1982, The occurrence of *Complexiopollis-Atlantopolis* zone (palynomorphs) in the Eagle Ford Group (Upper Cretaceous) of Texas: *Journal of Paleontology*, v. 56, p. 525-541.
- Combellas-Bigott, R.I., and Galloway, W.E., 2006, Depositional and structural evolution of the middle Miocene depositional episode, east-central Gulf of Mexico: *American Association of Petroleum Geologists, Bulletin*, v. 90, p. 335-362.
- Davies, R., Howell, J., Boyd, R., Flint, S., and Diessel, C., 2006, High-resolution sequence-stratigraphic correlation between shallow-marine and terrestrial strata: Examples from the Sunnyside Member of the Cretaceous Blackhawk Formation, Book Cliffs, eastern Utah: *American Association of Petroleum Geologists, Bulletin*, v. 90 (7), p. 1121-1140.
- Drake, C., and Woodward, H., 1963, Appalachian curvature, wrench faulting and offshore structures: *New York Academy of Science, Transactions, Series II*, v. 26, p. 48-63.
- Finley, R.J., and Tyler, N., 1986, Geological characterization of sandstone reservoirs, *in* Lake, L.W., and Carrol, H.B., eds., *Reservoir Characterization*: New York, Academic Press, p. 1-38.

- Fisher, W.L., and McGowan, J.H., 1969, Depositional systems in the Wilcox Group of Texas and their relationship to the occurrence of oil and gas: American Association of Petroleum Geologists, Bulletin, v. 53, p. 30-54.
- Galloway, W.E., 1975, Process framework for describing the morphologic and stratigraphic evolution of deltaic depositional systems, *in* Broussard, M.L., ed., Deltas; Models for Exploration: Houston, Texas, Houston Geological Society, p.87-98.
- Galloway, W.E., 1989, Genetic stratigraphic sequences in basin analysis II: Application to northwest Gulf of Mexico Cenozoic basin: American Association of Petroleum Geologists, Bulletin, v. 73, p. 143-154.
- Galloway, W.E., 2001, Cenozoic evolution of sediment accumulation in deltaic and shore-zone depositional systems, Northern Gulf of Mexico Basin: Marine and Petroleum Geology, v. 18, p. 1031-1040.
- Galloway, W.E., Garney-Curry, P.E., Li, X., and Buffler, R.T., 2000, Cenozoic depositional history of the Gulf of Mexico basin; American Association of Petroleum Geologists, Bulletin, v. 84, p. 1743-1774.
- Gani, M.R., and Bhattacharya, J.P., 2007, Basic building blocks and process variability of a Cretaceous delta: internal facies architecture reveals a more dynamic interaction of river, wave, and tidal processes than is indicated by external shape: Journal of Sedimentary Research, v. 77, p. 284-302.
- Grow, J.A., 1980, Deep structure and evolution of the Baltimore Canyon Trough in the vicinity of the COST No. B-3 well: United States Geological Survey, Circular 833, p. 117-132.
- Haq, B.U., Hardenbol, J., and Vail, P.R., 1987, Chronology of fluctuating sea levels since the Triassic (250 million years ago to present): Science, v. 235, p. 1156-1167.
- Keys, W.S., and MacCary, L.M., 1971, Application of borehole geophysics to water resource investigations: United States Geological Survey, Techniques of Water-Resource Investigations, Chapter E1, TWR12-E1A, 126 p.
- Kominz, M.A., Miller, K.G., and Browning, J.V., 1998, Long-term and short-term global Cenozoic sea-level estimates: Geology, v. 26, p. 311-314.
- Lanci, L., Kent, D.V., and Miller, K.G., 2002, Detection of Late Cretaceous and Cenozoic sequence boundaries on the Atlantic coastal plain using core log integration of magnetic susceptibility and natural gamma ray measurements at Ancora, New Jersey: Journal of Geophysical Research, v. 107, 2216, 12 p.

- Lee, K., McMechan, G.A., Gani, M.R., Bhattacharya, J.P., Zeng, X., and Howell, C.D., Jr., 2007, 3-D architecture and sequence stratigraphic evolution of a forced regressive top-truncated mixed-influence delta, Cretaceous Wall Creek Sandstone, Wyoming, U.S.A.: *Journal of Sedimentary Research*, v. 77, p. 303-323.
- Miller, K.G., Wright, J.D., and Fairbanks, R.G., 1991, Unlocking the ice house: Oligocene-Miocene oxygen isotopes, eustasy, and margin erosion: *Journal of Geophysical Research*, v. 96, p. 6829-6848.
- Miller, K.G., Mountain, G.S., the Leg 150 Shipboard Party, and Members of the New Jersey Coastal Plain Drilling Project, 1996, Drilling and dating New Jersey Oligocene-Miocene sequences: Ice-volume, global sea level, and Exxon records: *Science*, v. 271, p. 1092-1094.
- Miller, K.G., Mountain, G.S., Browning, J.V., Kominz, M.A., Sugarman, P.J., Christie-Blick, N., Katz, M.E., and Wright, J.D., 1998a, Cenozoic global sea-level, sequences, and the New Jersey transect: Results from coastal plain and slope drilling: *Reviews of Geophysics*, v. 36, p. 569-601.
- Miller, K.G., Sugarman, P.J., Browning, J.V., Olsson, R.K., Pekar, S.F., Reilly, T.J., Cramer, B.S., Aubry, M.-P., Lawrence, R.P., Curran, J., Stewart, M., Metzger, J.M., Uptegrove, J., Bukry, D., Burckle, L.H., Wright, J.D., Feigenson, M.D., Brenner, G.J., and Dalton, R.F., 1998b, Bass River Site, *in* Miller, K.G., Sugarman, P.J., Browning, J.V., et al., *Proceedings of the Ocean Drilling Program, Scientific results, Volume 174AX: College Station, Texas, Ocean Drilling Project*, p. 5-43.
- Miller, K.G., Sugarman, P.J., Browning, J.V., Cramer, B.S., Olsson, R.K., de Romero, L., Aubry, M.-P., Pekar, S.F., Georgescu, M.D., Metzger, K.T., Monteverde, D.H., Skinner, E.S., Uptegrove, J., Mullikin, L.G., Muller, F.L., Feigenson, M.D., Reilly, T.J., Brenner, G.J., and Queen, D., 1999, Ancora site, *in* Miller, K.G., Sugarman, P.J., Browning, J.V., et al., *Proceedings of the Ocean Drilling Program, Scientific results, Volume 174AX (supplement): College Station, Texas, Ocean Drilling Program*, p. 1-65.
- Miller, K.G., Sugarman, P.J., Browning, J.V., Kominz, M.A., Hernandez, J.C., Olsson, R.K., Wright, J.D., Feigenson, M.D., and Van Sickle, W., 2003, Late Cretaceous chronology of large, rapid sea-level changes: Glacioeustasy during the greenhouse world: *Geology*, v. 31, p. 585-588.
- Miller, K.G., Sugarman, P.J., Browning, J.V., Kominz, M.A., Olsson, R.K., Feigenson, M.D., and Hernandez, J.C., 2004, Upper Cretaceous sequences and sea-level history, New Jersey Coastal Plain: *Geological Society of America, Bulletin*, v. 116, p. 368-393.

- Miller, K.G., Kominz, M.A., Browning, J.D., Wright, J.D., Mountain, G.S., Katz, M.E., Sugarman, P.J., Cramer, B.S., Christie-Blick, N., and Pekar, S.F., 2005, The Phanerozoic record of global sea-level change: *Science*, v. 310, p. 1293-1298.
- Miller, K.G., Sugarman, P.J., Browning, J.V., Aubry, M.-P., Brenner, G.J., Cobbs, G., III, de Romero, L., Feigenson, M.D., Harris, A., Katz, M.E., Kulpecz, A., McLaughlin, P.P., Jr., Mizintseva, S., Monteverde, D.H., Olsson, R.K., Patrick, L., Pekar, S.J., and Uptegrove, J., 2006, Sea Girt site, *in* Miller, K.G., Sugarman, P.J., Browning, J.V., et al., *Proceedings of the Ocean Drilling Program, Scientific results, Volume 174AX (supplement): College Station, Texas, Ocean Drilling Program*.
- Mitchum, R.M., Vail, P.R., and Thompson, S., 1977, The depositional sequence as a basic unit for stratigraphic analysis, *in* Payton, C.E., ed., *Seismic stratigraphy, applications to hydrocarbon exploration: American Association of Petroleum Geologists, Memoir*, 26, p. 53-62.
- Olsson, R.K., 1991, Cretaceous to Eocene sea-level fluctuations on the New Jersey margin: *Sedimentary Geology*, v. 70, p. 195-208.
- Olsson, R.K., Gibson, T.G., Hansen, H.J., and Owens, J.P., 1988, Geology of the northern Atlantic Coastal Plain: Long Island to Virginia, *in* Sheridan, R.E., and Grow, J.A., eds., *The Atlantic Coastal Margin, U.S.: Boulder, Colorado, Geological Society of America, The Geology of North America*, v. 1-2, p. 87-105.
- Olsson, R.K., Miller, K.G., Browning, J.V., Habib, D., and Sugarman, P.J., 1997, Ejecta layer at the Cretaceous-Tertiary boundary, Bass River, New Jersey (Ocean Drilling Program Leg 174AX): *Geology*, v. 25, p. 759-762.
- Owens, J.P., 1970, Post-Triassic tectonic movements in the central and southern Appalachians as recorded by sediments of the Atlantic Coastal Plain, *in* Fisher, G.W., Pettijohn, F.J., and Reed, J.C., Jr., eds., *Studies of Appalachian Geology: Central and southern New York: New York, Interscience*, p. 417-427.
- Owens, J.P., and Gohn, G.S., 1985, Depositional history of the Cretaceous series in the U.S. Atlantic Coastal Plain: Stratigraphy, paleoenvironments, and tectonic controls of sedimentation, *in* Poag, C.W., ed., *Geologic Evolution of the United States Atlantic Margin: New York, Van Nostrand Reinhold*, p.25-86.
- Owens, J.P., and Sohl, N.F., 1969, Shelf and deltaic paleoenvironments in the Cretaceous-Tertiary formations of the New Jersey Coastal Plain, *in* Subitsky, S., ed., *Geology of Selected Areas in New Jersey and Eastern Pennsylvania and Guidebook of Excursions: New Brunswick, N.J., Rutgers University Press*, p. 235-278.

- Owens, J.P., Sugarman, P.J., Sohl, N.F., Parker, R., Houghton, H.H., Volkert, R.V., Drake, A.A., and Orndorff, R.C., 1998, Bedrock geology map of central and southern New Jersey: U.S. Geological Survey, Miscellaneous Investigations Series Map I-2540-b, scale 1:100,000, 4 sheets.
- Pitman, W.C., III, and Golovchenko, X., 1983, The effect of sea-level change on the shelf edge and slope of passive margins, *in* Stanley, D.J., and Moore, G.T., eds., *The Shelfbreak: Critical Interface on Continental Margins*: SEPM Special Publication, 33, p. 41-58.
- Plint, A.G., 2003, Clastic sediment partitioning in a Cretaceous delta system, western Canada: responses to tectonic and sea-level controls: *Geologica Croatica*, v. 56 (1), p. 39-68.
- Poag, C.W., and Sevon, W.D., 1989, A record of Appalachian denudation in postrift Mesozoic and Cenozoic sedimentary deposits of the U.S. middle Atlantic continental margin: *Geomorphology*, v. 2, p. 119-157.
- Posamentier, H.W., and Vail, P.R., 1988, Eustatic controls on clastic deposition II- sequence and systems tract models, *in* Wilgus, C.K., Hastings, B.S., Kendall, C.G. St. C., Posamentier, H.W., Ross, C.A., and Van Wagoner, J.C., eds., *Sea Level Changes- An Integrated Approach*: SEPM, Special Publication, 42, p. 125-154.
- Reynolds, D.J., Steckler, M.S., and Coakley, B.J., 1991, The role of sediment load in sequence stratigraphy; the influence of flexural isostasy and compaction, *in* Cloetingh, S., ed., *Special Section on Long-Term Sea-Level Change*: *Journal of Geophysical Research*, v. 96, p. 6931-6949.
- Rider, M.H., 1990, Gamma-ray log shape used as a facies indicator: critical analysis of an oversimplified methodology, *in* Hurst, A., Lovell, M.A., and Morton, A.C., eds., *Geological Applications of Wireline Logs*: Geological Society of London Special Publication 48, p. 27-37.
- Rider, M.H., 2002, *The Geological Interpretation of Well Logs*, Second Edition: Sutherland, Scotland, Rider-French Consulting Ltd., 280 p.
- Serra, O., and Sulpice, L., 1975, Sedimentological analysis of sand shale series from well logs: Society of Professional Well Log Analysts, 16th Annual Symposium, Transactions, Paper W, 23 p.
- Stanford, S.D., Ashley, G.M., and Brenner, G.J., 2001, Late Cenozoic fluvial stratigraphy of the New Jersey Piedmont: a record of glacioeustasy, planation, and incision on a low-relief passive margin: *The Journal of Geology*, v. 109, p. 265-276.

- Sugarman, P.J., and Miller, K.G., 1997, Correlation of Miocene sequences and hydrogeologic units, New Jersey Coastal Plain: *Sedimentary Geology*, v. 108, p. 3-18.
- Sugarman, P.J., Miller, K.G., Bukry, D., and Feigenson, M.D., 1995, Uppermost Campanian-Maestrichtian strontium isotopic, biostratigraphic, and sequence stratigraphic framework of the New Jersey Coastal Plain: *Geological Society of America, Bulletin*, v. 107, p.19-37.
- Sugarman, P.J., Miller, K.G., Browning, J.V., McLaughlin, P.P., Jr., Brenner, G.J., Buttari, B., Cramer, B.S., Harris, A., Hernandez, J.C., Katz, M.E., Lettini, B., Mizintseva, S., Monteverde, D.H., Olsson, R.K., Patrick, L., Roman, E., Wojtko, M.J., Aubry, M.-P., Feigenson, M.D., Barron, J.A., Baxter, S.J., Curtin, S., Cobbs, G., III, Bukry, D., and Huffman, B.A., 2005, Millville site, *in* Sugarman, P.J., Miller, K.G., Browning, J.V., et al., *Proceedings of the Ocean Drilling Program, Scientific results, Volume 174AX (supplement): College Station, Texas, Ocean Drilling Program, 2005.*
- Sugarman, P.J., Miller, K.G., Browning, J.V., Kulpecz, A.A., McLaughlin, P.P., Jr., and Monteverde, D.H., 2006, Hydrostratigraphy of the New Jersey Coastal Plain: Sequences and facies predict the continuity of aquifers and confining units: *Stratigraphy*, v. 2 (3), p. 259-275.
- Ta, T.K.O., Nguyen, V.L., Tateishi, M., Kobayashi, I., Saito, Y., and Nakamura, T., 2002, Sediment facies and Late Holocene progradation of the Mekong River Delta in Bentre Province, southern Vietnam: an example of evolution from a tide-dominated to a tide- and wave-dominated delta: *Sedimentary Geology*, v. 152, p. 313-325.
- Taylor, P.I., Zietz, I., and Dennis, L.S., 1968, Geologic implications of aeromagnetic data for the eastern continental margin of the U.S.: *Geophysics*, v. 33, p. 755-780.
- Vail, P.R., Mitchum, R.M., and Thompson, S., III, 1977, Seismic stratigraphy and global changes of sea level; Part 3; Relative changes of sea level from coastal onlap, *in* Payton, C.E., ed., *Seismic stratigraphy: applications to hydrocarbon exploration: American Association of Petroleum Geologists, Memoir*, 26, p. 63-81.
- Van Andel, T.J.H., 1967, The Orinoco delta: *Journal of Sedimentary Petrology*, v. 37, p. 297-310.
- Van Sickle, W.A., Kominz, M.A., Miller, K.G., and Browning, J.V., 2004, Late Cretaceous and Cenozoic sea-level estimates: Backstripping analysis of borehole data, onshore, New Jersey: *Basin Research*, v. 16, p. 451-465.
- Watts, A.B., 1982, Tectonic subsidence, flexure, and global changes of sea level: *Nature*, v. 297, p. 469-474.

- Watts, A.B., and Steckler, M.S., 1979, Subsidence and eustasy at the continental margin of eastern North America: American Geophysical Union, Maurice Ewing Symposium Series 3, p. 218-234.
- Weems, R.E., and Lewis, W.C., 2002, Structural and tectonic setting of the Charleston, South Carolina region: Evidence from the Tertiary stratigraphic record: Geological Society of America, Bulletin, v. 114, p. 24-42.
- Yang, B.C., Dalrymple, R.W., and Chun, S.S., 2005, Sedimentation on a wave-dominated, open-coast tidal flat, southwestern Korea: summer tidal flat - winter shoreface: *Sedimentology*, v. 52, p. 235-252.
- Zapczka, O.S., 1989, Hydrogeologic framework of the New Jersey Coastal Plain: United States Geological Survey, Professional Paper 1404-B, 49 p.

Figure Captions

Figure 1. Location map shows the location of ODP 174AX coreholes and additional geophysical logs used in this study. The location of basement structures is represented by the form line (in light gray) from Owens (1970). Coreholes (large gray circles, capital letters, boxed labels): AN- Ancora; BR- Bass River; MV- Millville; SG- Sea Girt. Geophysical logs (small circles, lowercase letters): Ap- Asbury Park; Bm- Browns Mills; Bu- Buena; Cw- Chatsworth; Do- Dorothy; Fr- Freehold; Hw- Howell; Ib- Island Beach; Ja- Jackson; La- Lavallette; Lb- Long Branch; Lh- Lakehurst; Lk- Lakehurst; Lw- Lakewood; Pp- Point Pleasant; Pw- Pittman West; Sh- Seaside Heights; Sm- South Mantoloking; Sp- Seaside Park; T1, T2, T3, T4, T5- Toms River area; Wg- Warren Grove; Wi- Williamstown; Wm- Woodmansie; Wt- Williamstown. OB represents an outcrop of the Magothy II sequence in Old Bridge, NJ. The inset map (after Poag and Sevon, 1989) presents a regional view with modern river courses and source terrains (filled with gray): H- Hudson River; D- Delaware River; S- Susquehanna River; C-

Connecticut River; CA- Central Appalachian Highlands; A- Adirondack Highlands; NE- New England Highlands; and NJ- New Jersey.

Figure 2. Generalized lithostratigraphy (after Owens and Gohn, 1985), sequence stratigraphy (after Miller et al., 2004), and hydrostratigraphy (after Zapecza, 1989) of the Upper Cretaceous New Jersey Coastal Plain.

Figure 3. Anatomy and well-log signature of typical New Jersey Upper Cretaceous sequences showing the primary lithologic components, their relationship to sequence stratigraphic units, and their characteristic gamma-ray and resistivity log characteristics (after Miller et al., 2004).

Figure 4. Paleogeographic maps showing the depositional evolution of Late Cretaceous deltaic facies. The thickness of highstand sands is represented by 10 m contour intervals. Facies are represented by both color and symbol where appropriate: AP- alluvial plain; CS- crevasse splay; DF- delta front; DP- delta plain and paleosols; ES- estuary; F- fluvial; L/S- lagoon and swamp; PD- prodelta; S- marine shelf; SF- shoreface; and TC- Tidal channel to Tidal delta. “Funnel, bell and box, and serrated” refer to the characteristic gamma log signatures of deltaic facies (listed to the left of each log) that are used to correlate facies away from continuous coreholes (after Rider, 2002). Approximate vertical scales are displayed to the right of each log signature.

Figure 5. Strike cross section of Upper Cretaceous sequences of the northern New Jersey Coastal Plain showing typical well-log characteristics. Correlation between ODP 174AX corehole Sea Girt (SG) and geophysical logs Lakewood (Lw) and Toms River (T3) shows the advantage of using both resistivity and gamma-log data (e.g., T3), particularly in identifying thin HST sand units. Changes in API values between coreholes represent differences in lithology, logging instruments, and borehole conditions.

Figure 6. Isopach maps of the Cenomanian Bass River sequences (I, II, III) from core and geophysical log data. Arrows represent the inferred location of sediment sources, with solid arrows representing a primary source and dashed arrows indicating a weaker secondary source. Contour interval is 3 meters. Large gray circles represent coreholes; small black circles represent well locations.

Figure 7. Subdivisions of the Magothy Formation showing sequences, facies, and log characteristics from the four ODP 174AX coreholes. Magothy sequences thicken to the north and contain diverse shallow marine to delta-plain facies. Outcrop photograph of the Old Bridge Member of the Magothy Formation (Magothy II sequence), Old Bridge, New Jersey. Note the change in orientation of the outcrop face represented by the thin black line. The letters indicate: A) an irregular-based interval of gray to white clean clays with fine-grained quartz sand; B) an irregular-based (30-40 cm) channel incised into clayey and sandy substrates; C) flaser and wavy beds of black to dark gray micaceous, organic clay draped over small (1-2 cm) ripples and planar cross-beds of fine- to medium-grained

quartz sand; D) planar cross stratification; and E) interlaminated (3-5 mm) black micaceous clay with yellow to gray fine quartz sands.

Figure 8. Isopach maps of the Turonian-Coniacian Magothy sequences (I, II, III, IVA, IVB) from core and geophysical log data. Solid arrows represent a primary sediment source and dashed arrows indicate a weaker secondary source. Contour interval is 3 meters. Large gray circles represent coreholes; small black circles represent well locations.

Figure 9. Isopach maps of the Santonian, Campanian, and Maastrichtian sequences (Cheesequake, Merchantville, upper Englishtown, Marshalltown, and Navesink) from core and geophysical log data. Solid arrows represent a primary sediment source and dashed arrows indicate a weaker secondary source. Contour interval is 3 meters. Large gray circles represent coreholes; small black circles represent well locations.

Figure 10. Chart shows: (1) Composite sequence recovery; (2) backstripped sea-level estimates (from Miller et al., 2005); (3) onshore depocenter isopach maps (contour interval 20 meters); (4) offshore depocenter isopach maps from Poag and Sevon (1989) (contour interval 100 meters); (5) inferred sediment source (black circle indicates primary role, open circle indicates secondary); and (6) appropriate facies system. The two isopach sets do not represent the same ages, as is indicated by each map title.

Age (Ma)	Formation		Sequence	Hydrogeologic unit	
70	Maastrichtian	Tinton Fm.	Navesink	Red Bank Sand composite confining bed	
		Redbank Fm.			
		Navesink Fm.			
75	Campanian	Mount Laurel Fm.	Marshalltown	Mount Laurel aquifer	
		Wenonah Fm.		Wenonah-Marshalltown confining bed	
		Marshalltown Fm.			
		U. Englishtown Fm.	Upper Englishtown	Englishtown aquifer system	
		L. Englishtown Fm.	Merchantville	Merchantville- Woodbury confining bed	
		Woodbury Fm.			
		Merchantville Fm.			
85	Sant.	Cheesequake Fm.	Cheesequake		
90	Conia.	Magothy Fm.	Magothy IVA/B	Potomac-Raritan-Magothy aquifer system	Upper aquifer
	Magothy III				
	Magothy II				
	Turonian		Magothy I		
95		Bass River/ Raritan Fm.	Bass River III		
			Bass River II		Middle aquifer
	Cenomanian		Bass River I		
					Confining bed
		Potomac Fm.	(nonmarine)		Lower aquifer

Figure 2

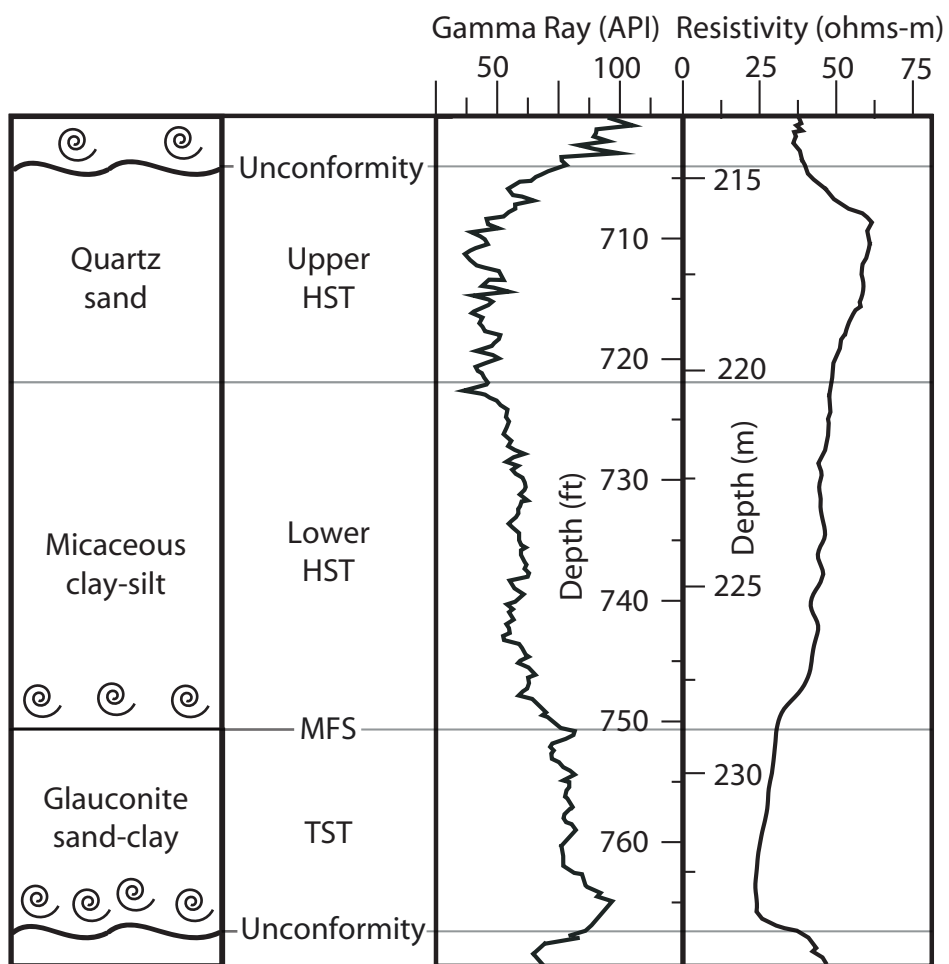


Figure 3

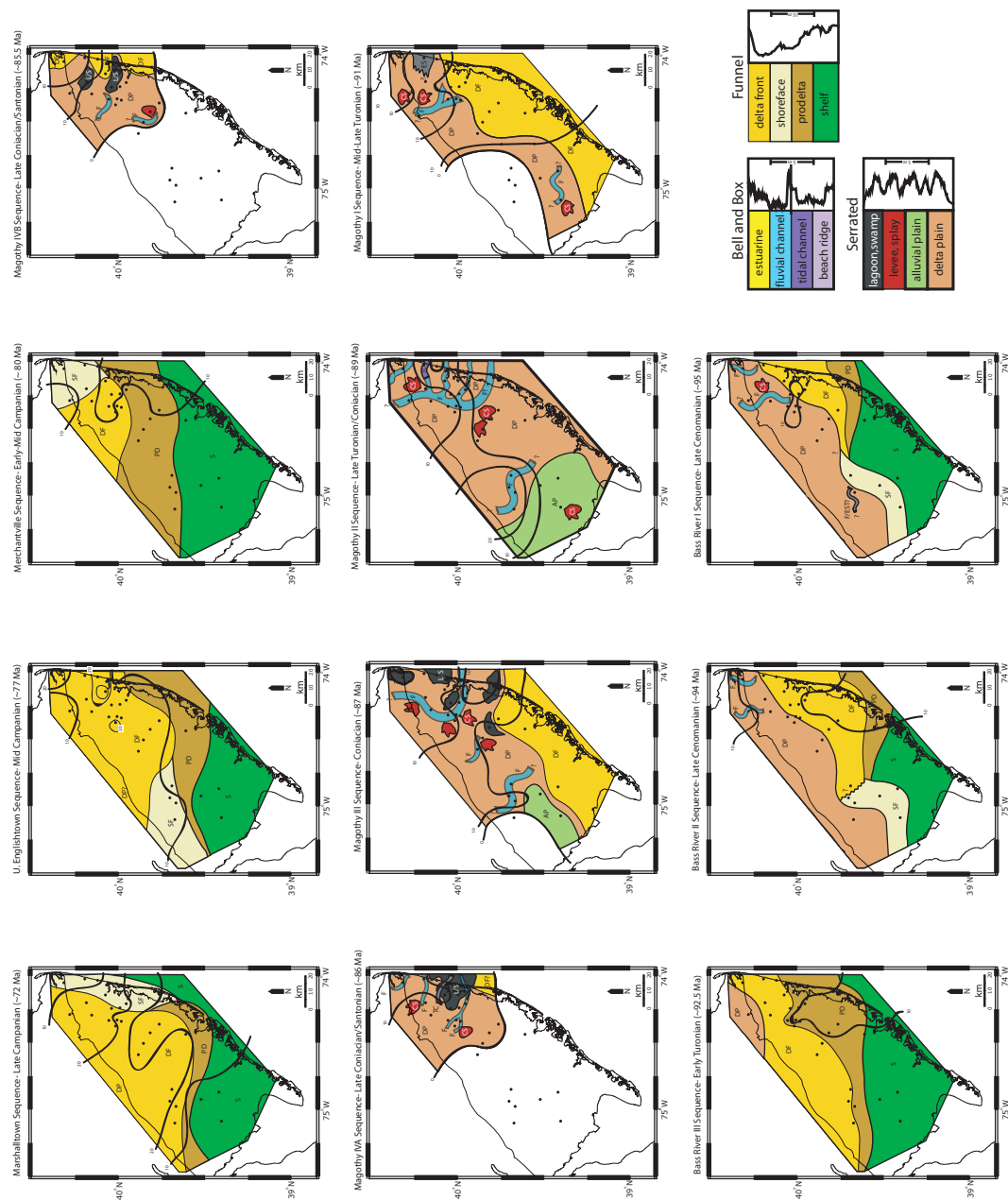


Figure 4

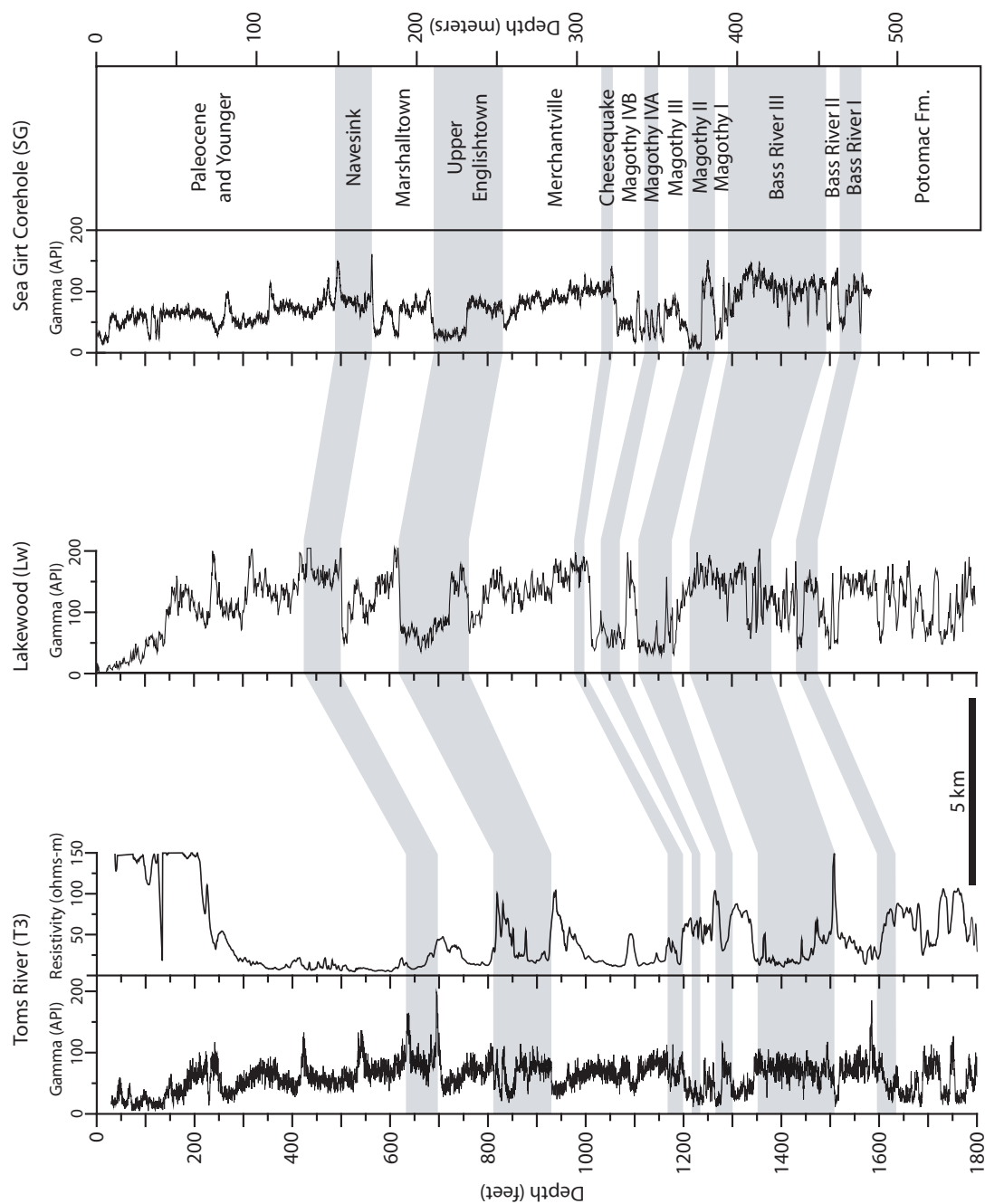


Figure 5

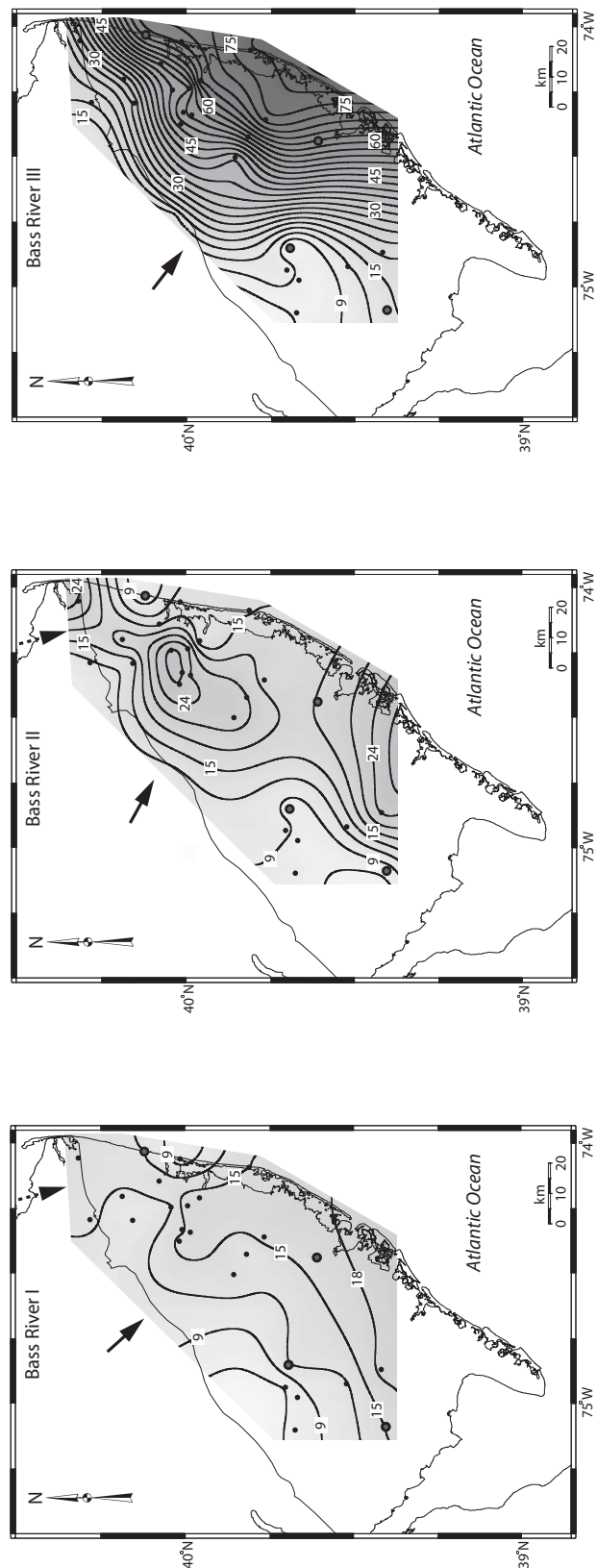


Figure 6

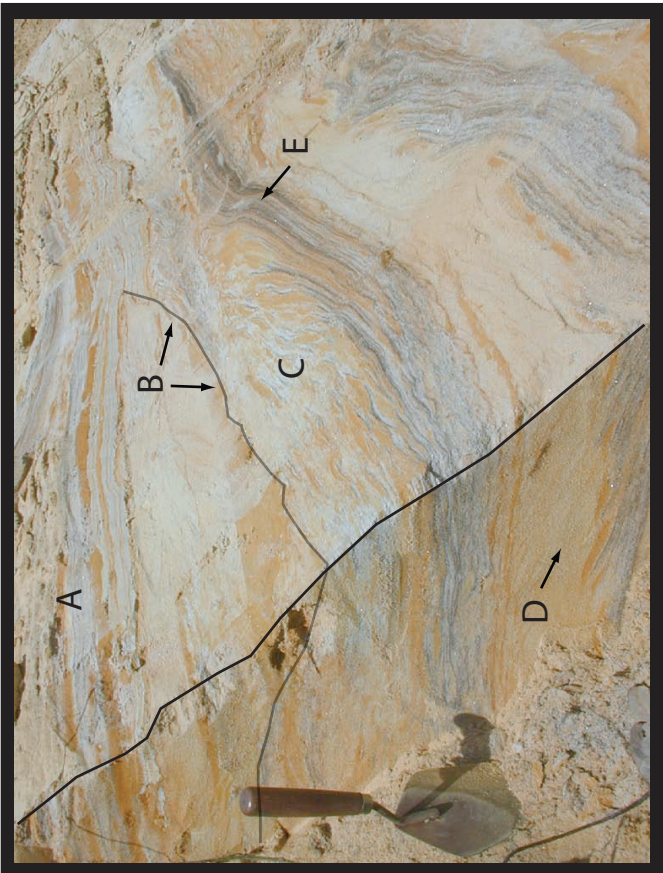
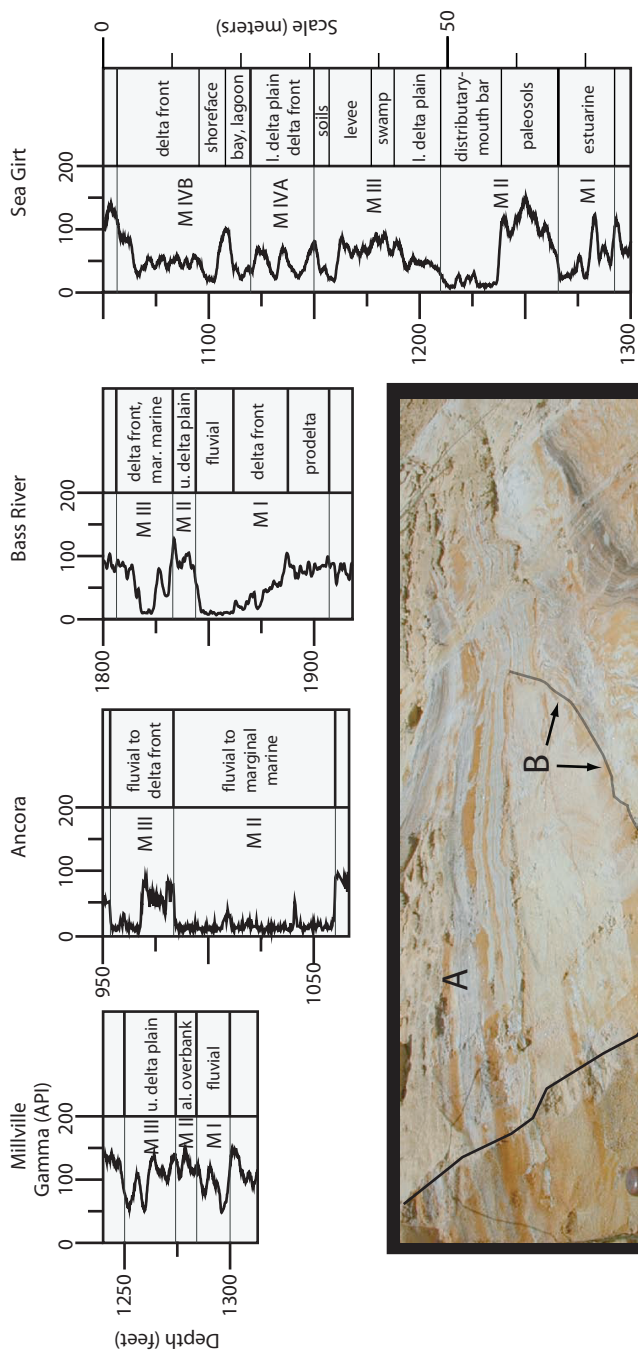


Figure 7

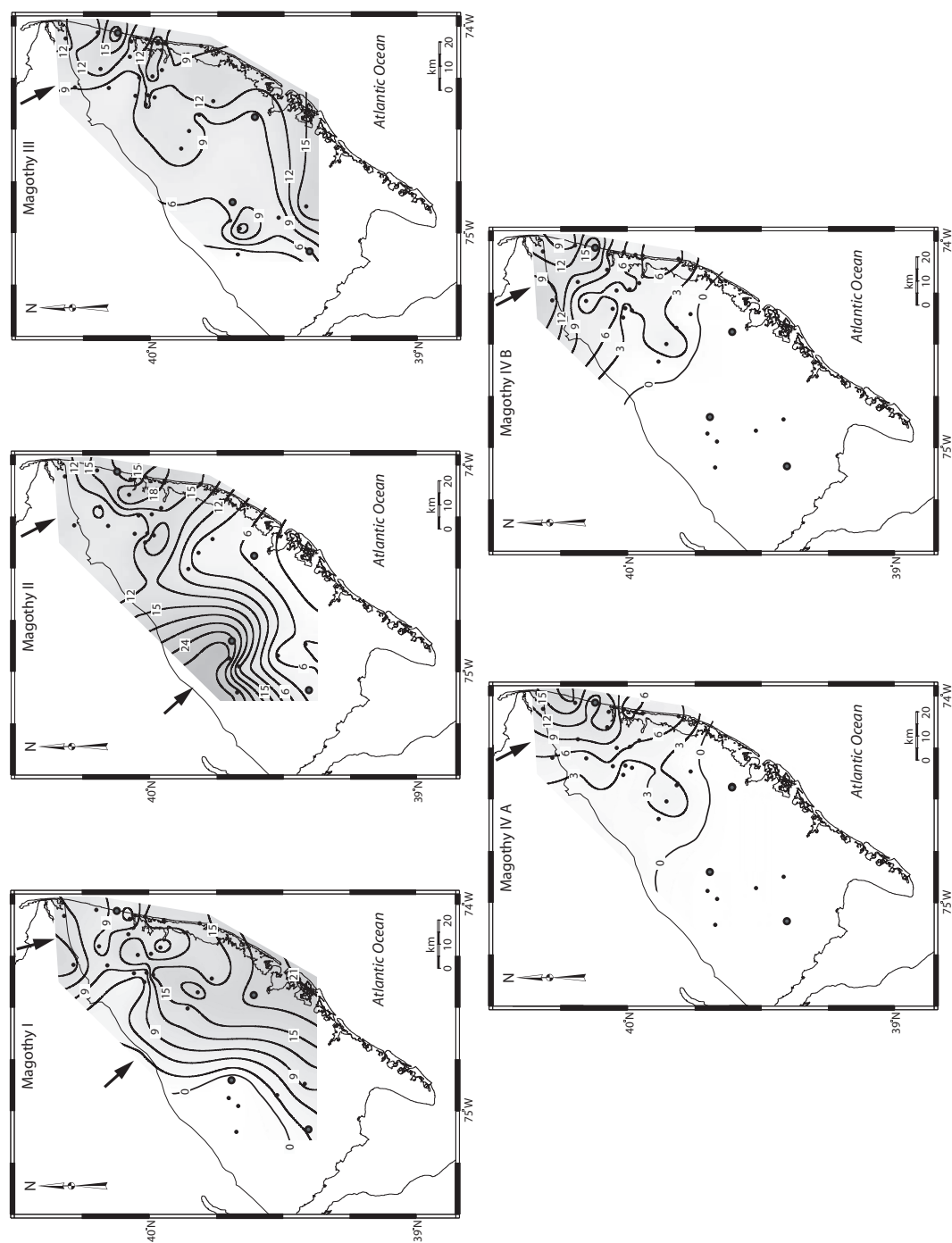


Figure 8

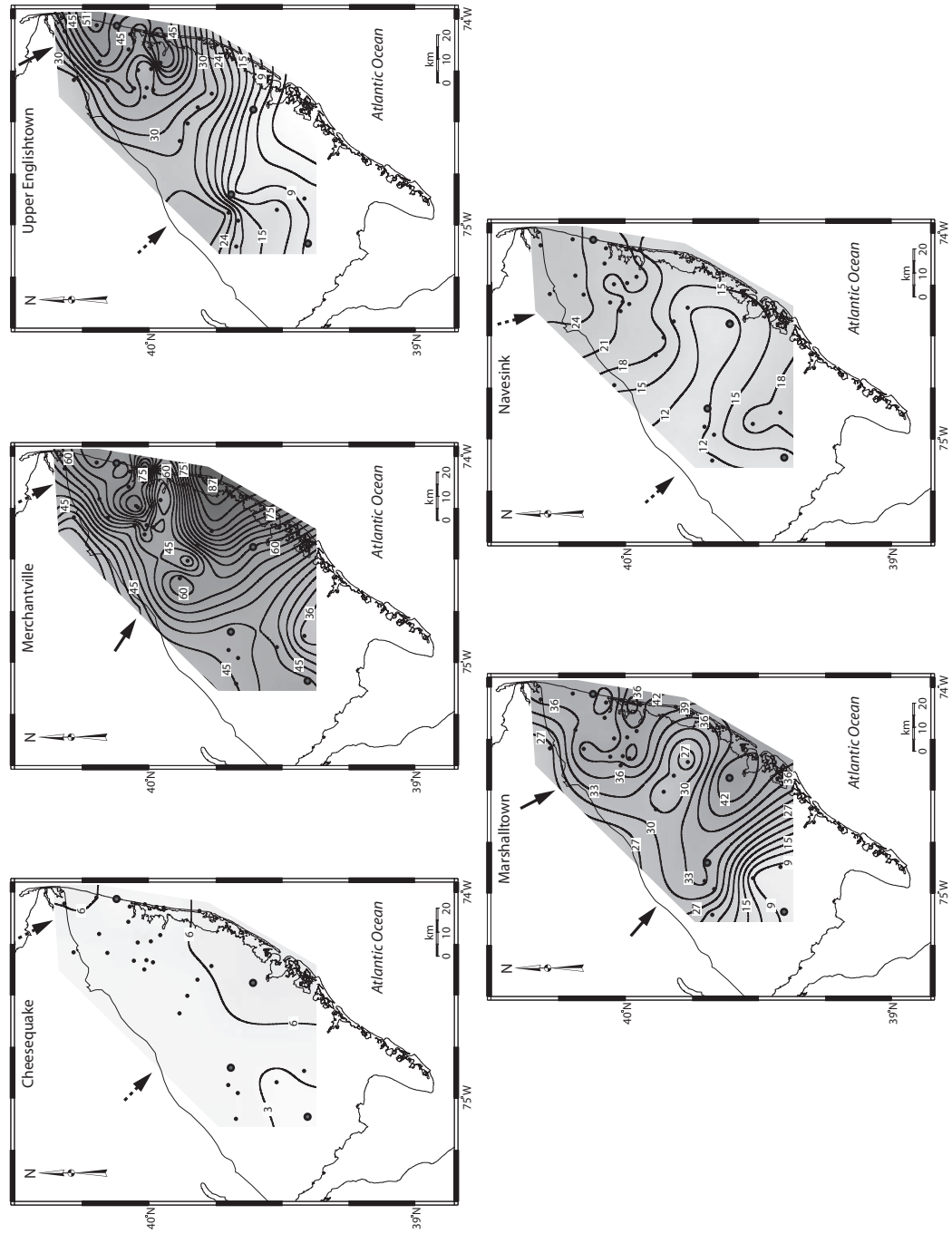


Figure 9

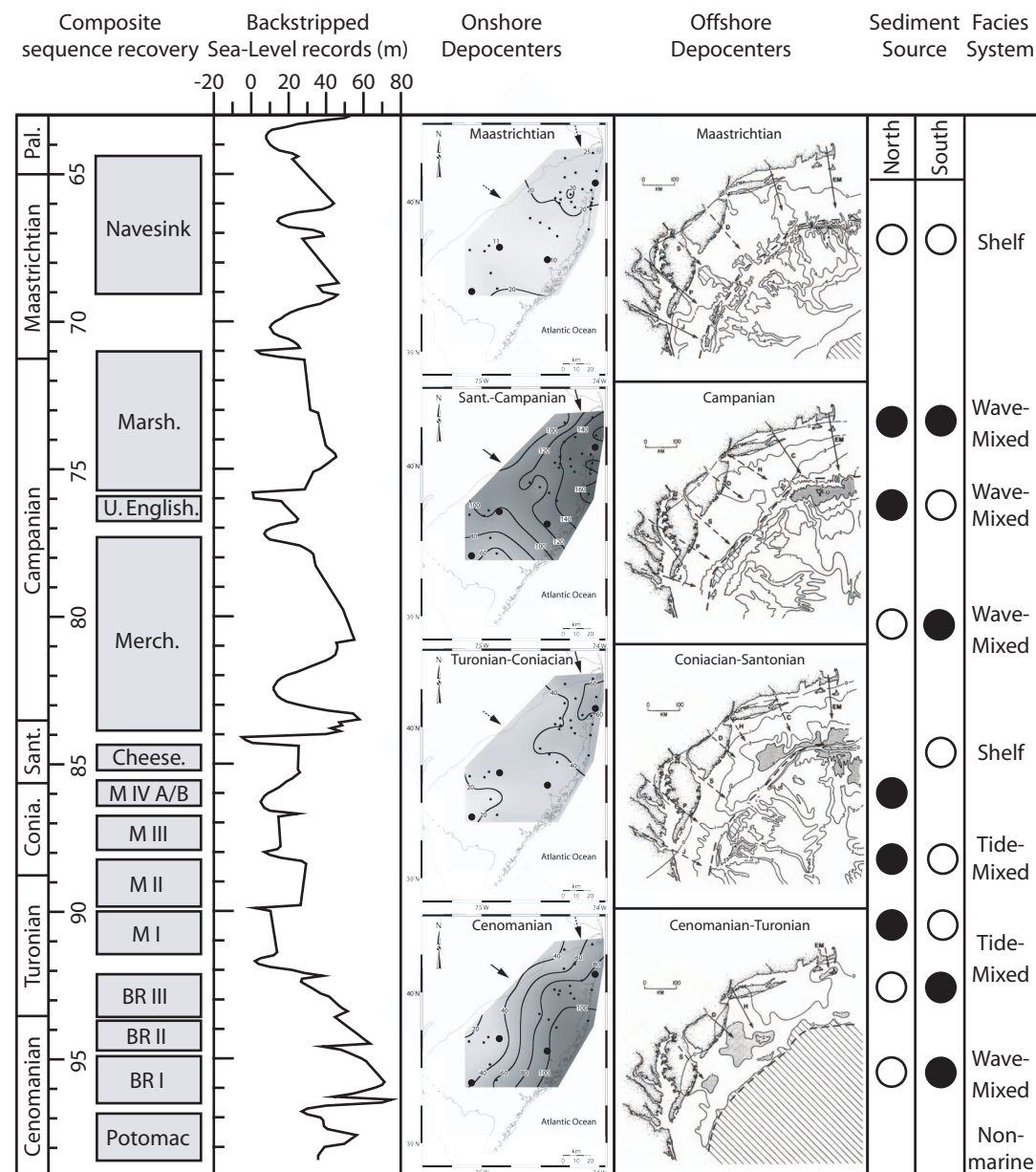


Figure 10

Chapter 2: Post-Impact Evolution of the Chesapeake Bay Impact Structure: Eustasy, Passive-Aggressive Tectonism, and Impactite Compaction

This chapter is currently under review as Kulpecz, A.A., Miller, K.G., Browning, J.V., Edwards, L.E., Powars, D.S., McLaughlin, P.P., Jr., Harris, A.D., and Feigenson, M.D., *submitted*, Post-Impact Evolution of the Chesapeake Bay Impact Structure:

Eustasy, Passive-Aggressive Tectonism, and Impactite Compaction: Geological Society of America Special Publication on the Chesapeake Bay Impact Structure.

Abstract: The Eyreville and Exmore, VA cores provide the first continuous, high-resolution ($> \sim 1$ myr) chronostratigraphic records linking the inner crater and annular trough of the late Eocene Chesapeake Bay Impact Structure (CBIS). We identify 12-16 post-impact depositional sequences within the annular trough (Exmore), integrate the results with sequences identified from cores in the inner crater (Eyreville), and place them within a regional framework extending from northern North Carolina through Delaware. CBIS, other Delmarva, and New Jersey sequence boundaries that are preserved correlate with $\delta^{18}\text{O}$ increases, indicating a primary glacioeustatic control. However, regional comparisons show that sequences are preserved and cut out in different time intervals in different regions: 1) the upper Eocene is thickest in the central crater but is thin immediately around the crater; 2) the Oligocene is generally thin and poorly represented throughout the mid-Atlantic region, except in the southeastern New Jersey Coastal Plain; 3) the lower lower Miocene is thick and well developed in New Jersey and Delaware, but very thin to absent in the CBIS and other Maryland-Virginia

sections (hiatus 27-18 Ma); 4) the middle Miocene is thick across the Delmarva but thin south of the CBIS, while late-mid Miocene (13-8.4 Ma) sections pinch out just north the CBIS; and the 5) upper Miocene-Pliocene is thick and well developed in the CBIS and adjacent regions, but poorly represented in New Jersey. We explain these observations by tectonic movements of crustal blocks, compaction of impact materials, and changes in sediment supply: 1) thick upper Eocene crater sequences are attributed to the rapid infilling of the crater and subsequent impactite compaction; 2) regional sediment starvation and tectonism resulted in thin, highly dissected Oligocene sequences; 3) regional uplift of the Norfolk arch occurred during the early Miocene, while the accumulation of thick prograding sediments occurred in New Jersey and Delaware; 4) progradation of thick sequences occurred throughout the region in the middle Miocene, with tectonic uplift of the Norfolk arch from 13-8.4 Ma; and 5) preservation of upper Miocene-Pliocene sequences in the CBIS and Virginia region reflect relative subsidence versus relative uplift in New Jersey and Delaware. We suggest that uplift and excess subsidence was caused by differential movement of basement structures in response to variations in intraplate stress.

Introduction

The late Eocene (35.4 ± 0.1 Ma; Pusz et al., in review) Chesapeake Bay Impact Structure (CBIS) is a remarkably intact 85-90-km diameter crater that underlies the Chesapeake Bay area and lower Delmarva Peninsula in eastern Virginia, U.S.A. (Fig. 1) (Poag et al., 1994, 2004; Powars and Bruce, 1999). The CBIS is a complex “inverted sombrero”

impact structure, consisting of a central peak ringed by a 38-km wide central basin, 24-km diameter annular trough, and extensive outer fracture zone (Figs. 1, 2) (Poag et al., 1994, Powars and Bruce, 1999; Powars, 2000). The CBIS, one of only a handful of well-preserved marine-impacts (Sanford et al., 2004), formed when a 2-3 km diameter bolide impacted the continental shelf. Following impact, the crater catastrophically infilled with impactites, mega-block breccias, and tsunamites that were subsequently buried by passive margin sediments (Poag et al., 1994; Powars and Bruce, 1999). Post-impact sediments consist of 400-500 m of upper Eocene to Recent marine shelf and coastal plain sediments that thicken into the impact structure (Fig. 2) (Powars and Bruce, 1999; Poag, et al., 1994).

Scientific investigation of CBIS dates back to its discovery by Poag et al. (1994). The United States Geological Survey (USGS) and the Virginia Department of Environmental Quality cooperatively drilled a series of coreholes, including those shown in Fig. 1: Exmore, Kiptopeke, Bayside, Cape Charles, Dismal Swamp, Fentress, and Langley (the latter a cooperative project with the Hampton Roads Planning District Commission) that penetrated both impact and post-impact sections. Cooperative drilling of the Eyreville coreholes (funded by the International Continental Scientific Drilling Project, USGS, and NASA) was completed in May 2006 and provided the first complete post-impact section (~444 m) from the inner crater moat (Fig. 2). Although previous studies examined post-impact strata within the annular trough (e.g., Powars, 2000; Horton et al., 2005), the lack of continuous core and associated data in the central moat limited our understanding of crater-wide evolution. Furthermore, a majority of previous interpretations were focused

on regional mapping (e.g., lithostratigraphic and hydrogeologic units) and had only broad biostratigraphic age control with limited isotopic data (e.g., Powars et al., 1992; Powars and Bruce, 1999; Powars, 2000; Poag et al., 1997; Poag et al., 2000). These previous studies lack high-resolution chronostratigraphic analysis and therefore provided limited information on temporal correlations and the processes that shape the evolution of post-impact strata. Detailed biostratigraphic work from the recently completed Langley corehole in the western annular trough (Fig. 1; Powars et al., 2005; Edwards et al., 2005) offers an excellent point of calibration to the inner crater at Eyreville.

We use sequence stratigraphy, the subdivision of the stratigraphic record into genetically related units bounded by unconformities and their correlative conformities (e.g., Mitchum et al., 1977; Posamentier et al., 1988; Miller et al., 1997), to recognize depositional sequences and present the first continuous, high-resolution (~ 1 myr) chronostratigraphic record from the CBIS annular trough (Exmore, this study) and inner crater (Eyreville, Browning et al., this volume). Because sequence boundaries form in response to base-level lowerings, sequence stratigraphic analysis of these coreholes enables the first process-based evaluation of the mechanisms that shape the post-impact record, namely: 1) global sea-level changes; 2) variations in sediment supply; 3) regional tectonism (uplift and subsidence) and; 4) crater-specific processes (e.g., cooling and related subsidence, differential compaction of impact-generated crater materials, movement of crater-related faults).

The cores within the CBIS also provide expanded upper Eocene through Pliocene sections useful for assessing the controls of sequence deposition across the entire mid-Atlantic Coastal Plain (Fig. 3; northern North Carolina to New Jersey). The mid-Atlantic Coastal Plain is underlain by a series of alternating crystalline basement basins and arches (e.g., from south to north: Cape Fear Arch, Albemarle embayment, Norfolk arch, Salisbury embayment, South Jersey high, and Raritan embayment) that extend inland from the offshore Baltimore Canyon Trough (Fig. 1; Brown et al., 1972; Olsson, 1988). Though differential movement on these basins and arches has occurred (whether by “wrench’ tectonic faulting”; Brown et al., 1972; thermoflexural loading or regional warping of “rolling basins”; Owens et al., 1997), regional similarities can be attributed to sea-level change (Miller et al., 2005). More specifically, global changes in ice volume (glacioeustasy), determine the template of available sequences on the Atlantic Margin through changes in base-level and accommodation (Miller et al., 2005; Browning et al., 2006), while changes in regional tectonics and sediment supply can influence sequence expression.

Extensive drilling of the New Jersey shelf-slope (Ocean Drilling Program [ODP] Legs 150 and 174A) and coastal plain (ODP Leg 150X and 174AX) identified 33 Cenozoic sequences and linked middle Eocene-Miocene sequence boundaries with $\delta^{18}\text{O}$ increases, implicating a glacioeustatic control on sequence boundary genesis (Miller et al., 1998, 2005). Because eustasy is the primary control on sequence boundary genesis in New Jersey and Delaware, any observed differences across the southern mid-Atlantic margin

(both temporal and physical) reveal the scale and timing (e.g., 10's m in 1-5 myr) of regional and local mechanisms that influence the stratigraphic record.

The main objectives of this study are: 1) to provide a high-resolution record of sequences at the Exmore corehole within the CBIS annular trough; 2) compare with similar results from the inner crater moat at Eyreville (Browning et al., this volume); 3) extend correlations to Delaware and northern North Carolina using well logs and age control; and 4) gain insight into the processes that control sequence development within the CBIS and across the greater mid-Atlantic Margin. This study builds on the lithostratigraphic descriptions (Edwards et al., this volume) and sequence stratigraphic framework (Browning et al., this volume) from the Eyreville corehole. We also incorporate results from previous studies of Exmore, VA (Powars et al., 1992; Powars and Bruce, 1999; Powars, 2000), Bethany Beach, DE (ODP Leg 174AX; Miller et al., 2003; Browning et al., 2006), Langley, VA (Horton et al., 2005; Edwards et al., 2005; Powars et al., 2005) and several New Jersey coreholes (Miller et al., 2005). We provide new sequence stratigraphic interpretations from the Exmore corehole (currently archived at the Rutgers Rift-Drift Core Repository, <http://geology.rutgers.edu/corerepository.shtml>), and use numerous geophysical logs, USGS coreholes (Powars et al., 1992; Powars and Bruce, 1999), and state geological survey reports to extend regional sequence correlations across the mid-Atlantic Coastal Plain (Fig. 3).

Methods

In this study sequence stratigraphic analyses of the USGS Exmore corehole are used to identify sequence boundaries, systems tracts, critical surfaces (e.g., maximum flooding surfaces [MFS], flooding surfaces [FS], etc.), and lithofacies patterns. The Exmore corehole was completed in 1986 and is located in the northern CBIS annular trough several kilometers south of the outer rim (Fig. 1), making it an ideal point of comparison between CBIS sequences and those established in New Jersey and Delaware. Prior interpretations examined the litho- and biostratigraphy of the ~350 m post-impact section (Powars et al., 1992; Powars and Bruce, 1999; De Verteuil and Norris, 1996). We provide new sequence stratigraphic interpretations, including; 1) semi-quantitative grain-size analysis; 2) lithofacies and paleoenvironmental interpretation (including trace fossil analysis); and 3) Sr-isotopic age estimates.

Sequence boundaries in cores can be represented by: 1) sharp unconformable contacts; 2) lag gravels, phosphate accumulations, and shell beds; 3) rip-up clasts; 4) extensively bioturbated surfaces and reworked microfossils; 5) significant changes in lithofacies successions; and 6) geophysical log characteristics (Miller et al., 2004; Sugarman et al., 1995). Sequence boundaries are also recognized by temporal hiatuses (e.g., Van Wagoner et al., 1988) established from Sr-isotope stratigraphy and biostratigraphy. Although each sequence boundary is unique, a combination of these criteria can be used to identify significant periods of erosion and nondeposition (Olsson et al., 1988; Sugarman et al., 1995). Other significant contacts, such the MFS and FS, were defined on the basis of lithofacies successions, mineralogy (e.g., increase of glauconite, phosphorite, and carbonate), and geophysical log signatures (e.g., Miller et al., 1998).

Procedures for evaluating the Exmore corehole follow those for Eyreville (Browning et al., this volume) and previous New Jersey and Delaware cores (Browning et al., 2006). Exmore was described for lithology, paying careful attention to changes in grain size, sorting, mineralogy, color, sedimentary structures, critical contacts, and lithofacies changes. Quantitative grain size data was collected for all three coreholes at 5 ft sampling intervals. Samples were weighed and then washed through 63 and 250 μ m sieves to establish the percentage of clay/silt, fine to medium sand, and coarse sand and gravel. The percentage of minerals (quartz, glauconite, lignite, mica, carbonate, pyrite, etc.) was visually estimated using a microscope. Such data are valuable in establishing fining or coarsening upward trends, which can be key indicators of depositional environment and facies stacking patterns.

Eocene-Pleistocene sequences within the CBIS and at Bethany Beach, DE are generally characterized by either transgressive-regressive “coarsening-upwards” facies successions typical of the mid-Atlantic Margin (Fig. 4; Owens and Sohl, 1969; Owens and Gohn, 1985; Sugarman et al., 1995), or transgressive, fine-grained, deep-water packages that exhibit very little coarse-grained material. Most mid-Atlantic sequences commonly consist of thin, basal quartz sand, clay and silt corresponding to the Transgressive Systems Tract (TST of Posamentier et al., 1988) that are overlain by a coarsening-upwards succession of regressive fine to coarse quartz sand equivalent to the Highstand Systems Tract (Fig. 4; HST of Posamentier et al., 1988). Lowstand Systems Tracts (LST) are largely absent in the coastal plain sediments of Virginia, Delaware, and New Jersey

due to the updip position of coastal plain strata. Lowstand wedges and fans are generally located much farther offshore, while transgressive ravinement often reworks the updip expression of such deposits. Occasionally, lowstand deposits are preserved within incised valleys (e.g., Miller et al., 2004). Although this succession is typical of many sequences at Exmore (C6-C8, SM, Ea1, Ea2) and Bethany Beach (C1-M1), many older sequences within the inner crater at Eyreville (e.g., Eocene, Oligocene, C4-C6) and Exmore (Eocene, Oligocene, C5) were deposited in deep paleodepths (outer neritic-upper bathyal; 100-200 m), the result of excess accommodation from the compaction of impactites. As a result, they are dominated by fine-grained clay and silt, and sequence expression is subtle and difficult to identify. In cases where HST are poorly expressed or eroded, sequences can fine upwards or show no coarsening upwards pattern (Fig. 7; consistent with several fining-upwards packages identified by Powars et al., 1992).

Lithofacies are similar among the three coreholes, and appear consistent with a wave-dominated shoreface facies model (Browning et al., 2006, this volume). Post-impact sediments in the CBIS generally exhibit some parts of the following coarsening-upwards succession of lithofacies: 1) basal offshore thinly laminated to bioturbated silt, clay, and fine sand deposited below storm wave-base; 2) distal lower shoreface very fine sand with abundant interbedded silt; 3) lower shoreface bioturbated silty fine sand with abundant whole shells deposited below fair-weather wave base; 4) distal upper shoreface fine to medium sand exhibiting moderate to-heavy bioturbation; 5) upper shoreface to foreshore fine to medium beach-like sand with abundant shell fragments and cross bedding; 6) foreshore fine to coarse sand with opaque heavy mineral laminations; 7) lower estuarine

poorly sorted sand interbedded with lignitic clay and fine sand; and 8) fluvial to upper estuarine sandy to gravely cut and fill channels with occasional lignite, mud clasts, and sporadic clay laminae (Fig. 4). The uppermost estuarine and fluvial facies often incise and rework upper shoreface and foreshore facies. Sequences in the CBIS and Delaware exhibit significantly different lithofacies than the deltaically influenced sequences recovered in the Cretaceous and Cenozoic New Jersey Coastal Plain (e.g., basal glauconite shelf sand overlain by prodelta clay, delta front quartz sand, and marginal to non-marine delta plain deposits; e.g., Miller et al., 2004; Kulpecz et al., 2008).

Age control for the late Eocene-Pleistocene sequences at Exmore was largely derived from 32 Sr-isotopic age estimates (Fig. 5; Sr-isotope ages for Eyreville are presented by Browning et al., this volume) and previously published dinocyst zonations by de Verteuil and Norris (1996). Carbonate material from mollusk shells (both whole shells and large fragments) was used. However, intervals lacking whole shells required the collection of 5-10 mg of benthic foraminifera for Sr-analysis. Careful attention was applied to the collection of carbonate material, avoiding shells that exhibited evidence of post-depositional diagenesis, alteration, or clear signs of reworking and redeposition. Sr was extracted using the ion-exchange techniques of Hart and Brooks (1974) and run on an Isoprime Mass Spectrometer at Rutgers University. We use the Miocene Sr-isotopic regressions of Oslick et al. (1994) and Reilly et al. (2002) and Pliocene regressions of McArthur et al. (2001). We assign ages using the Berggren et al. (1995) timescale. Age errors for the late Oligocene-early Miocene (22.8-27.5 Ma) are ± 1 Ma (Reilly et al., 2002). The regression for 15.5-22.8 Ma exhibits errors of ± 0.61 Ma while the period

from 9.7-15.5 Ma exhibits errors of ± 1.17 Ma (Miller et al., 1991). Pliocene-Pleistocene age errors are ± 0.35 Ma. These errors are calculated at the 95% confidence interval for a single analysis.

An age-depth plot (Fig. 5) depicting Sr-isotopic and dinocyst age data against lithostratigraphic observations from core established the geochronology of sequences, hiatuses, and the post-impact section. We inferred sedimentation rates consistent with other marginal-marine to marine sections of the mid-Atlantic Coastal Plain established by Browning et al. (2006; this volume). The error range (the shaded red interval surrounding the blue “best fit” line) represents the range of interpretations, based on the previously discussed errors of Sr-isotopic dating coupled with the limitations of dinocyst age control. Sequence ages were determined by establishing a best-fit line between bounding hiatuses (consistent with reasonable sedimentation rates) that honored the available data. However, in several intervals multiple interpretations exist due to the divergence of bio- and Sr-isotopic age data (e.g., sequences C6 and SM; Fig. 5). In these cases the preferred interpretation is presented, and the error range was extended to include alternative interpretations (represented by dotted grey lines; Fig. 5).

Downhole gamma ray logs, a measure of naturally occurring radiation in sediment, have emerged as a useful tool for log-based facies interpretation and sequence correlation. Because fine-grained sediments, clays, glauconite sands, and phosphorites retain high levels of radioactive elements (K, Ur, Th), gamma logs are a good indicator of lithology (Rider, 2002). Although the thick (10-20 m), coarse-grained HST sands observed at

Bethany Beach, DE and New Jersey (Browning et al., 2006) are rare within the upper Eocene-middle Miocene sections of the CBIS, many sequences (C7-Ea2) still exhibit gamma values that gradually decrease upsection until a rapid deflection to high values at the capping sequence boundary (Fig. 4). However, in many older CBIS sequences (Eocene, Oligocene, C1-C6), the fine-grained lithology, lack of thick HST sands, and presence of phosphorite and glauconite often results in an elevated gamma signature throughout (Fig. 2). In these instances, sequence boundaries are visible by rapid and pronounced gamma ray inflections often exceeding 100 API. Maximum flooding surfaces (MFS) also exhibit pronounced gamma peaks due to condensed sections, even in fine-grained lithologies. Because coarse-grained intervals are important freshwater aquifers of the mid-Atlantic coastal plain, resistivity logs (the measure of pore fluid resistance to an electrical current) generally exhibit low values (e.g., ~10-50 ohms-m) in fine-grained “confining” intervals (e.g., transgressive shelfal clays and silts) and grade upwards to increasingly higher values (e.g., ~50-150 ohms-m) in coarse-grained shoreface sands of the HST (Fig. 4) (e.g., Sugarman et al., 2006).

We correlate the sequences identified at the Exmore corehole (this study) to similar results from Eyreville, VA (Browning et al., this volume) and Bethany Beach, DE (Browning et al., 2006) on the basis of age, lithostratigraphy, sequence stratigraphy, and geophysical log character (Figs. 2, 3; Table 1). Core-geophysical log integration from the three coreholes was used to identify log patterns of each sequence (generally repetitive coarsening upwards packages in the Pliocene and middle Miocene; Browning et al., 2006; Powars and Bruce, 1999) and bounding sequence boundaries (rapid gamma spikes

in fine-grained Eocene, Oligocene, and lower Miocene CBIS sequences), although lateral facies variability, regional unconformities, and stratigraphic pinch-outs complicated log correlation on regional scales (We also provide the confidence in each sequence boundary pick in Tables 3, 4). To overcome these limitations, we also used published data (litho- and biostratigraphy) from several USGS coreholes and wells (e.g., Powars et al., 1992; Powars and Bruce, 1999; Powars, 2000; Powars et al., 2005; Edwards et al., 2005) to increase the accuracy of regional correlations (Fig. 1). Although these cores do not provide the same geochronologic resolution of Exmore, Eyreville, and Bethany Beach, they provide valuable age constraints with good (~1-3 myr) resolution.

For example, sequences SM and Ea1 (dated from Sr-isotopes at Eyreville as 8.3-8.0 Ma and 7.7-7.2 Ma, respectively; Table 1) are correlated to the USGS Langley corehole on the basis of log character and biostratigraphy by Edwards et al. (2005). The interval from 300.3-182.0 ft contains nannofossil zones NN 11-12 (~ 8.6-5.6 Ma) and dinocyst zones DN 9-10 (8.7-5.8 Ma) that confirm our correlations to sequences SM and Ea1. A similar methodology was applied to other USGS coreholes (Fig. 1; Kiptopeke, Cape Charles, Fentress, Dismal Swamp, Bayside) pending the availability of biostratigraphic data.

Correlation north of the crater (Figs. 1, 3) was more difficult due to the lack of coreholes between Exmore, VA and Bethany Beach, DE (118 kilometers). Correlations were accomplished using 38 geophysical logs (both gamma and electric) obtained from state geological surveys, the Virginia Tech Regional Geophysics Laboratory, U.S. Department of Energy, and USGS. We utilized existing publications (Olsson et al., 1987; Olsson,

1988) and numerous state geological survey reports (e.g., Hansen and Wilson, 1984; Hansen and Wilson, 1990; Andreason and Hansen, 1987; Hansen and Lang, 1980; and Andres, 2004) to constrain our correlations across the Maryland and Delaware Coastal Plains (Fig. 1). Many of these reports are founded on lithologic and biostratigraphic studies from outcrop and core, and contain useful information regarding regional age and lithostratigraphic trends. Although the geochronologic resolution is somewhat coarse (2-5 myr), several reports (e.g., Olsson et al., 1987) document the presence of significant unconformities that may coincide with sequence boundaries identified in our study. Additional reports from the Delmarva Peninsula were included in this study to lend regional context, but are not depicted on the regional transect (Figs. 1, 3).

Data and Results- Exmore Corehole

Twelve to sixteen late Eocene through Pleistocene depositional sequences were recovered in the Exmore (this study) and Eyreville (Browning et al., this volume) coreholes within the Chesapeake Bay Impact Structure (Figs. 5, 6, 7). These results were compared to the record from Bethany Beach, DE, where 16-19 uppermost Oligocene through Pleistocene sequences were identified by Browning et al. (2006). The different number of sequences represents both: 1) the differential preservation of sequences between coreholes; and 2) the presence of tentatively identified sequences that lack conclusive geochronology. We present the sequence stratigraphic and geochronologic interpretations of the USGS Exmore corehole and refer to Table 1 for a comparison of sequences at Eyreville and Bethany Beach.

Late Eocene Sequence(s)- 1191.2-1110.7 ft; 363.08-338.54 m

We identify one, and possibly two, fine-grained transgressive sequences within the upper Eocene Chickahominy Formation (Fig. 7). The lower sequence consists of transgressive outer shelf light gray clay with minor amounts of very fine sand, rare whole shells, trace glauconite, and abundant phosphatized fish scales. The interval exhibits moderate to intense bioturbation, except for laminated clays from 1181.1-1179.0 ft (360.0-359.36 m). Light gray clay extends upwards to a subtle burrowed contact and possible sequence boundary at 1160.0 ft (353.57 m). The overlying sequence is dominated by a bioturbated, occasionally shelly, slightly silty clay with several pyritic concretions and phosphatized bone material at 1159.2 ft (353.32 m). The abundance of small clay-filled *Planolites* and *Chondrites* trace fossils in concentrated intervals supports the interpretation of a mid- to outer shelf “reducing” depositional environment. The upper contact was not recovered due to a coring gap, and is placed at 1110.7 (338.54 m; consistent with Powars and Bruce, 1999) on the basis of a gamma shift, thus separating the underlying clays from slightly glauconitic sandy silt above (Fig. 7). No Sr- dates were obtained for this interval, and it is correlated to dated sections at Eyreville and Langley (Fig. 2; Table 1). We identify these sequences as transgressive in nature, with no clear HST sands due to the environment of deposition on a deep mid- to outer shelf within the initial bathymetric low of the CBIS (a result of excavation and infilling resulting in 50-200 m paleodepths in the annular trough versus middle shelf conditions [30-100 m] in nearby coreholes; Poag et al., 1994).

Oligocene Sequences- 1110.7-1024.1 ft; 338.54-312.15 m

The Oligocene section in the Exmore corehole is poorly preserved and highly desiccated; making the identification of primary sedimentary structures and contacts extremely difficult. We identify two bioturbated contacts within this Oligocene section, separating three individual sequences. Bioturbated silty clay (TST) overlies the basal sequence boundary (1110.7 ft; 338.54 m) and coarsens upwards (above a MFS at 1104.2 ft; 336.56 m) to slightly glauconitic, slightly micaceous, bioturbated fine sandy silt with scattered small (> 1 mm) shell fragments deposited in a distal lower shoreface environment (HST). A significant contact at 1069.4 ft (325.95 m) separates green to black glauconite sands above from the largely non-glauconitic sandy silt below and is interpreted as a sequence boundary. This contact was previously recognized as separating the lower Oligocene Delmarva beds (P 18-20) from the upper Oligocene Old Church Formation (P21a; Powars et al., 1992; Powars and Bruce, 1999). The Old Church was subsequently reclassified as the Drummonds Corner Beds (Powars et al., 2005). Several glauconite filled burrows are visible beneath the contact, including a spectacular *Teichichnus* burrow at 1070.1 ft (326.17 m) and an elongate 6-cm vertical burrow at 1071.5 ft (326.59 m).

The interval above 1069.4 ft (325.95 m) is dominated by coarse-grained glauconite sand with a silty and clayey matrix. Although the interval is poorly recovered, we identify a contact and possible sequence boundary at 1049.7 ft (319.95 m) on the basis of several indurated clasts of glauconitic clay within an interval of indurated silt and clay (Fig. 7). The overlying section is similarly glauconitic, and extends to a heavily indurated zone at

1037.6 ft (316.26 m) that preserves a bioturbated contact, also identified as a potential sequence boundary, between clay dominated section below and glauconite dominated section above. Clayey glauconite sands extend upwards to a spectacular contact at 1024.1 ft (312.15 m) that caps an extensive zone (0.7 ft; 0.21 m) of heavily bioturbated and reworked glauconite sand and silty clay from overlying mid-Miocene sediments (17.5-17.3 Ma). These glauconite rich Oligocene sequences were deposited in sediment starved, mid- to outer shelf paleoenvironments and are largely transgressive in nature.

We identify the interval from 1110.7-1069.4 ft (338.54-325.95 m) as lower Oligocene based on Sr-age estimates of 33.8-32.6 Ma and previous work (Powars et al., 1992; Powars and Bruce, 1999), and correlate it to sequence O1 defined from the New Jersey Coastal Plain (Pekar et al., 2000). Insufficient shell and benthic material in the interval from 1069.4 to 1024.1 ft (325.95-312.15 m) prevented Sr-isotopic analysis, although previous work (Powars et al., 1992; Powars and Bruce, 1999; De Verteuil and Norris, 1996) identified this interval as upper Oligocene (Old Church Formation) from planktonic foraminifera and dinocyst data. We tentatively identify two sequences in this section, separated by a likely sequence boundary at 1037.6 ft (316.26 m), and use geophysical logs and lithologic similarity to correlate them to the Eyreville (Browning et al., this volume) and Langley coreholes (Edwards et al., 2005). From correlation to dated section at Eyreville, the interval from 1069.4-1037.6 ft (325.95-316.26 m) is tentatively identified as sequence O4 (27.7-27.6 Ma) while the unit from 1037.6-1024.1 (316.26-312.15 m) is identified as sequence O5 (26.65-26.5 Ma) as defined in New Jersey (Pekar et al., 2000).

Sequence C5 (Lower Miocene)- 1024.1-1014.1 ft; 312.15-309.10 m

A heavily burrowed contact at 1024.1 ft (312.15 m) separates Oligocene glauconitic sand from overlying transgressive, slightly glauconitic, carbonaceous clay deposited on a marine shelf. This unit contains many small shell fragments and extends to a heavily bioturbated upper contact with overlying non-glauconitic silty clay at 1014.1 ft (309.10 m) interpreted as a sequence boundary (Fig. 7). The lack of whole shells makes Sr-dating difficult and a single sample retrieved from the lower reworked and burrowed zone (1027.1 ft; 313.06 m) yielded an age of 17.6 Ma (Fig. 5). De Verteuil and Norris (1996) identified this interval as DN3 (~19.0-16.7 Ma; sample from 1021.0 ft; 311.20 m), while Powars et al. (1992) classified this interval as the Newport News unit, and recorded possible planktonic foraminifera Zone N8 (~16.4-15.2 Ma). We tentatively identify this interval as sequence C5 (17.7-17.5 Ma) based on the overlap of DN3 with one Sr-isotope age estimate, and correlate it to similar sequences recognized at the Eyreville and Bethany Beach coreholes (Fig. 2; Table 1).

Sequence C6 (Middle Miocene)- 1014.1-786.7 ft; 309.10-239.79 m

Overlying a contact at 1014.1 ft (309.10 m) is an interval of shelfal bioturbated slightly silty clay with scattered small shell fragments, black phosphorite grains, fish scales, and abundant *Planolites* trace fossils interpreted as the TST (Fig. 7). This interval is assigned to the Calvert Formation (Powars and Bruce, 1999). Trace amounts of glauconite overlie this contact, but appear to be reworked from underlying units. The interval consists of

fairly uniform bioturbated silty clay to ~875 ft (266.70 m), although laminated clay with minor silt (1-3 mm laminae) extends from 972.1-953.4 ft (296.30-290.60 m). A gamma inflection and increase in clay and carbonate at 936.3 ft (285.38 m) is interpreted as an MFS. Above this interval, intensely bioturbated clay extends upsection and individual trace fossils are not well-defined. At 875.0 ft (266.70 m), the overall lithology coarsens to clayey silt with small amounts (2-5%) of carbonate material and very fine sand increasing upsection representing the lower HST. The percent of fine sand peaks below a surface at 836.7 ft (255.03 m), which may represent a flooding surface and parasequence boundary (Fig. 7). The section further coarsens upwards from clayey silt at 815.4 ft (248.53 m) to bioturbated silty fine quartz sand with abundant shell fragments deposited in a distal lower shoreface (upper HST). Several large *Thalassinoides*, sand-filled *Planolites*, and other back-filled burrows (e.g., large *Diplocraterion* trace fossil at 804.2 ft; 245.12 m) characterize this interval (*Skolithos* ichnofacies). A burrowed contact at 786.7 ft (239.79 m) separates the underlying fine sands from offshore silts above, and caps an extensive (790.4-786.7 ft; 240.91-239.79 m) heavily reworked zone that exhibits abundant trace fossils of the *Cruziana* ichnofacies (marine shelf). We interpret a shallowing upwards progression of paleoenvironments in this thick (227 ft; 69.19 m) sequence from basal outer shelf, to inner shelf, and distal lower shoreface.

Establishing the geochronology of this sequence was difficult due to the divergence of Sr-isotopic data and planktonic foraminifera zones from dinocyst zones. Four Sr-dates at the base of the sequence were clustered from 16.1-15.5 Ma, an interval of high confidence with low Sr-age errors (e.g., Miller et al., 1991). Planktonic foraminifera

Zones N8 and N9 (~16.4-14.8 Ma) reported by Powars and Bruce (1999) are consistent with this interpretation. However, de Verteuil and Norris (1996) identify five samples between 1013-951 ft (314.25-289.86 m) as DN3 (~19.0-16.7 Ma) which is not consistent with the Sr-isotopic and foraminiferal age constraints. Above this interval, de Verteuil and Norris (1996) identified zones of DN4 (~16.7-15.1 Ma; 941-901 ft; 286.82-274.62 m) and DN5 (~15.1-13.1 Ma; 883-799 ft; 269.14-237.44 m) that are consistent with other age estimates. We interpret the base of sequence C6 using planktonic foraminifera and Sr-isotopic data (~16.3 Ma), and the upper portion of the sequence with DN4 and DN5 assignments. The combination of these data sets date this interval as 16.3-14.8 Ma (Fig. 5), and it is correlated to sequence C6 as identified in the Eyreville and Bethany Beach coreholes (Fig. 2; Table 1).

Sequence C7 (Middle Miocene)- 786.7-650.9 ft; 239.79-198.39 m

Above a heavily burrowed contact at 786.7 ft (239.79 m), is very uniform light gray, fine sandy, slightly clayey, bioturbated silt with abundant backfilled and clay-lined burrows (*Teichichnus*, *Asterosoma*, and *Planolites*) deposited on a marine shelf (TST; Fig. 7). The section coarsens upwards to heavily bioturbated, silty fine sand with large (~1-cm diameter) sand-filled shafts of interconnected *Thalassinoides* burrows (e.g., 659.9-658.0; 201.14-200.56 m). A possible MFS at 739.8 ft (225.49 m) corresponds with a slight increase in clay, and a gamma ray inflection. These upper sands are interpreted as distal lower shoreface, represent the HST, and underlie a subtle burrowed contact at 650.9 ft (198.39 m) and shelfal fine sandy silt above. Previous studies (Powars et al., 1992;

Powars and Bruce, 1999) identified this interval as the Calvert Formation. Carbonate material in this interval was sparse, and three benthic foraminifera samples yielded Sr-ages of 14.4, 11.6, and 11.7 Ma (Fig. 5). De Verteuil and Norris (1996) identified this interval as DN5 (~15.1-13.1 Ma), while Powars et al. (1992) identified planktonic foraminifera Zone N9, both consistent with the older Sr-date of 14.4 Ma. The younger Sr-age estimates appear to have been diagenetically altered, and are excluded from age interpretations. We estimate the age of this sequence as 14.5-14.1 Ma, which correlates to Sequence C7 at Eyreville and Bethany Beach (Fig. 2; Table 1).

Sequence C8 (Middle Miocene)- 650.9-507.8 ft; 198.39-154.78 m

The interval from 650.9-507.8 ft (198.39-154.78 m) is a classic coarsening upward sequence and consists of fairly uniform bioturbated fine sandy silt (above the contact at 650.9 ft [198.39 m] interpreted as a sequence boundary) with several thin intervals of planar (below 638.2 ft; 194.52 m) and faint cross lamination (625.3 ft; 190.59 m). Above a burrowed surface and gamma peak at 632.1 ft (192.66 m; interpreted as a MFS), these shelfal silts (TST) shallow and coarsen upwards to burrowed silty fine sands deposited in a distal lower shoreface (HST; Figs. 6, 7). This sandy interval exhibits several small phosphate nodules at 539.7 ft (164.50 m) and contains 1-2% opaque heavy minerals. The entire section to 507.8 ft (154.78 m) was initially assigned to the Calvert Formation (Powars et al., 1992). However, this sand is sandwiched between finer grained units assigned to the Calvert and St. Marys Formations above and below, respectively; at the Eyreville corehole a similar coarser grained unit was assigned to the Choptank Formation

(Edwards et al., this volume). Two possibilities exist: 1) the sandy interval from 520.0-507.8 ft (158.50-154.78 m) represents the Choptank Formation; or 2) the underlying fine sands are included, and the interval from 628.0-507.8 ft (191.41-154.78 m) represents the Choptank Fm. Although we present both options (Figs. 5, 7), comparison with Eyreville (Edwards et al., this study) supports the first option and we assign the sandy interval from 158.50-507.8 ft (158.50-154.78 m) to the Choptank Formation. Regardless of the interpretation, the coarser-grained interval from 628.0-507.8 ft (191.41-154.78 m) is interpreted as the HST of sequence C8. Above 522.4 ft (159.23 m), the interval gradually fines to sandy, silty clay until a spectacular burrowed contact at 507.8 ft (154.78 m) characterized by a network of large chambers filled with coarse quartz sand of the overlying unit. We interpret this as a *Glossifungites* surface, representing an eroded firmground (e.g., Pemberton, 1998; Pemberton et al., 2004) and recording a major hiatus separating two sequences.

Two Sr-isotopic age estimates of 13.4 and 12.1 Ma were recovered in the uppermost portion of the sequence. The older of these is consistent with the interpretations of de Verteuil and Norris (1996), who classified the entire section as DN5 (~15.1-13.1 Ma). Subsequent work by L. Edwards reinterpreted sample 1712-22 (513 ft; 156.36 m) as DN6 (~13.1-12.6 Ma). Powars et al. (1992) also identified the section below 507.8 ft (154.78 m) as N9-10 (~15.1-12.8 Ma). Dinocyst and Sr-isotope age estimates date this sequence as 13.6-13.0 Ma, and it is identified as C8 as recovered at both Eyreville and Bethany Beach (Fig. 2; Table 1). The surface at 507.8 ft (154.78 m) records a major hiatus, from sediments below (13.6-13.0 Ma) to those immediately above, classified as DN9 (~7.4-8.6

at 501 [152.70 m] and 493 ft [150.27 m]; de Verteuil and Norris, 1996) and dated at 9.9-9.8 Ma by Sr-isotopic analysis.

Sequence M1 or LST Sequence SM (Upper Miocene)- 507.8-496.6 ft; 154.78-151.36 m

A thin (507.8-496.6.0 ft; 154.78-151.36 m) unit overlies the *Glossifungites* surface and consists of basal fine to medium sand that coarsens upward to coarse to slightly clayey very coarse quartzose sand at 506.4 ft (154.35 m; Fig. 6). This contact was initially recognized as a major unconformity separating the Calvert (middle Miocene) and St. Marys (upper Miocene) Formations by Powars and Bruce (1999), although subsequent work indicates the presence of the Choptank Formation below 507.8 ft (154.78 m). Within this interval are numerous shell fragments ranging from 0.3-2.5 cm (504.0-503.8 ft; 153.62-153.56 m), 2-3 cm long chocolate brown lignitic material with original woody textures preserved at 506.2 ft (154.29 m), and a clay rip up clast at 506.4 ft (154.35 m). Above 503.9 ft (153.59 m), the section fines to a fine to medium sand that is interbedded with silt and clay and contains sand-filled burrows. We interpret the lower sands of this interval as estuarine to nearshore, and the upper heterolithic interbeds as estuary fill. The upper contact is placed at 496.6.0 ft (151.36 m), coincides with the uppermost sand burrow, and caps the gradational transition from lower coarse sands to overlying marine clay. Multiple interpretations exist for the interval from 507.8-496.6 ft (154.78-151.36 m): 1) the upper contact is a sequence boundary on the basis of a major shift in depositional environments (estuarine below, deep shelf above) and records a possible hiatus; 2) the entire interval represents the LST of the overlying sequence SM (estuarine

sands preserved in a possible incised valley), and the upper contact represents a transgressive surface capped by marine shelf facies; or 3) the wood, shell fragments, rip up clasts, and broad range of ages in this interval represent part of the transgressive lag during a relative rise in sea level (TST).

Sr-isotope age estimates are inconclusive for this thin section. Two dates of 9.9 and 9.8 Ma occur within this interval, while a date of 10.8 Ma was recovered in the upper reworked zone. De Verteuil and Norris (1996) identified this interval as DN9 (~8.6-7.4 Ma) from samples at 501 and 493 ft (152.70 and 150.27 m, respectively). If the two Sr-dates are used, this thin interval is dated as 9.9-9.8 Ma, the upper contact is interpreted as a sequence boundary (overlying sequence SM dated 8.4-7.9 Ma) and this thin “sequence” can be correlated to M1 recovered at the Bethany Beach, DE corehole (Fig. 3; Table 1; Browning et al., 2006). The preferred interpretation classifies this interval as entirely DN9 (~8.6-7.4 Ma), and this thin unit is interpreted as the LST of sequence SM (approx. 8.4 Ma; Fig. 2; Table 1). The presence of older Sr-age estimates is interpreted as reworked material from lowstand valley incision and subsequent transgressive winnowing.

Sequence SM (Upper Miocene)- 496.6-397.0 ft; 151.36-121.01 m

Above a contact with the LST of sequence SM at 496.6 ft (151.36 m) is a very fine-grained interval (496.6-446.0 ft; 151.36-135.94 m) dominated by gray, slightly silty, bioturbated clay (interpreted as the TST) with trace amounts of mica, rare scattered shell

fragments, and numerous fish scales and phosphatized material (concentrated below 490 ft; 149.35 m) that is typical of transgressive lag deposits. Bioturbation is intense but dominated by small unidentifiable trace fossils, with several concentrated intervals of *Chondrites*. A slight increase in clay and corresponding gamma ray peak at 476.5 ft (145.24 m) may represent a MFS. We interpret the depositional environment as mid- to outer shelf, occurring within the St. Marys Formation. Above 446.0 ft (135.94 m), the section coarsens to brown to gray, slightly micaceous, bioturbated clayey silt with small amounts (5-10%) of fine quartz sand increasing upsection. Numerous large and well-developed trace fossils (distal *Cruziana* ichnofacies) are dominated by *Asterosoma*, but also include numerous *Planolites*, *Paleophycus* (410.5 ft; 125.12 m), and *Teichichnus* burrows (427.0 ft; 130.15 m). The interval from 446-406.7 ft (135.94-123.96 m) appears shallower than the underlying clays, and is interpreted as inner- to middle shelf (HST). An irregular, scoured contact at 406.7 ft (123.96 m) separates this interval of clayey silt from an overlying sandy, shelly interval that consists of numerous 1-2 cm diameter, well rounded, rip-up clasts composed of silty clay (similar to underlying units) and a fine-grained shell hash suspended in a clayey matrix. The unit above this reworked interval consists of bioturbated, occasionally shelly, slightly clayey, silty fine sand (interpreted as distal lower shoreface) that persists to a subtle, gradational contact at 397.0 ft (121.01 m) with overlying silty clay to clayey silt.

There are two possibilities for 406.7-397.0 ft (123.96-121.01 m); 1) the unit is an individual sequence, both the upper and lower contacts represent sequence boundaries; or 2) there is no hiatus at 406.7 ft (123.96 m) and the contact represents a possible wave

ravinement surface (accounting for the rip up clasts and concentration of shell material) and facies shift to the uHST of sequence SM. Sr-age estimates (10.6, 10.3 and 7.1 Ma) are inconclusive for this sequence. The two older values are not consistent with assignment to Zone DN9 (~8.6-7.4 Ma; De Verteuil and Norris (1996). The uppermost Sr-age estimate (7.1 Ma) is consistent with this zone. The sequence is dated as 8.4-7.9 Ma and identified as sequence SM recovered at the Eyreville corehole (Fig. 2; Table 1; Browning et al., this volume). Biostratigraphic work from the Langley (Edwards et al., 2005) and Kiptopeke coreholes (Powars and Bruce, 1999) also support this interpretation. Because no hiatus can be established across the contact at 406.7 (123.96 m), we believe it represents the transition to the uHST of sequence SM (507.8-397.0 ft; 154.78-121.01 m).

Sequences Ea1 and Ea2 (Upper Miocene)- 397.0-181.0 ft; 121.01-55.17 m

The interval from 397.0-360.1 ft (121.01-109.76 m) is characterized by very fine sandy, silty clay to clayey silt with abundant scattered shells, mainly turritellids. Although several faintly laminated intervals are visible (370.1-387.8 ft [112.81-118.20 m]; 391.0-391.3 ft [119.18-119.27 m]), bioturbation dominates the primary texture and numerous *Asterosoma* and *Planolites* trace fossils are evident. This paleoenvironment is interpreted as middle to inner shelf and represents the TST (Fig. 6). Above a MFS at 360.1 ft (109.76 m; clayey section with corresponding gamma peak), the section coarsens to alternating indurated and non-indurated micaceous, slightly clayey, very shelly, silty fine sand with extensive bioturbation (primarily *Asterosoma* trace fossils) and abundant whole and fragmented turritellids, oyster, and mollusk shells (lower HST). Powars and Bruce (1999)

placed the Eastover-St. Marys contact at the base of a non-recovered interval at 326 ft (99.36 m), separating sandy shelly fine sand above from finer-grained sediments below. The section from 315.2-312.0 ft (96.07-95.10 m) consists of very shelly bioturbated fine sand with evidence of cross lamination and is interpreted as distal lower shoreface, representing the transition from the lower to upper HST (Fig. 6). Cemented intervals effervesce slightly with hydrochloric acid, exhibit numerous vugs, moldic porosity, and appear localized around shelly intervals, the likely source of carbonate cement. These indurated zones continue upsection to 230.2 ft (70.16 m) and resulted in very poor recovery (< 20%) from 360-230 ft (109.73-70.10 m). We interpret the shelly, sandy interval from 360-181 ft (109.73-55.17 m) as predominantly lower shoreface with several coarser intervals representing possible upper shoreface (Fig. 6). A large coring gap from 221.0-186.0 ft (67.36-56.69 m) prevents analysis of lithology, although log correlation with Eyreville suggests a sequence boundary at 220 ft (67.06 m) coinciding with a gamma inflection (Fig. 2).

Although seven Sr-age dates cluster around 7.2-6.7 Ma, Sr-age estimates alone are inconclusive given the error ranges during the late Miocene (Fig. 5). Dinocyst data from de Verteuil and Norris (1996) identified DN9 (~8.6-7.4 Ma) at the base of the section, overlain by transitional DN9 and DN10 (~7.4-6.1 Ma), and exclusively DN10 between 220.0-181.0 ft (67.06-55.17 m). These changes in dinocyst zones across the contact at 220 ft (67.06 m), coupled with Sr-age data and regional correlation, lead to the interpretation of two sequences within the Eastover Formation. The sequence from 397-220.0 ft (121.01-67.06 m) is identified as Ea1 and dated at 7.7-7.3 Ma (Fig. 5), while the

poorly recovered interval from 220.0-185.0 (67.06-56.39 m) is identified as lower Ea2 (6.7-6.5 Ma). Both sequences are correlated to the Eyreville corehole (Fig. 2; Table 1; Browning et al., this volume). A bioturbated contact at 181.0 ft (55.17 m) caps a reworked interval (186.7-181.0 ft; 56.91-55.17 m) consisting of shelly, clayey, silty fine sand intermixed with down-burrowed coarse to very coarse quartz sand, pebbles, shell fragments, and phosphatic material. This contact represents a major erosive surface and is interpreted as the base of a Pleistocene Exmore paleochannel identified by Powars and Bruce (1999) that we date as 1.0-0.3 Ma. The late Miocene-Pliocene sequences (Yk1, Yk2, and CR) identified at the Eyreville corehole (Browning et al., this volume) are not recovered, and were eroded by the incision of the paleochannel (Fig. 2) as shown by regional mapping (Powars et al., 1992; Powars and Bruce, 1999).

Pleistocene sequences- 181.0-26.1 f; 55.17-7.96 m

The section from 181.0 to 26.1 ft (55.17-7.96 m) consists of a heterolithic interval of Pleistocene sediments (Fig. 6). Poor core recovery and condition (majority of sands are desiccated and disassociated) complicates lithofacies interpretations and the identification of primary sedimentary structures. A sharp basal contact at 181.0 ft (55.17 m) is overlain by slightly silty, poorly sorted, coarse to very coarse quartz sand. Although the interval from 181.0-136.0 ft (55.17-41.45 m) is poorly recovered, large indurated cobbles, clasts and pebbles were recovered at 180.6 (55.05 m) and 163.2 ft (49.74 m). At 132.5 ft (40.39 m), the medium to coarse sands are mixed with quartz granules, 2-3% opaque heavy minerals, and exhibit faint cross bedding. We interpret this succession as fluvial in origin,

consistent with the interpretation of Powars and Bruce (1999). A fining upwards gradational contact from 128.2-131.2 ft (39.08-39.99 m) shifts from fluvial coarse sand to interlaminated micaceous silty clay to clayey silt with very fine sand concentrated in planar interbeds. Several laminated intervals change orientation, inclination, and exhibit wavy bedding (e.g., 110.6 ft; 33.71 m). Burrows are generally sporadic, small and sand filled. Fine-grained shell debris is scattered throughout, and rare organic material is observed above 102.9 ft (31.36 m). Post-coring sulfur staining is visible from 83-73 ft (25.30-22.25 m), and we interpret this paleoenvironment as estuarine or lagoon. A sharp contact at 63.6 ft (19.39 m) separates finer-grained lithologies from structureless, slightly micaceous, fine to medium quartz sand with granules and small pebbles that extends to another sharp contact at 58.2 ft (17.74 m). Above this surface, a thin interval of white to gray bioturbated, sandy, silty clay extends to 52.8 ft (16.09 m), where it coarsens upwards to a yellow to white structureless fine to coarse quartz sand with 1-2 % opaque heavy minerals and occasional granules and small pebbles. Because of the poor condition of the core, we tentatively identify the depositional environment from 52.8-26.0 ft (16.09-7.92 m) as proximal upper shoreface to estuarine, with contacts at 41.4 ft (12.62 m) and 39.7 ft (12.10 m) representing facies changes (Powars, personal comm.). Sr- isotope dates of 1.0-0.5 Ma were obtained for the laminated silts below 73.0 ft (22.25 m). An additional date at 53.7 ft (16.37 m) yielded an age of 0.33 Ma, implicating one of the contacts at 63.6 ft (19.39 m) or 58.2 ft (17.74 m) as another sequence boundary (Fig. 6). We identify the contact at 63.6 ft (19.39 m) as an unconformity generated by the incision of an estuarine channel, overlain by finer-grained estuary fill deposits from 58.2-52.8 ft (17.74-16.09 m). These Pleistocene sequences are significantly thicker than those at

Eyreville (Fig. 2; Table 1), and are classified as part of the Omar Formation (Powars and Bruce, 1999). Mixon et al. (1992) estimated the Exmore paleochannel as either stage 8 (270 ka) or stage 12 (430 ka). The interval from 26.1 ft (7.92 m) to ground surface is interpreted as surficial.

Discussion

Post-Impact Evolution of the CBIS

Our study shows that post-impact sedimentation was largely controlled by global sea-level change, and overprinted by the differential compaction of impactites, variations in sediment supply, and periods of regional uplift and subsidence. The timing of sequence boundaries both outside (Bethany Beach) and within the CBIS (Eyreville, Exmore) show strong correspondence to ice volume increases inferred from oxygen isotopic changes from the Oligocene through late Miocene arguing for a global control (Fig. 8). However, there are significant differences between CBIS sequences and coeval sections dated outside the crater that can be attributed to regional tectonism and sedimentation changes.

The upper Eocene is thickest and best developed in the central crater but is thin immediately around the crater. This pattern reflects the initial depression after the impact (outer neritic to upper bathyal paleodepths ranging from 75-400 m; Poag, submitted) and subsequent compaction and settling of thick impactite deposits within the CBIS, providing high rates of accommodation and an expanded section. The Oligocene is

generally thin and poorly represented throughout the mid-Atlantic region and consists of glauconitic sand and clay deposited on a sediment starved shelf, except for the southeastern New Jersey Coastal Plain where the Oligocene is quite thick (30-60 m; Miller et al., 1997; Pekar et al., 2000; Fig. 3; Table 2). Oligocene sequences (~33-24 Ma) are very thin within the central crater (~15 m) compared to the annular trough (50 m at Langley, Fig. 2; Table 2), representing sediment starvation of the central crater. The lower lower Miocene is thick (>150 m) and well developed in New Jersey and Delaware, but is patchy and very thin to absent in the CBIS and other Maryland-North Carolina sections (hiatus 27-18 Ma; Table 2). Extensive lower Miocene sequences are not recovered at Exmore or Kiptopeke, but the thin and patchy distribution is evident through: 1) biostratigraphic work from the Langley corehole (Edwards et al., 2005) that identifies possible sequence C1 (20.0-19.4 Ma); 2) dinocyst data from Eyreville that identifies a very thin package of sediment from 19.7-19.2 Ma (Browning et al., this volume); and 3) 10-13 meters of lower Miocene sediment recovered at the Jamestown corehole (Powars and Bruce, 1999). This southward thinning and patchy distribution of Oligocene-lower Miocene sequences is interpreted as the result of regional uplift of the Norfolk arch, accentuated by decreased sediment supply and possible sediment starvation in the southern Delmarva and CBIS area (Fig. 3).

The middle Miocene is well represented in New Jersey and across the Delmarva Peninsula, consisting of thick sequences characterized by high sedimentation rates (Browning et al., 2006). These sequences persist into the CBIS at Exmore, Eyreville, and Kiptopeke, but pinch out rapidly between Kiptopeke and Langley (Fig. 2) and are largely

thin to absent south (Fentress, Dismal Swamp) of the crater (Fig. 3), interpreted as regional uplift of the Norfolk arch (Fig. 3). The lower-upper Miocene sequences (C9, C10, M1; 11.9-9.8 Ma) thin progressively southwards, ranging from 20-60 m across the Delmarva Peninsula before pinching out north of Exmore between Tasley and Hallwood based on a significant change in log character and thickness (Fig. 3; Table 2). No sediments of this age were recovered within, or south, of the CBIS (Fig. 3), although Powars and Bruce (1999) document DN8 (~11.1-8.6 Ma) at the Jamestown corehole west of the CBIS. This southward thinning similarly reflects the coupling of regional tectonic uplift and decreased sediment supply of the CBIS area.

Upper Miocene-Pliocene sequences are marine to marginal-marine, and are thick and well developed in both the CBIS and adjacent regions (120-200 m) but poorly represented to absent in New Jersey (e.g. Miller et al., 2005). This is attributed to excess subsidence of the Salisbury embayment relative to the New Jersey Coastal Plain. Within the CBIS, upper Miocene-Pliocene sections thicken into the crater relative to adjacent sections in Virginia. Mapping and seismic data (Powars and Bruce, 1999) show that these intervals are thickest on the southern side of the crater due to the excess accommodation relative to the northern CBIS, where thick middle Miocene prograding packages filled much of the available space. These changes are visible on our regional transect (Fig. 3; Table 2), and we discuss the roles of each contributing factor in subsequent sections.

Eustatic Variations

Previous studies of the mid-Atlantic margin (Miller et al., 1996, 1998, 2005; Browning et al., 2006) identified glacioeustasy, sea-level change driven by variations in ice volume, as the dominant control on sequence formation. The timing of sequence boundaries at Bethany Beach, DE exhibits a nearly one-to-one correspondence with ice volume increases inferred from oxygen isotopic changes from the Oligocene through late Miocene (Fig. 8), although a period of excess subsidence caused by offshore depocenter loading is observed from 21-12 Ma. Many of these sequences can be correlated across the Delmarva Peninsula towards the CBIS (Fig. 3).

The comparison of oxygen isotope records (Fig. 8; Miller et al., 2005) to sequences within the CBIS show that sequence boundary formation was controlled by glacioeustatic falls. Periods demonstrating a strong correspondence between sequence boundaries and $\delta^{18}\text{O}$ isotope increases include the middle Miocene (sequences C5-C8), the late Miocene (sequences SM, Ea1, Ea2; although each sequence boundary is only 100-200 ka in duration), the Pliocene recovered at Eyreville (sequences Yk1, Yk2 and CR; Browning et al., this volume), and the Pleistocene sequences (dated at 400-200 ka and correlated to MIC 11 at Eyreville; Browning et al., this volume) (Fig. 8). Late Miocene sequences C9, C10, and M1 are absent at both Eyreville and Exmore, but are recovered at Bethany Beach and are tied to $\delta^{18}\text{O}$ isotope increases (Fig. 8). Although this indicates glacioeustatic control on sequence genesis for these intervals, the thickness and preservation of sequences is also modified by impactite compaction, sediment supply

changes, and regional tectonics. Browning et al. (this volume) provides a comprehensive analysis linking sequence boundary genesis with oxygen isotopic events.

Periods exhibiting weak calibration to $\delta^{18}\text{O}$ isotopic records in Virginia include: 1) the Oligocene (sequences are poorly preserved and dated and cannot be conclusively tied to oxygen isotopic changes); 2) lower Miocene (sequences C1-C3 are poorly preserved or absent within the CBIS and south of the crater); and 3) mid- to late Miocene (sequences C9, C10, and M1 are absent within the CBIS, indicating regional uplift that overrides eustatic signals). These results from the late Eocene-Pleistocene show that although eustasy provides the template for sequences globally, regional tectonics (rates of uplift, subsidence, and accommodation), variations in sediment supply, and local factors can modify and determine the preservation of sequences in a particular region.

Impactite Compaction

Impactites (e.g., the Exmore Beds and crater units A and B of Poag, 1996; 1997; Poag et al., 1999; Powars and Bruce, 1999; Horton et al., 2008) are described as brecciated “polymict diamicton” (formalized by Flint et al., 1960) consisting of unsorted 2-40 m-diameter sedimentary megablocks with heterolithic cobble, pebble, and sand-sized grains suspended in a finer-grained matrix rapidly emplaced during the catastrophic infilling of the CBIS (e.g., Poag, 2002). The size of sedimentary megablocks generally increases with depth from the upper transition zone that separates impact-generated materials from overlying normal marine sedimentation (Poag, 1994). These large volumes of highly

porous (currently >25-35% from wet porosity samples; Sanford et al., this volume), poorly compacted materials resulting from unconventional burial exhibit an unusual compaction history, influenced by the settling of underlying megablocks and subsequent loading of overlying impact and post-impact units (e.g., Powars, 2000).

Previous work (Hayden et al., 2008) used one-dimensional backstripping (e.g., accounting for the effects of compaction and sediment loading; Watts, 1979; Kominz et al., 1998) of annular-trough corehole sections (Exmore, Kiptopeke, and Langley) and regional coreholes (Fentress, Dismal Swamp) to examine 10 myr-scale tectonic trends in and around the crater. They identified a period of excess accommodation in the annular trough for the first 3 myr caused by the rapid compaction of impact-generated materials. A period of Oligocene uplift of 50-125 m was attributed to thermal blanketing by cold impact materials and the onset of a large negative thermal anomaly, while the mid-Miocene through Pliocene was dominated by regional tectonic patterns (Hayden et al., 2008).

We show that the compaction of impactites was not limited to the first 3 myr as reported by Hayden et al. (2008), but continued to strongly influence sedimentation within the central crater over the past 35.4 myr through the Pleistocene. Our corehole-well log cross section (Fig. 3) shows that a majority of post-impact sequences (late Eocene, middle-late Miocene, and Pliocene) are thicker in the annular trough (Exmore, Langley) than correlative sequences outside the crater (Tasley and sections to the north). These sequences thicken further into the crater moat (Eyreville), but thin substantially onto the

central peak at Cape Charles (Fig. 3). We contend that differences in accommodation within the CBIS can be attributed to the different thickness and compaction of impactites within the crater moat (>1000 m thick at Eyreville) versus the annular trough (~100-200 m thick at Exmore) and the central uplift (~300 m thick at Cape Charles) (Fig. 3). While previous work revealed similar lithostratigraphic trends (Powars and Bruce, 1999; Powars, 2000), our results provide better geochronologic resolution (~ 0.5-1.0 myr) and a sequence by sequence examination of the timing and nature of the events that shape the post-impact record. These results are consistent with high resolution seismic profiles across the CBIS that show numerous compaction faults that extend to the floor of the modern Chesapeake Bay, offsetting post-impact sediments that dip and thicken into the crater (Poag et al., 2004; Catchings et al., 2007).

This unique compaction history apparently produced a bathymetric low within the inner crater, resulting in a restricted basin characterized by mid-outer shelf paleoenvironments for much of the late Eocene-middle Miocene (Fig. 2). This observation is founded on the comparison of lithofacies, quantitative grain-size measurements, and paleoenvironmental indicators between Eyreville (inner crater) and Exmore (annular trough): 1) Oligocene sections are substantially thicker in the annular trough (Exmore and Langley; 35-50 m) than the inner crater (15 m), representing enhanced sediment starvation within the inner basin; 2) Miocene sequences at Exmore are generally coarser-grained, exhibiting > 50-85 % fine sands versus < 10% at Eyreville in HST intervals (Fig. 2); and 3) while lower-middle Miocene sequences (C6-C8) are dominated by shelf sediments (silt and clay) at both coreholes, Exmore sequences shallow upwards to distal lower shoreface fine-

medium sands while Eyreville exhibits shelfal clayey silts even in the HST (Fig. 2). Notable facies differences are not observed during late Miocene-Pliocene deposition, with coarse-grained and shallow marine facies dominating both sections (Fig. 2).

Passive-Aggressive Tectonism: Regional Insights and Controlling Mechanisms

Although post-rift lithospheric cooling and the flexural response to offshore sediment loading are the dominant contributors to “classic” Atlantic-type passive margin subsidence (Watts, 1979; Kominz et al., 1998), it has been clear that non-thermoflexural subsidence and uplift have occurred on this margin (e.g., Brown et al., 1972; Owens and Gohn, 1985; Owens et al., 1997). The development of a high-resolution (> 1 myr) sequence stratigraphic framework across the mid-Atlantic Margin (New Jersey, Delaware) and within the CBIS (Virginia) provides the proper geochronologic resolution to identify such non-thermal events. We contend that the distribution of regional sequences reveals significant periods of non-thermal tectonic uplift and excess subsidence at a scale of tens of meters in 1-5 myr, overprinting subsidence from simple lithospheric cooling, flexure, and impactite compaction (within the CBIS). This style of “passive-aggressive” tectonism characterizes passive margins otherwise dominated by thermoflexural subsidence.

We attribute the significant crater-wide and regional unconformities south of Delaware during the Oligocene (33-25 Ma), early Miocene (24-18 Ma), and mid- to late Miocene (~13.0-8.4 Ma; Figs. 3, 8) to relative uplift of the Norfolk arch, possibly enhanced by low

rates of sedimentation in southern Virginia. Evidence for post-impact uplift of the Norfolk arch is visible from the differential preservation of sequences southwards across the CBIS and surrounding regions. At Exmore and Eyreville, sequences C5-C8 are well represented (sequence C4 is also recovered at Eyreville), while an unconformity spans from ~13.0-8.4 Ma. At the Langley corehole (10 km north of the Norfolk arch), correlation and biostratigraphy (Edwards et al., 2005) indicate the absence of sequences C4, C5, and C7, coupled with the thin, patchy preservation of sequences C1, C6 and C8. This pattern likely reflects the periodic uplift of the Norfolk arch during the lower Miocene, mid-Miocene, and lower upper Miocene, because thick and widespread Miocene sections are recovered farther north throughout the Salisbury embayment and New Jersey (Fig. 3). These results are consistent with previous work by Powars (2000).

The CBIS-area unconformities during the Oligocene and early Miocene are also consistent with patchy to absent Paleocene-Pliocene strata caused by episodic tectonic uplift of the Cape Fear arch ~300 km to the south (Gohn, 1988; Weems and Lewis, 2002). Although the Norfolk arch does not exhibit the modern or historical seismicity of the Cape Fear arch (Weems and Lewis, 2002), the two structures bear several similarities: 1) position adjacent to major structural embayments of the Atlantic Margin (the Norfolk arch borders the Salisbury and Albemarle embayments, while the Cape Fear arch is bracketed by the Albemarle and Southeast Georgia embayments; Gohn, 1988); 2) alternating periods of normal coastal plain deposition interspersed with periodic tectonic uplift and erosion/nondeposition (Coniacian-Campanian strata are undisturbed atop the Cape Fear arch before Paleocene uplift; Gohn, 1988); and 3) exposure to variations in the

North American stress field throughout the Cenozoic (e.g., reaction of the Cape Fear arch to a regional compressive stress field throughout the Neogene; Weems and Lewis, 2002).

Although we attribute the majority of Oligocene and Miocene uplift of the CBIS to regional tectonism, quantification of the amplitudes and rates of change are necessary to evaluate the controlling mechanisms. Previous efforts on the mid-Atlantic margin used one-dimensional backstripping to document numerous vertical tectonic events of uplift or excess (non-thermal) subsidence. Browning et al. (2006) and Hayden et al. (2008) identified periods of Miocene excess subsidence of 30 ± 10 m across the Delmarva Peninsula that were attributed to down-flexure from depocenter loading on the offshore shelf. Within the CBIS, Hayden et al. (2008) identified a period of intra-crater uplift of 50-120 m caused by the onset and removal of a negative thermal anomaly induced by the thermal blanketing of cold impact materials. We believe these estimates of thermally-induced crater uplift (both amplitude and timing) are complicated by: 1) the unique compaction history of the impact-generated column underlying the post-impact section and; 2) the presence of regional hiatuses during the Oligocene-early Miocene. Hayden et al. (2008) modeled the bulk of impactite compaction within ~ 3 myr after impact, and did not model the long-term, time-dependent compaction of impact breccias observed in this study and Gohn et al. (2008; Fig. 2). This resulted in deeper R1 estimates that require greater uplift ($100 +$ m) to achieve sub-aerial erosion required for unconformity genesis in the Oligocene. Second, these estimates of crater-specific uplift are complicated by the presence of regional hiatuses during the Oligocene-early Miocene (largely absent sections with occasional thin, patchy intervals identified from coreholes, geophysical log

correlations, and previous studies of the region; Fig. 3; Powars, 2000; Powars and Bruce, 1999). These thin Oligocene-lower Miocene sections stand in stark contrast to thicker coeval sections recovered in the New Jersey Coastal Plain (Miller et al., 1998, 2005; Pekar et al., 2000) and are attributed to a phase of regional uplift by the Norfolk arch and southern Salisbury embayment, further compounded by low sedimentation rates during the Oligocene. As a result, establishing the exact amplitude and rate of possible thermal CBIS uplift is difficult, and requires further modeling (using higher resolution geochronology, impactite compaction model, and comparison to eustatic estimates) to quantify and differentiate crater-specific effects from regional tectonic trends.

The genesis and behavior of the Norfolk arch and other mid-Atlantic basement structures is poorly understood due to the lack of deep regional seismic data and low seismicity along active faults in the mid-Atlantic coastal plain (Seeber and Armbruster, 1988). Brown et al. (1972) described these structures as a series of wrench fault-bounded grabens, while Owens et al. (1997) attributed regional stratigraphic differences to “rolling basins” or broad warping (~100-300 km wavelength) of the crust. While there is insufficient data to conclusively determine their origin, we believe these basement structures represent inherited tectonic trends (basement faults) and fault-bounded terranes emplaced during Paleozoic continental collisions. Such boundaries are critical structural components of passive margins, many of which are reactivated during the subsequent asymmetrical rift-stage of a margin (Wernicke, 1985; e.g., the border fault of the Newark Basin; Schlische, 1992; Withjack et al., 1998) and still react to intraplate stresses today (e.g., Cape Fear arch; Weems and Lewis, 2002). A comprehensive understanding of

terrane distribution, character, and structural history is limited by the small number of coreholes that penetrate the Paleozoic basement underlying the Coastal Plain, resulting in numerous interpretations. However, several studies (e.g, Horton et al., 1989; Glover et al., 1997; Maguire et al., 2004) identify a mosaic of fault bounded terranes across the mid-Atlantic Margin (Fig. 9), each of which has the capacity for vertical movement given the proper stress conditions. The James River structural zone (Powars, 2000), a structural boundary associated with the Norfolk arch, appears to separate two accreted terranes emplaced during the assemblage of Pangaea: Grenville-Laurentia crystalline basement and Avalonia (Fig. 9). Movement along this fault, among others, could contribute to the differential preservation of sequences observed on the mid-Atlantic margin.

We suggest two mechanisms that could cause regional upwarping/downwarping and influence existing basement structures: 1) variations in intraplate stress (e.g., Cloetingh, 1988; Karner et al., 1993); and 2) density-driven mantle processes related to the interaction of eastern North America with the subducted Farallon plate (e.g., Mueller et al., 2008; Moucha et al., 2008). The accumulation and relaxation of intra-plate stresses tied to variations and reorganizations of far-field stress direction and intensity (e.g., changes in mid-ocean ridge spreading rates, ridge extensions, onset of margin subduction, etc.) could provide the mechanism behind the influence of basement structure on coastal plain strata. Cloetingh (1988) invoked these stress-field reorganizations as a possible explanation for 3rd order sea-level cycles (1-3 m.y.) with amplitudes of 10-20 m. Although this mechanism fails to account for the observed eustatic driver of sequence boundary formation (evidenced by the calibration of sequence boundaries with oxygen

isotope records), these variations in intra-plate stress can be propagated over large distances (1000's km; Letouzey, 1986; Ziegler and Van Hoorn, 1989; Cloetingh et al., 1990), enhance or diminish unconformity genesis on intra-basinal scales (Karner et al., 1993), account for the pronounced thinning or truncation of thick (~50-100 m) sedimentary packages (e.g., Norfolk arch), or result in the complete removal of entire series in the stratigraphic record (e.g., Norfolk arch; largely absent Paleogene section atop Cape Fear arch, North Carolina; Weems and Lewis, 2002; Self-Trail et al., 2004).

The periodic uplift of the Cape Fear and Norfolk arches may represent the adjustment of these structures from prior stress conditions to the current maximum horizontal stress direction of east northeast- west southwest, with the fault-bounded Cape Fear arch accommodating much of the modern stress and seismicity (Weems and Lewis, 2002).

The Oligocene and early Miocene uplift of these structures are coincident with a major reorganization of the North American stress field (~90° shift) from 35-28 Ma (Bird, 2002) due to the collision of the East Pacific Rise along the western North American margin and consequent cessation of subduction, onset of Basin and Range extension, and development of the Pacific-North American transform margin through the Miocene (Bird, 2002; Nicholson et al., 1994), among other events (e.g., onset of Cayman Trough transform margin; e.g., Ten Brink et al., 2002).

Alternatively, recent studies (Mueller et al., 2008; Forte et al., 2007; Spasojević et al., 2008; Moucha et al., 2008) have shown that variations in the mantle density structure can result in dynamic topographic changes (e.g., response of Earth's surface to convectively-

driven vertical stresses; Mitrovica et al., 1989) and broad epeirogenic uplift and downwarp of large crustal segments. Both Mueller et al. (2008) and Spasojević et al. (2008) attribute the comparatively low long-term (10 myr-scale) sea level events established from the New Jersey margin (Miller et al., 2005) to periods of dynamic subsidence (50-200 m) superimposed on long-term sea level fall since the Eocene. This subsidence is driven by the interaction of the Eastern U.S. with the underlying subducted Farallon plate (Spasojević et al., 2008). While implications of such studies are profound, they primarily focus on long-term (10-100 myr) tectonic trends (e.g., Moucha et al., 2008) that fail to account for higher frequency sequence and unconformity genesis on the mid-Atlantic and other margins that appear to be on the 1-5 myr scale. Recent studies by Forte et al. (2007) invoke mantle density perturbations coupled to the subducted Farrallon slab as a possible explanation for the intraplate seismicity observed in the New Madrid fault zone, showing that dynamic topography can drive smaller scale processes than broad crustal warping. Further research is needed to determine if sub-regional high-frequency (1-10 myr) tectonic uplift and subsidence, which may at times be synchronous (as observed on the mid-Atlantic margin; e.g., Cape Fear and Norfolk arch uplift versus relative subsidence in the Salisbury embayment), can effectively be explained by dynamic topography, or if they represent the blending of several tectonic processes. Quantitatively modeling (through one-dimensional backstripping) the rates, amplitudes, and lateral scale of these changes is a topic of ongoing research, and will provide better constraints on differentiating these mechanisms.

Regional Sediment Supply variations

Variations in sediment supply cannot alone cause the formation of sequence boundaries (Christie-Blick et al., 1991), but they can contribute significantly to the distribution of sequences and lithofacies on both regional and local scales. While Cenozoic sequences of the mid-Atlantic margin primarily reflect eustatic and tectonic controls, an increase or reduction of sediment supply can affect sequence thickness, the position of key stratal surfaces, and the presence of litho- and biofacies (e.g., Reynolds et al., 1991; Galloway, 1989). The mid-Atlantic region was influenced by several major fluvial systems during the Cenozoic (Poag and Sevon, 1989). The ancestral Susquehanna, Potomac, Delaware, and Hudson Rivers, as well as several smaller rivers (e.g. James, York), each influenced regional and local sedimentation (Poag and Sevon, 1989; Powars, 2000). Changes in sediment input, tied to variation in the rates of Appalachian uplift and denudation, are often reflected by different styles of regional sedimentation. The Cretaceous-Miocene New Jersey margin was strongly influenced by two deltaic systems that controlled the distribution of sequences, depocenter location, and lithofacies (Sugarman et al., 1995; Sugarman et al., 2006; Miller et al., 2004; Kulpecz et al., 2008). Coeval Miocene sections in Delaware, Maryland, and Virginia reveal low deltaic influence and exhibit wave-dominated shoreline facies (e.g., Browning et al., 2006), representing increased distance from primary margin sediment sources.

We contend that regional changes in sediment supply, caused by the concentration of major fluvial and deltaic axes in New Jersey, contributed to the preservation of sequences

across the mid-Atlantic margin and within the CBIS. While eustasy controls sequence boundary formation, and regional tectonics can account for absent sequences, decreased sediment supply can result in thin sequences more prone to erosion during base-level lowerings. The overall decrease in deltaic influence southward, from thick deltaic sections at Cape May, NJ (Fig. 1; Sugarman et al., 2007), to wave-dominated sequences at Bethany Beach, DE (Browning et al., 2006), and finer-grained shelf to lower shoreface-dominated sequences in southern Virginia likely contributed to: 1) an Oligocene sediment starved margin (e.g., Miller et al., 1997; Browning et al., 2008) with areas of intense starvation concentrated within the inner crater; and 2) early (C1-C5) and mid- to late Miocene (C9, C10, M1) sequences that persist across the Delmarva but pinch out southwards and are patchy, thin, and absent within the CBIS, representing uplift of the Norfolk arch coupled with decreased sediment supply. Although the large unconformities in the Oligocene, lower Miocene, and mid-to late Miocene are controlled by regional tectonic uplift, we believe the effects are exacerbated by low sedimentation. Seismic data from Powars and Bruce (1999) and Catchings et al. (2007) shows the southerly downlap of Miocene units, the northern infilling of the CBIS during the middle Miocene (and subsequent thickening of late Miocene-Pliocene packages in the southern crater), and are thus consistent with a strong northern sediment source prograding southwards and lower levels of sediment delivery in Virginia relative to the north.

Conclusions

The Exmore and Eyreville, VA cores provide the first continuous, high-resolution ($> \sim 1$ myr) chronostratigraphic records linking the annular trough and inner crater of the late Eocene Chesapeake Bay Impact Structure. We use integrated sequence stratigraphic analyses to identify 12-16 post-impact depositional sequences within the inner crater and the annular trough, and place them within a regional framework spanning the mid-Atlantic margin. Results indicate that post-impact sedimentation was largely controlled by global sea-level changes (as indicated with calibration to oxygen isotopic records), long-term impactite compaction, and periods of regional tectonic uplift and subsidence. Differential compaction of the impact-generated column was greatest in the inner crater, and caused a bathymetric low during the late Eocene-mid-Miocene, resulting in deeper water lithofacies than coreholes in the annular trough.

While many CBIS sequence boundaries show a strong correspondence with ice volume increases inferred from oxygen isotopic changes (indicating a eustatic control on sequence genesis), an evaluation of the CBIS in relation to the U.S. mid-Atlantic margin reveals five primary phases of crater evolution influenced by sediment supply changes and regional tectonism: 1) rapid late Eocene deposition was dominated by the initial depression caused by impact and a rapid phase of impactite compaction; 2) regional Oligocene uplift and sediment starvation characterized the inner basin; 3) a phase of continued lower Miocene regional uplift; 4) mid-upper Miocene uplift of the Norfolk arch coupled with low sedimentation rates; and 5) late Miocene to Pliocene subsidence of

the southern Salisbury embayment relative to New Jersey. We identify periods of regional uplift and excess subsidence at a scale of tens of meters in 1-5 myr that overprint subsidence from simple lithospheric cooling, flexure, and impactite compaction, and suggest these events were caused by the differential movement of basement structures and fault-bounded terranes in response to variations in intraplate stress.

Acknowledgements

We thank members of the USGS-ICDP onsite science party for the collection of data at the Eyreville corehole, and the members of the New Jersey Coastal Plain Drilling Project for their assistance with datasets from ODP Leg 174AX. We thank Greg Gohn and J. Wright Horton for provision of the Exmore corehole. We thank Pete McLaughlin for insight into regional stratigraphy in Delaware and Maryland, and Steve Curtain for providing several geophysical logs used in this study. We thank the Byrne family for use of their land for the Eyreville corehole, and DOSECC, G. Cobb III, and Major Drilling for drilling operations. This research was supported by EAR0506720 and EAR0606693 (Miller, Browning, Kominz)

References

- Andreason, D.C., and Hansen, H.J., 1987, Summary of hydrogeologic data from a test well (1,725 ft.) drilled in Tuckahoe State Park, Queen Anne's County, Maryland: Maryland Geological Survey Open File Report No. 87-02-3, 47 p.
- Andres, A.S., 2004, The Cat Hill Formation and Bethany Beach Formation of Delaware: Delaware Geological Survey Report of Investigations No. 67, 8 p.

- Berggren, W.A., Kent, D.V., Swisher, C.C., and Aubry, M.-P., 1995, A revised Cenozoic geochronology and chronostratigraphy, *in* Berggren, W.A., Kent, D.V., Aubry, M.-P., and Hardenbol, J., eds., *Geochronology, Time Scales and Global Stratigraphic Correlations: A Unified Temporal Framework for an Historical Geology*, Volume 54: Tulsa OK, SEPM (Society for Sedimentary Geology) Special Publication, p. 129-212.
- Bird, P., 2002, Stress direction history of the western United States and Mexico since 85 Ma: *Tectonics*, v. 21, p. 1-12.
- Brown, P.M., Miller, J.A., and Swain, F.M., 1972, Structural and stratigraphic framework, and spatial distribution of permeability of the Atlantic Coastal Plain, North Carolina to New York: U.S. Geological Survey Professional Paper 796, p. 1-79.
- Browning, J.V., Miller, K.G., McLaughlin, P.P., Kominz, M.A., Sugarman, P.J., Monteverde, D., Feigenson, M.D., and Hernández, J.C., 2006, Quantification of the effects of eustasy, subsidence, and sediment supply on Miocene sequences, Mid-Atlantic margin of the United States: *Geological Society of America Bulletin*, v. 118, p. 567-588.
- Browning, J.V., Miller, K.G., Sugarman, P.J., Kominz, M.A., McLaughlin, P.P., and Kulpecz, A.A., 2008, A 100 million year record of sequences, sedimentary facies and sea-level change from Ocean Drilling Program onshore coreholes, U.S. Mid-Atlantic coastal plain: *Basin Research*, v. 20, p. 227-248.
- Browning, J.V., Miller, K.G., McLaughlin, P.P., Jr., Edwards, L.E., Powars, D.S., Kulpecz, A.A., Wade, B.S., and Feigenson, M.D., *this volume*, Post-impact integrated litho-, sequence, Sr-isotopic, and bio-stratigraphy of the Eyreville corehole, Chesapeake Bay impact structure inner basin: Geological Society of America Special Publication.
- Catchings, R.D., Powars, D.S., Goldman, M.R., Gohn, G.S., Horton, J.W., Jr., Rymer, M.J., Gandhok, G., and Edwards, L.E., 2007, High-resolution seismic reflection images across the 1.76-km-deep Eyreville corehole within the moat of the Chesapeake Bay Impact Structure: *Geological Society of America Abstracts with Programs*, 450, abstract 167-3.
- Christie-Blick, N., 1991, Onlap, offlap, and the origin of unconformity-bounded depositional sequences: *Marine Geology*, v. 97, p. 35-56.
- Cloetingh, S., 1988, Intraplate stresses: a tectonic cause for third-order cycles in apparent sea level?: *Society of Economic Paleontologists and Mineralogists Special Publication*, v. 42, p. 19-29.

- Cloetingh, S., Gradstein, F.M., Kooi, H., Grant, A.C., and Kaminski, M., 1990, Plate reorganization: a cause of rapid late Neogene subsidence and sedimentation around the North Atlantic?: *Journal of the Geological Society*, v. 146, p. 495-506.
- de Verteuil, L. and Norris, G., 1996, Miocene dinoflagellate stratigraphy and systematics of Maryland and Virginia: *Micropaleontology*, v. 42 supplement, 172 p.
- Edwards, L.E., Barron, J.A., Bukry, D., Bybell, L.M., Cronin, T.M., Poag, C.W., Weems, R.E., and Wingard, G.L., 2005, Paleontology of the Upper Eocene to Quaternary Postimpact Section in the USGS-NASA Langley Core, Hampton, Virginia, *in* Horton, J.W., Jr., Powars, D.S., and Gohn, G.S., Eds. 2005, *Studies of the Chesapeake Bay Impact Structure- The USGS-NASA Langley Corehole, Hampton, Virginia, and Related Coreholes and Geophysical Survey*: U.S. Geological Survey Professional Paper 1688, p. H1-47, 9 pls.
- Edwards, L.E., Powars, D.S., Wade, B.S., Self-Trail, J.M., Kulpecz, A.A., Browning, J.V., Miller, K.G., McLaughlin, P.P., Jr., and Elbra, T., *this volume*, Geologic columns for the ICDP-USGS Eyreville A and C coreholes, Chesapeake Bay Impact Structure: Post-Impact Sediments, 0 to 444 m depth: Geological Society of America Special Publication.
- Flint, R.F., Sanders, J.E., and Rodgers, J., 1960, Diamictite, a substitute term for symmictite: *Geological Society of America Bulletin*, v. 71, p. 1809.
- Forte, A.M., Mitrovica, J.X., Moucha, R., Simmons, N.A., and Grand, S.P., 2007, Descent of the ancient Farallon slab drives localized mantle flow below the New Madrid seismic zone: *Geophysical Research Letters*, v. 34, L04308, doi: 10.1029/2006GL027895.
- Galloway, W.E., 1989, Genetic stratigraphic sequences in basin analysis II: Application to northwest Gulf of Mexico Cenozoic basin: *American Association of Petroleum Geologists Bulletin*, v. 73, p. 143-154.
- Glover, L., III., Sheridan, R.E., Holbrook, W.S., Ewing, J.I., Talwani, M., Hawman, R.B., and Wang, P., 1997, Paleozoic collisions, Mesozoic rifting and structure of the Middle-Atlantic states continental margin: an 'EDGE' Project report: *Geological Society of America Special Paper* 314, p. 107-135.
- Gohn, G.S., 1988, Atlantic coastal plain: North Carolina to Florida, *In* Sheridan, R.E., and Grow, J.A., eds., *The Atlantic Coastal Margin, U.S.*: Boulder, Colorado, Geological Society of America, *Geology of North America*, v. 1-2, p. 107-130.
- Gohn, G.S., Sanford, W.E., Powars, D.S., Horton, J.W., Jr., Edwards, L.E., Morin, R.H., and Self-Trail, J.M., 2007, Site report for the USGS test holes drilled at Cape Charles, Northampton County, Virginia, in 2004: U.S. Geological Survey Open File Report 1094, 27 p.

- Gohn, G.S., Koeberl, C., Miller, K.G., Reimold, W.U., Browning, J.V., Cockell, C.S., Horton, J.W., Jr., Kenkmann, T., Kulpecz, A.A., Powars, D.S., Sanford, W.E., and Voytek, M.A., 2008, Deep Drilling Yields New Insights into the Chesapeake Bay Impact Event: Science, *in press*.
- Hansen, H.J., 1977, Geologic and Hydrologic data from two core holes drilled through the Aquia Formation (Eocene-Paleocene) in Prince George's and Queen Anne's counties, Maryland: Miscellaneous Open File Report, Maryland Geological Survey, 77 p.
- Hansen, H.J., and Lang, C.M., 1980, unpublished well log transect from Smith Island to Ocean City Airport, MD: Maryland Geological Survey, 1 plate.
- Hansen, H.J., and Wilson, J.M., 1984, Summary of hydrogeologic data from a deep (2,678 ft.) well at Lexington Park, St. Mary's County, Maryland: Maryland Geological Survey Open File Report No. 84-02-1, 61 p.
- Hansen, H.J., and Wilson, J.M., 1990, Hydrogeology and stratigraphy of a 1,515-foot test well drilled near Princess Anne, Somerset County, Maryland: Maryland Geological Survey Open File Report No. 91-02-5, 59 p.
- Hart, S.R., and Brooks, C., 1974, Clinopyroxene-matrix partitioning of K, Rb, Cs, and Ba: *Geochimica et Cosmochimica Acta*, v. 38, p. 1799-1806.
- Hayden, T., Kominz, M., Powars, D.S., Edwards, L.E., Miller, K.G., Browning, J.V., and Kulpecz, A.A., 2008, Impact effects and regional tectonic insights: Backstripping the Chesapeake Bay impact structure: *Geology*, v. 36, p. 327-330.
- Horton, J.W., Jr., Drake, A.A., Jr., and Rankin, D.W., 1989, Tectonostratigraphic terranes and their Paleozoic boundaries in the central and southern Appalachians: Geological Society of America Special Paper 230, p. 213-245.
- Horton, J.W., Jr., Powars, D.S., and Gohn, G.S., Eds. 2005a, Studies of the Chesapeake Bay Impact Structure- The USGS-NASA Langley Corehole, Hampton, Virginia, and Related Coreholes and Geophysical Survey: U.S. Geological Survey Professional Paper 1688.
- Horton, J.W., Jr., Aleinikoff, J.N., Kunk, M.J., Gohn, G.S., Edwards, L.E., Self-Trail, J.M., Powars, D.S., and Izett, G.A., 2005b, Recent research on the Chesapeake Bay impact structure, USA- impact debris and reworked ejecta: Geological Society of American Special Paper 384, p. 147-170.
- Horton, J.W., Jr., Gohn, G.S., Powars, D.S., and Edwards, L.E., 2008, Origin and emplacement of impactites in the Chesapeake Bay impact structure, Virginia, USA: Geological Society of America Special Paper 437, p. 73-97.

- Karner, G.D., Driscoll, N.W., Weissel, J.K., 1993, Response of the lithosphere to in-plane force variations: *Earth and Planet Science Letters*, v. 114, p. 397-416.
- Kominz, M.A., Miller, K.G., and Browning, J.V., 1998, Long-term and short-term global Cenozoic sea-level estimates: *Geology*, v. 26, p. 311-314.
- Kulpecz, A.A., Miller, K.G., Sugarman, P.J., and Browning, J.V., 2008, Response of Late Cretaceous migrating deltaic facies systems to sea level, tectonics, and sediment supply changes, New Jersey Coastal Plain U.S.A.: *Journal of Sedimentary Research*, v. 78, p. 112-129.
- Letouzey, J., 1986, Cenozoic paleo-stress pattern in the Alpine foreland and structural interpretation in a platform basin: *Tectonophysics*, v. 132, p. 215-231.
- Maguire, T.J., Sheridan, R.E., and Volkert, R.A., 2004, Geophysical modeling of the northern Appalachian Brompton-Cameron, Central Maine, and Avalon terranes under the New Jersey Coastal Plain: *Journal of Geodynamics*, v. 37, p. 457-485.
- McArthur, J.M., Howarth, R.J., and Bailey, T.R., 2001, Strontium isotope stratigraphy: LOWESS Version 3. Best-fit line to the marine Sr-isotope curve for 0 to 509 Ma and accompanying look-up table for deriving numerical age (Look-Up Table Version 4: 08/03): *Journal of Geology*, v. 109, p. 155-169.
- Miller, K.G., Wright, J.D., and Fairbanks, R.G., 1991, Unlocking the ice house: Oligocene-Miocene oxygen isotopes, eustasy, and margin erosion: *Journal of Geophysical Research*, v. 96, p. 6829-6848.
- Miller, K.G., Mountain, G.S., the Leg 150 Shipboard Party, and Members of the New Jersey Coastal Plain Drilling Project, 1996, Drilling and dating New Jersey Oligocene-Miocene sequences: Ice volume, global sea level, and Exxon records: *Science*, v. 271, p. 1092-1094.
- Miller, K.G., Rufolo, S., Sugarman, P.J., Pekar, S.F., Browning, J.V., and Gwynn, D.W., 1997, Early to middle Miocene sequences, systems tracts, and benthic foraminiferal biofacies, New Jersey coastal plain, *in* Miller, K.G., and Snyder, S.W., eds., *Proceedings of the Ocean Drilling Program, Scientific results, Volume 150X*: College Station, Texas, Ocean Drilling Program, p. 169-186.
- Miller, K.G., Mountain, G.S., Browning, J.V., Kominz, M.A., Sugarman, P.J., Christie-Blick, N., Katz, M.E., and Wright, J.D., 1998, Cenozoic global sea-level, sequences, and the New Jersey transect: Results from coastal plain and slope drilling: *Reviews of Geophysics*, v. 36, p. 569-601.
- Miller, K.G., McLaughlin, P.P., Browning, J.V., Benson, R.N., Sugarman, P.J., Hernandez, J., Ramsey, K.W., Baxter, S.J., Feigenson, M.D., Aubry, M.-P., Monteverde, D.H., Cramer, B.S., Katz, M.E., McKenna, T.E., Strohmeier, S.A.,

- Pekar, S.F., Uptegrove, J., Cobbs, G., Cobbs, G., III, and Curtin, S.E., 2003, Bethany Beach Site, *in* Miller, K.G., Sugarman, P.J., Browning, J.V., and et al., eds., *Proceedings of the Ocean Drilling Program, Initial reports, Volume 174AX (Suppl.)*: College Station, TX, Ocean Drilling Program, p. 1–84.
- Miller, K.G., Sugarman, P.J., Browning, J.V., Kominz, M.A., Olsson, R.K., Feigenson, M.D., and Hernández, J.C., 2004, Upper Cretaceous sequences and sea-level history, New Jersey coastal plain: *Geological Society of America Bulletin*, v. 116, p. 368-393.
- Miller, K.G., Kominz, M.A., Browning, J.V., Wright, J.D., Mountain, G.S., Katz, M.E., Sugarman, P.J., Cramer, B.S., Christie-Blick, N., and Pekar, S.F., 2005, The Phanerozoic record of global sea-level change: *Science*, v. 310, p. 1293-1298.
- Mitchum, R.M., Vail, P.R., and Thompson, S., 1977, The depositional sequence as a basic unit for stratigraphic analysis: *American Association of Petroleum Geologists Memoir*, v. 26, p. 53-62.
- Mitrovica, J.X., Beaumont, C., and Jarvis, G.T., 1989, Tilting of continental interiors by the dynamic effects of subduction: *Tectonics*, v. 8, p. 1079-1094.
- Mixon, R.B., Powars, R.B., and Daniels, D.L., 1992, Nature and timing of deformation of Upper Mesozoic and Cenozoic deposits in the inner Atlantic Coastal Plain, Virginia and Maryland, *in* Gohn, G.S., ed., *Proceedings of the 1988 U.S. Geological Survey Workshop on the Geology and Geohydrology of the Atlantic Coastal Plain*: U.S. Geological Survey Circular 1059, p. 65-74.
- Moucha, R., Forte, A.M., Mitrovica, J.X., Rowley, D.B., Quere, S., Simmons, N.A., and Grand, S.P., 2008, Dynamic topography and long-term sea level variations: there is no such thing as a stable continental platform: *Earth and Planetary Science Letters*, doi: 10.1016/j.epsl.2008.03.056
- Mueller, R.D., Sdrolias, M., Gaina, C., Steinberger, B., and Heine, C., 2008, Long-term sea-level fluctuations driven by ocean basin dynamics: *Science*, v. 319, p. 1357-1362.
- Nicholson, C., Sorlien, C.C., Atwater, T., Crowell, J.C., and Luyendyk, B.P., 1994, Microplate capture, rotation of the western Transverse Ranges, and initiation of the San Andreas as a low-angle fault system: *Geology*, v. 22, p. 491-495.
- Olsson, R.K., Melillo, A.J., and Schreiber, B.L., 1987, Miocene sea level events in the Maryland Coastal Plain and the offshore Baltimore Canyon Trough: *Cushman Foundation for Foraminiferal Research, Special Publication 24*, p. 85-97.
- Olsson, R.K., Gibson, T.G., Hansen, H.J., and Owens, J.P., 1988, Geology of the northern Atlantic Coastal Plain: Long Island to Virginia, *in* Sheridan, R.E., and

- Grow, J.A., eds., The Atlantic Coastal Margin, U.S.: Boulder, Colorado, Geological Society of America, Geology of North America, v. 1-2, p. 87-105.
- Oslick, J.S., Miller, K.G., Feigenson, M.D., and Wright, J.D., 1994, Oligocene-Miocene strontium isotopes: Stratigraphic revisions and correlations to an inferred glacioeustatic record: *Paleoceanography*, v. 9, p. 427-443.
- Owens, J.P., and Sohl, N.F., 1969, Shelf and deltaic paleoenvironments in the Cretaceous-Tertiary formations of the New Jersey Coastal Plain, *in* Subitzky, S., ed., *Geology of Selected Areas in New Jersey and Eastern Pennsylvania and Guidebook of Excursions*: New Brunswick, NJ, Rutgers University Press, p. 390-408.
- Owens, J.P., and Gohn, G.S., 1985, Depositional history of the Cretaceous series in the U.S. Atlantic Coastal Plain: Stratigraphy, paleoenvironments, and tectonic controls of sedimentation, *in* Poag, C.W., ed., *Geologic evolution of the United States Atlantic Margin*: New York, Van Nostrand Reinhold, p. 25-86.
- Owens, J.P., Miller, K.G., and Sugarman, P.J., 1997, Lithostratigraphy and paleoenvironments of the Island Beach borehole, New Jersey Coastal Plain Drilling Project, *In* Miller K.G., and Snyder, S.W., eds. *Proceedings of the Ocean Drilling Program, Scientific Results*, v. 150X, p. 15-24.
- Pekar, S.J., Miller, K.G., and Kominz, M.A., 2000, Reconstructing the stratal geometry of latest Eocene to Oligocene sequences in New Jersey: Resolving a patchwork distribution into a clear pattern of progradation: *Sedimentary Geology*, v. 134, p. 93-109.
- Pemberton, S.G., 1998, Stratigraphic applications of the *Glossifungites* ichnofacies delineating discontinuities in the rock record: *American Association of Petroleum Geologists Bulletin*, v. 82, p. 2155.
- Pemberton, S.G., MacEachern, J.A., and Saunders, T., 2004, Stratigraphic applications of substrate-specific ichnofacies: delineating discontinuities in the rock record. *In*: McIlroy, D. (Ed.), *The Application of Ichnology to Paleoenvironmental and Stratigraphic Analysis*. Geological Society, Special Publications, v. 228, p. 29-62.
- Poag, C.W., 1996, Structural outer rim of Chesapeake Bay impact crater- Seismic and bore hole evidence: *Meteoritics & Planetary Science*, v. 31, no. 2, p. 218-226.
- Poag, C.W., 1997, The Chesapeake Bay bolide impact: a convulsive event in Atlantic Coastal Plain evolution: *Sedimentary Geology*, v. 108, p. 45-90.
- Poag, C.W., 2000, Nature and distribution of deposits derived from the Chesapeake Bay submarine impact [abs.]: *Geological Society of American Abstracts with Programs*, v. 32, no. 7, p. A-163.

- Poag, C.W., and Sevon, W.D., 1989, A record of Appalachian denudation in postrift Mesozoic and Cenozoic sedimentary deposits of the U.S. middle Atlantic continental margin: *Geomorphology*, v. 2, p. 119-157.
- Poag, C.W., Powars, D.S., Poppe, L.J., and Mixon, R.B., 1994, Meteorid mayhem in Ole Virginny: Source of the North American tektite strewn field: *Geology*, v. 22, p. 691-694.
- Poag, C.W., Hutchinson, D.R., Coleman, S.M., and Lee, M.W., 1999, Seismic expression of the Chesapeake Bay impact crater; Structural and morphologic refinements based on new seismic data, *in* Dressler, B.O., and Sharpton, V.L., eds., *Large meteorite impacts and planetary evolution; II: Geological Society of America Special Paper 339*, p. 149-164.
- Poag, C.W., Koeberl, C., and Reimold, W.U., 2004, *The Chesapeake Bay Crater: Geology and Geophysics of a Late Eocene Submarine Impact Structure*: New York, Springer-Verlag, 522 p.
- Posamentier, H.W., Jervey, M.T., and Vail, P.R., 1988, Eustatic controls on clastic deposition I -- Conceptual framework: *Society of Economic Paleontologists and Mineralogists Special Publication*, v. 42, p. 109-124.
- Powars, D.S., 2000, The effects of the Chesapeake Bay impact crater on the geological framework and correlation of hydrogeologic units of southeastern Virginia, south of James River: *U.S. Geological Survey Professional Paper 1622*, 53 p.
- Powars, D.S., and Bruce, T.S., 1999, The effects of the Chesapeake Bay impact crater on the geologic frame-work and the correlation of hydrogeologic units of southeastern Virginia, south of the James River: *U.S. Geological Survey Professional Paper 1612*, 82 p.
- Powars, D.S., Mixon, R.B., and Bruce, T.S., 1992, Uppermost Mesozoic and Cenozoic geologic cross section, outer coastal plain of Virginia, *in* Gohn, G.S., ed., *Proceedings of the 1988 U.S. Geological Survey Workshop on the Geology and Geohydrology of the Atlantic Coastal Plain: U.S. Geological Survey Circular 1059*, p. 85-101.
- Powars, D.S., Bruce, T.S., Edwards, L.E., Gohn, G.S., Self-Trail, J.M., Weems, R.E., Johnson, G.H., Smith, M.J., and McCartan, C.T., 2005, Physical stratigraphy of the upper Eocene through Quaternary postimpact section in the USGS-NASA Langley core, Hampton, Virginia: *U.S. Geological Survey Professional Paper 1688*, p. G1-44.
- Pusz, A., Miller, K.G., Wright, J.D., and Kent, D.V., submitted March 2008, Global carbon cycle perturbation associated with late Eocene impacts: *Geology*.

- Reilly, T.J., Miller, K.G., and Feigenson, M.D., 2002, Late Eocene to Oligocene Sr-isotopic reference section, Site 522, eastern South Atlantic,: *Paleoceanography*, v.18, p. 1-9.
- Reynolds, D.J., Steckler, M.S., and Coakley, B.J., 1991, The role of sediment load in sequence stratigraphy: the influence of flexural isostasy and compaction, *in* Cloetingh, S. ed., Special section on long-term sea-level change: *Journal of Geophysical Research, B, Solid Earth and Planets*. v. 96, p. 6931-6949.
- Rider, M.H., 2002, The geological interpretation of well logs (2nd edition): Rider-French Consulting Ltd., Scotland, 280p.
- Sanford, W.E., and Powars, D.S., this volume, Porewater chemistry of the central Chesapeake Bay impact structure and its implications for groundwater resources. GSA Special Publication XX, XX p.
- Sanford, W.E., Gohn, G.S., Powars, D.S., Horton, J.W., Jr. , Edwards, L.E., Self-Trail, J.M., and Morin, R.H., 2004, Drilling the central crater of the Chesapeake Bay impact structure: A first look: *Eos Transactions*, v. 85, p. 369, 377.
- Schlische, R.W., 1992, Structural and stratigraphic development of the Newark extensional basin, eastern North America: Evidence for the growth of basin and its bounding structures: *Geological Society of America Bulletin*, v. 104, p. 1246-1263.
- Seeber, L., and Armbruster, J.G., 1988, Seismicity along the Atlantic seaboard of the U.S.: Intraplate neotectonics and earthquakes, *in* Sheridan, R., and Grow, J., eds., *The Atlantic continental margin, U.S.: Geological Society of America, Decade of North American Geology*, v. 1-2, p.437-444.
- Self-Trail, J.M., Powell, D.C., and Christopher, R.A., 2004, The Collins Creek and Pleasant Creek Formations: Two new Upper Cretaceous subsurface units in the Carolina/Georgia Coastal Plain: *Southeastern Geology*, v. 42, p. 237-252.
- Spasojević, S., Liu, L., Gurnis, M., and Muller, R.D., 2008, The case for dynamic subsidence of the U.S. east coast since the Eocene: *Geophysical Research Letters*, v. 35, L0835, doi: 10.1029/2008GL033511.
- Sugarman, P.J., Miller, K.G., Bukry, D., and Feigenson, M.D., 1995, Uppermost Campanian-Maestrichtian strontium isotopic, biostratigraphic, and sequence stratigraphic framework of the New Jersey Coastal Plain: *Geological Society of America Bulletin*, v. 107, p. 19-37.
- Sugarman, P.J., Miller, K.G., Browning, J.V., Kulpecz., A.A., McLaughlin, P.P., Jr., Monteverde, D.H., 2006, Hydrostratigraphy of the New Jersey Coastal Plain:

Sequences and facies predict the continuity of aquifers and confining units:
Stratigraphy, v. 2, p. 259-275.

- Sugarman, P.J., Miller, K.G., Browning, J.V., Monteverde, D.H., Uptegrove, J., McLaughlin, P.P., Jr., Stanley, A.M., Wehmiller, J., Kulpecz, A.A., Harris, A.D., Pusz, A., Kahn, A., Friedman, A., Feigenson, M.D., Barron, J., and McCarthy, F.M.G., 2007, Cape May Zoo site. *In* Miller, K.G., Sugarman, P.J., Browning, J.V., et al., *Proc. ODP, Init. Repts.*, 174AX (Suppl.): College Station, TX (Ocean Drilling Program) p. 1-66.
- Ten Brink, U.S., Coleman, D.F., and Dillon, W.P., 2002, The nature of the crust under Cayman Trough from gravity: *Marine and Petroleum Geology*, v. 19, p. 971-987.
- Van Wagoner, J.C., Posamentier, H.W., Mitchum, R. M., Vail, P.R., Sarg, J.F., Loutit, T.S., and Hardenbol, J., 1988, An overview of the fundamentals of sequence stratigraphy and key definitions: *Society of Economic Paleontologists and Mineralogists Special Publication*, v. 42, p. 39-45.
- Watts, A.B., and Steckler, M.S., 1979, Subsidence and eustasy at the continental margin of eastern North America, *in* Talawani, M., Hay, W., and Ryan, W.B.F., eds., *Deep drilling results in the Atlantic Ocean: continental margins and paleoenvironments: American Geophysical Union Maurice Ewing series*, v. 3, p. 218-234.
- Weems, R.E., and Lewis, W.C., 2002, Structural and tectonic setting of the Charleston, South Carolina, region: Evidence from the Tertiary stratigraphic record: *Geological Society of America Bulletin*, v. 114, p. 24-42.
- Wernicke, B., 1989, Uniform-sense normal simple shear of the continental lithosphere: *Canadian Journal of Earth Sciences*, v. 22, p. 108-125.
- Withjack, M.O., Schlische, R.W., and Olsen, P.E., 1998, Diachronous rifting, drifting, and inversion on the passive margin of central eastern North America: an analog for other passive margins: *American Association of Petroleum Geologists Bulletin*, v. 82, p. 817-835.
- Ziegler, P.A., and Van Hoorn, B., 1989, Evolution of the North Sea rift system. *In* Tankard, A.J., and Balkwell, H., eds., *Extensional tectonics and stratigraphy of the North Atlantic margins. American Association of Petroleum Geologists Memoir*, v. 46, p. 471-500.

Figure Captions

Figure 1. Location map of the mid-Atlantic margin showing the distribution of coreholes and geophysical logs used in this study. Yellow dots represent USGS coreholes, red dots represent ODP 150X and 174AX coreholes, while black dots are geophysical logs. Coreholes used in this study are further identified by letter; E- Eyreville (Browning et al., this volume; Edwards et al., this volume; Gohn et al., in press); X- Exmore; K- Kiptopeke; F- Fentress; D- Dismal Swamp (Powars and Bruce, 1999); C- Cape Charles (Gohn et al., 2007); B- Bayside (Horton et al., 2008); L-Langley (Horton et al., 2005a); CM- Cape May (Sugarman et al., 2007); and BB- Bethany Beach (Browning et al., 2006). Well logs shown in Figure 3 are identified by letters; Ea-Eastville; Ta- Tasley; Ha- Hallwood; Wa- Wallops Island; Sh- Snow Hill; Wo- Wor-Dd80; Oa- Ocean City C30A; and Ob- Ocean City C43B. The regional transect (Fig. 3) is represented by the blue line that runs from A-A1. Figure 2 occurs along this same line, and depicts the wells within the CBIS. The outline of the CBIS is modified from Powars and Bruce (1999). An approximate basement contour (adapted from Olsson, 1988) marks the primary basement features of the mid-Atlantic Margin: 1) the Norfolk arch; 2) Salisbury embayment; and 3) South Jersey high. The base map is adapted from USGS Digital Line Graph 1:2,000,000, 1990.

Figure 2. Corehole-well log cross section from Langley, VA–Bethany Beach, DE (A-A1) modified from Gohn et al. (in press). Bethany Beach (Browning et al., 2006), Langley, Kiptopeke, Cape Charles, Exmore are coreholes; Eastville and Tasley are

gamma ray logs. Sequence ages based on age-depth plots primarily using Sr-isotopes. Sequences C1-10 and M1 defined at Bethany Beach (Browning et al., 2006) while YK, Ea1, Ea2, and SM were first identified at Eyreville (Browning et al., this volume; this study). Blue lines represent sequence boundaries. Wavy red lines indicate coalesced sequence boundaries where one or more sequences are absent. Blue age ranges at Langley and Kiptopeke are established from biostratigraphy (Edwards et al., 2005; Powars and Bruce, 1999). Green ages are single Sr-age estimates from Powars and Bruce (1999). Lithologic columns are coded by the following colors: bright yellow- coarse quartz sand; pale yellow- fine quartz sand; blue- carbonate sand; brown- silt and clay; green- glauconite sand; and pink/white- mica or other. The underlying diagram of the CBIS is not to scale, and is intended to show the position of post-impact sequences relative to crater morphology. Note the change in transect orientation at Kiptopeke from N-S to NE-SW.

Figure 3. Regional corehole-well log transect from Fentress, VA to Bethany Beach, DE (A-A1) showing Oligocene-Pleistocene sequence distribution as defined at the Bethany Beach (Browning et al., 2006), Eyreville (Browning et al., this volume), and Exmore coreholes (this study). Published reports were used to supplement correlations outside the crater (e.g., Powars and Bruce, 1999; Olsson et al., 1987). Thin blue lines represent sequence boundaries. Thick wavy red lines indicate coalesced sequence boundaries where one or more sequences are absent. Thin green lines indicate significant contacts or hiatuses identified from lithologic or biostratigraphic breaks from previous studies. Dotted lines indicate lower confidence in correlations, while hachured areas indicate

insufficient data to render interpretations. Sequences are packaged and color coded by time. Blue age ranges at Langley and Kiptopeke are established from biostratigraphy (Edwards et al., 2005; Powars and Bruce, 1999). Green ages are single Sr-age estimates from Powars and Bruce (1999). The underlying diagram of the CBIS is not to scale, and is intended to show the position of post-impact sequences relative to crater morphology. Note the change in transect orientation at Kiptopeke from N-S to NE-SW.

Figure 4. Generalized transgressive-regressive, “shallowing-upwards” sequence of the Cenozoic mid-Atlantic Margin (modified from Miller et al., 1996; Miller et al., 2004; and Kulpecz et al., 2008). Diagram depicts the relationships between paleoenvironment, lithology, sequence components, and geophysical log character.

Figure 5. Diagram shows age-depth relationships for the early through late Miocene sequences identified within the Exmore corehole. Sequence boundaries identified in core are represented by the thick horizontal red lines. Blue lines extend from the lower to upper unconformities and indicate the time represented by a sequence, assuming a consistent sedimentation rate. Horizontal blue bars represent dinocyst zones from De Verteuil and Norris (1996). Zone DN6 at 513 ft represents a reinterpretation of De Verteuil and Norris (1996) sample 1712-22 by L. Edwards. The inferred ages for the top and base of each sequence are annotated. Black circles represent valid Sr- isotope datum points, while red circles represent Sr- isotope ranges compromised by diagenetic alteration. Error bars are included for all dates. Red shading represents the error range for each sequence. Lithologic units are from Powars et al. (1992), Powars and Bruce

(1999), and Powars et al. (2005).). Lithologic columns are coded by the following colors: bright yellow- coarse quartz sand; pale yellow- fine quartz sand; blue- carbonate sand; brown- silt and clay; green- glauconite sand; and pink/white- mica or other.

Figure 6. Figure shows lithologic, geochronologic, and sequence stratigraphic interpretations of the Exmore corehole. From left to right: 1) Gamma log response; 2) percent lithology (color key described in Figure 2); 3) depth column; 4) Sr- isotope dates; 5) paleoenvironmental interpretations; 6) sequence stratigraphic interpretations (e.g., systems tracts, MFS, etc.); 7) the identified sequence; and 8) respective lithostratigraphic Formation. Solid horizontal red lines indicate sequence boundaries identified from core, while dashed red lines represent potential sequence boundaries. Dashed blue lines represent the position of Maximum Flooding Surfaces identified from core and geophysical logs. Lithologic units are from Powars et al. (1992), Powars and Bruce (1999), and Powars et al. (2005). LHST- lower Highstand Systems Tract; uHST- upper Highstand Systems Tract; TST- Transgressive Systems Tract; LST- Lowstand; FS- Flooding surface; MFS- Maximum Flooding Surface; Chop- Choptank Fm.; and NN-Newport News Beds.). Lithologic columns are coded by the following colors: bright yellow- coarse quartz sand; pale yellow- fine quartz sand; blue- carbonate sand; brown- silt and clay; green- glauconite sand; and pink/white- mica or other.

Figure 7. See Figure 6 caption.

Figure 8. Diagram shows the temporal distribution of sequences for three coreholes (Exmore, Eyreville, and Bethany Beach) plotted against oxygen isotope data (Miller et al., 2005). Geochronology of each sequence was derived from Sr- isotope age analysis, with biostratigraphy at Bethany Beach and Eyreville (Browning et al., 2006; this volume). Hachured sequences are poorly dated. Oxygen 18 inflections represent ice volume increases, are marked by the arrowed blue lines, and identified next to the right axis.

Figure 9. Map showing the distribution of subsurface terranes, boundaries, and key structural elements across the mid-Atlantic Magrin (modified from Maguire et al., 2004 and Glover et al., 1997). Terranes are colored according to the underlying key. Blue dashed lines represent major synforms (b- Shellburne Falls and Chester domes; d- Connecticut Valley-Gaspe Synclinorium) while orange dashed lines represent major antiforms (a- Manhattan prong-Berkshire Massif; c- Prehlan dome-Bronson Hill anticlinorium). The mid-Atlantic coastline and CBIS are overlain to add geographic perspective. Terranes and other features are identified by letters: rr- Roanoke Rapids; ch- Charleston; ha- Hatteras; bc- Brompton-Cameron; and cm- central Maine. JRSZ marks the James River Structural Zone (northern edge of the Norfolk arch) from Powars (2000). Horton et al. (2005a, b) note the presence of Avalon basement at the Bayside corehole, different from the shown map.

Figure 10. Diagram shows the preservation of sequences (in time) plotted against geographic distance (south to north transect from Fentress, VA to Island Beach, NJ).

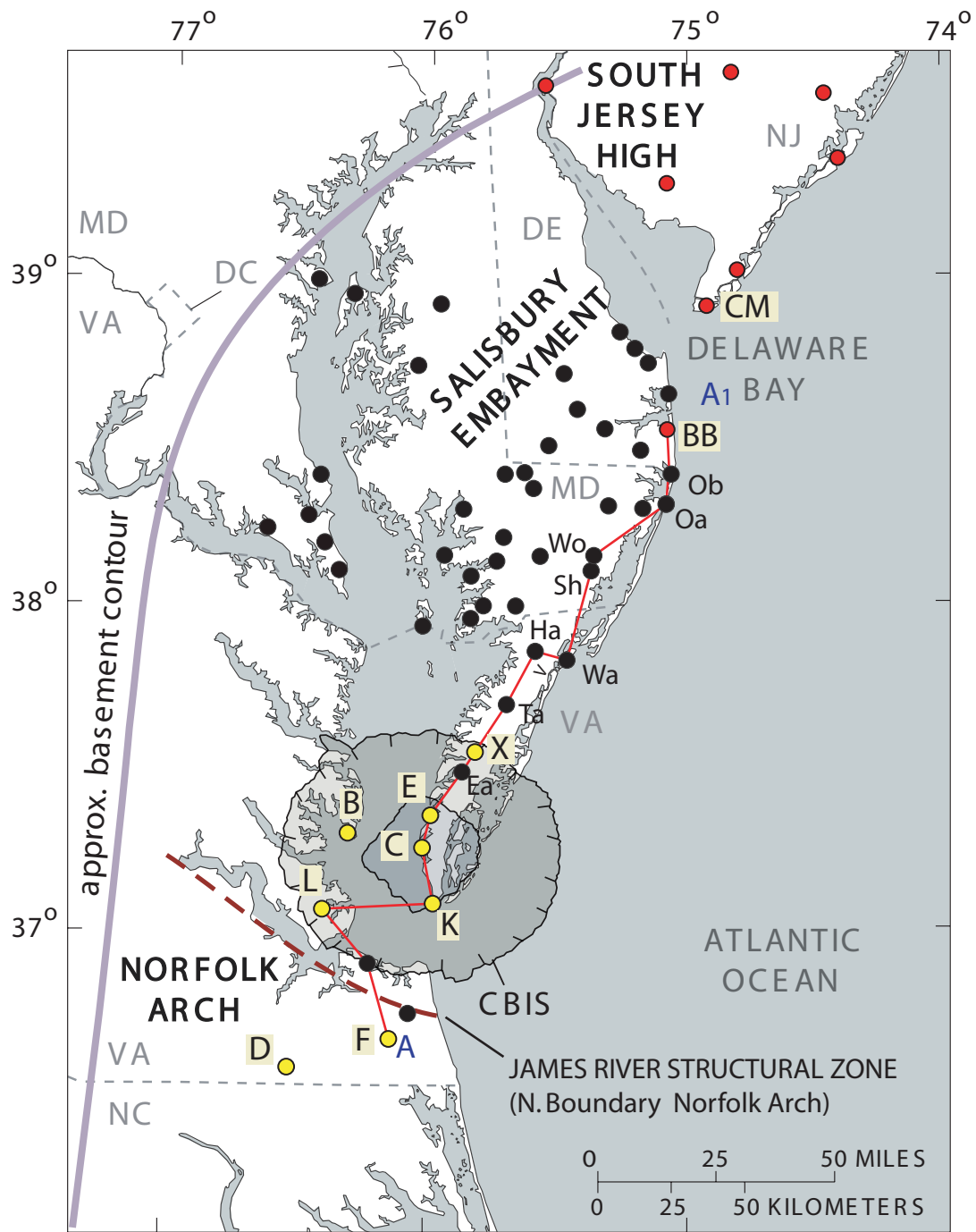
The basement contour is modified from Olsson et al., 1989). Faint red background is used to represent regional hiatuses.

Table 1. Table shows the Sr- isotopic age ranges for sequences recovered at the three coreholes used in this study; Bethany Beach (Browning et al., 2006); Eyreville (Browning et al., this volume); and Exmore (this study). All ages are in Ma. Undated (no carb) indicates that intervals provided insufficient carbonate material to extract Sr-ratios. The letters “xxx” indicate the absence of a sequence at a corehole.

Table 2. Table summarizes the primary lithologic, paleoenvironmental, and regional thickness trends of strata from Delaware/ New Jersey to the CBIS and southern Virginia.

Table 3. Criteria used for sequence boundary analysis for the Eyreville corehole. A confidence level of ‘2’ indicates that there is a substantial hiatus, and the presence of several key defining characteristics. A confidence level of ‘1’ indicates a shorter hiatus, or a poorly defined sequence boundary.

Table 4. Criteria used for sequence boundary analysis for the Exmore corehole. A confidence level of ‘2’ indicates that there is a substantial hiatus, and the presence of several key defining characteristics. A confidence level of ‘1’ indicates a shorter hiatus, or a poorly defined sequence boundary. Age estimates with superscript “*” represent ages derived from correlation with nearby coreholes.



Base from U.S. Geological Survey
Digital Line Graph, 1:2,000,000, 1990

Figure 1

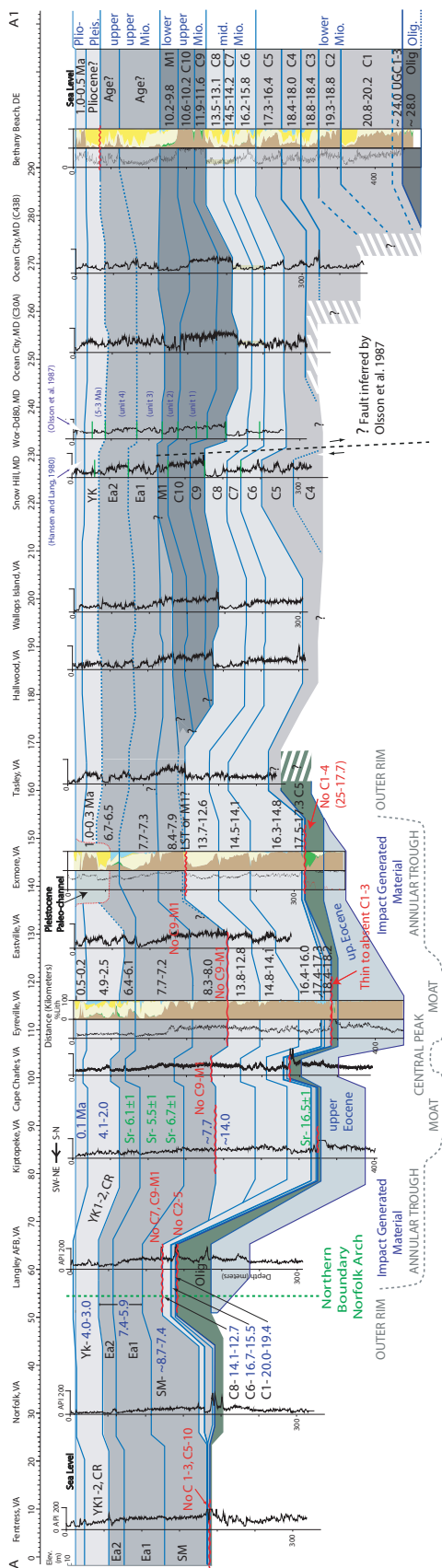


Figure 3

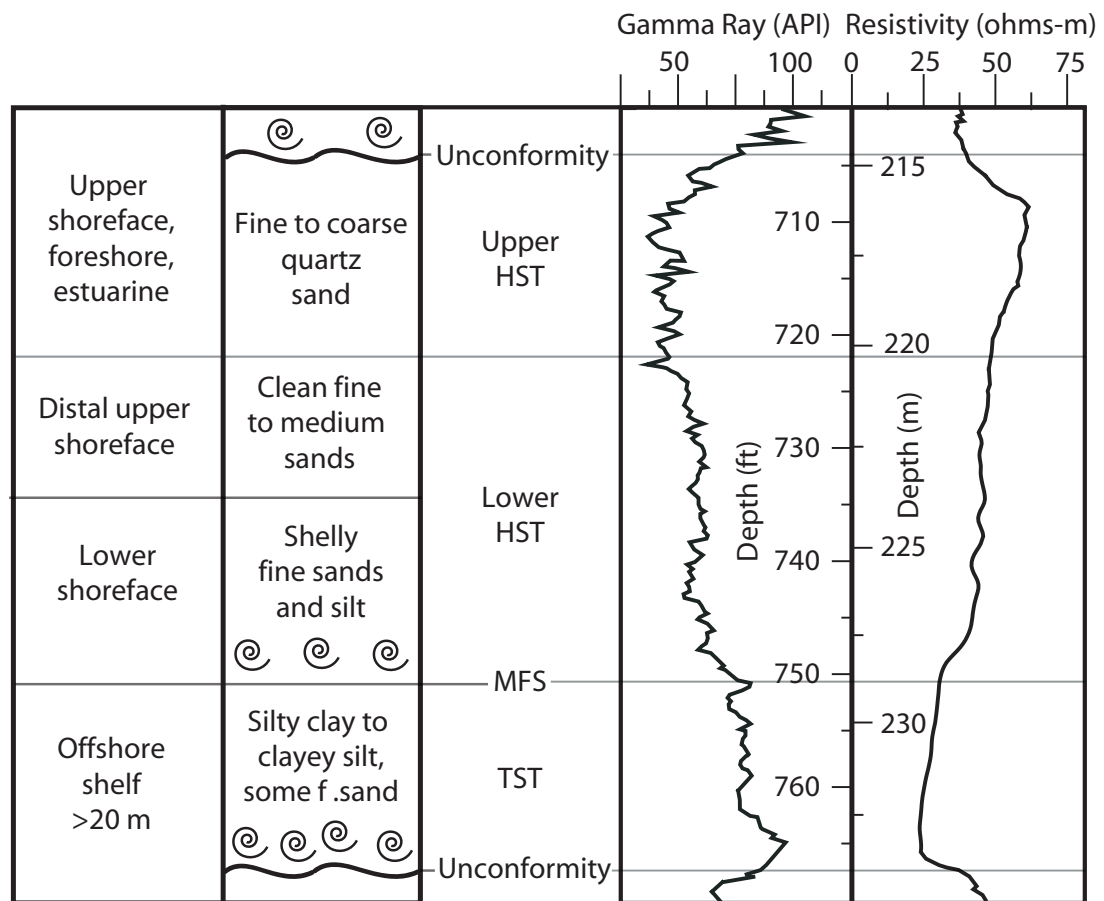


Figure 4

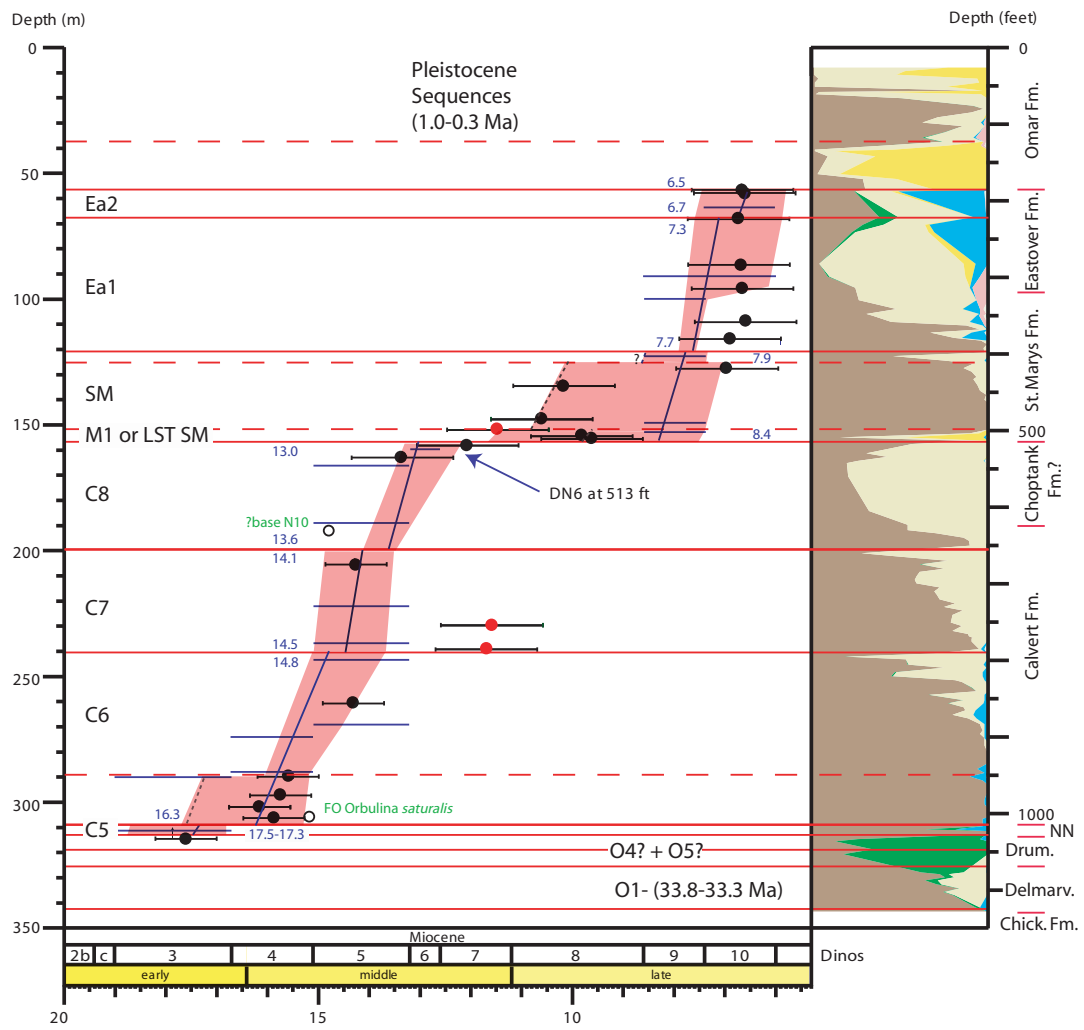


Figure 5

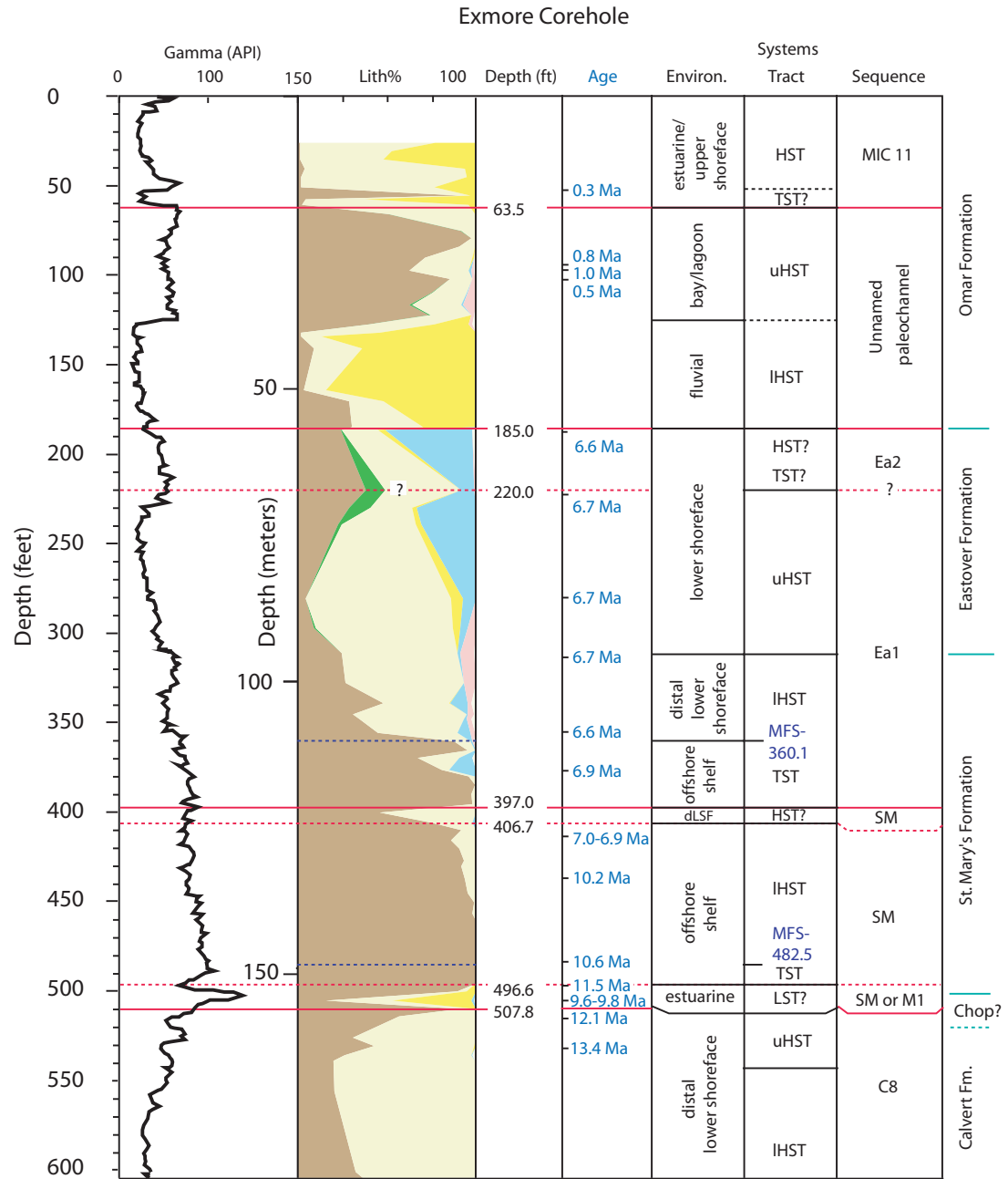


Figure 6

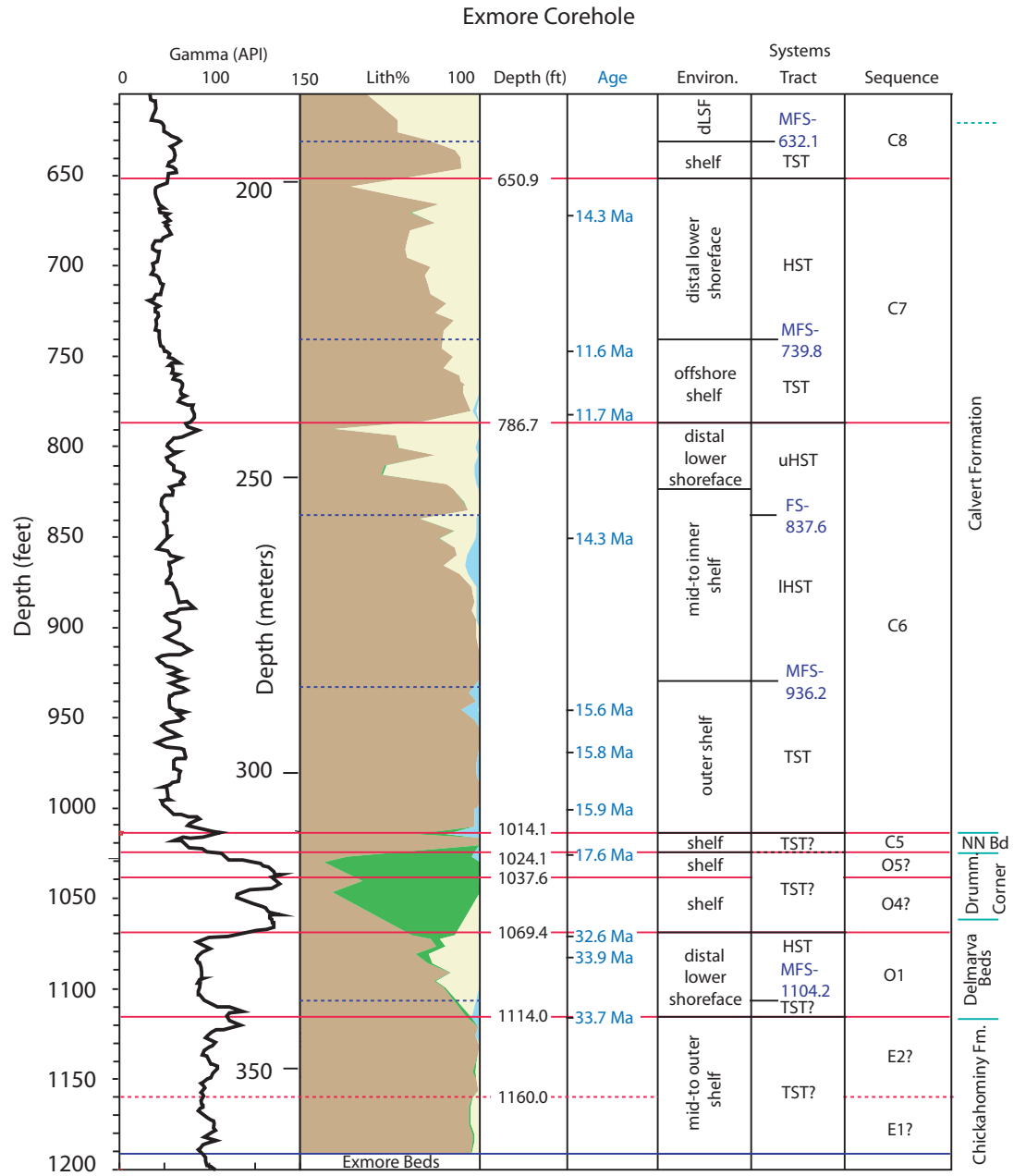


Figure 7

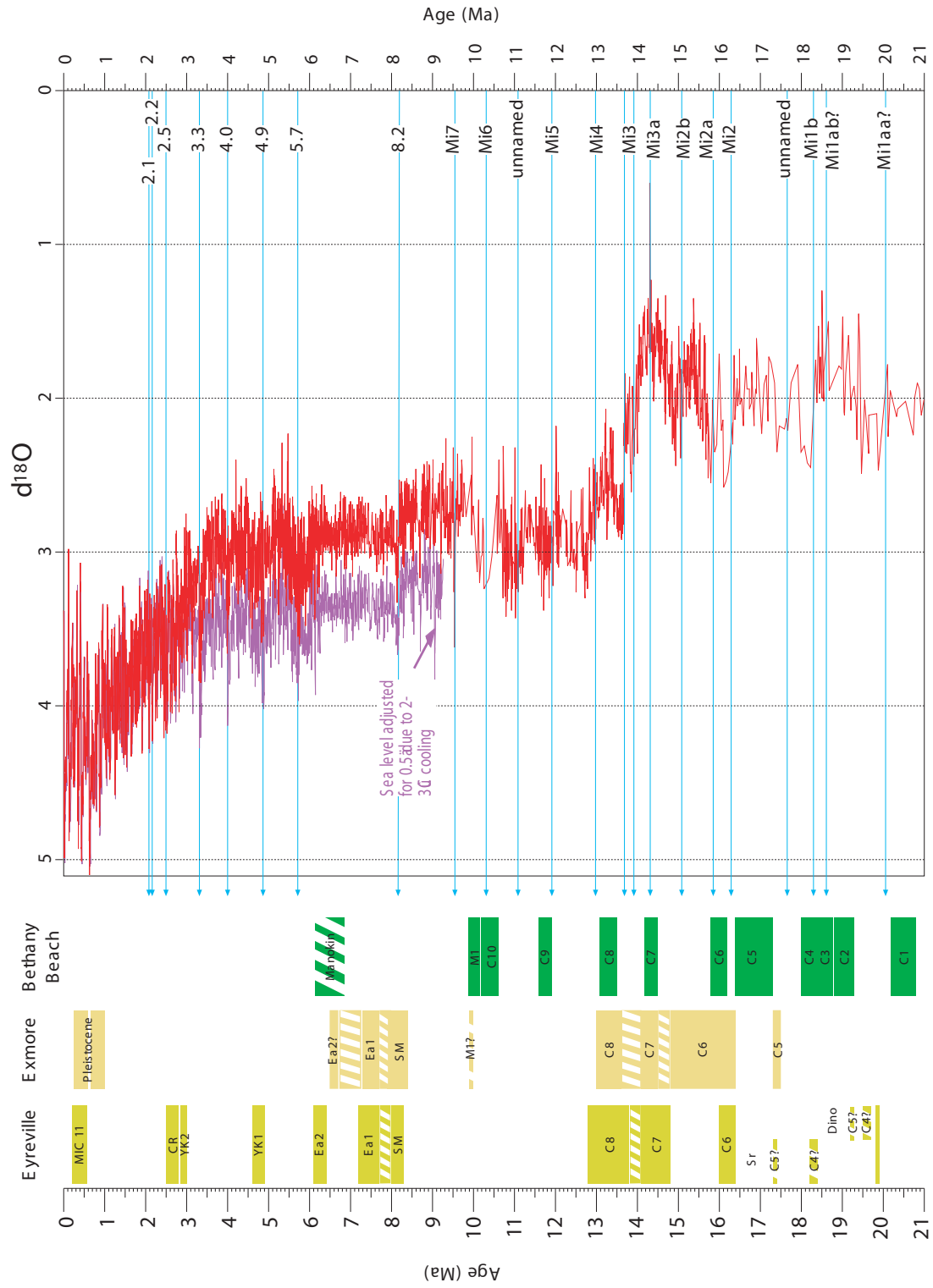


Figure 8

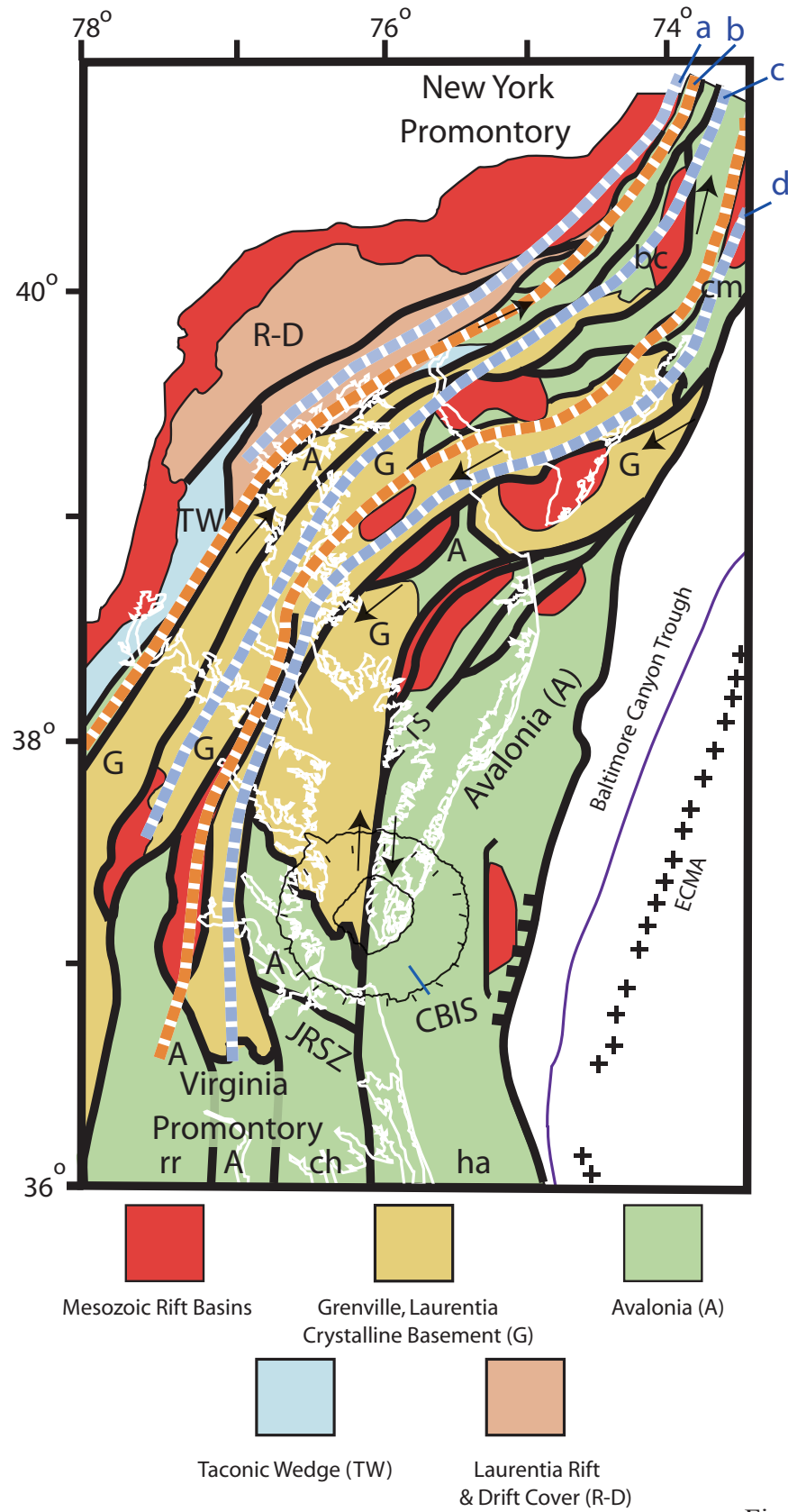
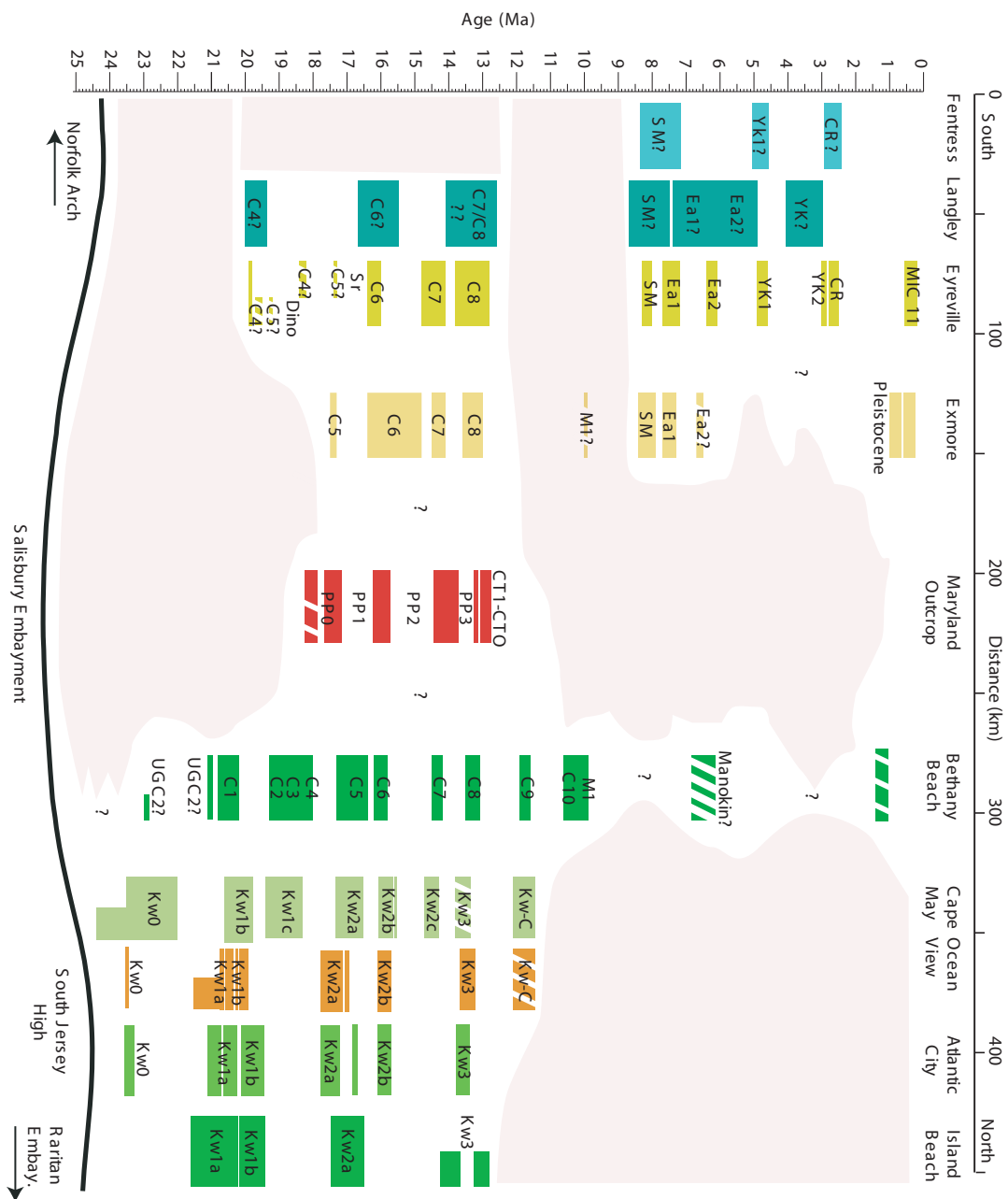


Figure 9



Sequence	Eyreville, VA	Exmore, VA	Bethany Beach, DE
Pleis	0.55-0.2	1.0-0.3	1.0-0.5
CR	2.8-2.5	xxx	xxx
Yk2	3.0-2.8	xxx	xxx
Yk1	4.9-4.6	xxx	xxx
Ea2	6.4-6.1	6.7-6.5	undated (no carb)
Ea1	7.7-7.2	7.7-7.3	undated (no carb)
SM	8.3-8.0	8.4-7.9	xxx
M1	xxx	9.8-9.9?	10.2-9.8
C10	xxx	xxx	10.6-10.2
C9	xxx	xxx	11.9-11.6
C8	13.8-12.8	13.6-13.0	13.5-13.1
C7	14.8-14.1	14.5-14.1	14.5-14.2
C6	16.4-16.0	16.3-14.8	16.2-15.8
C5	17.4-17.3	17.5-17.3	17.3-16.4
C4	18.4-18.2	xxx	18.4-18.0
C3	xxx	xxx	18.8-18.4
C2	xxx	xxx	19.3-18.8
C1	xxx	xxx	20.8-20.2
UGC	xxx	xxx	24.0-28.0
O5?	26.65-26.5	undated (no carb)	not cored
O4?	27.7-27.6	undated (no carb)	not cored
O1?	xxx	33.8-32.6	not cored
E2	???	???	not cored
E1	35.4-???	35.4-???	not cored

all ages in Ma

Table 1

Late Miocene-Pliocene	CBIS Central Basin Eyreville	Fine grained (St. Marys) to coarse grained (Eastover) Marine shelf to shoreface Thick and widespread Persists south of CBIS Hiatus: 12.8-8.3 Ma	CBIS Annular Trough Exmore	Fine grained (St. Marys) to coarse grained (Eastover) Marine shelf to shoreface Thick and widespread Pleis. channel removed Pliocene Hiatus: 13.0-8.4 Ma	Delaware and New Jersey Bethany Beach Predominantly coarse grained Marine shelf to shoreface in DE Deltaic in NJ L.Miocene-Pliocene absent Hiatus: 7-2 Ma
	Middle Miocene	Fine grained Shelf, distal lower shoreface HSTs 20-50 m thick sequences Thickens into central crater Absent south of crater	Fine grained base, coarsens upwards Shelf to shoreface 20-50 m thick sequences Thickens into the annular trough Abundant in annular trough	Coarse grained Shoreface in DE, deltaic in NJ 10-20 m thick sequences Prograding wedges Consistent across Delmarva	
Early-Middle Miocene	Very fine grained Marine shelf Thin to absent within inner crater Thin, patchy, absent further south	Very fine grained Marine shelf Largely absent within annular trough	Coarse grained Upper shoreface to shelf in DE Prograding wedges, deltaic in NJ Thick and continuous (20-60 m)		
Oligocene	Heavily glauconitic clay and sand Sediment starved shelf Restricted inner basin Thinly preserved (15 m)	Heavily glauconitic clay and sand Sediment starved shelf Thicker in annular trough (25-50m) Thins significantly to south	Glaucconitic clay and sand Sediment starved shelf Locally thick (40-60 m) Patchy distribution		
Late Eocene	Very fine grained Deep shelf, deeper inner basin Thick in central basin (94 m) Thin to absent in surrounding regions	Very fine grained Deep shelf Thinner than inner basin (24 m) Thins outside of crater	Fine grained Deep shelf Thick sequences (50 m) Continuous and widespread		

Table 2

Exmore Sequence	Unconformity	Depth (ft)	Depth (m)	Age (Ma)	Hiatus (my)	Confidence	Sharp Contact	Burrowed	Rip ups, lag	Shell lag	Facies shift	Gamma kick
Pleistocene				0.2								
				0.55								
	Unconformity				0.05	1	Y		Y		Y	Y
Paleochannel		63.6	19.39	0.6								
		181	55.17	1								
	Unconformity				5.5	2	Y		Y	Y	Y	Y
Ea2		181	55.17	6.5								
		220.0	67.06	6.7								
	Unconformity				0.6	2						Y
Ea1		220.0	67.06	7.3								
		397	121.01	7.7								
	Unconformity				0.2	1	Y	Y	Y			Y
SM		397	121.01	7.9								
		507.8	154.78	8.4								
	Unconformity				4.6	2	Y	Y	Y	Y	Y	Y
C8		507.8	154.78	13								
		650.9	198.39	13.6								
	Unconformity				0.5	2	Y	Y				Y
C7		650.9	198.39	14.1								
		786.7	239.79	14.5								
	Unconformity				0.3	1	Y	Y				Y
C6		786.7	239.79	14.8								
		1014.1	309.10	16.3								
	Unconformity				1.0	1	Y	Y				Y
C5		1014.1	309.10	17.3								
		1024.1	312.15	17.5								
	Unconformity				9.0*	2	Y	Y			Y	Y
O3		1024.1	312.15	26.5*								
		1037.6	316.26	26.65*								
	Unconformity				0.95*	1			Y			Y
O2		1037.6	316.26	27.6*								
		1049.7	319.95	27.7*								
	Unconformity				4.9*	1	Y	Y		Y	Y	Y
O1		1069.4	325.95	32.6								
		1110.7	338.54	33.8								
	Unconformity				0.2	2				Y	Y	Y
Eocene		1110.7	338.54	34								
		1191.2	363.08	35.5								

Table 4

Chapter 3: Quantifying Regional Tectonics and Impact-Related Effects: Backstripping the Inner Crater, Chesapeake Bay Impact Structure, Virginia, USA

This chapter is in preparation for submission to a peer-reviewed journal as Kulpecz, A.A., Kominz, M.A., Miller, K.G., Browning, J.V., and Hayden, T.G., Quantifying Regional Tectonics and Impact-Related Effects: Backstripping the Inner Crater, Chesapeake Bay Impact Structure, Virginia, USA.

Abstract: We develop a new time-dependent compaction model for impact-generated materials and use one-dimensional backstripping to differentiate and quantify the rates and amplitudes of impact-related effects, regional tectonics, and eustatic change on the post-impact section of the late Eocene (35.5 Ma) Chesapeake Bay Impact Structure (CBIS) and surrounding mid-Atlantic Coastal Plain. While eustasy and thermoflexural subsidence are the dominant controls on margin sedimentation, the presence of basinal-scale unconformities (3-7 myr hiatus) across the CBIS area implicates periodic regional tectonic uplift. Comparison of backstripped records in and around the CBIS reveals several interesting trends: 1) the long-term, time-dependent compaction of impactites strongly influenced deposition within the inner crater, shown by the growth of post-impact sequences into the CBIS and excess subsidence of 285 ± 50 m in the late Eocene that progressively decreases to 20 ± 15 m by the late Miocene; 2) excess accommodation at Exmore was 115 ± 50 m immediately after impact, but decreased to overlap with eustasy from the late Eocene-Miocene, a reflection of thinner (~ 200 m) impactites within the annular trough; 3) late Eocene-early Oligocene uplift/shallowing of 95 ± 45 m at Exmore and 225 ± 125 m at Eyreville resulted from the combination of the major Eocene-Oligocene sea level fall and the removal of a negative thermal anomaly within

the CBIS; 4) basin-scale unconformities during the Oligocene, early Miocene, and late middle Miocene contrast with thick sections in New Jersey and Delaware, and appear to correspond with known basement structural boundaries of the mid-Atlantic margin; and 5) this segment of the margin exhibits distinct periods of “passive-aggressive” non-thermal tectonic uplift (10-50 m /1-5 myr) and excess subsidence (10-55/10 myr, with peaks of 75-100 m/5 myr). We conclude that while eustasy is largely responsible for changes in accommodation and the margin-wide genesis of sequence boundaries, the vertical movement of basement structures in response to intraplate stress, depocenter loading, and other tectonic mechanisms, results in significant differential preservation of sequences across the margin. The post-impact section of the CBIS, although strongly influenced by the initial impact and subsequent time-dependent compaction of impact materials, is primarily dominated by regional tectonic patterns after the latest Eocene and may provide valid eustatic estimates for the late Miocene and Pliocene: 25 ± 9 m to 15 ± 5 m from 8.4 to 8.0 Ma; 22 ± 5 m and 14 ± 5 m from 7.7 to 7.2 Ma; 12 ± 2 m from 6.4-6.1 Ma; 10 ± 2 m at 4.9 Ma; 10 ± 2 m at 2.95 Ma shallowing to 4 ± 3 m at 2.8 Ma; and 18 ± 5 m from 2.75-2.55 Ma.

Introduction

The late Eocene Chesapeake Bay Impact Structure (CBIS; dated at 35.4 Ma; Pusz et al., in press) is an 85-90 km diameter marine impact crater that underlies the modern Chesapeake Bay and adjacent lower Delmarva Peninsula (Fig 1; Poag et al., 1994). This “wet-target” impact structure formed when a ~3 km bolide (Crawford, 2002) struck a

passive margin continental shelf consisting of a marine water column (mean value 85 m, 0-170 m paleodepth range; Poag et al., 1994; Horton et al., 2005), mid-Cretaceous through Paleogene unconsolidated sediments, and Paleozoic crystalline basement (Gohn et al., 2008). The structure exhibits complex “inverted sombrero” morphology with a central uplift surrounded by a 35-40 km diameter inner crater, ~25 km annular trough, and extensive outer fracture zone (Fig. 1; Poag et al., 1994; Powars and Bruce, 1999). The impact location on a marine shelf not only enabled exceptional preservation of impact-generated crater fill deposits (e.g., suevite, resurge flows, granite megablocks, tsunamiites, sedimentary lithic breccia; Gohn et al., 2008; Horton et al., 2008), but also resulted in the deposition of an expanded (~140-450 m) post-impact record of normal marine upper Eocene-Holocene sediments (Poag et al., 1994; Powars and Bruce, 1999).

The CBIS was initially identified from marine seismic profiles (Poag et al., 1994) and impact breccia in the Exmore coreholes (Fig. 1), and was later correlated to the North American Tektite strewn field (Glass, 1989; Koeberl, 1989; Poag et al., 1994). Early work on the post-impact section focused on hydrogeology and regional stratigraphy, but was largely restricted to a series of coreholes and geophysical logs within the annular trough (e.g., Powars et al., 1992). Over the last decade, the United States Geological Survey (USGS), Virginia Department of Environmental Quality, and Hampton Roads Planning District Commission drilled a series of coreholes that penetrated both impact and post-impact sections (Fig. 1). However, these studies (with the exception of the Langley corehole; Horton et al., 2005) produced primarily lithostratigraphic observations with relatively coarse biostratigraphic control (Powars and Bruce, 1999; Powars, 2000).

Cooperative drilling of the Eyreville corehole (funded by the International Continental Scientific Drilling Project, USGS, and NASA) was completed in May 2006 and provided the first complete continuous post-impact section (~444 m) from the inner crater with high-resolution geochronology from biostratigraphic and Sr-isotopic analyses (e.g., Gohn et al., 2008; Browning et al., submitted; Kulpecz et al., submitted).

Recent studies by Hayden et al. (2008) used one-dimensional backstripping of coreholes within the annular trough and surrounding area to differentiate crater effects from regional tectonic trends. The authors identified a period of excess accommodation within the CBIS of 3 myr after the impact that was attributed to the rapid compaction of impact-generated materials. This was followed by a period of Oligocene uplift of 50-125 m attributed to crustal-scale heating from the impact event, subsequent to thermal blanketing by cold sedimentary materials, and the onset of a large negative thermal anomaly that was removed by 30 ± 2 Ma (Hayden et al., 2008). Following a large hiatus from 30-20 Ma, the mid-Miocene through Pliocene was primarily dominated by regional trends, with several periods of excess subsidence and uplift (10's m) superimposed on passive margin subsidence. Although Hayden et al. (2008) provided the first backstripped records of the CBIS post-impact section, the study is limited by several factors: 1) the lack of a time-dependent model for the compaction of the impactites that underlie post-impact sediments (regional studies indicate the growth of post-impact sequences into the crater; Poag, 1997; Gohn et al., 2008); 2) the absence of a continuous record from the inner crater; 3) the lack of high resolution (~ 1 myr) geochronology and sequence

stratigraphic interpretations; and 4) limited paleobathymetric data for coreholes in and around the CBIS.

The Eyreville corehole (situated within the inner crater; Fig. 1) addresses many of these limitations, and thus allows for more accurate backstripping of the CBIS. Recent studies used litho-, bio-, and Sr-isotopic analyses to produce a high resolution (> 1 myr) sequence stratigraphic framework in the inner crater (Eyreville; Edwards et al., submitted; Browning et al., submitted) and annular trough (Exmore; Kulpecz et al., submitted). Recent studies (Gohn et al., 2008; Kulpecz et al., submitted) also provided regional correlations of CBIS sequences across the mid-Atlantic margin to other coreholes in Delaware and New Jersey (Browning et al., 2006; Miller et al., 2005).

Although these results document eustatic control on sequence boundary formation within the CBIS (as shown by the strong correspondence of sequence boundaries with $\delta^{18}\text{O}$ isotope increases), they also indicate that periods of regional tectonic uplift and subsidence, variations in regional sediment supply, and the long-term compaction of impact materials influenced the post-impact record (Kulpecz et al., submitted; Browning et al., submitted). Recent studies (Gohn et al., 2008; Kulpecz et al., submitted) established the presence of significant regional unconformities around the CBIS and across the southern mid-Atlantic margin during the Oligocene (thin, patchy distribution from 34-25 Ma), early Miocene (25-18 Ma) and late middle Miocene (13-8.4 Ma). The geographic extent of these unconformities appear to coincide with the Norfolk arch and associated structural boundaries. These represent periods of regional non-thermal

“passive-aggressive” tectonic uplift of 10-50 m on 3-5 myr scales. These studies also show the long-term (35.4 myr) growth of most post-impact sequences into the CBIS (indicating excess accommodation that we attribute to the persistent compaction of impact materials). New wet porosity samples of the impactites from Eyreville (Sanford et al., submitted) yield valuable constraints on porosity-depth relationships and have been used as a partial constraint on the construction of a new time-dependent model for the compaction of impact-generated materials. In previous backstripping efforts impactites compacted solely with depth like a normal sedimentary unit (Hayden et al., 2008). Furthermore, in this study we provide new paleobathymetric depth estimates from lithofacies and benthic foraminiferal analysis for the Eyreville corehole, significantly improving constraints on water-depth estimates.

Although the CBIS is located on a passive margin typically dominated by thermoflexural subsidence and eustasy (Watts and Steckler, 1979; Kominz et al., 1998; Miller et al., 2005), recent studies (Powars, 2000; Kulpecz et al., submitted) note the proximity of the CBIS to the Norfolk arch (10-15 km to the south), one of a series of alternating crystalline basement arches and embayments (e.g., from south to north: Cape Fear arch, Albemarle embayment, Norfolk arch, Salisbury embayment, South Jersey high, and Raritan embayment) that underlie the mid-Atlantic margin (Fig. 1) (Brown et al., 1972; Olsson, 1988). Although the presence of these basement structures has been recognized for some time (e.g., Owens and Sohl, 1969; Owens and Gohn, 1985), the timing, scale, and mechanism responsible for tectonic activity remains uncertain due to the lack of regional seismic data, small number of deep coreholes that penetrate basement, and lack

of significant seismic activity north of the Cape Fear arch (Seeber and Ambruster, 1988). Brown et al. (1972) attributed the origin of these basement structures to large-scale crustal wrench faulting, while Owens et al. (1997) invoked regional crustal warping responsible for long-wavelength (100-200 km) “rolling basins.”

Recent studies (Moucha et al., 2008; Mueller et al., 2008; Spasojević et al., 2008) demonstrate the influence of long-term dynamic topographic changes (e.g., epeirogenic crustal response to convectively-driven vertical stresses; Mitrovica et al., 1989) on the eastern U.S. margin related to its passage over the subducted Farallon slab. However, such studies focus on long-term (10-20 myr) and broad margin-wide trends, and their implications for myr-scale, sub-regional tectonic variations remain uncertain. Although not unique to this margin, variations and reorganizations of intra-plate stress fields can result in 1-3 myr-scale events with amplitudes of 10-50 m (Cloetingh, 1988). These changes in intra-plate stress can be propagated over large distances (1000's km; Letouzey, 1986; Ziegler and Van Hoorn, 1989; Cloetingh et al., 1990), influence unconformity genesis on basinal scales (Karner et al., 1993), or result in the thinning, truncation, or the complete removal of entire series in the stratigraphic record (e.g., Cape Fear arch, North Carolina; Weems and Lewis, 2002; Self-Trail et al., 2004). Other studies (Browning et al., 2006; Hayden et al., 2008) noted periods of excess subsidence and uplift on this margin attributed to the flexural response of sediment loads prograding onto the continental shelf. However, the amplitudes and timing of these tectonic events is largely unclear due to the limited high-resolution geochronology on the margin, and lack

of detailed backstripped records (myr-scale) south of the New Jersey Coastal Plain (e.g., Kominz et al., 2008).

The primary objective of this study is to provide new backstripped results from the inner crater and annular trough of the Chesapeake Bay Impact Structure (at Eyreville and Exmore, respectively), using enhanced geochronology, paleobathymetry, and impactite porosity data from the Eyreville corehole in the central basin (Gohn et al., 2008; Browning et al., submitted; Kulpecz et al., submitted). We also present a new model for the time-dependent compaction of impact materials, the first applications of such a model in backstripping efforts. We use a sequence stratigraphic framework (e.g., genetically related stratigraphic units bounded at their top and base by unconformities, or their correlative conformities; Mitchum et al., 1977) to evaluate how variations in eustasy (e.g., Posamentier et al., 1988; Van Wagoner et al., 1988), tectonics, sediment supply (e.g., Christie-Blick et al., 1990), and impact-related processes (e.g., Hayden et al., 2008) influence the evolution of the CBIS. These results are compared to previously backstripped records from the U.S. mid-Atlantic margin (Miller et al., 2005; Browning et al., 2006; Hayden et al., 2008; Kominz et al., 2008) to differentiate impact effects from both eustatic and regional tectonic signals. Furthermore, one-dimensional backstripping provides quantitative estimates of the rates and amplitudes of tectonic uplift and subsidence on the mid-Atlantic margin, allowing for an evaluation of the non-thermoflexural mechanisms that influence this “passive-aggressive” margin.

Methods

The backstripping method has been described by Steckler and Watts (1978) and Bond et al. (1989). In this study it has been modified by erosion of a significant package of pre-impact strata followed by time-dependent compaction of the rapidly-deposited impact materials. One-dimensional backstripping is an inverse modeling technique that provides an estimate of tectonic subsidence in water (e.g., accommodation, the vertical capacity for sediment to accumulate) by removing the effects of sediment and sea level loading. Tectonic subsidence (TS) is represented by the following equation (Eq. 1), after Steckler and Watts (1978):

$$TS = S * \frac{(\rho_m - \rho_s)}{(\rho_m - \rho_w)} - \Delta SL \frac{(\rho_m)}{(\rho_m - \rho_w)} + Wd$$

Eq.1

Where the variables are defined as decompacted sediment thickness (S^*), density of decompacted sediment (ρ_s), density of the mantle ($\rho_m = 3.18 \text{ g/cm}^3$), density of seawater ($\rho_w = 1.03 \text{ g/cm}^3$), water depth (Wd), and global sea level change (ΔSL).

The first reduction (R1 of Bond et al., 1989) progressively unloads the decompacted sediment packages to yield a combination of tectonic subsidence and eustasy (Eq. 2). Each sediment package must be decompacted before unloading, and porosity-depth estimates are used to restore each unit to its ‘true’ thickness at the time of deposition. Water depth estimates are derived from lithofacies and benthic foraminiferal

analysis from core. The resultant R1 estimate (Eq. 3) represents a combination of both tectonic subsidence and eustasy:

Eq.2

$$\begin{aligned} R1 &= S * \frac{(\rho_m - \rho_s)}{(\rho_m - \rho_w)} + Wd \\ &= TS + \Delta SL \frac{(\rho_m)}{(\rho_m - \rho_w)}. \end{aligned}$$

Eq. 3

The second reduction (R2 of Bond et al., 1989) removes theoretical thermal subsidence (McKenzie, 1978) to provide an estimate of sea-level change and non-thermal tectonics. R2 is represented by the following equation:

$$R2_{SL} = (R1 - TS) \left(\frac{\rho_a - \rho_w}{\rho_a} \right)$$

Eq. 4

The time-dependent nature of theoretical thermal subsidence requires age estimates for each sedimentary unit. These are established from core and in this study include micropaleontology (planktonic foraminifera and dinocyst zones) and Sr-age estimates and that provide geochronologic resolution of 1 myr or better for most sections (Fig. 2; Table 1).

Recent sea level studies of the New Jersey margin (Miller et al., 2005; Kominz et al., 2008) assume negligible non-thermal tectonic effects to generate eustatic estimates for the Late Cretaceous-Miocene. Although we anticipate non-thermal tectonics (both regional uplift/subsidence and crater effects), the comparison of our R2 results to eustatic estimates allows an evaluation and quantification of these non-thermal processes. In the backstripping equation, the assumption of R2 as an approximation of eustasy results in an underestimate of tectonic subsidence by $(\rho_a - \rho_s)/\rho_a$ (Eq. 4).

Due to the position of the CBIS on the mid-Atlantic passive margin, R1 results may be compared to theoretical models of passive margin subsidence (e.g., Bond and Kominz, 1984). These are based largely on the empirical thermal decay of heated oceanic crust (decay constant of $\tau = 62.5$ myr, Watts, 1981; McKenzie, 1978). This model quantifies the timing and magnitude of margin subsidence due to thermal cooling seaward of the hinge zone. Because the cores from the CBIS are located near the hinge zone, subsidence on the coastal plain (the area landward of the hinge zone) follows thermal decay curves due to the flexure of unstretched continental crust in response to sediment loading on the shelf (e.g., thermoflexural subsidence of Kominz et al., 1998). The breakup of the mid-Atlantic margin and onset of offshore thermal subsidence occurred at 155 Ma around the Maryland-Virginia area (Grow et al., 1980). As expected for thermoflexural subsidence, onshore subsidence and coastal plain deposition show a substantial lag (first coastal plain sediments of the Potomac Formation were deposited 140-120 Ma; Grow and Sheridan, 1989).

In this study, the normal backstripping model has been modified to account for normal pre-impact sediments that were instantaneously removed by the impact event. The entire sediment column and uppermost crust was removed within the inner crater (Eyreville), while only a portion of the sediment column was removed in the annular trough (Exmore). These units were catastrophically redeposited within seconds to minutes (Poag et al., 1994; Horton et al., 2008) of the impact event as impactites (suevite, crystalline-clast breccias, and lithic-clast breccias; Horton et al., 2005; Horton et al., 2008). The rapid rate of deposition, unconventional burial history, and growth of most post-impact units into the CBIS (Powars and Bruce, 1999; Kulpecz et al., submitted) indicates the compaction of impact-generated materials was long-term (late Eocene-Miocene) and time-dependent, and we generate a new model that accounts for these unique characteristics.

Normal sedimentary units are decompacted using porosity-depth curves established from the New Jersey Coastal Plain (Island Beach) and margin (COST-B2; Van Sickel et al., 2004). Porosity estimates from the Eyreville coreholes (Sanford et al., submitted) measure current impactite porosity ranges of 15-20% below 800 m to 35% at ~450 m depth, although expansion during core recovery may have caused higher porosities than *in situ* values. Estimates of impactite porosity immediately after deposition (although poorly constrained) are significantly higher, ranging from 45-70% (Sanford et al., submitted). In our model the impactite unit is assumed to compact exponentially through time, and is represented by the following equations:

$$\phi = \phi_0 e^{(-z/k(t))}$$

Eq. 5

Where:

$$k(t) = k_{\infty} e^{[(c/(t+t_0))^2]}$$

Eq. 6

Where k_{∞} is the exponential decay constant (in the case where k is independent of time). We use physical porosity-depth measurements from impactites within the Eyreville core (Fig. 3) (Sanford et al., submitted) to establish k_{∞} values for Eyreville (900 m) and Exmore (700 m). The compaction equation is designed so that initial decay constants are higher than k_{∞} , and exponentially approach k_{∞} through time. The time decay variable (c) is designed so that larger values result in slower, protracted compaction of the impactites (values of 50 and 40 are assigned for Eyreville and Exmore, respectively), while “ t ” represents time since the deposition of the impactites. The constant “ t_0 ” controls porosity-depth relationships through time: low values result in high initial porosity throughout the entire section, while high values yield increased compaction with depth (similar to normal compaction curves). We assign t_0 values of 6 and 8 for Eyreville and Exmore, respectively.

We assigned different “ c ” and “ t_0 ” values for the two coreholes because of the different impactite thicknesses at Eyreville (~ 950 m) and Exmore (~ 200 m), and the timing of

compaction at each location. Stratigraphic cross sections show minor growth of sequences into the annular trough, and significant thickening of sequences into the inner crater (Gohn et al., 2008; Kulpecz et al., submitted). Thus, we assume that impactite compaction in the annular trough was rapid while the thick impactite unit at Eyreville took significantly longer to fully compact. Extreme-range scenarios for the Eyreville impactites were tested before selecting the compaction constants. Figure 3 shows the time-dependent compaction curves for Eyreville and Exmore, compared to physical porosity measurements from the Eyreville core.

Data

Although most of the data used in this study was derived from Eyreville and Exmore, in the backstripping model normal pre-impact sedimentary units were removed by the impact and consequently replaced. At Exmore, these sediments were replaced by 200 m of impact-generated material. Because the Exmore corehole did not penetrate pre-impact strata, unit thicknesses, ages, and lithologies were projected along-strike from regional studies (Powars et al., 1992; Powars and Bruce, 1999). At Eyreville, where the entire pre-impact section and several kilometers of continental crust were removed (Catchings et al., 2008), the “pre-impact” units were replaced by a thick (~950 m) lithic breccia impactite unit (~300 m of granite megablocks are non-compactable and thus were not modeled).

The Eyreville and Exmore coreholes provide the data necessary for backstripping: 1) age-estimates from biostratigraphy and Sr-isotopic analyses; 2) paleowater depth estimates

from lithofacies and benthic foraminifera; and 3) the current thickness and lithology of sedimentary units that must be decompacted to restore the unit to its original thickness at the time of deposition. Sixteen post-impact sequences were identified in the central moat at Eyreville (Edwards et al., submitted; Browning et al., submitted), while 13-15 sequences were recovered in the annular trough at Exmore (Fig. 2) (Kulpecz et al., submitted). Late Eocene-Pleistocene age control for these sequences was established from the integration of Sr-isotopic age estimates and biostratigraphic data (planktonic foraminifera, dinocyst, and nannofossil zones), yielding age estimates with ~ 1 myr resolution for most sequences (Fig. 2, Tables 2, 3; Browning et al., submitted; Kulpecz et al., submitted).

Previous studies (Browning et al., submitted; Kulpecz et al., submitted) provided lithologic descriptions (from standard core analysis) and semi-quantitative grain size analysis that established the percentage of coarse sand, fine sand, and silt/clay. The percentage of quartz, glauconite, mica, carbonate, and other minerals was visually estimated (Browning et al., submitted; Kulpecz et al., submitted). These results were expanded by estimating the percent sandstone, silt, clay, micrite, calcarenite, and the mineralogy of cemented intervals. Density estimates for the mineralogy of these largely unconsolidated quartz- and clay-rich sediments generally range between 2.65-2.75 gm/cm³ (Tables 2, 3). Porosity-depth relationships of post-impact units are tied to sediments of similar age and lithology (unconsolidated silts, sands, and clays) from the New Jersey Margin (Van Sickel et al., 2004).

We provide new paleo-water depth estimates (Tables 1-3) for each sequence based on lithofacies interpretations and benthic foraminiferal biofacies depth ranges established from the New Jersey Coastal Plain (Fig. 4; Miller et al., 1997; Pekar et al., 1997).

Lithofacies descriptions follow the wave-dominated shoreface facies model of Browning et al. (2006), and include primary sedimentary structures, textures, lithology, color, fossil content (shells and microfossils), and ichnologic observations (Edwards et al., submitted; Browning et al., submitted; Kulpecz et al., submitted). This facies model distinguishes lagoonal, estuarine, foreshore, proximal upper shoreface, distal upper shoreface, lower shoreface, and shelf facies and infers water depth ranges (Fig. 4).

Multiple samples were taken from each sequence in the Eyreville corehole (at 3-10 m intervals), and benthic foraminifera were evaluated for each sample (bio- and lithofacies interpretations are indicated on Figure 2 and Tables 1, 2). Due to dissolution, dilution, and/or non-fossiliferous zones most analyses were semi-quantitative, although complete analysis (300 individual benthic tests) was possible in several intervals. The dominant and most abundant faunas were identified for each sample (Table 1), and the results were compared to previous studies for the Oligocene (Pekar et al., 1997) and Miocene (Miller et al., 1997) that identified benthic biofacies (with inferred depth ranges from paleoslope analysis) from coreholes on the New Jersey Coastal Plain (Fig. 4; ODP Leg 150X). When applicable, we also used previously published benthic foraminiferal data (e.g., Poag, submitted) to supplement our paleodepth estimates for specific intervals (e.g., upper Eocene Chickahominy Formation).

The broad range of paleodepth estimates constitutes the greatest source of uncertainty in the backstripping equation. For shallow marine sections (<30 m), our interpretations are primarily based on lithofacies successions and substantiated by benthic foraminiferal data, and provide depth estimates with ± 5 -10 m accuracy (Fig. 4; Table 1). Resolution decreases in middle to outer neritic environments due to the wider habitat ranges of benthic foraminifera and lack of distinct lithofacies. As a result, paleodepth estimates range from ± 20 -30 m for middle neritic biofacies (30-100 m) to ± 50 m or greater for outer neritic biofacies (100-200 m), although the abundance of certain species and calibration to lithofacies observations can increase resolution. While these benthic analyses are valuable, they must be considered preliminary at this point in time pending further quantitative analysis to improve paleodepth constraints.

We also incorporate previously backstripped results from Bethany Beach, DE (Browning et al., 2006) and multiple coreholes from the CBIS and mid-Atlantic region (Fig. 1) (Hayden et al., 2008). The latter includes three coreholes drilled by the USGS within the CBIS (Kiptopeke, Langley, and Exmore) and three from the surrounding areas (Fentress, MW4-1, and Dismal Swamp; Mixon, 1985; Powars et al., 1992; 2005; Powars and Bruce, 1999; Powars, 2000; Edwards et al., 2005). Although the work of Hayden et al. (2008) does not account for time-dependent impactite compaction and is founded on geochronologic and paleobathymetric data of coarser resolution than our studies at Eyreville and Exmore, the results provide an excellent point of comparison to differentiate impact effects from regional tectonic trends.

Results

Time-Dependent Compaction Model

This backstripping model is unique because it enables the reconstruction of temporal as well as vertical changes in porosity. In the model, we assume that compaction begins immediately after the deposition of the impactites and the rate of time-dependent compaction decreases exponentially with time (see equation 5). We tested different scenarios for time-dependent compaction, including high and low extremes using the thickest compacting unit, the Eyreville corehole. Figure 5 shows the sensitivity of the compaction model to changes in the constants ‘ c ’ and ‘ t_0 ’ of equation 6.

During backstripping, the high initial porosity (45%) of the impactite results in a significantly thicker decompacted unit than the ~ 950 m observed in core today (the unit is restored to “true” thickness at time of deposition). Thus, as initial porosity values increase (models A and C), the predicted tectonic response (e.g., excess subsidence immediately after the impact) also increases. However, if time-dependent compaction is not used (e.g., depth-dependent; model D), then initial R1 and R2 values exhibit less excess subsidence immediately after impact, while the subsequent loading from normal marine deposition results in a period of gentle subsidence (Fig. 5).

In the scenarios where the compaction of impact materials is time-dependent (models A and C), significant accommodation is generated. Because there is no change in the

observed water depth ranges during this period (35.4-33.8 Ma), tectonic uplift is required to offset impactite compaction and maintain the basin-floor within paleodepth ranges. The lower slope (slower uplift rate) of model C implies that compaction occurred over a longer time period, thus requiring less tectonic uplift to match bathymetric data. The higher slope and greater magnitude of model A indicates a period of rapid compaction and thus greater tectonic uplift. In each scenario tested, a majority of impactite compaction ends by the early Miocene, with relatively minor amounts occurring through the mid- and late Miocene (Fig. 5).

Figure 5 also illustrates the potential influence of different model scenarios on our interpretations of crater history, particularly in regards to estimating the magnitude and cause of late Eocene-Oligocene uplift or shallowing. The modeling of rapid time-dependent compaction (models A and C) results in deeper R1 depths for the late Eocene, thus requiring greater “tectonic uplift” to reach shallower Oligocene values (Fig. 5). Furthermore, it influences the magnitude and rate of the previously mentioned tectonic uplift during the late Eocene (Fig. 5). To generate a realistic model, we constrain our results with stratigraphic observations that identify the timing of major compaction episodes (e.g., periods of thickening into the crater; Gohn et al., 2008; Kulpecz et al., submitted) as model A of Figure 5.

R1 results

We generate R1 curves for the Eyreville and Exmore coreholes (Fig. 6), and compare the results to R1 estimates of Hayden et al. (2008) from the CBIS (Langley, Kiptopeke, Exmore) and the mid-Atlantic region (Fig. 7) (MW4-1, Fentress, Dismal Swamp, and Bethany Beach; the latter from Browning et al., 2006). This places our new CBIS results in regional context, and enables differentiation of crater-effects from regional subsidence and uplift patterns.

We observe initial late Eocene R1 values of 890 ± 80 m for Eyreville and 590 ± 70 m for Exmore that shallow to 820 ± 75 m and 525 ± 25 m, respectively, by the end of the late Eocene (90 ± 70 m for Eyreville, 90 ± 65 m for Exmore). Both the time-dependent compaction model and the different thicknesses of impact-materials influence these R1 backstripped results. Because the impact-generated column was deposited seconds to minutes after the impact (Poag et al., 1994), both coreholes exhibit significant compaction and excess accommodation during the late Eocene (Figs. 6, 7), as the impactite compacted under its own mass despite the lack of significant loading from overlying sediments. At Exmore, the relatively thin impact-generated column (~ 200 m) compacted rapidly and the effects of time-dependent compaction were largely over by the late Eocene-early Oligocene (Fig. 6). At Eyreville, both rapid (late Eocene) and long-term (Oligocene-Miocene) compaction is observed due to the greater thickness (~ 950 m) of impactites within the structure (Fig. 6).

A pronounced late Eocene-Oligocene uplift or shallowing event is recorded in both coreholes and in the cores from the annular trough analyzed by Hayden et al. (2008). At Exmore, this event is extremely rapid and shallowing/uplift of 95 ± 45 m occurs between 34.0 and 33.8 Ma (Fig. 7). Within the inner crater, the magnitude of uplift is substantially greater (225 ± 125 m) although a regional hiatus from 33.7 Ma to 27.7 Ma obscures the exact timing of this event. Hayden et al. (2008) quantified this event at 50-125 m and attributed it to the onset and removal of a large negative thermal anomaly. We further elucidate on the potential mechanisms behind this event in the discussion.

A regional hiatus from 33-18 Ma resulted in only minor deposition within and around the CBIS. Oligocene R1 depths for Eyreville are 600 ± 50 m at 27.7 Ma and 540 ± 10 m at 26.6 Ma (Fig. 6). R1 depths for Exmore are substantially shallower (450 ± 25 m at 27.7 Ma) and indicate marginal shallowing from late Eocene R1 depths (525 ± 25 m). Significant sedimentation resumed during the late early Miocene, with R1 depths of 570 ± 15 m at 18.4 Ma at Eyreville, and 475 ± 25 m at Exmore (Fig. 7). During this time of regional nondeposition compaction of the impactite likely continued. Although the presence of this broad unconformity indicates the region was above base level, there was likely sufficient mass within the impact-column for lower impactites to compact without additional overburden (e.g., time-dependent compaction; Fig. 5). However, there is no discernable change in water depth estimates, indicating that uplift occurred within the inner crater to maintain the basin floor within observed paleodepths (Fig. 7).

A long-term, gradual phase of uplift of 45 ± 20 m occurred at Eyreville from 18.4 to 0.2 Ma and is characterized by the gradual “shoaling-upwards” of litho- and biofacies observed in core (Fig. 7) (Browning et al., submitted; Kulpecz et al., submitted). Conversely, a long-term subsidence event of 55 ± 15 m occurred at Exmore from 14.8 to 6.5 Ma, followed by a minor subsidence event of 15 ± 2 m during the Pleistocene. The overall effect of these trends is the near convergence of the two R1 records during the middle to late Miocene (Fig. 7), and suggesting the end of significant time-dependent compaction of impact-generated materials.

The crater exterior coreholes of Hayden et al. (2008) each record similar trends that are interpreted as regional signals of vertical tectonic uplift and subsidence. While MW4-1, Fentress, and Dismal Swamp (Fig. 1) are all in close proximity to the CBIS (< 25 -30 km), Bethany Beach is 120-km to the north (northern end of the Salisbury embayment) and thus experienced differences in tectonic evolution. Hayden et al (2008) documented a southward regional subsidence event (20-30 m vertical scale) that started 22 Ma at Bethany Beach, 14 Ma in the MW4-1 corehole, and 13 Ma at Fentress (Fig. 7), followed by a minor regional uplift event of 2-20 m around 2.5 Ma. The authors suggested the southward progradation of large depocenters and consequent down-flexure of the crust during the Miocene as the mechanism behind the first of these two events (Hayden et al., 2008). While our results from Exmore are consistent with the Miocene subsidence event (55 ± 15 m starting at 14.8 Ma), the coeval period of uplift at Eyreville indicates that the inner crater is controlled by a mechanism other than these regional tectonic trends (Fig. 7).

Discussion- Integration with R2 results and Controls on Post-Impact Evolution

The development of a time-dependent compaction model for the impactites, generation of backstripped R1 results from the CBIS, and comparison with previously published regional R1 curves, allows for a quantitative reconstruction regional subsidence and uplift events on the mid-Atlantic margin. However, the comparison of R2 curves from Eyreville and Exmore with sea-level estimates established from the New Jersey margin (backstripped R2_{SL} curves; Kominz et al., 2008) offers a unique opportunity to further differentiate eustatic from tectonic influences. In the absence of non-thermal tectonics, R2 results from the CBIS should yield estimates of eustasy. However, there are numerous marked differences between eustatic estimates from New Jersey and CBIS R2 results (Fig. 8). These differences represent a combination of non-thermal tectonics and impact related-effects, and offer a quantitative method to extract the timing, amplitude, and rates of such changes. Our results show that although the evolution of the CBIS is superimposed on regional trends of uplift and subsidence, the inner crater is characterized by long-term lithospheric uplift (late Eocene-Miocene) required to counter the excess accommodation from the time-dependent compaction of impact-generated materials, while the annular trough is primarily dominated by eustatic change and secondarily by regional tectonic patterns after the late Eocene.

Late Eocene- Excess Accommodation and “Shoaling-Upwards” Trends

Following the impact event at 35.4 Ma, Eyreville R2 results record a significant period of excess accommodation that “shallows” through the late Eocene from 285 ± 50 m at 35.5 Ma to 240 ± 40 m at 33.7 Ma (Fig. 8). R1 results quantify this uplift event as 90 ± 70 m (Fig. 7). Exmore also records this decrease in excess accommodation (90 ± 65 m from R1 results), shoaling from 115 ± 50 m at 35.5 Ma to 65 ± 15 m at 33.0 Ma (Fig. 8). These results are substantially deeper than eustatic estimates during the late Eocene that range from 60 ± 20 m at 35.7 Ma, to 40 ± 5 m at 34.8 Ma, and 60 ± 30 m at 33.8 Ma (Kominz et al., 2008). The excess accommodation immediately following the impact is attributed to the crater-wide bathymetric low resulting from impact excavation, with the time-dependent compaction of impact-generated materials during the late Eocene having been removed during backstripping (Figs. 3, 8).

Following this early period of excess accommodation, a late Eocene “shoaling” upwards trend is observed at both Eyreville and Exmore, which is consistent with R1 estimates of the same event (Figs. 6, 7), and requires uplift of the lithosphere. Although the rapid compaction of impact-materials generated excess accommodation during the late Eocene (water flux and thermal data from Eyreville identifies as much as ~ 320 m of impactite compaction and associated dewatering within the first several thousand years after the impact; Sanford et al., submitted), paleodepth estimates indicate the depth of the basin floor remained largely unchanged (although the wide error ranges permit some vertical variation). Thus, basement uplift is required to resolve the modeled rapid compaction of

impact materials. The mechanism behind this lithospheric uplift is unclear, but could be related to thermal effects (e.g., Hayden et al., 2008).

By the late Eocene, R2 results from Exmore shallow, fall in line with eustatic estimates, and remain consistent with eustasy throughout the overlap of these records into the Miocene (Fig. 8), despite the presence of several notable hiatuses in the Oligocene (33-24 Ma), early Miocene (24-17 Ma), and late middle Miocene (13-9 Ma; Fig. 8). R2 results from Eyreville continue to exhibit excess accommodation during the late Eocene (240 ± 40 m at 33.7 Ma), Oligocene, and Miocene.

The differences between late Eocene R1 and R2 results from Exmore and Eyreville represent changes in accommodation due to the time-dependent compaction model (Fig. 3), and the inherent differences between the annular trough and inner crater. Exmore is located in the northern annular trough (Fig. 1) and is underlain by ~200 m of impactites (e.g., Exmore beds) that overlie impact-altered slump blocks of pre-impact mid-Cretaceous sediments (Powars and Bruce, 1999). Conversely, Eyreville is situated within the inner crater that experienced removal of the entire pre-impact sediment column and several kilometers of the upper crust (Catchings et al., 2008). This was followed by the deposition of at least 950 m of lithic-clast impactites (this number does not include ~350 m of granite megablocks and other non-compactable material; Gohn et al., 2008).

Because the Eyreville corehole did not reach the shocked *in situ* crater floor, but instead penetrated material that apparently slumped in from the transient crater wall (Gohn et al., 2008), these impactites are underlain by 1.5 to 3.5 km of melt-rock, fractured and altered

basement, and impact-generated crystalline and sediment-clast breccias within the central moat (estimated from deep seismic profiles; Catchings et al., 2008).

Thus, the timing and magnitude of late Eocene excess accommodation was strongly influenced by the rapid compaction of impact materials, both known (accounted for by our time-dependent compaction model) and unknown (units not penetrated by the Eyreville corehole and thus not modeled). The inner crater is also ringed by a series of deep, impact-generated, concentric faults that bound the central moat (Catchings et al., 2008), providing a possible ‘detachment’ mechanism for uplift and subsidence events within the inner crater that are not observed in the annular trough.

Late Eocene-early Oligocene Uplift within the CBIS

Both R1 and R2 results document a significant period of uplift or shallowing between the late Eocene, a period of high excess accommodation within the CBIS, and the early Oligocene, a period where R2 depths are significantly closer to eustatic estimates. We attribute this event to a combination of several factors: 1) a substantial drop in sea level across the Eocene-Oligocene boundary; 2) a decrease in the rate of impactite compaction; and 3) uplift of the lithosphere in response to the crustal-scale restoration of the geothermal gradient and reheating of cold impactites and post-impact sediments (e.g., thermal anomaly of Hayden et al., 2008)

The uplift/shallowing event at Exmore is very rapid, measuring 55 ± 20 m between 34.0 to 33.8 Ma. This change appears to coincide with the major Eocene-Oligocene eustatic fall of 50 ± 28 m identified by Kominz et al. (2008) (Fig. 8) and therefore implies eustatic, not tectonic, control for the shallowing event at Exmore. Although a large hiatus prevents the quantification of this event at Eyreville during the early Oligocene, late Oligocene R2 results (80 ± 30 m at 27.7 Ma) are still significantly deeper (60-100 m) than eustatic estimates at this time. Thus, although 50 ± 28 m of the total observed shallowing (160 ± 80 m) may be attributed to this eustatic lowering, the remaining difference (~ 110 m) requires a mechanism other than eustasy for the observed uplift.

Hayden et al. (2008) attributed 50-125 m of annular trough uplift to a crustal-scale negative thermal anomaly. This uplift was generated by the impact event, crater excavation, and the redeposition of cold, low thermal-conductivity, impact-generated and post-impact sediments. These cold materials “reset” the geothermal gradient, contributing to excess subsidence during the late Eocene (Fig. 9). This subsidence event was followed by the gradual restoration of the geothermal gradient and reheating of the upper crust and sediment package, resulting in thermal uplift that ended by 30 ± 2 Ma (Fig. 9). The low-thermal conductivity of the sediment package enabled the establishment of a higher geothermal gradient than normally possible before eventual stabilization (Fig. 9). Although this thermal anomaly was only modeled for coreholes in the annular trough, the thicker impactite section within the inner crater suggests that these thermal effects could have been even greater, and may account for the remaining ~ 110 m of shallowing at Eyreville not explained by eustasy (Fig. 8).

However, our new backstripped results from the inner crater and annular trough (using a time-dependent compaction model for the impactites) show *uplift* during the late Eocene, as opposed to the subsidence predicted by the thermal anomaly model of Hayden et al. (2008). However, the broad error ranges and limited age control (base of section is dated by superposition above impactites, top of section by several Sr-isotope age estimates) do not preclude brief subsidence prior to the observed uplift (Fig. 8). Furthermore, the late Eocene “shoaling” upward trend observed at Eyreville and Exmore (Fig. 8) may require tectonic uplift to maintain the basin floor within paleo-water depth ranges. A potential mechanism for this lithospheric uplift could be early thermal reheating of the crust and sediments during the restoration of the geothermal gradient. This thermal anomaly could extend well into the Oligocene (Hayden et al., 2008), accounting for both the late Eocene shoaling upwards trend, and the Oligocene uplift event.

Miocene through Pliocene Trends and Sea-Level Estimates

Exmore R2 results are generally consistent with eustatic estimates from the late Eocene through the late Miocene (error ranges normally overlap), indicating the end of significant excess accommodation in the northern annular trough from the compaction of the relatively thin (~200 m) impact-generated column. However, R1 results document a late Miocene subsidence trend of 55 ± 15 m at Exmore from 14.8 to 6.5 Ma, followed by a minor subsidence event of 15 ± 2 m during the Pleistocene (Figs. 6, 7). The late Miocene event is consistent in magnitude and timing with the regional Miocene

subsidence event of Hayden et al. (2008), and may be attributed to the southward progression of regional subsidence due to down-flexure from deltaic depocenter loading in the northern Salisbury embayment (e.g., Browning et al., 2006). However, these subsidence trends are also similar to broad eustatic trends during this time (Fig. 8), suggesting at least some of the observed signal may be from long-term eustatic lowering.

Although Eyreville R2 results briefly overlap the eustatic record (55 ± 15 m) at 26.7 Ma, they are characterized by excess accommodation throughout the Miocene (Fig. 8). While a majority of the modeled time-dependent compaction ceases by the early to middle Miocene (Fig. 3), recent estimates from seismic data indicate between 1.5 and 3.5 km of impact-generated and modified debris exists within the central moat depending on the interpretation of deep layered materials (Catchings et al., 2008). Because the true thickness, porosity, and lithology of this debris are unknown, it was not considered during our modeling of impactite compaction, and could be the source of middle to late Miocene excess accommodation at Eyreville.

The magnitude of excess accommodation progressively decreases through time so that R2 results approach eustatic estimates (Fig. 8); from 50 ± 15 m (18.4 Ma), 30 ± 15 m (17.4 Ma; although the lower error range overlaps eustasy), and 35 ± 15 m (14.1 Ma) before converging with eustatic estimates (20 ± 15 m) from 14.8-12.8 Ma (Fig. 8; eustatic estimates and R2 results are presented in Appendices 1-3).

By the time deposition resumed in the CBIS (~9 Ma), the record in New Jersey is incomplete and no backstripped eustatic estimates are available for comparison.

However, after 8 Ma there is convergence of the records from Eyreville and Exmore (10-20 m difference between mean R2 values with overlapping error ranges), suggesting the cessation of significant impact-related subsidence in the inner crater (significant impact-related subsidence within the annular trough ceased around 34 Ma). These long-term differences in accommodation between the inner crater (Eyreville) and annular trough (Exmore) reflect the complexity of marine impact structures, and the significant control the impact-generated column plays on post-impact sedimentation.

Based on the similarity of the records in the late Miocene, and the apparent end of significant impact-related effects at this time, the CBIS backstripped R2 results may offer the first sea level estimates for the late Miocene and Pliocene previously unavailable to sea level studies of the mid-Atlantic margin (a large hiatus dominates New Jersey after ~9 Ma; Miller et al., 2005; Kominz et al., 2008). While much of the Pliocene at Exmore was removed by the incision of a Pleistocene paleo-channel (Powars and Bruce, 1999; Kulpecz et al., submitted), the results from Eyreville provide late Miocene and mid-Pliocene sea-level estimates of 25 ± 9 m to 15 ± 5 m from 8.4 to 8.0 Ma; 22 ± 5 m and 14 ± 5 m from 7.7 to 7.2 Ma; 12 ± 2 m from 6.4-6.1 Ma; 10 ± 2 m at 4.9 Ma; 10 ± 2 m at 2.95 Ma shallowing to 4 ± 3 m at 2.8 Ma; and 18 ± 5 m from 2.75-2.55 Ma. Although these results are preliminary, and require additional benthic foraminiferal analysis to further constrain water depth estimates, they provide some of the first eustatic estimates from the mid-Atlantic margin for this time interval.

Quantifying Oligocene and Miocene Uplift and Unconformity Genesis

Following the CBIS uplift event, large unconformities span the region during the Oligocene (~33-25 Ma), early Miocene (~24-18 Ma), and late Miocene (12.8-9 Ma) (Fig. 10). These unconformities contrast with thick, coeval sections in Delaware and New Jersey and are significantly longer in duration (~3-5 myr) than hiatuses (interpreted as sequence boundaries) caused by eustatic base level lowering (0.5-3 myr). Oligocene sequences are generally thin (< 15 m, although a localized ~50 m thick interval was recovered at the Langley corehole; Edwards et al., 2005), exhibit discontinuous and patchy distribution (Fig. 10), and are characterized by glauconite-rich lithology consistent with a sediment starved margin (Powars and Bruce, 1999; Edwards et al., submitted). Lower lower Miocene units are largely absent from this segment of the mid-Atlantic Coastal Plain, although biostratigraphy indicates the presence of thin (< 2m) packages of isolated lower Miocene sediments at the Eyreville corehole (Fig. 10) (Edwards et al., submitted; Browning et al., submitted). The early late Miocene (12.0-9.8 Ma) is absent across the CBIS and south, and regional correlations suggest it pinches out just north of the CBIS (Fig. 10) (Kulpecz et al., submitted). Each of these hiatuses contrasts with thick, well represented, coeval sections in New Jersey and Delaware. The Oligocene is ~90 m thick in New Jersey (Pekar et al., 2000), while thick lower and upper Miocene shoreface sands (~200 m; Browning et al., 2006) grade into thick deltaic packages in New Jersey (Fig. 10) (Sugarman et al., 2007).

The regional nature of these unconformities (observed in each Virginia corehole used in this study of the mid-Atlantic Coastal Plain) and presence of thick coeval packages ~200 km north implies regional tectonic uplift associated with the Norfolk arch, a significant basement structure that lies 15-20 km south of the CBIS (Fig. 10). Although the exact role of the Norfolk arch on margin deposition is unclear due to the lack of regional seismic lines, recent studies (Powars, 2000) document periodic uplift, erosion, and subsidence along the James River structural zone, a series of faults associated with the northern boundary of the arch (Fig. 1). Previous studies also noted the thinning, differential preservation, and erosion of units onto the Norfolk arch (Olsson et al., 1988).

The presence of these broad hiatuses prevents the comparison of eustatic estimates and our backstripped results. However, stratigraphic observations from Kulpecz et al. (submitted) suggest that a minimum of 10-50 m of uplift over the duration of these unconformities (3-7 myr) was required for unconformity genesis. These estimates are not inconsistent with our R2 results (Fig. 8), although backstripping is unable to further quantify these uplift events during the Oligocene, early Miocene, and late middle Miocene. We attribute the genesis of these unconformities to the regional uplift of the Norfolk arch. Although the mechanism for their genesis and Norfolk arch uplift is currently unknown, the minimum rate of 10-50 m/1-5 myr allows the evaluation of possible tectonic mechanisms (Fig. 11).

Discussion of Tectonic Mechanisms

The U.S. mid-Atlantic margin is considered the type-section for passive continental margins, given the large volume of work focused on its tectonic and stratigraphic history over the past several decades (e.g., Owens and Sohl, 1969; Watts and Steckler, 1979; Poag, 1979; Olsson, 1980; Watts, 1981; Klitgord et al., 1988; Grow and Sheridan, 1988; Grow et al., 1988; Poag and Sevon, 1989; Kominz et al., 1998; Miller et al., 2005). These studies identified eustatic changes, post-rift lithospheric cooling, and subsequent flexural subsidence from large-scale sedimentation on the continental shelf as the dominant controls on margin sedimentation. While this “thermoflexural” mechanism is evident on the New Jersey margin (making it an ideal location for the extraction of sea-level estimates; Miller et al., 1996; Kominz et al., 1998; Van Sickel et al., 2004; Miller et al., 2005; Kominz et al., 2008), numerous studies also note apparent structural or non-thermal tectonic influences on deposition across the greater mid-Atlantic margin.

These mechanisms include: 1) large-scale, ambiguous uplift and subsidence events controlling margin sedimentation (Owens and Sohl, 1969; Owens and Gohn, 1985); 2) the broad regional warping (100-200 km-wavelength) of rolling basins (Owens et al., 1997); 3) wrench fault-bounded grabens comprising the structural basement fabric (Brown et al., 1972); and 4) the influence of regionally-significant basement structures on margin sedimentation (alternating highs and embayments; Fig. 1; Olsson, 1988). Recent studies explored the long-term (10^7 yr) influence of dynamic topographic changes related to the passage of the eastern U.S. margin over the subducted Farallon slab (Moucha et al.,

2008; Mueller et al., 2008; Spasojević et al., 2008). Kulpecz et al. (submitted) identified significant regional unconformities across the CBIS and surrounding region, and attributed their genesis to the periodic uplift of the Norfolk arch and associated fault-bounded terranes (e.g., Maguire et al., 2004; Glover et al., 1997) in response to variations in intraplate stress, using the seismically active (and geologically similar) Cape Fear arch (~200 km to the south) as an analog.

Regardless of the mechanism, numerous non-thermoflexural tectonic events (both uplift and subsidence) occurred on this margin and influenced regional deposition during the Cenozoic. The recent development of a high resolution (> 1 myr) sequence stratigraphic framework from New Jersey (e.g., Miller et al., 2005) to Delaware (Browning et al., 2006) and Virginia (Browning et al., submitted; Kulpecz et al., submitted) provides the necessary geochronologic resolution to distinguish myr-scale or better eustatic and tectonic influences on deposition (previous studies were complicated by coarse geochronologic resolution from biostratigraphy). Furthermore, backstripped results from this and other studies are among the first for this region, allowing the quantification of amplitudes, timing, and rates of change.

The work of Hayden et al. (2008) and Browning et al. (2006) identified periods of excess subsidence on the mid-Atlantic margin on the order of 10-30 m throughout the Miocene, although higher excess subsidence estimates at Exmore (75-100 m/4 myr) and Kiptopeke (55 m/3 myr and 50 m/2 myr) were identified by Hayden et al. (2008) (Fig. 7). This study further refines estimates of Miocene-Pliocene subsidence to 55 ± 20 m at Exmore. The

Miocene subsidence event of Hayden et al. (2008) begins with 20-30 m of excess subsidence at Bethany Beach, DE at 21 Ma, and proceeds south during the Miocene, culminating at 5 Ma within and around the CBIS (Fig. 7). While this study is consistent with these results (Fig. 7), interpreting subsidence is complicated due to significant excess accommodation (Fig. 8). Previous studies (Hayden et al., 2008; Browning et al., 2006) attributed this excess subsidence event to the progradation of large depocenters southwards from New Jersey and Delaware during the Miocene, while seismic profiles verify the downlap of these units just north of the CBIS (Catchings et al., 2007). Although this is a valid interpretation, several uncertainties remain whether these loads sufficient to elicit this crustal response on a mature, flexurally rigid, late-stage rifted margin with a break-up age of 160-150 Ma. Furthermore, it is unclear if this flexural mechanism is working independently, or in conjunction with other mechanisms that could enhance or diminish the observed subsidence. To fully understand the nature of these excess subsidence events, they must be placed in the context with regional uplift events described on this margin.

Stratigraphic observations provide rough estimates for the rates and amplitudes of regional uplift as $>10\text{-}50\text{ m}/1\text{-}5\text{ myr}$ (the minimum limit of uplift required for erosion or nondeposition, although actual uplift could be substantially higher) while backstripping quantifies long-term excess subsidence as $10\text{-}55\text{ m}/10\text{ myr}$, with occasional peaks of $75\text{-}100\text{ m}/2\text{-}3\text{ myr}$ (e.g., Hayden et al., 2008). These non-thermoflexural changes are essentially 3-5 myr-scale, broad in geographic scope (100-200 km lateral scale), and

appear to coincide with known (although poorly defined) structural boundaries that underlie the mid-Atlantic Coastal Plain (Fig. 1).

Although we provide amplitudes and rates of uplift and subsidence, the mechanism controlling these events remains unclear. A variety of different tectonic drivers have been suggested as possible controls on “passive-aggressive” tectonism that characterizes passive margins otherwise dominated by thermoflexural subsidence (Fig. 11): 1) the adjustment of minor faults (localized effects ~ 10 m/myr); 2) depocenter loading resulting in both excess subsidence 10-30 m/5-10 myr and an associated flexural bulge ~ 10 -20 m (e.g., Galloway, 1989); 3) lower crustal flow and long-wavelength flexural isostasy from the cyclic loading and unloading of sediments (e.g., hinterland erosion and subsequent crustal response; Westaway, 2007); 4) long-term dynamic topographic changes (50-100 m/10-20 myr-scale; Mueller et al., 2008); and 5) third-order changes in the direction and intensity of intraplate stress fields (10-50 m/1-3 myr, e.g., Cloetingh, 1988; Karner et al., 1993). The magnitude and time scales of these mechanisms are presented in Figure 11.

Although clouded by the lack of subsurface seismic data and detailed stress-field reconstruction for the eastern United States, we propose that variations in Oligocene-Pliocene intraplate stress, and their influence on regionally significant fault-bounded basement structures, are the primary mechanism responsible for periods of uplift and excess subsidence. We base this interpretation on the following criteria: 1) the regional nature of these trends (100-200 km hiatuses during intervals of known eustatic dominance elsewhere on the margin); 2) the association of these events with known

structural boundaries capable of accommodating stress-field changes by the adjustment of significant fault-bounded basement blocks or broad-scale regional flexure (e.g., Cloetingh, 1988; Cloetingh et al., 1989; Karner, 1993); 3) rate and amplitude consistent with regional, stress-induced third-order trends identified in other depositional basins (Jean D'arc basin; Karner et al., 1993); 4) broad similarities of the Norfolk and Cape Fear arches (~200 km south) that both record periods of uplift that at times are synchronous at both structures (e.g., Weems and Lewis, 2002; Kulpecz et al., submitted); 5) historical seismicity of the Cape Fear arch due to the current maximum horizontal stress direction of E-SE-W-SW, accommodating much of the stress on the eastern U.S. margin (Weems and Lewis, 2002); and 6) variations in the North American stress field during the Paleogene and Neogene (e.g., Bird, 2002; Zoback and Zoback, 1980; Zoback et al., 1989).

The long-term influence of dynamic topographic changes was also considered as a possible mechanism. Recent studies (Mueller et al., 2008; Forte et al., 2007; Spasojević et al., 2008; Moucha et al., 2008) have shown that variations in the mantle density structure can result in dynamic topographic changes (e.g., response of Earth's surface to convectively-driven vertical stresses; Mitrovica et al., 1989) and broad epeirogenic uplift and downwarp of large crustal segments. Both Mueller et al. (2008) and Spasojević et al. (2008) attribute the comparatively low long-term (10-20 myr-scale) sea-level estimates established from the New Jersey margin (Miller et al., 2005) to periods of dynamic subsidence (50-200 m) superimposed on long-term sea level fall since the Eocene. This subsidence is driven by the interaction of the Eastern U.S. with the underlying subducted

Farallon plate (Spasojević et al., 2008). While implications of such studies are profound, they primarily focus on long-term (10-100 myr) tectonic trends (e.g., Moucha et al., 2008) that fail to account for higher frequency sequence and unconformity genesis (1-5 myr-scale) on the mid-Atlantic and other margins.

Kominz et al. (2008) included Mueller et al.'s (2008) model of this slab effect (Fig. 8) in an error analysis of their sea level results from New Jersey and Delaware cores. This slab correction results in substantially higher long-term sea level estimates for the Eocene-Miocene (orange curve; Fig. 8). A comparison of the slab-corrected sea-level curve to the CBIS R2 curves reveals interesting patterns. While Exmore tracks the original eustatic estimates fairly well after the Oligocene (Fig. 8), Eyreville is actually consistent with the slab-corrected long-term sea level values, eliminating the long-term excess accommodation. Given the close proximity of these two records (< 20 km), this raises an interesting question of which of these divergent records better approximates eustasy, and if the subducted Farallon plate is imparting dynamic topographic changes in Virginia (~250 km south) similar to New Jersey during this time period.

However, the slab effect has not been modeled south of New Jersey, and further research is needed to determine the regional scope and vertical amplitude of such dynamic topographic effects. Our data suggests that the Virginia Coastal Plain is not recording the same dynamic topographic response given the dissimilarity of the two records, and the known role of impactite compaction (e.g., Gohn et al., 2008). Furthermore, additional work is required to determine if regional high-frequency (1-5 myr) tectonic uplift and

subsidence, which may at times be synchronous (as observed on the mid-Atlantic margin; e.g., Norfolk arch uplift versus relative subsidence in the Salisbury embayment), can be explained by dynamic topography, or if they represent the blending of several tectonic processes. New phases of quantitative modeling (through one- and two-dimensional backstripping) of the rates, amplitudes, and lateral scale of these changes will provide better constraints on differentiating these mechanisms.

Conclusions

We generate a new time-dependent compaction model for impact-generated materials and use one-dimensional backstripping to quantify the rates and amplitudes of impact-related effects, regional tectonics, and eustatic change on the post-impact section of the late Eocene (35.5 Ma) Chesapeake Bay Impact Structure (CBIS). The generation of R1 and R2 results, and comparison to previously published backstripped records (Hayden et al., 2008) and sea-level estimates (Kominz et al., 2008), also allows an evaluation of the mechanisms that shape the surrounding mid-Atlantic Coastal Plain. While thermoflexural subsidence and eustatic changes are the dominant controls on sequence distribution on the mid-Atlantic margin, the presence of significant (3-7 myr) regional unconformities across the CBIS area (Kulpecz et al., submitted) implicates periodic regional tectonic uplift and erosion/nondeposition.

Comparison of backstripped records in and around the CBIS reveals several interesting trends: 1) the long-term compaction of impact-generated materials strongly influenced

deposition within the inner crater, shown by the growth of post-impact sequences into the structure and high (285 ± 50 m) excess subsidence during the late Eocene that gradually declines to 20 ± 15 m by the late Miocene; 2) excess accommodation in the annular trough was 115 ± 50 m after the impact, and decreases significantly by the late Eocene due to a thinner impact-generated column underlying the post-impact section (~ 200 m); 3) late Eocene-early Oligocene uplift or “shallowing” of 95 ± 45 m at Exmore and 225 ± 125 m at Eyreville likely resulted from a major Eocene-Oligocene sea-level fall coupled with the removal of a negative thermal anomaly; 4) regional unconformities during the Oligocene, lower Miocene, and upper middle Miocene within the CBIS-region contrast thick sections in New Jersey and Delaware and correspond with known basement structures; and 5) unlike much of the mid-Atlantic Coastal Plain otherwise dominated by eustasy and thermoflexural subsidence, this segment of the margin exhibits periods of “passive-aggressive” non-thermal tectonic uplift (10-50 m /1-5 myr; from stratigraphic observations) and excess subsidence (10-55/10 myr with peaks of 75-100 m/2-3 myr; from backstripping).

We conclude that while eustasy is largely responsible for changes in accommodation and the margin-wide genesis of sequence boundaries, the vertical movement of basement structures in response to intraplate stress, depocenter loading, and other large-scale tectonic mechanisms, results in significant differential preservation of sequences across the mid-Atlantic margin. The post-impact section of the CBIS, although strongly influenced by the impact event and subsequent long-term, time-dependent compaction of impact materials, is dominated by regional tectonic patterns after the Oligocene and may

provide valid eustatic estimates for the late Miocene and Pliocene: 25 ± 9 m to 15 ± 5 m from 8.4 to 8.0 Ma; 22 ± 5 m and 14 ± 5 m from 7.7 to 7.2 Ma; 12 ± 2 m from 6.4-6.1 Ma; 10 ± 2 m at 4.9 Ma; 10 ± 2 m at 2.95 Ma shallowing to 4 ± 3 m at 2.8 Ma; and 18 ± 5 m from 2.75-2.55 Ma.

References

- Bird, P., 2002, Stress direction history of the western United States and Mexico since 85 Ma: *Tectonics*, v. 21, p. 1-12.
- Bond, G.C., and Kominz, M.A., 1984, Construction of tectonic subsidence curves for the early Paleozoic miogeocline, southern Canadian Rocky Mountains: Implications for subsidence mechanisms, age of breakup, and crustal thinning: *Geological Society of America Bulletin*, v. 95, p. 155-173.
- Bond, G.C., Kominz, M.A., Steckler, M.S., and Grotzinger, J.P., 1989, Role of thermal subsidence, flexure, and eustasy in the evolution of early Paleozoic passive-margin carbonate platforms, *in* Crevello, J.L., et al., eds., *Controls on carbonate platform and basin development*: Society of Economic Paleontologists and Mineralogists Special Publication 44, p. 39-61.
- Brown, P.M., Miller, J.A., and Swain, F.M., 1972, Structural and stratigraphic framework, and spatial distribution of permeability of the Atlantic Coastal Plain, North Carolina to New York: U.S. Geological Survey Professional Paper 796, p. 1-79.
- Browning, J.V., Miller, K.G., McLaughlin, P.P., Kominz, M.A., Sugarman, P.J., Monteverde, D., Feigenson, M.D., and Hernández, J.C., 2006, Quantification of the effects of eustasy, subsidence, and sediment supply on Miocene sequences, Mid-Atlantic margin of the United States: *Geological Society of America Bulletin*, v. 118, p. 567-588.
- Browning, J.V., Miller, K.G., McLaughlin, P.P., Jr., Edwards, L.E., Powars, D.S., Kulpecz, A.A., Wade, B.S., and Feigenson, M.D., *submitted*, Post-impact integrated litho-, sequence, Sr-isotopic, and bio-stratigraphy of the Eyreville corehole, Chesapeake Bay impact structure inner basin: *Geological Society of America Special Publication XX*, XXX p.

- Catchings, R.D., Powars, D.S., Goldman, M.R., Gohn, G.S., Horton, J.W., Jr., Rymer, M.J., Gandhok, G., and Edwards, L.E., 2007, High-resolution seismic reflection images across the 1.76-km-deep Eyreville corehole within the moat of the Chesapeake Bay Impact Structure: Geological Society of America Abstracts with Programs, 450, abstract 167-3.
- Catchings, R.D., Powars, D.S., Gohn, G.S., Horton, J.W., Jr., Goldman, M.R., and Hole, J.A., 2008, Anatomy of the Chesapeake Bay impact structure revealed by seismic imaging, Delmarva Peninsula, Virginia, USA: Journal of Geophysical Research, v. 113, BO8413, doi:10.1029/2007JB005421, 2008.
- Christie-Blick, N., 1991, Onlap, offlap, and the origin of unconformity-bounded depositional sequences: Marine Geology, v. 97, p. 35-56.
- Cloetingh, S., 1988, Intraplate stresses: a tectonic cause for third-order cycles in apparent sea level?: Society of Economic Paleontologists and Mineralogists Special Publication, v. 42, p. 19-29.
- Cloetingh, S., Gradstein, F.M., Kooi, H., Grant, A.C., and Kaminski, M., 1990, Plate reorganization: a cause of rapid late Neogene subsidence and sedimentation around the North Atlantic?: Journal of the Geological Society, v. 146, p. 495-506.
- Collins, G.S., and Wünnemann, K., 2005, How big was the Chesapeake Bay impact? Insight from numerical modeling: Geology, v. 33, p. 925-928.
- Crawford, D.A., 2002, A computational model of the Chesapeake Bay impact structure [abstract]: Geological Society of America Abstracts with Programs, v. 34, no. 6, p. 465.
- Edwards, L.E., Barron, J.A., Bukry, D., Bybell, L.M., Cronin, T.M., Poag, C.W., Weems, R.E., and Wingard, G.L., 2005, Paleontology of the Upper Eocene to Quaternary Postimpact Section in the USGS-NASA Langley Core, Hampton, Virginia, *in* Horton, J.W., Jr., Powars, D.S., and Gohn, G.S., Eds. 2005, Studies of the Chesapeake Bay Impact Structure- The USGS-NASA Langley Corehole, Hampton, Virginia, and Related Coreholes and Geophysical Survey: U.S. Geological Survey Professional Paper 1688, p. H1-47, 9 pls.
- Edwards, L.E., Powars, D.S., Wade, B.S., Self-Trail, J.M., Browning, J.V., Miller, K.G., McLaughlin, P.P., Jr., Kulpecz, A.A., and Elbra, T., *submitted*, Geologic columns for the ICDP-USGS Eyreville A and C coreholes, Chesapeake Bay Impact Structure: Post-Impact Sediments, 0 to 444 m depth: Geological Society of America Special Publication XX, XX
- Galloway, W.E., 1989, Genetic sequence stratigraphic sequences in basin analysis II: application of northwest Gulf of Mexico Cenozoic basin: American Association of Petroleum Geologists Bulletin, v. 73, p. 143-154.

- Glass, B.P., 1989, North American tektite debris and impact ejecta from DSDP site 612: *Meteoritics*, v. 24, p. 209-218.
- Glover, L., III., Sheridan, R.E., Holbrook, W.S., Ewing, J.I., Talwani, M., Hawman, R.B., and Wang, P., 1997, Paleozoic collisions, Mesozoic rifting and structure of the Middle-Atlantic states continental margin: an 'EDGE' Project report: Geological Society of America Special Paper 314, p. 107-135.
- Gohn, G.S., 1988, Atlantic coastal plain: North Carolina to Florida, *In* Sheridan, R.E., and Grow, J.A., eds., *The Atlantic Coastal Margin, U.S.*: Boulder, Colorado, Geological Society of America, *Geology of North America*, v. 1-2, p. 107-130.
- Gohn, G.S., Sanford, W.E., Powars, D.S., Horton, J.W., Jr., Edwards, L.E., Morin, R.H., and Self-Trail, J.M., 2006, Chesapeake Bay impact structure drilled: *Eos Transactions American Geophysical Union*, v. 87, p. 349-355.
- Gohn, G.S., Koeberl, C., Miller, K.G., Reimold, W.U., Browning, J.V., Cockell, C.S., Horton, J.W., Jr., Kenkmann, T., Kulpecz, A.A., Powars, D.S., Sanford, W.E., and Voytek, M.A., 2008, Deep Drilling Yields New Insights into the Chesapeake Bay Impact Event: *Science*, *in press*.
- Grow, J.A., 1980, Deep structure and evolution of the Baltimore Canyon Trough in the vicinity of the COST No. B-3 well: U.S. Geological Survey Circular 833, p. 117-132.
- Grow, J.A., and Sheridan, R.E., 1988, U.S. Atlantic continental margin; A typical Atlantic-type or passive continental margin, *in* Sheridan, R.E., and Grow, J.A., eds., *The Atlantic Coastal Margin, U.S.*: Boulder, Colorado, Geological Society of America, *Geology of North America*, v. 1-2, p. 1-7.
- Hayden, T., Kominz, M., Powars, D.S., Edwards, L.E., Miller, K.G., Browning, J.V., and Kulpecz, A.A., 2008, Impact effects and regional tectonic insights: Backstripping the Chesapeake Bay impact structure: *Geology*, v. 36, p. 327-330.
- Horton, J.W., Jr., Powars, D.S., and Gohn, G.S., Eds. 2005, *Studies of the Chesapeake Bay Impact Structure- The USGS-NASA Langley Corehole, Hampton, Virginia, and Related Coreholes and Geophysical Survey*: U.S. Geological Survey Professional Paper 1688.
- Horton, J.W., Jr., Gohn, G.S., Powars, D.S., and Edwards, L.E., 2008, Origin and emplacement of impactites in the Chesapeake Bay impact structure, Virginia, USA: Geological Society of America Special Paper 437, p. 73-97.
- Karner, G.D., Driscoll, N.W., Weissel, J.K., 1993, Response of the lithosphere to in-plane force variations: *Earth and Planet Science Letters*, v. 114, p. 397-416.

- Kenkmann, T., 2004, A structural comparison between the Chesapeake Bay impact crater, USA, and the Reis crater, Germany: How did the central crater basin form?: in ICDP-USGS Workshop on the Deep Drilling in the Central Crater of the Chesapeake Bay Impact Structure, Virginia USA, September 22-24, 2003, USGS Open File Report 2004-1016, eds., Edwards, L.E., Horton, J.W., Jr., and Gohn, G.S., p. 30-31.
- Klitgord, K.D., Hutchinson, D.R., and Schouten, H., 1988, U.S. Atlantic continental margin; structural and tectonic framework, *in* Sheridan, R.E., Grow, J.A., eds., The Atlantic Continental Margin, U.S.: Boulder, Colorado, The Geological Society of America, Geology of North America, v. 1-2, p. 19-56.
- Koeberl, C., 1989, New estimates of area and mass for the North American tektite strewn field, *in* Proceedings, 19th Lunar and Planetary Science Conference: Houston, Texas, Lunar and Planetary Science Institute, p. 745-751.
- Kominz, M.A., Miller, K.G., and Browning, J.V., 1998, Long-term and short-term global Cenozoic sea-level estimates: *Geology*, v. 26, p. 311-314.
- Kominz, M.A., Browning, J.V., Miller, K.G., Sugarman, P.J., Mizintseva, S., and Scotese, C.R., 2008, Late Cretaceous to Miocene sea-level estimates from the New Jersey and Delaware coastal plain coreholes: and error analysis: *Basin Research*, v. 20, p. 211-226.
- Kulpecz, A.A., Miller, K.G., Browning, J.V., Edwards, L.E., Powars, D.S., McLaughlin, P.P., Jr., Harris, A.D., Feigenson, M.D., *submitted*, Post-impact of the Chesapeake Bay impact structure: eustasy, passive-aggressive tectonism, and impactite compaction: Geological Society of America Special Publication XX, XX
- Letouzey, J., 1986, Cenozoic paleo-stress pattern in the Alpine foreland and structural interpretation in a platform basin: *Tectonophysics*, v. 132, p. 215-231.
- Maguire, T.J., Sheridan, R.E., and Volkert, R.A., 2004, Geophysical modeling of the northern Appalachian Brompton-Cameron, Central Maine, and Avalon terranes under the New Jersey Coastal Plain: *Journal of Geodynamics*, v. 37, p. 457-485.
- McKenzie, D., 1978, Some remarks on the development of sedimentary basins: *Earth and Planetary Science Letters*, v. 40, p. 25-32.
- Miller, K.G., Mountain, G.S., the Leg 150 Shipboard Party, and Members of the New Jersey Coastal Plain Drilling Project, 1996, Drilling and dating New Jersey Oligocene-Miocene sequences: Ice volume, global sea level, and Exxon records: *Science*, v. 271, p. 1092-1094.

- Miller, K.G., Rufolo, S., Sugarman, P.J., Pekar, S.F., Browning, J.V., and Gwynn, D.W., 1997, Early to middle Miocene sequences, systems tracts, and benthic foraminiferal biofacies, New Jersey coastal plain, *in* Miller, K.G., and Snyder, S.W., eds., *Proceedings of the Ocean Drilling Program, Scientific results, Volume 150X*: College Station, Texas, Ocean Drilling Program, p. 169-186.
- Miller, K.G., Kominz, M.A., Browning, J.V., Wright, J.D., Mountain, G.S., Katz, M.E., Sugarman, P.J., Cramer, B.S., Christie-Blick, N., and Pekar, S.F., 2005, The Phanerozoic record of global sea-level change: *Science*, v. 310, p. 1293-1298.
- Mitchum, R.M., Vail, P.R., and Thompson, S., 1977, The depositional sequence as a basic unit for stratigraphic analysis: *American Association of Petroleum Geologists Memoir*, v. 26, p. 53-62.
- Mitrovica, J.X., Beaumont, C., and Jarvis, G.T., 1989, Tilting of continental interiors by the dynamic effects of subduction: *Tectonics*, v. 8, p. 1079-1094.
- Mixon, R.B., 1992, Stratigraphic and geomorphic framework of the uppermost Cenozoic deposits in the southern Delmarva Peninsula, Virginia and Maryland: U.S. Geological Survey Professional Paper 1067-G, 53 p.
- Moucha, R., Forte, A.M., Mitrovica, J.X., Rowley, D.B., Quere, S., Simmons, N.A., and Grand, S.P., 2008, Dynamic topography and long-term sea level variations: there is no such thing as a stable continental platform: *Earth and Planetary Science Letters*, doi: 10.1016/j.epsl.2008.03.056
- Mueller, R.D., Sdrolias, M., Gaina, C., Steinberger, B., and Heine, C., 2008, Long-term sea-level fluctuations driven by ocean basin dynamics: *Science*, v. 319, p. 1357-1362.
- Olsson, R.K., 1980, The New Jersey Coastal Plain and its relationship with the Baltimore Canyon Trough, *in* Manspeizer, W., ed., *Field studies of New Jersey geology and guide to field trips: 52nd annual meeting of the New York State Geological Association*, Newark, N.J., p. 116-129.
- Olsson, R.K., Gibson, T.G., Hansen, H.J., and Owens, J.P., 1988, Geology of the northern Atlantic Coastal Plain: Long Island to Virginia, *in* Sheridan, R.E., and Grow, J.A., eds., *The Atlantic Coastal Margin, U.S.*: Boulder, Colorado, Geological Society of America, *Geology of North America*, v. 1-2, p. 87-105.
- Owens, J.P., and Sohl, N.F., 1969, Shelf and deltaic paleoenvironments in the Cretaceous-Tertiary formations of the New Jersey Coastal Plain, *in* Subitsky, S., ed., *Geology of selected areas in New Jersey and eastern Pennsylvania and guidebook of excursions*: Rutgers University Press, New Brunswick, N.J., p. 235-278.

- Owens, J.P., and Gohn, G.S., 1985, Depositional history of the Cretaceous series in the U.S. Atlantic Coastal Plain: Stratigraphy, paleoenvironments, and tectonic controls of sedimentation, *in* Poag, C.W., ed., *Geologic evolution of the United States Atlantic Margin*: New York, Van Nostrand Reinhold, p.25-86.
- Owens, J.P., Miller, K.G., and Sugarman, P.J., 1997, Lithostratigraphy and paleoenvironments of the Island Beach borehole, New Jersey Coastal Plain Drilling Project, *In* Miller K.G., and Snyder, S.W., eds. *Proceedings of the Ocean Drilling Program, Scientific Results*, v. 150X, p. 15-24.
- Pekar, S.F., Miller, K.G., and Browning, J.V., 1997, New Jersey Coastal Plain Oligocene sequences, *in* Miller, K.G., and Snyder, S.W., eds., *Proceedings of the Ocean Drilling Program, Scientific results*, Volume 150X: College Station, Texas, Ocean Drilling Program, p. 187-206.
- Pekar, S.J., Miller, K.G., and Kominz, M.A., 2000, Reconstructing the stratal geometry of latest Eocene to Oligocene sequences in New Jersey: Resolving a patchwork distribution into a clear pattern of progradation: *Sedimentary Geology*, v. 134, p. 93-109.
- Poag, C.W., 1979, Stratigraphy and depositional environments of the Baltimore Canyon Trough, *American Association of Petroleum Geologists Bulletin*, v. 63, p. 1452-1466.
- Poag, C.W., and Sevon, W.D., 1989, A record of Appalachian denudation in postrift Mesozoic and Cenozoic sedimentary deposits of the U.S. middle Atlantic continental margin: *Geomorphology*, v. 2, p. 119-157.
- Poag, C.W., and Norris, R.D., 2005, Stratigraphy and paleoenvironments or early postimpact deposits at the USGS-NASA Langley corehole, Chesapeake Bay impact crater, *in* Horton, J.W., Jr., Powars, D.S., and Gohn, G.S., eds. 2005, *Studies of the Chesapeake Bay Impact Structure- The USGS-NASA Langley Corehole, Hampton, Virginia, and Related Coreholes and Geophysical Survey*: U.S. Geological Survey Professional Paper 1688, p. F1-52, 2 pls.
- Poag, C.W., Powars, D.S., Poppe, L.J., and Mixon, R.B., 1994, Meteoroid mayhem in Ole Virginny: Source of the North American Tektite strewn field: *Geology*, v. 22, p. 691-694.
- Poag, C.W., 1997, The Chesapeake Bay bolide impact: a convulsive event in Atlantic Coastal Plain evolution: *Sedimentary Geology*, v. 108, p. 45-90.
- Poag, C.W., 1989, Foraminiferal stratigraphy and paleoenvironments of Cenozoic strata cored near Haynesville, Virginia: *in* Mixon, R.B., ed., *Geology and paleontology of the Haynesville cores- Northeastern Virginia Coastal Plain*: U.S. Geological Survey Professional Paper 1489, p. D1-20, 5. pls.

- Posamentier, H.W., Jervey, M.T., and Vail, P.R., 1988, Eustatic controls on clastic deposition I -- Conceptual framework: Society of Economic Paleontologists and Mineralogists Special Publication, v. 42, p. 109-124.
- Powars, D.S., 2000, The effects of the Chesapeake Bay impact crater on the geological framework and correlation of hydrogeologic units of southeastern Virginia, south of James River: U.S. Geological Survey Professional Paper 1622, 53 p.
- Powars, D.S., and Bruce, T.S., 1999, The effects of the Chesapeake Bay impact crater on the geologic frame-work and the correlation of hydrogeologic units of southeastern Virginia, south of the James River: U.S. Geological Survey Professional Paper 1612, 82 p.
- Powars, D.S., Mixon, R.B., and Bruce, T.S., 1992, Uppermost Mesozoic and Cenozoic geologic cross section, outer coastal plain of Virginia, *in* Gohn, G.S., ed., Proceedings of the 1988 U.S. Geological Survey Workshop on the Geology and Geohydrology of the Atlantic Coastal Plain: U.S. Geological Survey Circular 1059, p. 85-101.
- Powars, D.S., Poag, C.W., and Mixon, R.B., 1993, The Chesapeake Bay "impact crater," stratigraphic and seismic evidence [abstract]: Geological Society of America Abstracts with Programs, v. 25, no. 6, A-378.
- Pusz, A., Miller, K.G., Wright, J.D., and Kent, D.V., *submitted March 2008*, Global carbon cycle perturbation associated with late Eocene impacts: Geological Society of America Special Publication.
- Sanford, W.E., and Powars, D.S., *submitted*, Porewater chemistry of the central Chesapeake Bay impact structure and its implications for groundwater resources. GSA Special Publication XX, XX p.
- Seeber, L., and Armbruster, J.G., 1988, Seismicity along the Atlantic seaboard of the U.S.: Intraplate neotectonics and earthquakes, *in* Sheridan, R., and Grow, J., eds., The Atlantic continental margin, U.S.: Geological Society of America, Decade of North American Geology, v. 1-2, p.437-444.
- Self-Trail, J.M., Powell, D.C., and Christopher, R.A., 2004, The Collins Creek and Pleasant Creek Formations: Two new Upper Cretaceous subsurface units in the Carolina/Georgia Coastal Plain: Southeastern Geology, v. 42, p. 237-252.
- Spasojević, S., Liu, L., Gurnis, M., and Muller, R.D., 2008, The case for dynamic subsidence of the U.S. east coast since the Eocene: Geophysical Research Letters, v. 35, L0835, doi: 10.1029/2008GL033511.

- Steckler, M.S., and Watts, A.B., 1978, Subsidence of Atlantic-type continental margins off New York: *Earth and Planetary Science Letters*, v. 41, p. 1-13.
- Sugarman, P.J., Miller, K.G., Browning, J.V., Monteverde, D.H., Uptegrove, J., McLaughlin, P.P., Jr., Stanley, A.M., Wehmiller, J., Kulpecz, A.A., Harris, A.D., Pusz, A., Kahn, A., Friedman, A., Feigenson, M.D., Barron, J., and McCarthy, F.M.G., 2007, Cape May Zoo site. *In* Miller, K.G., Sugarman, P.J., Browning, J.V., et al., *Proc. ODP, Init. Repts.*, 174AX (Suppl.): College Station, TX (Ocean Drilling Program) p. 1-66.
- Van Sickel, W.A., Kominz, M.A., Miller, K.G., and Browning, J.V., 2004, Late Cretaceous and Cenozoic sea-level estimates; backstripping analysis of borehole data, onshore New Jersey: *Basin Research*, v. 16, p. 451-465.
- Van Wagoner, J.C., Posamentier, H.W., Mitchum, R. M., Vail, P.R., Sarg, J.F., Loutit, T.S., and Hardenbol, J., 1988, An overview of the fundamentals of sequence stratigraphy and key definitions: *Society of Economic Paleontologists and Mineralogists Special Publication*, v. 42, p. 39-45.
- Watts, A.B., and Steckler, M.S., 1979, Subsidence and eustasy at the continental margin of eastern North America, *American Geophysical Union, Maurice Ewing Symposium Series* 3, p. 218-234.
- Watts, A.B., 1981, The U.S. Atlantic continental margin: Subsidence history, crustal structure, and thermal evolution: *in* Bally, A.B., ed., *Geology of passive continental margins: History, structure, and sedimentologic record (with special emphasis on the Atlantic margin)*, *American Association of Petroleum Geologists Education Course Notes Series*, No. 19, p. 2-i-2-75.
- Weems, R.E., and Lewis, W.C., 2002, Structural and tectonic setting of the Charleston, South Carolina, region: Evidence from the Tertiary stratigraphic record: *Geological Society of America Bulletin*, v. 114, p. 24-42.
- Westaway, R., 2007, Late Cenozoic uplift of the eastern United States revealed by fluvial sequences of the Susquehanna and Ohio river systems: coupling between surface processes and lower crustal flow: *Quaternary Science Reviews*, v. 26, p. 2823-2843.
- Ziegler, P.A., and Van Hoorn, B., 1989, Evolution of the North Sea rift system. *In* Tankard, A.J., and Balkwell, H., eds., *Extensional tectonics and stratigraphy of the North Atlantic margins*. *American Association of Petroleum Geologists Memoir*, v. 46, p. 471-500.
- Zoback and Zoback, 1980, State of stress in the conterminous United States: *Journal of Geophysical Research*, v. 85, p. 6113-6156.

Zoback, M.L., M.D. Zoback, J. Adams, M. Assumpcao, S. Bell, E.A. Bergman, P. Bluemling, D. Denham, J. Ding, K. Fuchs, S. Gregersen, H.K. Gupta, K. Jacob, P. Knoll, M. Magee, J.L. Mercier, B.C. Muller, C. Paquin, O. Stephansson, A. Udias, and Z.H. Xu, Global patterns of intraplate stress: A status report on the world stress map project of the International Lithosphere Program. *Nature*, 341, 291-298.

Figure Captions

Figure 1. Location map showing the mid-Atlantic Coastal Plain and the location of the CBIS, key basement features, and the location of backstripped records used in this study. Coreholes are coded by color and letter: BB- Bethany Beach, DE; X- Exmore, VA; E- Eyreville, VA; K- Kiptopeke, VA; L- Langley, VA; M- MW4-1, VA; F- Fentress, VA; and D- Dismal Swamp, VA. New backstripped records from Eyreville and Exmore are unique to this study, while the other coreholes are modified from Hayden et al. (2008). Red circles indicate ODP Leg 150X and 174AX coreholes, some of which (along with Bethany Beach, DE) were used in the construction of the New Jersey sea-level estimates (Miller et al., 2005; Kominz et al., 2008).

Figure 2. Diagram shows the data inputs for backstripping from the Eyreville (Browning et al., submitted) and Exmore (Kulpecz et al., submitted) coreholes. Plots include the percentage lithology (brown- clay/silt; pale yellow- fine sand; bright yellow- medium/coarse sand; green- glauconite; blue- carbonate; white- other), age interpretations for each sequence (based on bio- and Sr-isotope stratigraphy, sequence name, benthic zone interpretations, and lithofacies/paleoenvironmental interpretation. Biofacies U- *Uvigerina*; Bul- *Bulimina*; Hanz- *Hanzawaia*; Non; *Nonionella*; and Elph- *Elphidium* are defined by the studies of Miller et al. (1997). Biofacies A-G are defined by

Pekar et al. (1997) while 'n' indicates no foraminifera. Lithofacies: USF- upper shoreface; LSF- lower shoreface; Est.- Estuarine; while p- proximal and d- distal.

Figure 3. Eyreville fraction porosity data is from Sanford et al. (submitted) and provided estimates used in the construction of our time-dependent compaction model. The compaction models for Eyreville and Exmore are shown next to the physical data. Each multi-colored line represents a time-step (see key below for both age after impact and true geologic age) in the time-dependent compaction of these impact materials.

Figure 4. Figure presents the litho- and biofacies models used for paleodepth assignment. Lithofacies are modified from the wave-dominated shoreface model of Browning et al. (2006), while benthic foraminiferal biofacies for Miocene sequences are from Miller et al. (1997; shown on lithofacies diagram) and Oligocene sequences from Pekar et al. (1997; noted in blue beneath lithofacies diagram).

Figure 5. The lower three graphs depict different scenarios of time-dependent compaction and the sensitivity of the models to changes in c and t_0 . Model C represents the maximum rate of compaction scenario (rapid late Eocene compaction); Model A represents the scenario used in this study that best approximated stratigraphic observations; and Model D represents the end-case of no time-dependent compaction (impactite compacts as a function of depth). The sensitivity of R1 and R2 results to changes in model inputs are portrayed at the top of the page. R1 results are plotted along with the best-fit theoretical

subsidence curve of McKenzie (1978). Each scenario is color coded to match the appropriate model.

Figure 6. Backstripped R1 results from Eyreville (red) and Exmore (green). ‘Tsubs’ is defined as tectonic subsidence (minimum = min, best, maximum = max, and sed = no water depth correction; obs sed = observed sediment) while ‘WD’ stands for water depth.

Figure 7. New backstripped R1 estimates from Eyreville (red) and Exmore (green) plotted against the previous records of Hayden et al. (2008) and Browning et al. (2006). The regional hiatuses of Gohn et al. (2008) and Kulpecz et al. (submitted) are represented by the semi-transparent boxes. The base of the graph classifies the events that shaped the post-impact evolution of the CBIS, as defined by Hayden et al. (2008) and this study. The black bar represents the impact event.

Figure 8. Backstripped R2 estimates from Eyreville (red) and Exmore (green) plotted against the eustatic estimates of Kominz et al. (2008). Purple indicates the best eustatic estimate, while the black line represents the approximated lowstand sea level estimates. Light and dark purple depict minimum and maximum values, respectively. The light blue line represents long-term sea level, while the orange line represents long-term sea level from New Jersey with a slab correction (to account for dynamic topographic changes). Error ranges of CBIS estimates are represented by the broad color fills.

Figure 9. Thermal anomaly model of Hayden et al. (2008) that shows the normal geothermal gradient, the post-impact cooling from the deposition of cold impact materials after impact, the maximum subsidence event, and subsequent uplift phase and restoration of a new geothermal gradient (higher than original values due to the low thermal conductivity of impactites and post-impact sediments).

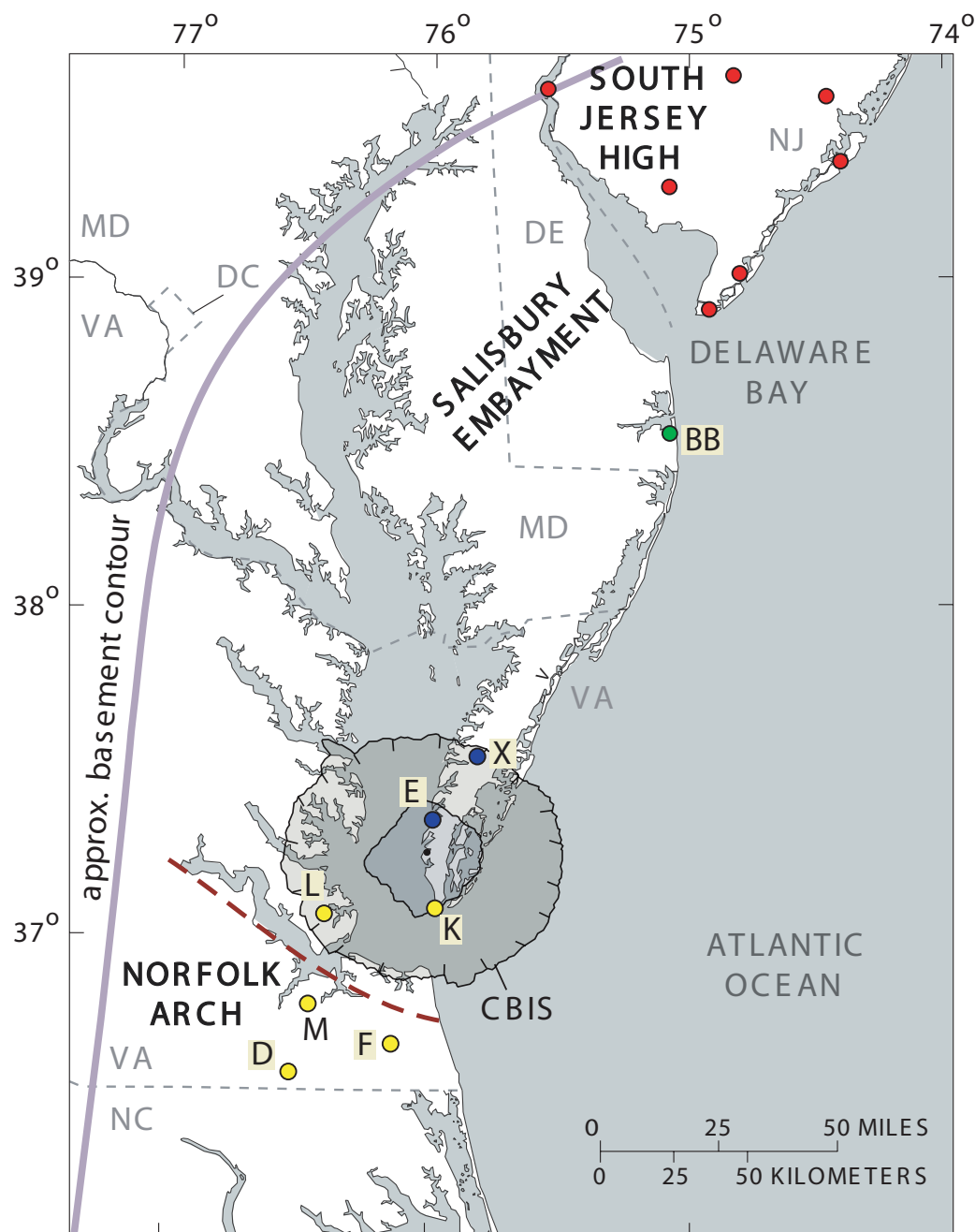
Figure 10. Figure depicts the geographic distribution of unconformities during the Oligocene, lower Miocene, and upper middle Miocene established from regional studies by Kulpecz et al. (submitted) and Powars and Bruce (1999). Thickness of these intervals in New Jersey, Delaware, and Maryland is established from geophysical log correlation (Kulpecz et al., submitted) and reports and publications from coreholes drilled by the Ocean Drilling Program (e.g., Browning et al., 2006; Sugarman et al., 2007; etc.). Note the different contour intervals between maps. Blank areas on the coastal plain indicate the presence of known unconformities.

Figure 11. Graph depicts the amplitude and timing of important mechanisms responsible for tectonic uplift and subsidence on typical passive margins. Lithospheric flexure and intraplate stress values are derived from Cloetingh (1988) and Karner et al. (1993). Dynamic topographic ranges are from Mueller et al. (2008). Thermoflexural subsidence estimates are from Steckler and Watts (1978) and Kominz et al. (1998), while lower crustal flow is derived from Westaway (2007). The dashed line for the upper intraplate stress box represents high amplitudes of uplift tied to major stress field reorganizations (e.g., Cloetingh, 1988; Cloetingh et al., 1990).

Table 1. Chart shows sample depth, sequence, paleoenvironmental interpretation, abundant benthic fauna, biofacies interpretations, and paleodepth estimates for the Eyreville corehole.

Table 2. Backstripping inputs for the Eyreville corehole. Thickness is in meters, density is in g/cm^3 , % clay-sand-silt is out of 100, sorting (1 = dirty, 4= clean), Age (Ma), paleoenvironmental interpretation from core, and water depth estimates.

Table 3. Backstripping inputs for the Exmore corehole. Thickness is in meters, density is in g/cm^3 , % clay-sand-silt is out of 100, sorting (1 = dirty, 4= clean), Age (Ma), paleoenvironmental interpretation from core, and water depth estimates.



Base from U.S. Geological Survey
Digital Line Graph, 1:2,000,000, 1990

● Backstripped coreholes (Miller et al., 2005; Kominz et al., 2008)

● Backstripped coreholes (Hayden et al., 2008)

● Backstripped corehole (Browning et al., 2006)

● Backstripped coreholes (this study)

James River Structural Zone
(N. boundary of Norfolk Arch)

Figure 1

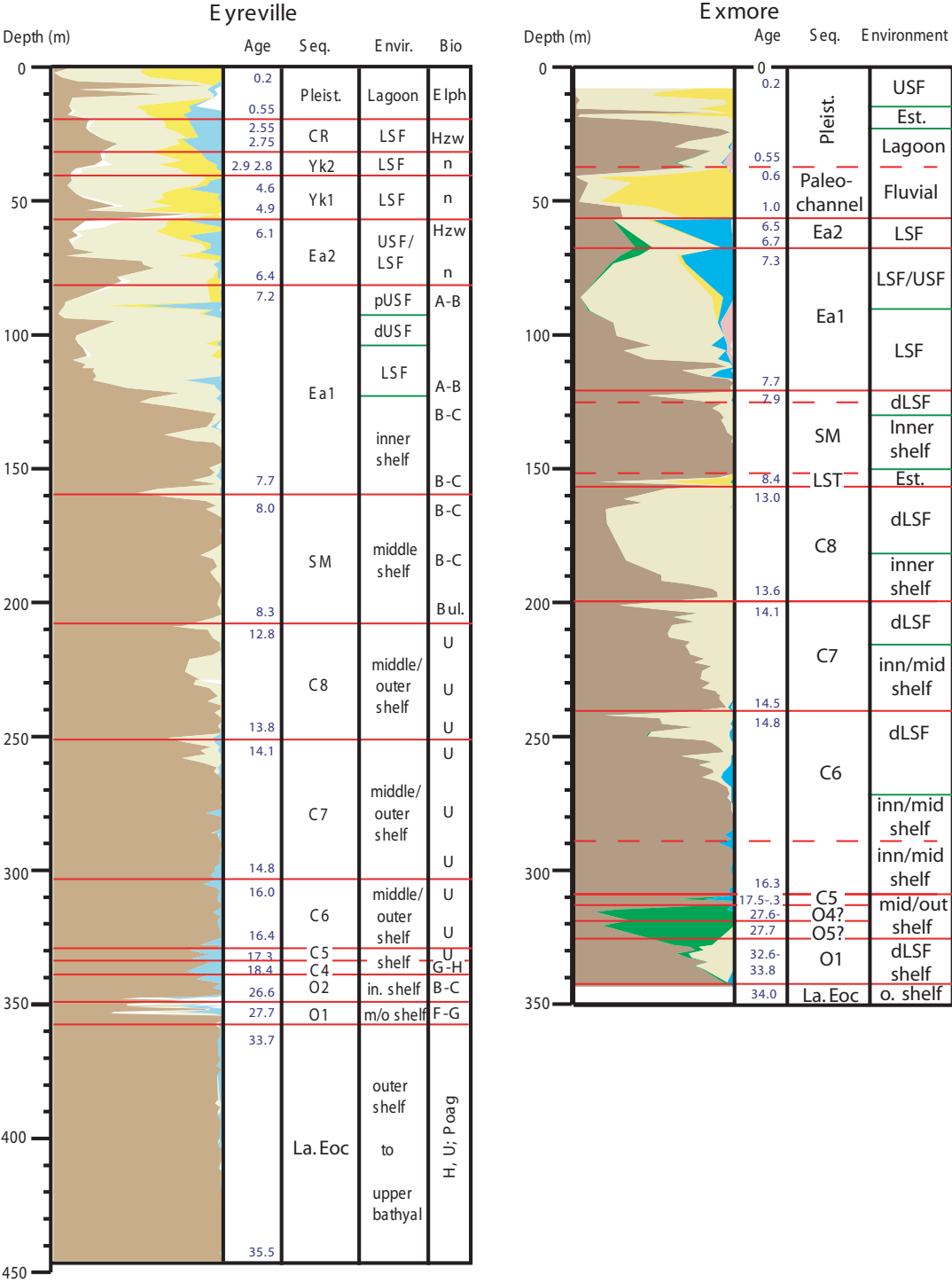


Figure 2

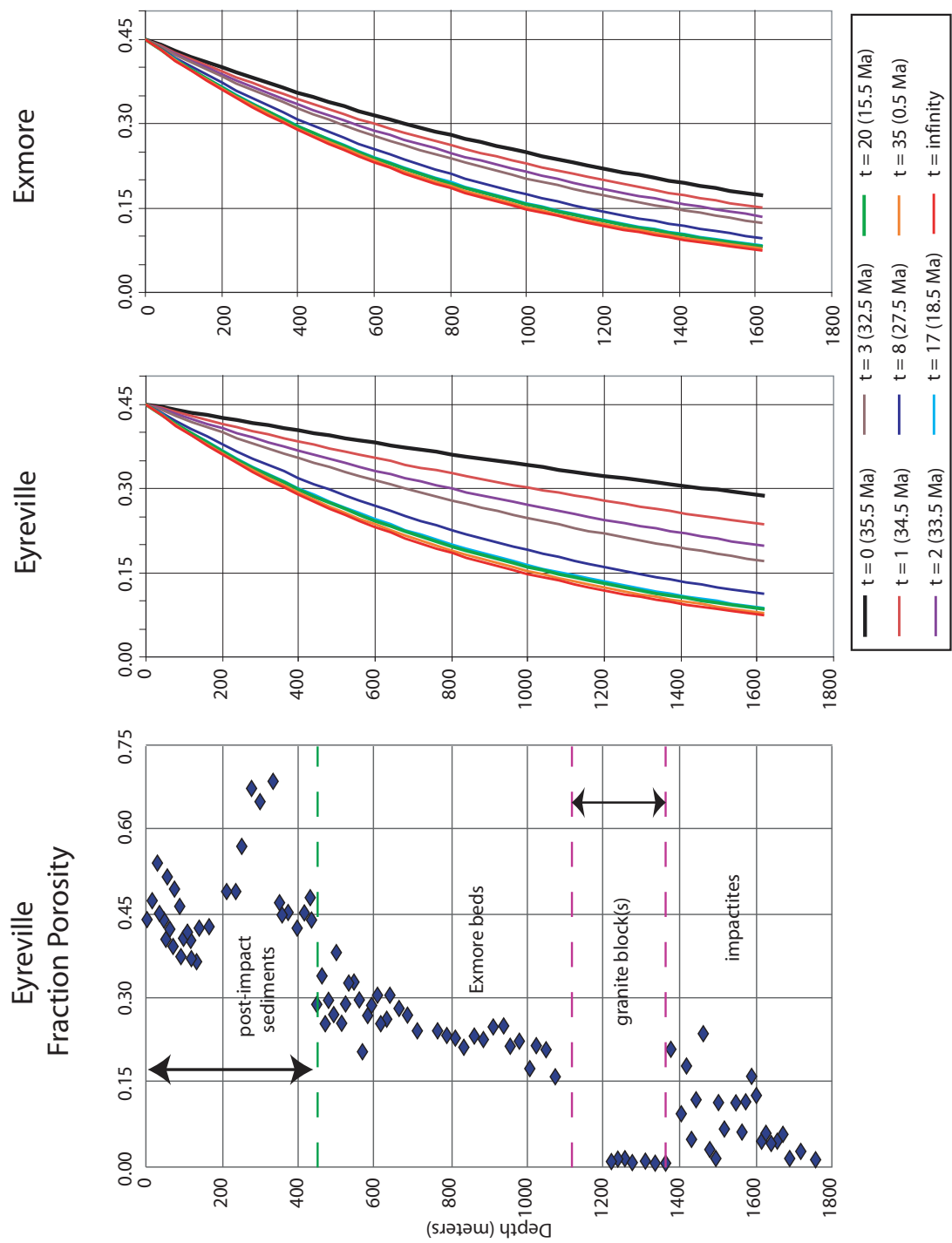


Figure 3

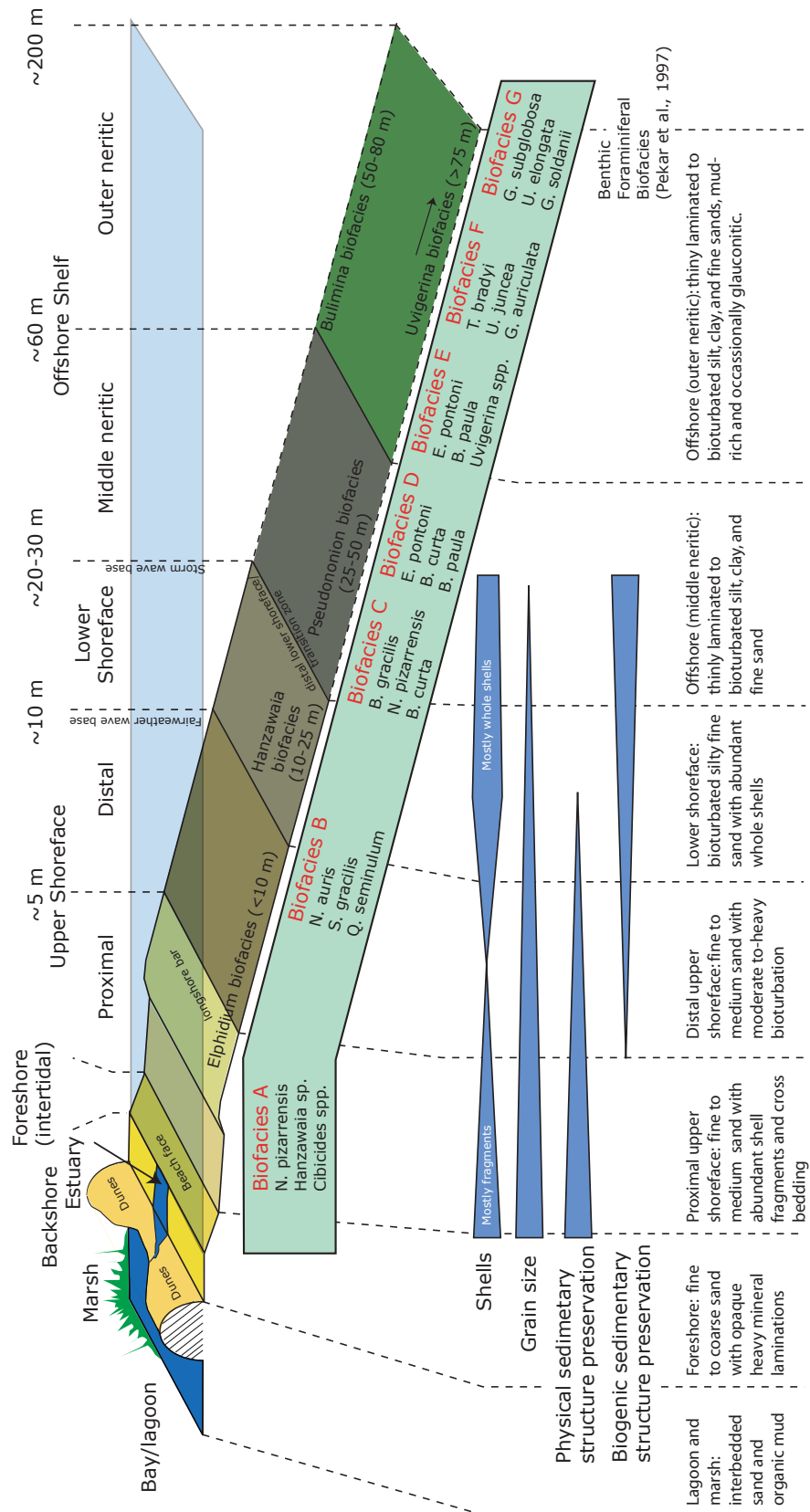


Figure 4

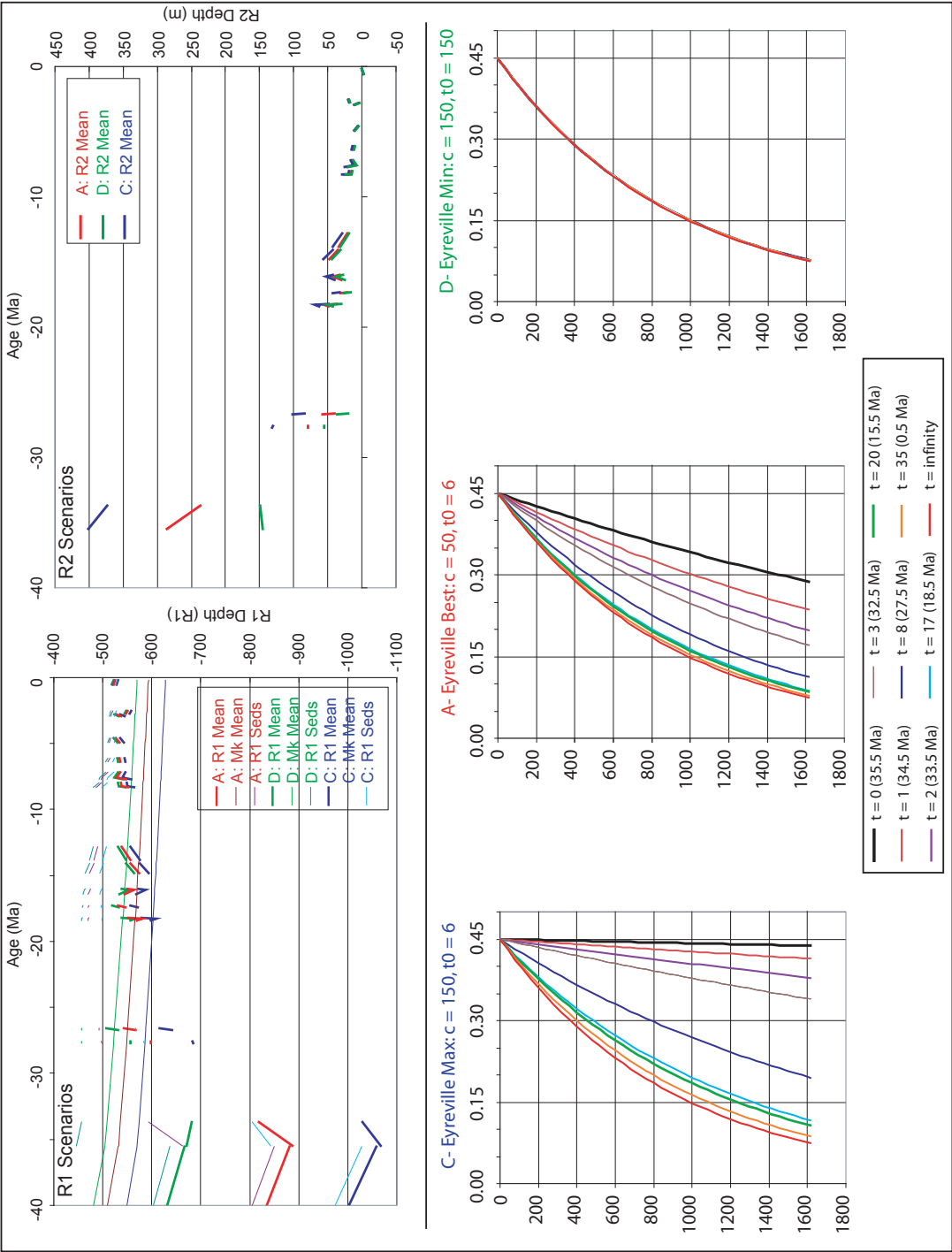


Figure 5

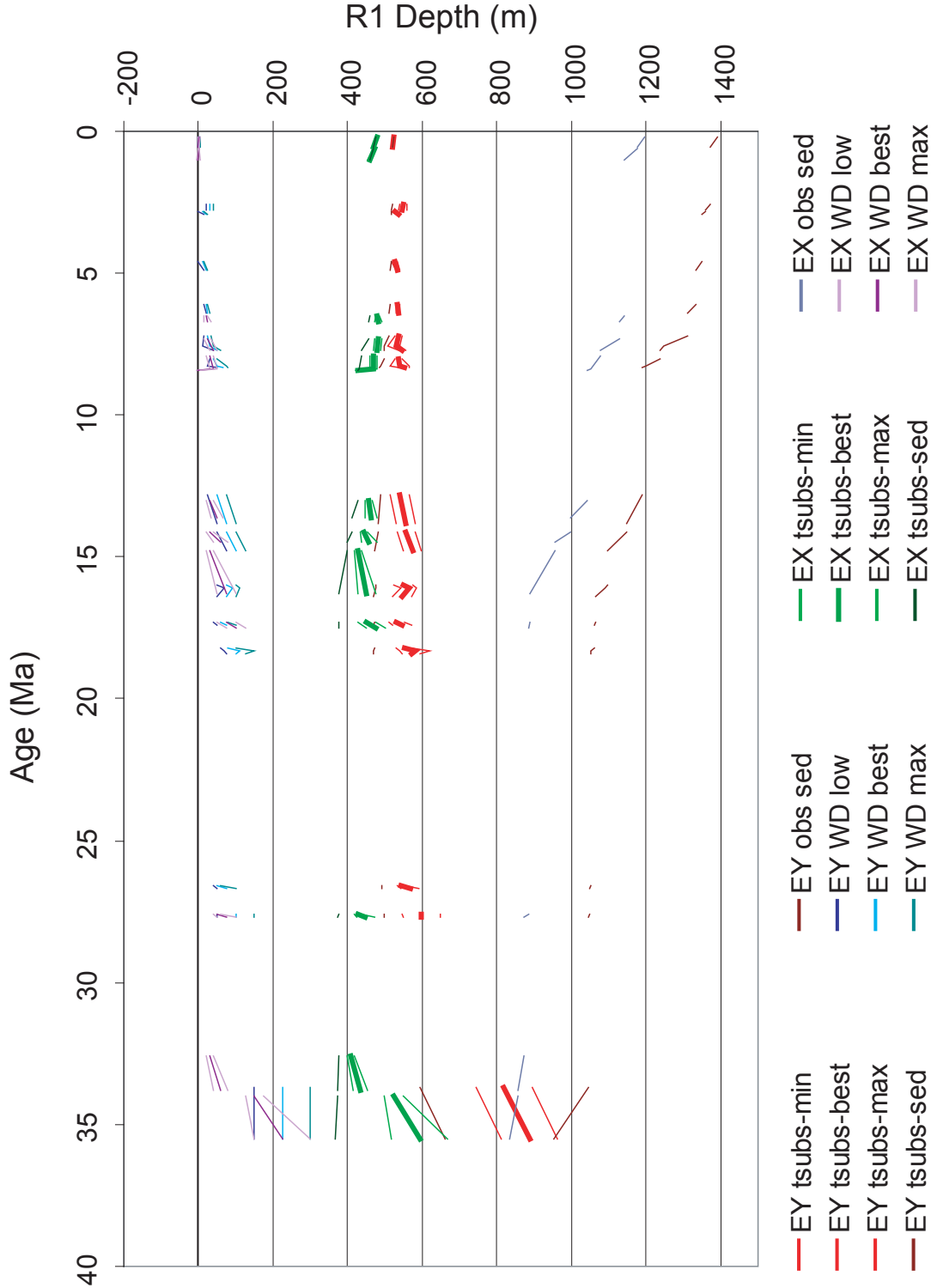


Figure 6

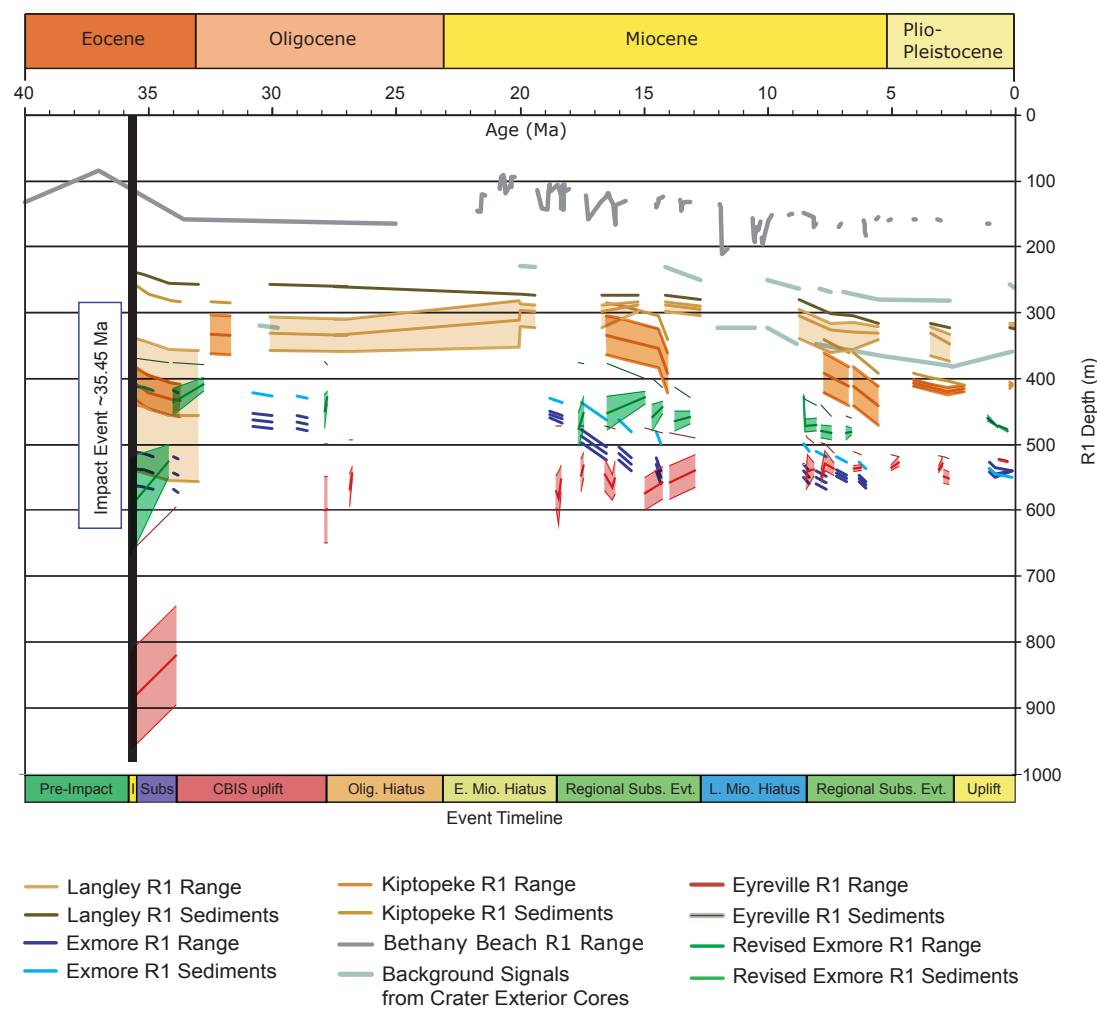


Figure 7

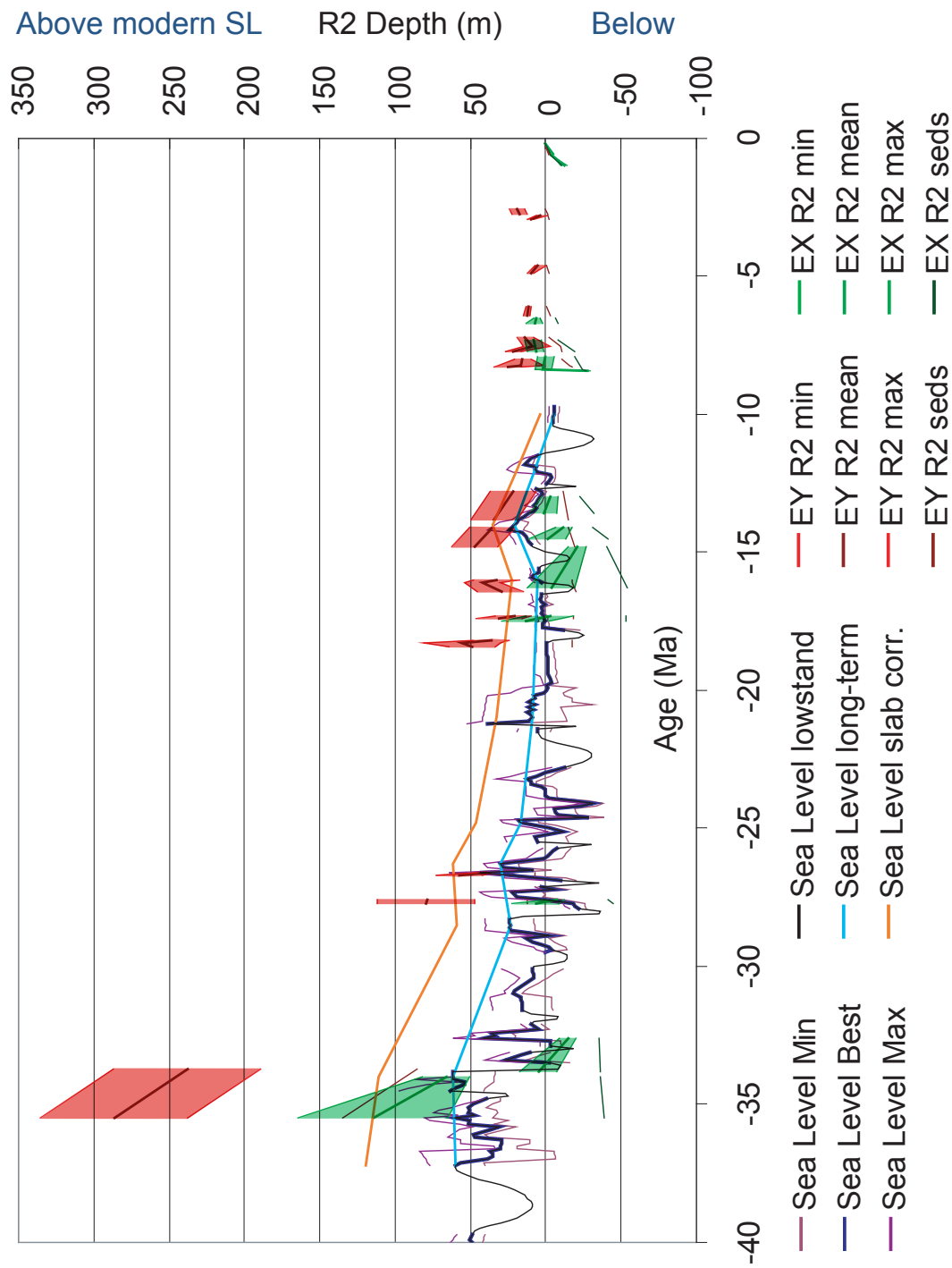


Figure 8

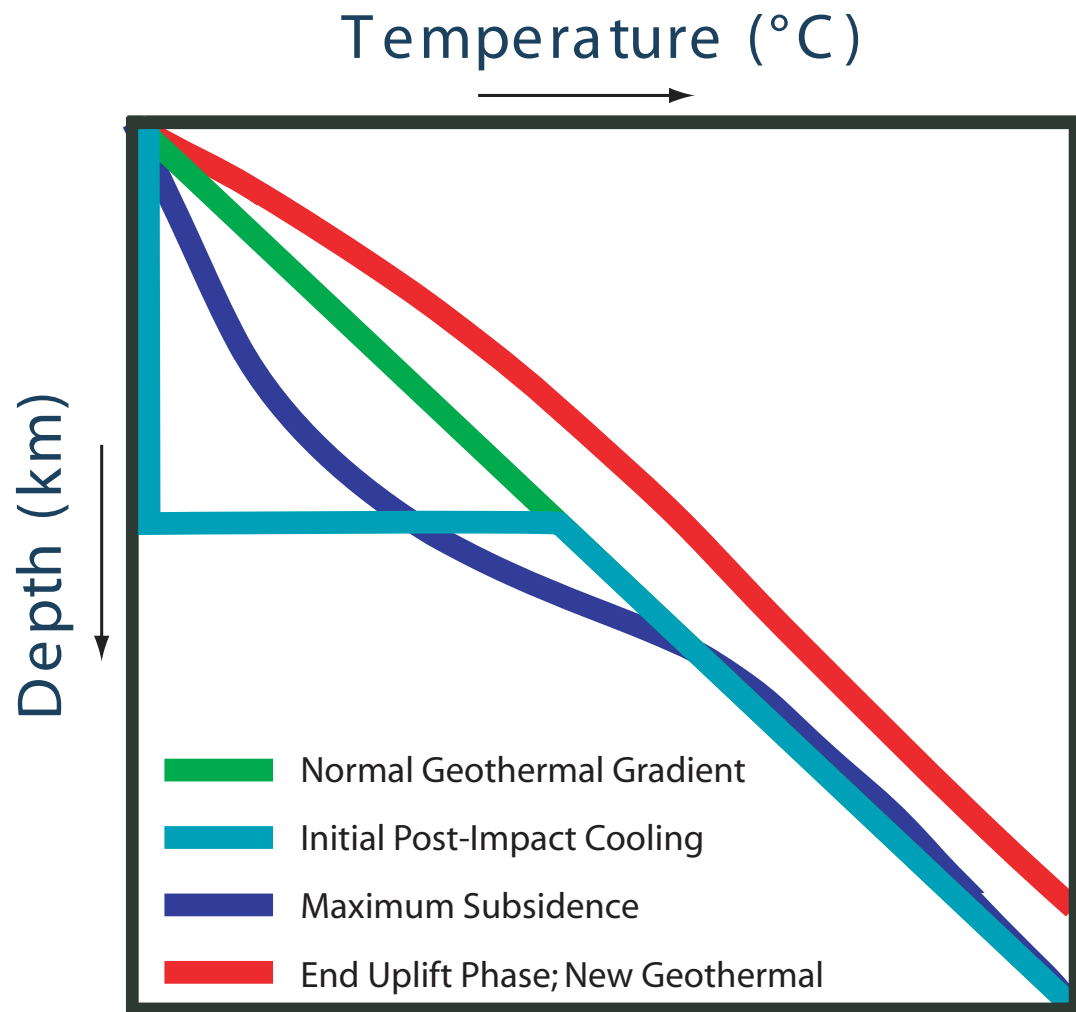


Figure 9

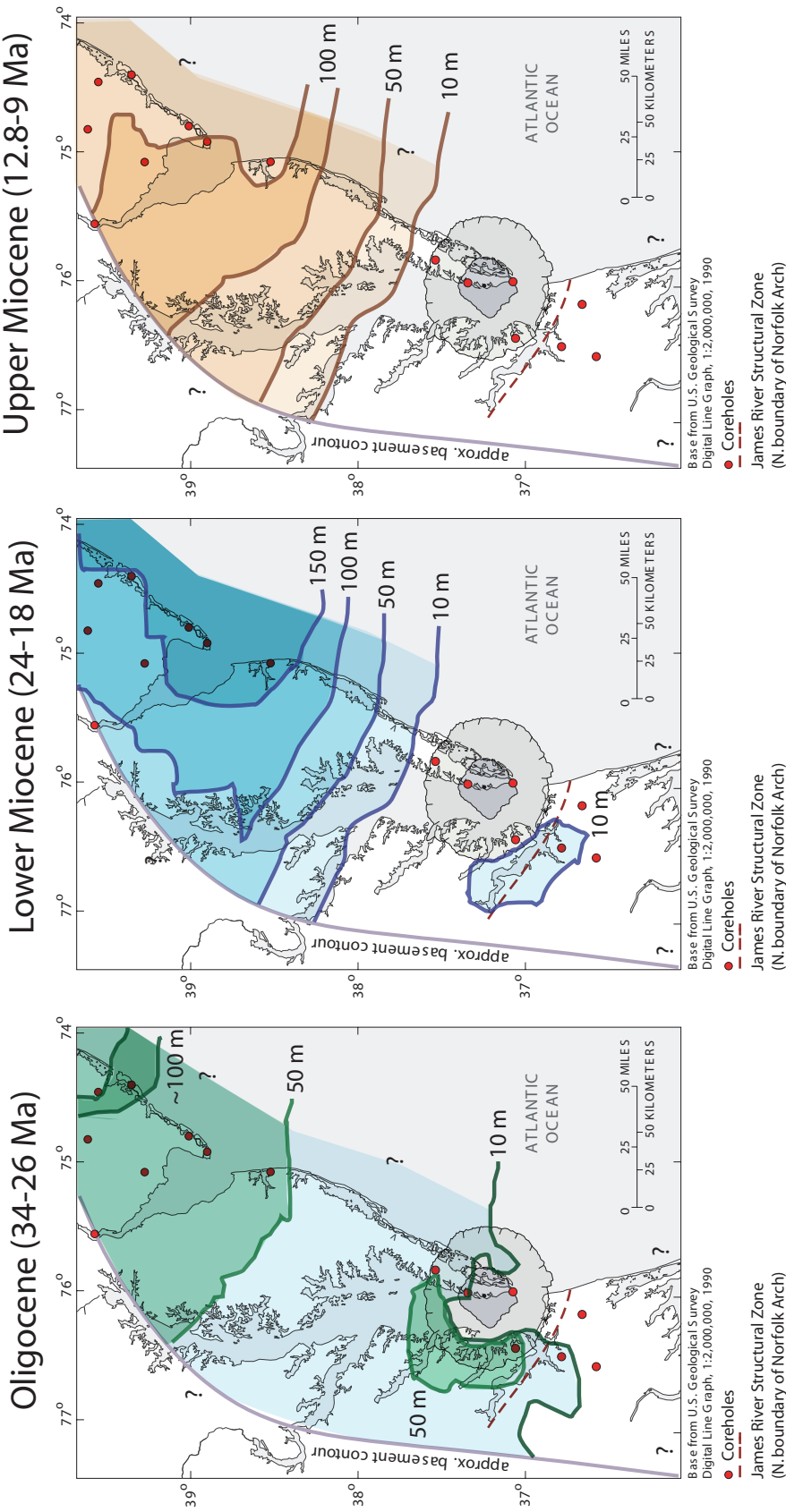


Figure 10

Tectonic influence on passive margins

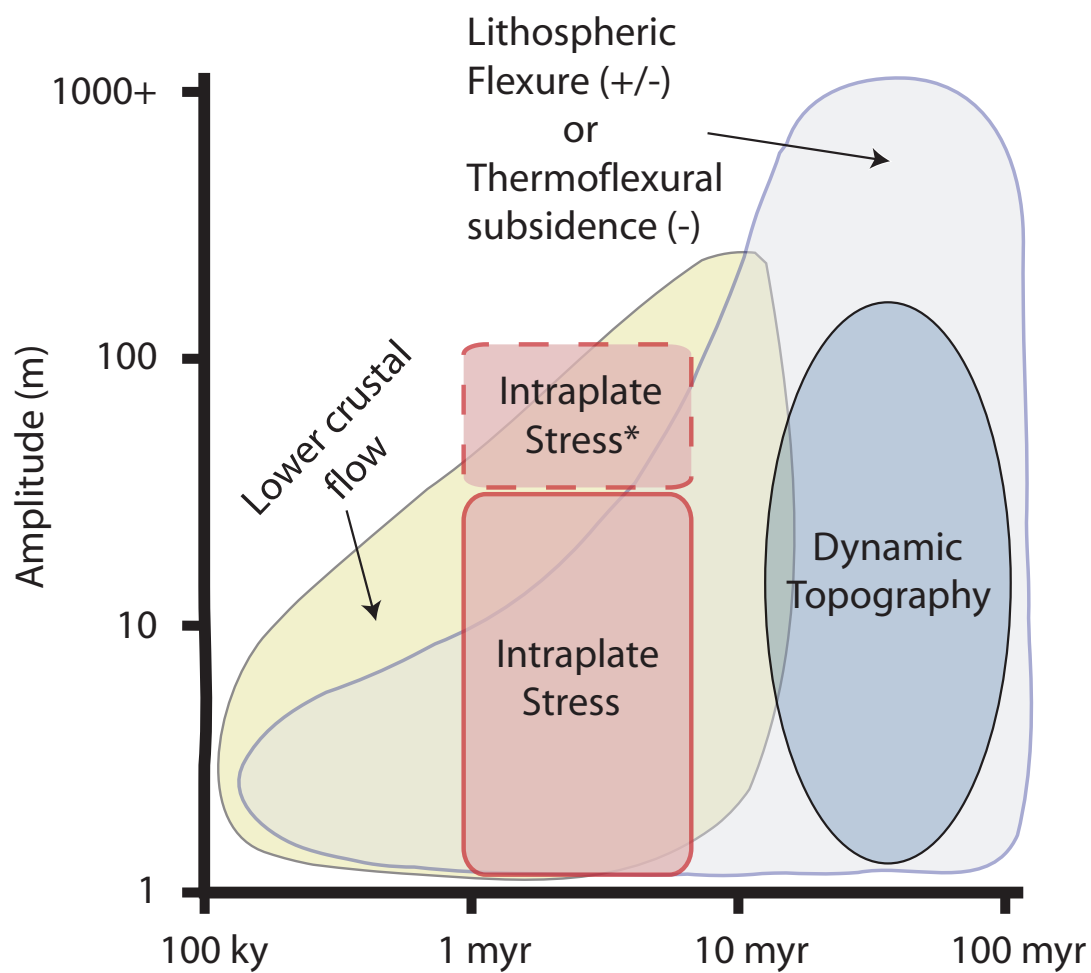


Figure 11

Eyreville Corehole						
Sample	Sequence	Lithofacies Interpretation	Abundant Benthic Foraminifera	Benthic Foraminiferal Biofacies	WD min	WD best WD max
12.7	Butler's Bluff	Lagoon	<i>Elphidium</i> spp., <i>Buccella</i> spp.	Elphidium Biofacies	0	2
95.2	Chowan River	LSF to inner shelf	<i>Hanzawaia</i> spp.	Hanzawaia Biofacies (A)	15	25
121	Yorktown 2	Lower Shoreface	No foraminifera	No foraminifera	15	25
171	Yorktown 1	Lower to Upper Shoreface	No foraminifera	No foraminifera	5	15
216	Eastover 2	Lower to Upper Shoreface	<i>Hanzawaia</i> spp., Largely barren	Hanzawaia Biofacies (A)	10	15
261	Eastover 2	Lower Shoreface	No foraminifera	No foraminifera	20	25
266	Eastover 2	Lower Shoreface	No foraminifera	No foraminifera	20	25
401	Eastover 1	dLSF/inner shelf	<i>Nonionella pizarrensis</i> , <i>Bulimina curta</i>	Biofacies A-B	15	25
430.7	Eastover 1	dLSF/inner shelf	<i>N. pizarrensis</i> , <i>Buccella</i> spp., <i>Nonionella</i> spp., <i>Eponides</i> spp.	Biofacies A-B	15	25
466	Eastover 1	Inner shelf	<i>Nonionella pizarrensis</i> , <i>Bulimina curta</i>	Biofacies B-C	40	50
511	Eastover 1	Inner shelf	<i>Nonionella pizarrensis</i> , <i>Bulimina curta</i> , <i>Buliminella gracilis</i>	Biofacies B-C	40	50
520	SM	Inner shelf	<i>Buliminella curta</i> , <i>N. pizarrensis</i> , <i>Eponides</i> spp.	Biofacies B-C, Sh. Lithofacies	30	40
645	SM	Inner to middle shelf	<i>N. pizarrensis</i> , <i>Lenticulina</i> spp., <i>Cassidulina</i> spp., <i>Bolivina</i> spp.	Biofacies B-C	25	50
667	SM	Middle shelf (MFS)	<i>Buliminella curta</i> , <i>N. pizarrensis</i> , <i>Eponides</i> spp.	Bulimina Biofacies	50	65
701	C8	Middle shelf	<i>Pseudonion</i> spp., <i>Nonionella pizarrensis</i>	Nonionella Biofacies	25	50
736	C8	Middle to outer shelf	<i>Uvigerina</i> spp.	Uvigerina Biofacies	75	90
796	C8	Middle to outer shelf	<i>Uvigerina</i> spp.	Uvigerina Biofacies	75	90
811	C8	Middle to outer shelf	<i>Uvigerina</i> spp.	Uvigerina Biofacies	75	90
826	C7	Middle to outer shelf	<i>Uvigerina</i> spp., <i>Bolivina</i> spp.	Uvigerina Biofacies	75	90
851	C7	Middle to outer shelf	<i>Uvigerina</i> spp., <i>N. pizarrensis</i>	Uvigerina Biofacies	75	90
891	C7	Middle to outer shelf	<i>Uvigerina</i> spp., <i>Gavelinella</i> spp.	Uvigerina Biofacies	75	90
926	C7	Middle to outer shelf	<i>Uvigerina</i> spp.	Uvigerina Biofacies	75	90
941	C7	Middle to outer shelf	<i>Loxostomoides applanata</i> , <i>Uvigerina</i> spp., <i>U. elongata</i> , <i>N. pizarrensis</i>	Uvigerina Biofacies	75	90
951	C7	Middle to outer shelf	<i>Uvigerina</i> spp., <i>N. pizarrensis</i>	Uvigerina Biofacies	75	90
981	C7	Outer shelf	<i>Uvigerina</i> spp., <i>Rectuvigerina</i> spp., <i>Gavelinella</i> spp., <i>Lenticulina</i> spp.	Uvigerina to Biofacies H?	100	125
986	C6	Middle shelf	<i>Rectuvigerina</i> spp., <i>Cibicides</i> spp.	Uvigerina Biofacies, Sh. lithofacies	50	75
1011	C6	Middle to outer shelf	<i>Loxostomoides applanata</i> , <i>Uvigerina</i> spp., <i>Rectuvigerina</i> spp.	Uvigerina Biofacies	75	90
1021	C6	Middle to outer shelf	<i>Uvigerina</i> spp., <i>Rectuvigerina</i> spp., <i>Lenticulina</i> spp.	Uvigerina Biofacies	75	90
1031	C6	Middle to outer shelf	<i>Loxostomoides applanata</i> , <i>Gavelinella</i> spp., <i>Gyronoides</i> spp.	Uvigerina Biofacies	75	90
1041	C6	Middle to outer shelf	<i>Uvigerina</i> spp., <i>Loxostomoides applanata</i> , <i>Rectuvigerina</i> spp.	Uvigerina Biofacies	75	90
1051	C6	Middle to outer shelf	<i>Loxostomoides applanata</i> , <i>Bolivina</i> spp., <i>Rectuvigerina</i> spp.	Uvigerina Biofacies	75	90
1071	C6	Middle to outer shelf	<i>Uvigerina</i> spp., <i>Rectuvigerina</i> spp., <i>Bulimina elongata</i>	Uvigerina Biofacies	75	90
1081	C6	Middle to outer shelf	<i>Loxostomoides applanata</i> , <i>Bulimina elongata</i> , <i>Uvigerina</i> spp.	Uvigerina Biofacies	50	75
1086	C5	Inner to middle shelf	<i>Bulimina elongata</i> , <i>Loxostomoides applanata</i> , <i>Uvigerina</i> spp.	Bulimina Biofacies	40	60
1096	C5	Inner to middle shelf	<i>Loxostomoides applanata</i> , <i>Bulimina elongata</i> , <i>Gyronoides</i> spp.	Bulimina Biofacies	50	75
1101	C4	Middle to outer shelf	<i>Uvigerina</i> spp., <i>Globocassidulina subglobosa</i> , <i>N. pizarrensis</i>	Uvigerina Biofacies, Biofacies G-H	60	80
1106	C4	Middle to outer shelf	<i>Uvigerina</i> spp., <i>Bulimina</i> spp., <i>N. pizarrensis</i> , <i>Bolivina</i> spp.	Uvigerina Biofacies	75	90
1111	C4	Middle to outer shelf	<i>Globocassidulina subglobosa</i>	Biofacies G-H	75	100
1119	C4	Outer shelf	<i>Rectuvigerina</i> spp., <i>Uvigerina</i> spp., <i>Gyronoides</i> spp.	Biofacies G-H	70	110
1126	C4	Outer shelf	<i>Globocassidulina subglobosa</i> , <i>Rectuvigerina</i> spp.	Biofacies G-H	75	100
1136.2	Olig 2	Inner shelf	No foraminifera	No foraminifera	40	50
1140	Olig 2	Inner to middle shelf	<i>Uvigerina costata</i> , <i>N. pizarrensis</i> , <i>Globobulimina</i> spp., <i>Lenticulina</i> spp.	Biofacies B-C, Uvigerina Biofacies	50	75
1143.55	Olig 1	Middle to outer shelf	<i>Loxostomoides applanata</i> , <i>Globobulimina arciculata</i> , <i>Trifarina</i> spp.	Biofacies F-G	50	100
1150	Chickahominy	Outer shelf to upper bathyal	<i>Bulimina jacksonensis</i> , <i>B. cooperensis</i> , <i>Uvigerina</i> spp.	Biofacies H and U. Bathyal of Poag	150	225
						300

Table 1

Backstripping inputs											
Exmore corehole											
Units	Thickness	Density	% Clay	% Sand	% Silt	Age (Ma)	Environment	WD low	WD best	WD high	
Impactites	-215	2.67	0	0	0	35.5	-	150	225	300	
Chickahominy Fm.	23.5	2.72	0.6	0.1	0.3	34	Outer shelf	125	150	175	
Oligocene 1 base	0.01	2.65	0	0	0	33.8	dLSF to inner shelf	40	60	80	
Oligocene 1 top	13.6	2.66	0.1	0.7	0.2	32.6	Distal lower shoreface	20	30	40	
Oligocene 1&2 base	0.01	2.64	0	0	0	27.7	Inner to middle shelf	50	75	100	
Oligocene 1&2 top	13.8	2.64	0.6	0.3	0.1	27.6	Inner to middle shelf	40	50	60	
C5 base + unconf.	0.01	2.65	0	0	0	17.5	Outer shelf	75	100	125	
C5 top	3	2.63	0.6	0.1	0.3	17.3	Inner to middle shelf	50	75	100	
C6 base + unconf.	0.01	2.65	0	0	0	16.3	Inner to middle shelf	50	75	100	
C6 top	69.3	2.65	0.7	0.25	0.05	14.8	dLSF to inner shelf	20	30	40	
C7 base + unconf.	0.01	2.62	0	0	0	14.5	Inner to middle shelf	40	60	80	
C7 top	41.4	2.65	0.5	0.3	0.2	14.1	dLSF to inner shelf	20	30	40	
C8 base + unconf.	0.01	2.62	0	0	0	13.6	Inner shelf	35	50	65	
C8 top	43.6	2.65	0.2	0.6	0.2	13	dLSF to inner shelf	20	30	40	
SM base + unconf.	0.01	2.62	0	0	0	8.4	Estuarine	-5	0	5	
SM MFS	10	2.62	0	0.9	0.1	8.35	Inner shelf	30	40	50	
SM top	23.8	2.62	0.7	0.1	0.2	7.9	dLSF to inner shelf	20	30	40	
Ea1 base + unconf.	0.01	2.62	0	0	0	7.7	Inner shelf	30	40	50	
Ea1 top	54	2.67	0.1	0.7	0.2	7.3	Lower shoreface	15	25	35	
Ea2 base + unconf.	0.01	2.65	0	0	0	6.7	LSF to inner shelf	15	25	35	
Ea2 top	10.6	2.67	0.1	0.8	0.1	6.5	Lower shoreface	15	20	25	
Paleochannel base	0.01	2.65	0	0	0	1	Fluvial	-5	0	5	
Paleochannel top	36.7	2.65	0.2	0.6	0.2	0.6	Bay or lagoon	0	1	2	
Pleistocene base	0.01	2.65	0	0	0	0.55	Estuarine	-2	0	2	
Pleistocene top	18	2.65	0.2	0.8	0	0.2	Upper shoreface	0	2	4	

Table 3

Eyreville R1 Results									
age	tsubs-min	tsubs-best	tsubs-max	t.subs-sed	sstar	obs sed	Ywd1	Ywdbest	Ywd3
120	-5	0	5	0	0	0	-5	0	5
35.55	865.4	880.4	910.4	850.4	2329.75	2151.11	15	30	60
35.5									
35.5	812.217	887.217	962.217	662.217	1285.94	951	150	225	300
33.7	744.013	819.013	894.013	594.013	1273.78	1045	150	225	300
27.7									
27.7	547.745	597.745	647.745	497.745	1177.52	1045.01	50	100	150
27.6	547.454	597.454	647.454	497.454	1178.37	1047.01	50	100	150
26.7									
26.7	542.255	567.255	592.255	492.255	1173.18	1047.02	50	75	100
26.6	532.4	542.4	552.4	492.4	1175.58	1051.02	40	50	60
18.4									
18.4	545.24	570.24	595.24	470.24	1153.42	1051.03	75	100	125
18.3	540.413	580.413	620.413	470.413	1154.73	1053.03	70	110	150
18.2	531.359	551.359	571.359	471.359	1159.64	1060.03	60	80	100
17.4									
17.4	520.355	545.355	570.355	470.355	1158.65	1060.04	50	75	100
17.3	511.031	531.031	551.031	471.031	1162.13	1065.04	40	60	80
16.4									
16.4	520.028	545.028	570.028	470.028	1161.14	1065.05	50	75	100
16.1	543.998	563.998	583.998	473.998	1179.05	1090.05	70	90	110
16	524.726	549.726	574.726	474.726	1182.59	1095.05	50	75	100
14.8									
14.8	548.597	573.597	598.597	473.597	1181.47	1095.06	75	100	125
14.1	531.694	556.694	581.694	481.694	1218.21	1146.56	50	75	100
13.8									
13.8	531.453	556.453	581.453	481.453	1217.97	1146.57	50	75	100
12.8	513.996	538.996	563.996	488.996	1248.52	1188.77	25	50	75
8.3									
8.3	536.453	551.453	566.453	486.453	1245.99	1188.78	50	65	80
8.25	513.642	538.642	563.642	488.642	1253.51	1198.78	25	50	75
8	526.948	536.948	546.948	496.948	1281.57	1236.48	30	40	50
7.7									
7.7	536.819	546.819	556.819	496.819	1281.44	1236.49	40	50	60
7.55	508.48	528.48	538.48	498.48	1288.54	1246.49	10	30	40
7.2	525.599	535.599	545.599	510.599	1336.09	1312.49	15	25	35
6.4									
6.4	530.29	535.29	540.29	510.29	1335.79	1312.5	20	25	30
6.1	529.061	534.061	539.061	514.061	1350.36	1332.7	15	20	25
4.9									
4.9	528.65	533.65	538.65	513.65	1349.95	1332.71	15	20	25
4.6	516.778	526.778	531.778	516.778	1362.8	1350.71	0	10	15
2.95									
2.95	531.29	536.29	541.29	516.29	1362.32	1350.72	15	20	25
2.8	517.527	527.527	532.527	517.527	1367.32	1357.72	0	10	15
2.75									
2.75	537.513	547.513	557.513	517.513	1367.31	1357.73	20	30	40
2.55	540.049	550.049	560.049	520.049	1377.36	1371.73	20	30	40
0.55									
0.550003	519.555	521.555	523.555	519.555	1376.87	1371.74	0	2	4
0.199997	522.981	524.981	526.981	522.981	1389.79	1389.74	0	2	4

Exmore R1 Results									
age	tsubs-min	tsubs-best	tsubs-max	t.subs-sed	sstar	obs sed	wd1	wdbest	wd3
120	-5	0	5	0	0	0	-5	0	5
95	299.9	304.9	309.9	304.9	697.744	634	-5	0	5
45	382.533	397.533	427.533	367.533	1412.39	703.855	15	30	60
35.5									
35.5	517.533	592.533	667.533	367.533	874.856	834	150	225	300
34	499.331	524.331	549.331	374.331	894.419	857.5	125	150	175
33.8									
33.8	413.961	433.961	453.961	373.961	894.056	857.51	40	60	80
32.6	397.311	407.311	417.311	377.311	905.061	871.11	20	30	40
27.7									
27.7	423.057	448.057	473.057	373.057	900.814	871.12	50	75	100
27.6	417.681	427.681	437.681	377.681	913.16	884.92	40	50	60
17.5									
17.5	450.002	475.002	500.002	375.002	910.488	884.93	75	100	125
17.3	426.116	451.116	476.116	376.116	913.234	887.93	50	75	100
16.3									
16.3	425.999	450.999	475.999	375.999	913.124	887.94	50	75	100
14.8	417.802	427.802	437.802	397.802	973.728	957.24	20	30	40
14.5									
14.5	437.77	457.77	477.77	397.77	973.703	957.25	40	60	80
14.1	432.503	442.503	452.503	412.503	1011	998.65	20	30	40
13.6									
13.6	447.45	462.45	477.45	412.45	1010.95	998.66	35	50	65
13	447.416	457.416	467.416	427.416	1049.52	1042.26	20	30	40
8.4									
8.4	422.034	427.034	432.034	427.034	1049.15	1042.27	-5	0	5
8.35	460.284	470.284	480.284	430.284	1057.74	1052.27	30	40	50
7.9	458.49	468.49	478.49	438.49	1078.4	1076.07	20	30	40
7.7									
7.7	468.477	478.477	488.477	438.477	1078.4	1076.08	30	40	50
7.3	471.023	481.023	491.023	456.023	1124.77	1130.08	15	25	35
6.7									
6.7	470.986	480.986	490.986	455.986	1124.74	1130.09	15	25	35
6.5	474.142	479.142	484.142	459.142	1133.56	1140.69	15	20	25
1									
1	453.874	458.874	463.874	458.874	1133.3	1140.7	-5	0	5
0.599998	470.54	471.54	472.54	470.54	1163.69	1177.4	0	1	2
0.55									
0.550003	468.538	470.538	472.538	470.538	1163.7	1177.41	-2	0	2
0.199997	475.651	477.651	479.651	475.651	1178.3	1195.41	0	2	4

Eyreville R2 results					Exmore R2 results				
Age	EYR2min	EYR2mean	EYR2max	EYR2seds	Age	EXR2min	EXR2mean	EXR2max	EXR2seds
-35.55	273.951	281.749	300.68	261.826	-35.55	-26.4601	-17.6704	2.24543	-38.5633
-35.5					-35.5				
-35.5	237.914	286.281	335.639	134.514	-35.5	64.7501	114.108	164.448	-38.6273
-33.7	189.006	237.439	286.797	85.7374	-34	50.4364	65.9875	82.4667	-35.9299
-27.7					-33.8				
-27.7	47.56	79.2938	111.748	12.3131	-33.8	-7.54928	4.62111	17.7126	-36.4301
-27.6	47.2243	78.9613	111.416	11.9838	-32.6	-20.3723	-14.9632	-8.67529	-35.6463
-26.7					-27.7				
-26.7	42.471	57.3336	72.8847	7.28836	-27.7	-9.0519	6.49915	22.765	-44.2829
-26.6	35.6713	40.3951	45.8042	7.25636	-27.6	-12.8061	-7.39704	-1.27644	-41.2693
-18.4					-17.5				
-18.4	33.8825	48.9931	64.5442	-17.7078	-17.5	-2.06013	13.4909	29.454	-53.5912
-18.3	30.499	55.7545	81.4475	-17.705	-17.3	-18.4124	-2.86139	13.0962	-53.0293
-18.2	24.2583	35.9939	48.1643	-17.1787	-16.3				
-17.4					-16.3	-19.4927	-3.9416	11.989	-54.0557
-17.4	15.8722	31.0106	46.5617	-18.7592	-14.8	-26.5066	-21.0976	-15.3486	-40.7067
-17.3	9.45038	21.2108	33.3812	-18.4143	-14.5				
-16.4					-14.5	-13.2956	-1.12523	11.3772	-41.0027
-16.4	14.485	29.6507	45.2017	-20.092	-14.1	-17.2415	-11.8324	-6.10158	-31.4052
-16.1	30.346	42.1391	54.3095	-17.7375	-13.6				
-16	17.201	32.3775	47.9285	-17.3545	-13.6	-7.61231	1.17741	10.276	-31.8924
-14.8					-13	-8.20339	-2.79433	2.90831	-22.311
-14.8	31.9754	47.1837	62.7348	-19.4196	-8.4				
-14.1	19.7621	34.9888	50.5398	-14.6929	-8.4	-29.5386	-27.5102	-25.3008	-26.5186
-13.8					-8.35	-3.72061	1.68845	7.27736	-24.3629
-13.8	19.2662	34.5007	50.0518	-15.1732	-7.9	-5.32512	0.0839386	5.66228	-19.1851
-12.8	6.36305	21.6233	37.1743	-11.1216	-7.7				
-8.3					-7.7	1.25467	6.66373	12.2375	-19.3573
-8.3	16.8119	25.4215	34.2112	-17.3548	-7.3	2.63122	8.04028	13.6047	-7.82024
-8.25	1.33757	16.7097	32.2607	-15.9234	-6.7				
-8	10.0816	15.3176	20.7266	-10.5483	-6.7	2.0937	7.50277	13.0533	-8.33023
-7.7					-6.5	4.05733	6.08573	8.2511	-6.35744
-7.7	16.4531	21.6962	27.1052	-10.924	-1				
-7.55	-2.85826	9.1497	14.5588	-9.94428	-1	-14.1073	-12.0789	-10.0339	-10.7598
-7.2	8.36644	13.6212	19.0303	-2.0839	-0.6	-3.14853	-3.82467	-4.49246	-3.165
-6.4					-0.55				
-6.4	10.7463	12.639	14.6674	-3.04763	-0.55	-4.54021	-4.54021	-4.5329	-3.20235
-6.1	9.62078	11.5203	13.5487	-0.778766	-0.2	0	0	0	0
-4.9									
-4.9	8.17904	10.1058	12.1342	-2.16611					
-4.6	-0.135403	5.17875	7.20715	-0.32515					
-2.95									
-2.95	8.12061	10.0905	12.1189	-2.13838					
-2.8	-1.32412	4.02964	6.05804	-1.4346					
-2.75									
-2.75	12.1427	17.4975	22.9066	-1.48833					
-2.55	13.6721	19.0313	24.4404	4.98E-02					
-0.55									
-0.55	-2.00414	-2.01144	-2.01144	-2.01874					
-0.2	0	0	0	0					

Age	S.L. Min	S.L. Mid	S.L. Max	Age	S.L. Min	S.L. Mid	S.L. Max	Age	S.L. Min	S.L. Mid	S.L. Max	Age	S.L. Min	S.L. Mid	S.L. Max	Age	S.L. Min	S.L. Mid	S.L. Max
-35.5	34.9	59.9	80.7	-30.1	-11.2	9.2	29.5	-24.4	-20.3	-6.7	8.0	-18.4	-4.7	-0.6	6.2	-12.3	-6.8	-3.5	-0.3
-35.4	33.3	46.8	57.8	-30				-24.3	-19.3	-5.6	8.0	-18.3	-4.4	-0.5	6.0	-12.2	-6.5	-3.2	-0.1
-35.3	31.8	51.8	74.8	-29.4	-14.2	-3.8	6.7	-24.2	-33.9	-23.5	-13.2	-18.2	-22.9	-11.5	6.6	-12.1	-6.3	5.3	21.9
-35.2	32.5	50.6	71.0	-29.3	-12.8	-2.4	7.9	-24.3	-37.9	-31.1	-24.3	-17.7	-20.1	1.2	7.2	-12	-6.1	6.9	25.8
-35.1	39.6	51.7	62.6	-29.2	-9.1	3.1	15.3	-24	-28.8	-18.4	-7.9	-17.7	-20	1.7	7.6	-11.9	-5.8	6.6	24.2
-35	34.9	48.1	54.4	-29.1	-5.4	8.7	22.8	-23.9	-7.7	-2.4	5.0	-17.6	-1.9	1.7	7.5	-11.8	9.3	14.1	21.4
-34.9	30.2	43.5	46.2	-29	-2.2	12.8	27.8	-23.8	-7.6	0.1	12.9	-17.5	0.7	0.7	4.9	-11.7	8.4	12.4	18.3
-34.8	30.3	39.3	40.6	-28.9	-12.7	-2.4	7.9	-23.7	-7.4	0.3	13.1	-17.4	-1.5	1.0	5.3	-11.6	6.8	9.8	14.0
-34.6	41.3	63.7	97.6	-28.8	-2.8	10.6	24.0	-23.6	-7.2	0.5	13.2	-17.3	-1.3	1.2	5.8	-11.5	4.3	5.8	7.5
-34.5	40.6	60.7	91.3	-28.6	7.4	24.1	40.7	-23.5	-5.1	2.7	13.4	-17.2	1.2	2.7	6.3	-11.4			
-34.4	40.6	60.7	91.3	-28.6	7.4	24.1	40.7	-23.4	6.2	9.8	13.6	-17.1	0.2	2.3	6.8	-10.3	-7.9	-4.6	-1.3
-34.3	37.0	53.6	78.6	-28.5	7.3	23.4	39.5	-23.3	6.3	9.8	13.8	-17	0.9	2.8	7.3	-10.2	-8.1	-4.8	-1.5
-34.2	34.7	54.0	58.1	-28.4	7.8	23.9	40.0	-23.2	1.7	12.4	32.3	-16.9	-4.6	0.5	11.4	-10.1	-8.3	-5.0	-1.7
-34.1	34.7	61.6	87.1	-28.3	8.4	24.5	40.6	-23.1	-3.0	6.2	23.1	-16.8	-0.8	2.9	8.3	-10	-8.5	-5.2	-1.9
-34	34.0	61.7	61.7	-28.2				-23	-7.6	0.0	14.0	-16.7	0.0	3.5	8.8	-9.9	-8.7	-5.4	-2.1
-33.9	33.9	61.8	61.8	-27.9	-26.8	-21.4	-16.1	-22.9	-12.3	-6.2	4.9	-16.6	-1.2	2.8	9.3	-9.8	-8.9	-5.6	-2.3
-33.8	33.8	61.9	61.9	-27.8	-26.2	-19.4	-12.6	-22.8	-16.9	-12.4	-4.3	-16.5	-0.7	3.3	9.8	-9.7	-9.1	-5.7	-2.5
-33.6				-27.7	-25.7	-18.7	-11.8	-21.6				-16.2							
-33.5	-15.6	-2.0	11.6	-27.6	-11.7	0.3	12.3	-21.5	-3.2	5.9	19.3	-16.1	-0.9	2.6	6.8				
-33.4	13.3	27.0	40.6	-27.5	2.4	19.4	36.4	-21.4	-3.6	5.3	18.5	-16	3.5	5.7	9.6				
-33.3	7.9	21.6	35.2	-27.4	0.6	21.1	41.6	-21.3				-15.9	8.8	9.5	9.9				
-33.2	2.6	16.2	29.8	-27.3	2.2	22.8	43.5	-21.2	27.6	38.7	52.1	-15.8	6.9	8.2	10.3				
-33.1	-2.7	10.9	24.4	-27.2	-13.8	-5.5	2.9	-21.1	-14.4	11.7	42.0	-15.7	2.1	4.8	9.8				
-33				-27.1	-1.6	2.8	7.2	-21	-13.6	9.0	41.7	-15.6	0.6	4.5	11.0				
-32.9	-10.3	-3.4	3.5	-27				-20.9	-12.7	9.4	41.3	-14.8							
-32.8	-10.1	-3.2	3.6	-26.9	-20.1	-9.6	0.9	-20.8	-11.8	12.1	41.0	-14.7	4.1	10.0	19.9				
-32.7	-9.9	-3.0	3.8	-26.8	-12.9	7.5	27.8	-20.7	-10.8	8.3	40.7	-14.6	5.1	11.1	21.0				
-32.6	21.2	41.5	61.8	-26.7	18.9	23.4	27.8	-20.6	-9.9	11.1	40.3	-14.5	6.1	12.1	22.0				
-32.5	19.8	33.4	47.0	-26.6	23.3	43.8	64.3	-20.5	-31.3	7.5	40.0	-14.4	7.2	13.1	23.0				
-32.4	22.4	36.0	49.6	-26.5	-4.0	7.7	19.5	-20.4	-17.2	11.3	39.6	-14.3	9.9	15.8	24.1				
-32.3	-2.1	4.7	11.6	-26.4	17.5	28.1	38.8	-20.3	-17.3	7.2	39.3	-14.2	14.8	24.2	38.9				
-32.2	0.4	7.2	14.0	-26.3	18.6	30.1	41.6	-20.2	-12.4	8.2	38.9	-14.1	13.6	22.4	36.1				
-32.1	2.9	9.7	16.5	-26.2	4.0	15.6	27.3	-20.1	-11.8	1.1	23.7	-14	12.4	20.7	33.4				
-31.7				-26.1	-10.6	1.2	13.1	-20	-14.6	-0.1	19.9	-13.9	11.3	18.9	30.6				
-31.6	-4.3	15.5	35.2	-26	-12.1	-0.9	10.4	-19.9	-20.2	-1.4	16.0	-13.8	17.0	18.4	22.5				
-31.5	-4.3	15.7	35.5	-25.9	-13.6	-2.9	7.8	-19.8	-1.0	-0.2	1.4	-13.7	11.7	14.7	19.7				
-31.4	-4.2	15.9	35.9	-25.8	-15.1	-5.0	5.1	-19.7	-7.8	-4.0	2.1	-13.6	7.7	11.0	17.0				
-31.3	-4.1	16.1	36.3	-25.7	-16.6	-7.0	2.5	-19.6	-7.0	-3.3	2.9	-13.5	6.6	8.2	11.6				
-31.2	-4.1	16.3	36.6	-25.6				-19.5	-6.3	-2.6	3.6	-13.4	5.4	6.0	6.2				
-31.1	-4.0	16.5	37.0	-25.5	-15.0	5.5	25.9	-19.4	-7.4	-1.5	8.4	-13.3	4.2	8.3	14.0				
-31	15.4	21.3	27.1	-25.4	-14.1	6.3	26.7	-19.3	-7.1	-1.4	8.2	-13.2	3.1	6.5	11.3				
-30.9	14.4	20.8	27.3	-25.3	-13.2	7.1	27.5	-19.2	-6.8	-1.3	7.9	-13.1	2.2	5.1	9.0				
-30.8	11.3	18.2	25.2	-25.2	-16.9	-2.0	12.9	-19.1	-6.6	-1.2	7.7	-13	1.2	3.7	6.8				
-30.7	8.2	15.7	23.2	-25.1	-20.6	-11.1	-1.6	-19	-6.3	-1.1	7.5	-12.9	0.5	2.3	4.5				
-30.6	5.1	13.1	21.2	-25	-13.3	-2.1	9.1	-18.9	-1.0	-1.0	7.3	-12.8	-0.6	2.7	7.7				
-30.5	2.0	10.6	19.2	-24.9	-6.0	6.9	19.9	-18.8	-5.7	-0.9	7.1	-12.7	4.8	6.7	9.9				
-30.4	-1.1	8.1	17.2	-24.8	4.5	16.6	28.7	-18.7	-5.5	-0.8	6.9	-12.6							
-30.3	-4.5	8.4	21.3	-24.7	5.6	17.9	30.2	-18.6	-5.2	-0.7	6.6	-12.5	-3.6	-0.3	2.9				
-30.2	-7.9	8.8	25.4	-24.6	-38.9	-28.9	-18.7	-18.5	-4.9	-0.7	6.4	-12.4	-5.2	-1.9	1.3				

CONCLUSIONS OF THE DISSERTATION

This study evaluates the relative influence of eustatic, tectonic, and sediment supply changes on the U.S. mid-Atlantic margin using high resolution geochronology from biostratigraphy and Sr-isotope age estimates, lithofacies analysis (from continuous coreholes), and geophysical log correlation to develop a detailed framework of sequence preservation, distribution, and character across the margin. Furthermore, continuous coreholes from the late Eocene Chesapeake Bay Impact Structure allow the differentiation and quantification (through one-dimensional backstripping) of regional tectonic uplift and subsidence from impact-related processes (impactite compaction, crustal rebound, etc.).

Late Cretaceous of New Jersey

We use core and geophysical log correlation to map upper Cretaceous sequences and deltaic facies across the New Jersey Coastal Plain and refine well-log predictions in the absence of core control. Core-log correlations from four continuously cored ODP sites (Ancora, Bass River, Millville and Sea Girt) establish a clear link between sequences (based on lithology, biostratigraphy, and Sr-isotope dating) and their respective gamma ray and resistivity geophysical log signatures.

Paleogeographic, deltaic lithofacies, and isopach maps of thirteen sequences establish the 35 million year, high-resolution (> 1 myr) record of Late Cretaceous deltaic evolution of

the New Jersey Coastal Plain. Our study demonstrates the widely known variability of deltaic systems, but also documents the relative stability of deltaic facies systems on the 10^6 - 10^7 yr scale, with long periods of cyclically repeating systems tracts (primarily TST and HST) controlled by eustatic change.

This study reveals five phases of paleodeltaic evolution during the Late Cretaceous: (1) Cenomanian-early Turonian deltaic facies shift from delta plain to fully marine and are centered in the central coastal plain; (2) high sediment input, coupled with low long-term sea level and high rates of accommodation in the northern coastal plain resulted in thick, marginal to nonmarine mixed-influenced deltaic facies during the Turonian-Coniacian; (3) low sediment rates and high long-term sea level during the Santonian resulted in a sediment-starved margin with little deltaic influence; (4) Campanian deltaic sequences exhibit wave reworking and longshore transport of sands and thicken to the north; and (5) low sedimentation rates and high long-term sea level during the Maastrichtian resulted in a sediment-starved glauconitic shelf with little to no deltaic influence.

Deltaic facies characteristics are strongly influenced by long-term eustatic changes, allogenic variations in sediment supply, and proximity to two long-lived fluvial axes (potentially related to the ancestral Hudson and Delaware Rivers). Sequence depocenters migrate gradually northeastward from the Cenomanian (ca. 98 Ma) through the earliest Danian (ca. 64 Ma) and reflect the interplay of dominant sediment source location and flexural subsidence from large sediment loads prograding across the offshore shelf. Results from the Late Cretaceous show that although eustasy provides the template for

sequences globally, regional tectonics (rates of subsidence and accommodation), autogenic changes in sediment supply, proximity to sediment input, and flexural subsidence from depocenter loading can strongly influence the regional to local preservation and facies expression of sequences.

Regional Studies of the Chesapeake Bay Impact Structure

The Exmore and Eyreville, VA cores provide the first continuous, high-resolution ($> \sim 1$ myr) chronostratigraphic records from the Chesapeake Bay Impact Structure, and provide a unique opportunity to differentiate impact-effects from regional tectonic patterns during the Cenozoic. We use integrated sequence stratigraphic analyses to identify 12-16 post-impact depositional sequences within the inner crater and the annular trough, and place these sequences in a regional framework covering the mid-Atlantic margin (New Jersey to Virginia). Results indicate that post-impact sedimentation was largely controlled by global sea-level change, the long-term compaction of impact-generated materials, and periods of regional uplift and subsidence linked to known basement structures. The differential compaction of impactites also caused a bathymetric low within the inner crater during the late Eocene-mid-Miocene, resulting in deeper water lithofacies than coreholes in the annular trough.

While many CBIS sequence boundaries show a strong correspondence with ice volume increases inferred from oxygen isotopic changes (indicating a eustatic control on sequence genesis), an evaluation of the CBIS in relation to the U.S. mid-Atlantic margin

reveals five primary phases of crater evolution influenced by sediment supply changes and regional tectonism: 1) the rapid late Eocene deposition was dominated by the initial bathymetric low from the impact event and phase of rapid impactite compaction; 2) regional Oligocene uplift and sediment starvation of the inner basin; 3) continued lower Miocene regional uplift; 4) mid-upper Miocene uplift of the Norfolk arch coupled with low sedimentation rates; and 5) late Miocene to Pliocene subsidence of the southern Salisbury embayment relative to New Jersey. We identify periods of regional uplift and excess subsidence at a scale of tens of meters in 1-5 myr that overprint subsidence from simple lithospheric cooling, flexure, and impactite compaction. We suggest that uplift and excess subsidence was caused by differential movement of basement blocks and fault-bounded terranes in response to variations in intraplate stress.

Quantifying impact-effects and regional tectonism

We use one-dimensional backstripping to quantify the rates and amplitudes of impact-related effects, regional tectonics, and eustatic change on the post-impact section of the late Eocene Chesapeake Bay Impact Structure. The generation of R1 and R2 curves, and comparison to previously published backstripped records and eustatic estimates, further allows an evaluation of the mechanisms that shape the surrounding mid-Atlantic Coastal Plain. While thermoflexural subsidence and eustatic changes are the dominant controls on sequence distribution on the mid-Atlantic margin, the presence of significant (3-7 myr) regional unconformities across the CBIS area implicates periods of regional tectonic uplift resulting in erosion and/or nondeposition.

Comparison of backstripped records in and around the CBIS reveals: 1) the long-term compaction of impact-generated materials strongly influenced deposition within the inner crater, shown by the growth of post-impact sequences into the structure and high (100 ± 50 m) excess subsidence during the late Eocene that gradually decreases to 10 ± 5 m by the late Miocene; 2) excess accommodation in the annular trough was 50 ± 25 m in the late Eocene but rapidly decreases by the Oligocene, reflecting the thin impactite-column underlying post-impact sediments (~ 200 m); 3) late Eocene-early Oligocene uplift of 80-140 m may have resulted from the crustal rebound of the fault-bounded CBIS; 4) regional unconformities during the Oligocene (patchy, discontinuous distribution from 33-27 Ma), lower Miocene (largely absent from 27-19 Ma), and upper middle Miocene (hiatus from 12-9.8 Ma) within the CBIS-region contrast thick sections in New Jersey and Delaware and loosely correspond with known basement structures; 5) comparison of backstripped R2 results with eustatic curves establishes minimum levels of uplift required for unconformity genesis at 10-50 m/ 1-5 myr; and 6) unlike much of the mid-Atlantic Coastal Plain otherwise dominated by eustasy and thermoflexural subsidence, this segment of the margin exhibits periods of “passive-aggressive” non-thermal tectonic uplift (10-50 m /1-5 myr) and excess subsidence (10-30/10 myr with peaks exceeding 75-100 m/5 myr)

We conclude that while eustasy is largely responsible for changes in accommodation and the margin-wide genesis of sequence boundaries, the vertical movement of basement structures in response to intraplate stress, depocenter loading, and other large-scale

tectonic mechanisms, results in significant differential preservation of sequences across the mid-Atlantic margin. The post-impact section of the CBIS, although strongly influenced by the initial impact and subsequent long-term compaction of impact materials, is dominated by regional tectonic patterns after the latest Eocene and may provide valid eustatic estimates for the late Miocene and Pliocene:

FUTURE WORK

While this study provided valuable insight regarding the distribution of sequences across the mid-Atlantic Coastal Plain, generated the first quantitative estimates of non-thermal “passive-aggressive” tectonic uplift and subsidence on this margin, and resolved the primary controls on the post-impact evolution of the Chesapeake Bay Impact Structure, it is important that these results are built upon by new generations of research. Further studies of the mid-Atlantic margin provide a unique opportunity to test the fundamental controls on margin evolution with excellent age-control and the integration of numerous data sources, including coreholes, geophysical logs, outcrops, and seismic data.

The calibration of geophysical logs with continuous coreholes from ODP Leg 174AX allowed the reconstruction of the paleogeographic evolution of the Late Cretaceous New Jersey Coastal Plain. However, similar high-resolution (> 1 myr) mapping efforts for the mid-Cretaceous Potomac Formation and overlying Paleocene-late Miocene sequences remain incomplete and are necessary to fully understand the long-term (120 Ma) development of the New Jersey Coastal Plain and adjacent continental shelf. The

Cenozoic section of New Jersey is an ideal location for the continuation of sequence and paleogeographic mapping efforts due to: 1) the presence of numerous onshore coreholes from ODP Legs 150X and 174AX that provide continuous sections with excellent recovery (Fig. 1; Miller et al., 1996; Miller et al., 2004); 2) full-suite geophysical logs from these coreholes vital to core-log integration and the establishment of characteristic sequence and facies signatures; and 3) a vast network of shallow (< 150 m) geophysical logs from water-resource companies and the New Jersey Geological Survey required for detailed mapping of sequence systems tracts and facies variability. Preliminary mapping of the Paleocene is ongoing (Fig. 2), and demonstrates trends similar to underlying upper Cretaceous units, namely: 1) slight thickening into the Raritan embayment; 2) identification of northern and southern depocenters; and 3) sediment-starved, glauconitic shelf lithofacies with little to no deltaic influence similar to the Maastrichtian Navesink Formation (Miller et al., 2004; Harris, 2006; Kulpecz et al., 2008).

Establishing the onshore distribution of Paleocene- late Miocene sequences in New Jersey also provides the unique opportunity for correlation with offshore seismic profiles (e.g., Monteverde et al., 2008), existing offshore coreholes (e.g., AMCORR 611 and A COW 1 and 2), and three future coreholes of the mid-Atlantic transect (MAT 1-3) scheduled for completion during the summer of 2009. Linking these records is an important step in not only understanding the evolution of the onshore coastal plain in regards to eustasy, sediment supply, and tectonics, but the entire New Jersey margin. The upcoming offshore coring efforts are also expected to penetrate sediments of the Lowstand Systems Tract (Posamentier and Vail, 1988), a sequence component that is

rarely captured on the updip coastal plain. These results will further increase our understanding of the controls on sequence geometry and our estimates of sea-level during lowstands and sequence boundary formation.

Another important step is the linkage of Cenozoic sequences from the New Jersey Coastal Plain to the recently established sequence stratigraphic framework of Virginia, Maryland, and Delaware (Browning et al., 2006; Browning et al., submitted; Kulpecz et al., submitted). Although the coreholes of Cape May, NJ (Miller et al., 1996) and Bethany Beach, DE (Browning et al., 2006) are separated by the geographic boundary of the Delaware Bay (Fig. 1) the coreholes stand only ~30 km apart. Numerous geophysical logs along the northern shore of Delaware (Andres, 2004) and southern New Jersey (archived at the New Jersey Geological Survey) could provide the vital link connecting the sequence stratigraphic frameworks of New Jersey and the Delmarva Peninsula. The result would be impressive: a series of near-continuous 250-300 km maps of Cenozoic sequence distribution across the mid-Atlantic margin (Fig. 1). Such results would allow the identification of regional-scale variability of sequence distribution, and allow greater insight into margin tectonics and broad sediment supply changes.

The improvement of age-control for USGS coreholes in and around the Chesapeake Bay Impact Structure could also further our understanding of post-impact processes and controls on regional sedimentation. Numerous coreholes within the CBIS (e.g., Langley, Kiptopeke, Bayside; Edwards et al., 2005; Powars and Bruce, 1999; Powars et al., 1992) provide relatively coarse biostratigraphic age-control with lithostratigraphic

interpretations. A reevaluation of these cores, using the integrated sequence stratigraphic method applied in this and other studies (e.g., Browning et al., 2006), namely Sr-isotopes, and enhanced biostratigraphy, will increase the geochronologic resolution of these studies and enable better analysis. Possible sequence stratigraphic studies of the Jenkins Bridge corehole (located on the Maryland-Virginia border; Fig. 1) could provide valuable constraints on log correlations between Bethany Beach, DE and the Exmore, VA corehole. These high resolution geochronologic studies, coupled with paleodepth analysis from benthic foraminifera biofacies and lithofacies, would also enable the generation of new backstripped results for coreholes across the entire mid-Atlantic margin. The comparison of these results would lend greater context to the timing, amplitude, and geographic scale of the tectonic changes identified by Hayden et al. (2008) and this study.

References

- Andres, A.S., 2004, The Cat Hill Formation and Bethany Beach Formation of Delaware: Delaware Geological Survey Report of Investigations No. 67, 8 p.
- Browning, J.V., Miller, K.G., McLaughlin, P.P., Kominz, M.A., Sugarman, P.J., Monteverde, D., Feigenson, M.D., and Hernández, J.C., 2006, Quantification of the effects of eustasy, subsidence, and sediment supply on Miocene sequences, Mid-Atlantic margin of the United States: Geological Society of America Bulletin, v. 118, p. 567-588.
- Browning, J.V., Miller, K.G., McLaughlin, P.P., Jr., Edwards, L.E., Powars, D.S., Kulpecz, A.A., Wade, B.S., and Feigenson, M.D., *submitted*, Post-impact integrated litho-, sequence, Sr-isotopic, and bio-stratigraphy of the Eyreville corehole, Chesapeake Bay impact structure inner basin: Geological Society of America Special Publication XX, XXX p.
- Edwards, L.E., Barron, J.A., Bukry, D., Bybell, L.M., Cronin, T.M., Poag, C.W., Weems, R.E., and Wingard, G.L., 2005, Paleontology of the Upper Eocene to Quaternary Postimpact Section in the USGS-NASA Langley Core, Hampton, Virginia, *in* Horton, J.W., Jr., Powars, D.S., and Gohn, G.S., Eds. 2005, Studies of the

- Chesapeake Bay Impact Structure- The USGS-NASA Langley Corehole, Hampton, Virginia, and Related Coreholes and Geophysical Survey: U.S. Geological Survey Professional Paper 1688, p. H1-47, 9 pls.
- Harris, A.D., Paleocene sea-level changes, New Jersey Coastal Plain, 2006: Master's thesis, Rutgers University Press, New Brunswick, NJ, USA: 122 p.
- Hayden, T., Kominz, M., Powars, D.S., Edwards, L.E., Miller, K.G., Browning, J.V., and Kulpecz, A.A., 2008, Impact effects and regional tectonic insights: Backstripping the Chesapeake Bay impact structure: *Geology*, v. 36, p. 327-330.
- Kulpecz, A.A., Miller, K.G., Sugarman, P.J., and Browning, J.V., 2008, Response of Late Cretaceous migrating deltaic facies systems to sea level, tectonics, and sediment supply changes, New Jersey Coastal Plain U.S.A.: *Journal of Sedimentary Research*, v. 78, p. 112-129
- Kulpecz, A.A., Miller, K.G., Browning, J.V., Edwards, L.E., Powars, D.S., McLaughlin, P.P., Jr., Harris, A.D., Feigenson, M.D., *submitted*, Post-impact of the Chesapeake Bay impact structure: eustasy, passive-aggressive tectonism, and impactite compaction: Geological Society of America Special Publication XX, XX
- Miller, K.G., Liu, C., Browning, J.V., Pekar, S.F., Sugarman, P.J., Van Fossen, M.C., Mullikin, L., Queen, D., Feigenson, M.D., Aubry, M.-P., Burckle, L.D., Powars, D., and Heibel, T., 1996. Cape May site report. *In* Miller, K.G., et al., *Proc. ODP, Init. Repts.*, 150X (Suppl.): College Station, TX (Ocean Drilling Program), 5-28.
- Miller, K.G., Sugarman, P.J., Browning, J.V., Kominz, M.A., Olsson, R.K., Feigenson, M.D., and Hernández, J.C., 2004, Upper Cretaceous sequences and sea-level history, New Jersey coastal plain: *Geological Society of America Bulletin*, v. 116, p. 368-393.
- Monteverde, D.H., Mountain, G.S., and Miller, K.G., 2008, Early Miocene sequence development across the New Jersey margin: *Basin Research*, v. 20, p. 249-267.
- Posamentier, H.W., and Vail, P.R., 1988, Eustatic controls on clastic deposition II- sequence and systems tract models: *Society of Economic Paleontologists and Mineralogists Special Publication*, v. 42, p. 125-154.
- Powars, D.S., and Bruce, T.S., 1999, The effects of the Chesapeake Bay impact crater on the geologic frame-work and the correlation of hydrogeologic units of southeastern Virginia, south of the James River: U.S. Geological Survey Professional Paper 1612, 82 p.
- Powars, D.S., Mixon, R.B., and Bruce, T.S., 1992, Uppermost Mesozoic and Cenozoic geologic cross section, outer coastal plain of Virginia, *in* Gohn, G.S., ed., *Proceedings of the 1988 U.S. Geological Survey Workshop on the Geology and*

Geohydrology of the Atlantic Coastal Plain: U.S. Geological Survey Circular 1059, p. 85-101.

Figure Captions

Figure 1. Location map of the mid-Atlantic margin showing the location of ODP Leg 150X and 174AX coreholes (red dots) that could be used for extensive mapping of Cenozoic sequences. JB represents the location of the Jenkins Bridge (USGS) corehole, a vital component for improving regional correlations across the Delmarva Peninsula.

Figure 2. Isopach map showing the thickness and distribution of Paleocene sequences on the New Jersey Coastal Plain. Red dots indicate the location of ODP Leg 174 AX coreholes used in Kulpecz et al. (2008), while black dots indicate geophysical logs used for correlation. Thickness trends mirror those of the Late Cretaceous identified by Kulpecz et al. (2008), but further mapping is required to establish the distribution of Eocene- late Miocene sequences on the Coastal Plain.

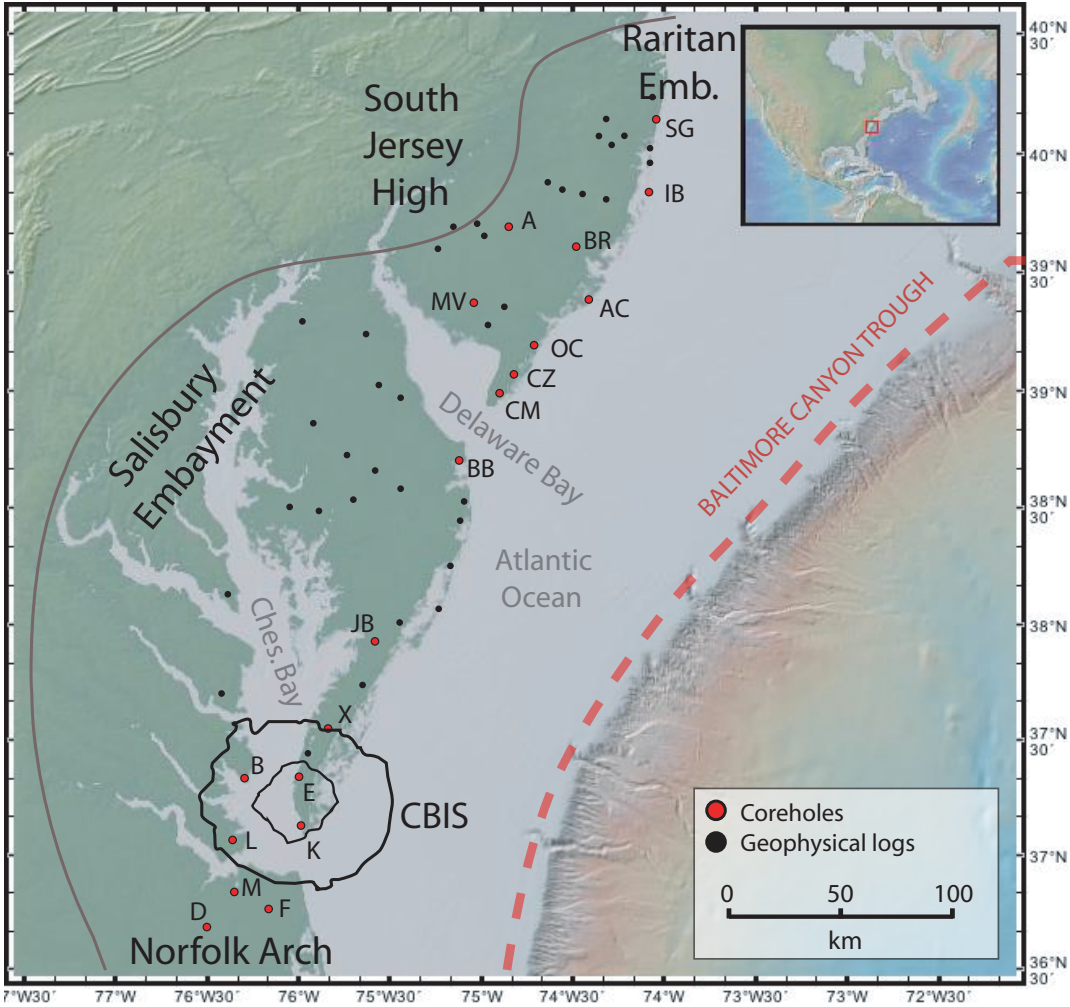


Figure 1

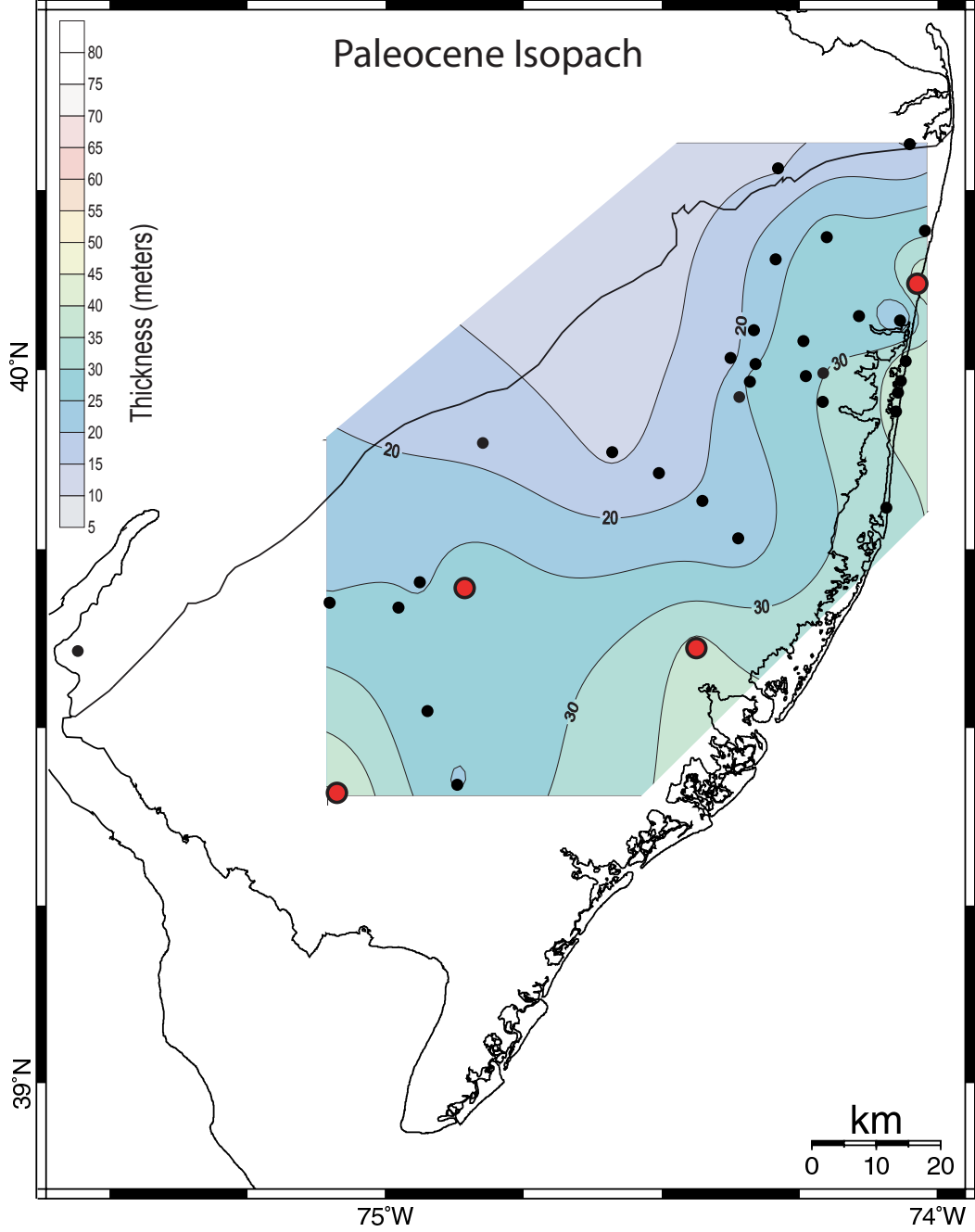


Figure 2

CURRICULUM VITAE

Andrew Alexander Kulpecz

Job Title: Geoscientist, Chevron Energy Technology Company, 1500 Louisiana Street,
Houston TX 77002

Current Address: 636 W. 17th Street, Houston, TX 77008

Permanent Address: 90 Bryant Road, Waretown, NJ 08758

Education:

B.A., Geology, 1998-2002, Wheaton College (IL)

M.Sc., Geological Sciences, 2002-2005, Rutgers University (NJ)

Ph.D., Geological Sciences, 2005-2008, Rutgers University (NJ)

Professional Experience:

- 6/2007-8/2007: **Chevron Energy Technology Company**
Summer intern with Shallow Marine Stratigraphy Team, San Ramon, CA
- 9/2005-11/2005: **Official Volunteer, United States Geological Survey**
Onsite work at Chesapeake Bay Impact Structure coring
- 6/2005-9/2007: **Part-time Employee, New Jersey Geological Survey**
Regional stratigraphic mapping
- 8/2002-5/2008: **Teaching Assistant, Rutgers University**
Planet Earth lecture, Stratigraphy and Sedimentology laboratories
- 6/2004-8/2004: **Shell International Exploration and Production, Inc.**
Summer internship with Regional Studies Team, Houston, TX
- 5/2003-12/2003: **Graduate Research Assistant, Rutgers University**
- 2/2002-5/2002: **Teaching Assistant, Wheaton College**
- 5/2000-7/2000: **Boston Consulting Group (Management Consultant)**
Summer intern, London, United Kingdom
- 5/1999-7/1999: **Booz Allen & Hamilton; London (Management Consultant)**
Summer intern, London United Kingdom

Professional Memberships:

American Geophysical Union, Geological Society of America, American Association for the Advancement of Science, Society of Economic Petrologists and Sedimentologists

Publications:

Kulpecz, A.A., Miller, K.G., Sugarman, P.J., and Browning, J.V., 2008. Response of Late Cretaceous Migrating Deltaic Facies Systems to Sea Level, Tectonics, and Sediment

- Supply Changes, New Jersey Coastal Plain, U.S.A. *Journal of Sedimentary Research*, v. 78, p. 112-129.
- Gohn, G.S., Koeberl, C., Miller, K.G., Reimold, W.U., Browning, J.V., Cockell, C.S., Horton, J.W., Jr., Kenkmann, T., Kulpecz, A.A., Powars, D.S., Sanford, W.E., and Voytek, M.A., 2008. Deep drilling into the Chesapeake Bay Impact Structure: *Science*, v. 320, p. 1740-1745.
- Miller, K.G., Browning, J.V., Aubry, M-P., Wade, B., Katz, M.E., Kulpecz, A.A., and Wright, J.D., 2008. Eocene-Oligocene Global Climate and Sea-level Changes: St. Stephens Quarry, Alabama. *Geological Society of America Bulletin*, v. 120 (2). p. 34-53.
- Hayden, T., Kominz, M.A., Powars, D.S., Edwards, L.E., Miller, K.G., Browning, J.V., and Kulpecz, A.A., 2008. Impact Effects and Regional Tectonic Insights: Backstripping the Chesapeake Bay Impact Structure: *Geology*, v. 36 (4), p.327-330.
- Browning, J.V., Miller, K.G., Sugarman, P.J., Kominz, M.A., McLaughlin, P.P., Kulpecz, A.A., and Feigenson, M.D., 2008. A 100 million year record of sequences, facies, and sea-level change from Ocean Drilling Program onshore coreholes, U.S. Mid-Atlantic coastal plain: *Basin Research*, v. 20, 227-248.
- Sugarman, P.J., Miller, K.G., Browning, J.V., Monteverde, D.H., Uptegrove, J., McLaughlin, P.P., Jr., Stanley, A.M., Wehmiller, J., Kulpecz, A.A., Harris, A.D., Pusz, A., Kahn, A., Friedman, A., Feigenson, M.D., Barron, J., and McCarthy, F.M.G., 2007, Cape May Zoo site. In Miller, K.G., Sugarman, P.J., Browning, J.V., et al., *Proc. ODP, Init. Repts., 174AX (Suppl.)*: College Station, TX (Ocean Drilling Program) p. 1-66.
- Sugarman, P.J., Miller, K.G., Browning, J.V., Kulpecz, A.A., McLaughlin, P.P., Jr., and Monteverde, D.H., 2006. Hydrostratigraphy of the New Jersey Coastal Plain: Sequences and facies predict the continuity of aquifers and confining units. *Stratigraphy*, v. 2 (3), p. 259-275.
- Miller, K.G., Sugarman, P.J., Browning, J.V., Aubry, M.P., Brenner, G.J., Cobbs, G., III, de Romero, L., Feigenson, M.D., Harris, A., Katz, M.E., Kulpecz, A.A., McLaughlin, P.P., Jr., Misintseva, S., Monteverde, D.H., Olsson, R.K., Patrick, L., Pekar, S.J., and Uptegrove, J., 2006. Sea Girt site. In Miller, K.G., Sugarman, P.J., Browning, J.V., et al., *Proc. ODP, Init.Repts., 174AX (Suppl.)*: College Station, TX (Ocean Drilling Program), p. 1-104.
- Kulpecz, A.A., Miller, K.G., Browning, J.V., Edwards, L.E., Powars, D.S., McLaughlin, P.P., Jr., Harris, A.D., and Feigenson, M.D., under review, Post-impact evolution of the Chesapeake Bay Impact Structure. *Submitted to Geological Society of America, Special Publication on Chesapeake Bay Impact Structure*

Browning, J.V., Miller, K.G., McLaughlin, P.P., Jr., Edwards, L.E., Powars, D.S., Kulpecz, A.A., Wade, B.S., and Feigenson, M.D., under review, Post-impact litho-, sequence, Sr-isotopic, and bio-stratigraphy of the Eyreville coreholes, Chesapeake Bay impact structure inner basin. *Submitted to* Geological Society of America, Special Publication on Chesapeake Bay Impact Structure

Edwards, L.E., Powars, D.S., Browning, J.V., McLaughlin, P.P., Jr., Miller, K.G., Self-Trail, J.M., Kulpecz., A.A., and Elbra, T., under review, Geologic columns for the ICDP-USGS Eyreville A and C coreholes, Chesapeake Bay Impact Structure: Post-impact sediments, 0 to 444 m depth. *Submitted to* Geological Society of America, Special Publication on Chesapeake Bay Impact Structure